UCLA
UCLA Electronic Theses and Dissertations

Title
Heparin Mimicking Polymer Fibroblast Growth Factor 2 Conjugates for Improved Therapeutics

Permalink
https://escholarship.org/uc/item/2qr1r1h3

Author
Paluck, Samantha Joy

Publication Date
2017

Peer reviewed|Thesis/dissertation

eScholarship.org Powered by the California Digital Library
University of California

UNIVERSITY OF CALIFORNIA

Los Angeles

Heparin Mimicking Polymer Fibroblast Growth Factor 2 Conjugates for Improved Therapeutics

A dissertation submitted in partial satisfaction of the requirements for the degree Doctor of Philosophy in Chemistry

by

Samantha Joy Paluck

2017

© Copyright by

Samantha Joy Paluck

2017

ABSTRACT OF THE DISSERTATION

Heparin Mimicking Polymer
Fibroblast Growth Factor 2 Conjugates
for Improved Therapeutics

by

Samantha Joy Paluck
Doctor of Philosophy in Chemistry
University of California, Los Angeles, 2017
Professor Heather D. Maynard, Chair

Heparin is a naturally occurring highly sulfated polysaccharide that plays a critical role in a range of different biological processes. Due to the diverse functions of this polysaccharide in the body and drawbacks of its use, analogous heparin-mimicking materials are widely studied for therapeutic applications. Fibroblast growth factor 2 (FGF2) is a heparin-binding protein involved in cellular functions in applications such as wound healing and tissue regeneration. Stabilization of this protein is important for its use as a therapeutic since the native protein is unstable during storage and delivery. Additionally, the ability to increase the activity of FGF2 is important for its application, particularly in chronic wound healing and the treatment of various ischemic

conditions. This dissertation focuses on the development of a new superagonist heparin-mimicking block copolymer FGF2 conjugate, the structure activity relationship of one of the polymer blocks, and the use of that polymer to covalently dimerize FGF2.

In Chapter 1, the synthesis and biological activity of heparin-mimicking polymers are outlined. Utilization of these polymers provides significant benefits compared to heparin, including enhancing therapeutic efficacy and reducing side effects as a result of fine-tuning heparin-binding motifs and other molecular characteristics. The major types of synthetic heparin-mimicking polymers are summarized in this chapter, as well as their applications. In Chapter 2 we report a heparin mimicking block copolymer, p(SS-*co*-PEGMA)-*b*-VS, that contains one segment that enhances the stability of FGF2 and one that binds to the FGF2 receptor. The FGF2 conjugate retained activity after exposure to refrigeration (4 °C) and room temperature (23 °C) for 7 days, while unmodified FGF2 was inactive after these standard storage conditions. A cell study and receptor-based enzyme-linked immunosorbant assay (ELISA) indicated that the conjugated block copolymer facilitated binding of FGF2 to its receptor to the same extent as the addition of heparin to FGF2. Furthermore, the conjugate increased the migration and angiogenesis of endothelial cells when compared to FGF2 alone.

In Chapter 3 the structure activity relationship of the stabilizing block, p(SS-*co*-PEGMA), was examined. A library was synthesized to contain nine polymers with degrees of sulfonation ranging from 0-100%. These polymers were tested for their ability to enhance FGF2 binding with its receptor as both covalent conjugates and as excipients. In a receptor based enzyme-linked immunosorbant assay (ELISA), as well as a cell-based study, the polymer with 81% SS incorporation enhanced receptor binding compared to FGF2 alone, and to a greater extent than the

other polymers. Furthermore, a polymer size study did not show any further increase in receptor binding in relation to polymer chain length. These results provide important information for the use of p(SS-*co*-PEGMA) as a potential heparin-mimicking therapeutic.

In its active form, FGF2 is dimerized, typically with heparan sulfate threaded through the heparin binding domain. In Chapter 4 we show that we are able to increase the *in vitro* angiogenesis activity of FGF2 by covalently dimerizing it with 2 kDa poly(ethylene glycol) (PEG). We hypothesized that replacing the PEG linker with a heparin-mimicking polymer could increase the biological activity of the dimer. To fabricate a FGF2 dimer with heparin-mimicking linker, p(SS-*co*-PEGMA) was functionalized to contain maleimide end groups. The polymer was used to successfully dimerize FGF2. The purification of the dimer from unconjugated protein proved difficult and in the future we hope to purify the conjugate and asses its ability to stabilize FGF2 and increase the biological activity of the protein.

While bio-mimicking polymers provide unique characteristics for conjugates, the most commonly used polymer for protein conjugation is PEG. The covalent attachment of PEG to proteins (PEGylation) improves protein stability and bioavailability. However, there are still some downfalls to using PEG, including the non-degradable nature of the protein. Fabricating PEG-like polymers with degradable backbones is one way to overcome problems with bioaccumulation. In Chapter 5 we report the step growth polymerization of PEG-like polymers containing degradable oxime and hydrazone linkages. The polymers were shown to be degradable over 12 months with hydrazone linkages fully degrading, and oxime linkages partially degrading.

The dissertation of Samantha Joy Paluck is approved.

Timothy J. Deming

Daniel T. Kamei

Heather D. Maynard, Committee Chair

University of California, Los Angeles

2017

This dissertation is dedicated to my family.

Without your support and encouragement,

I would not be where I am today.

TABLE OF CONTENTS

Abstract of the Dissertation ii

Table of Contents vii

List of Figures xi

List of Tables xix

List of Schemes xx

List of Abbreviations xxii

Acknowledgements xxix

Vita xxxii

Chapter 1. Heparin-Mimicking Polymers: Synthesis and Biological Applications 1

1.1 Introduction to Heparin 2

1.2 Heparin-Mimicking Polymers 5

1.2.1 Introduction to Heparin-Mimicking Polymers 5

1.2.2 Carboxymethyl Benzylamide Sulfonate Dextrans (CMDBS) 7

1.2.3 Polyaromatic Anionic Compounds 11

1.2.4 Sulfated Synthetic Glycopolymers 15

1.2.5 Polysulfonated Compounds 27

1.2.6 Polyionomers as Heparin Mimics 45

1.3 Conclusions and Perspectives 50

1.4 References 52

Chapter 2. A Heparin-Mimicking Block Copolymer Stabilizes and Increases the Activity of Fibroblast Growth Factor 2 (FGF2) 65

2.1 Introduction 66

2.2 Results and Discussion 70

2.2.1 Stability Study of FGF2-pVS Conjugate 70

2.2.2 Synthesis of p(SS-*co*-PEGMA)-*b*-VS 73

2.2.3 Cytotoxicity Study of p(SS-*co*-PEGMA)-*b*-VS 75

2.2.4 Conjugation of p(SS-*co*-PEGMA)-*b*-VS to FGF2 76

2.2.5 Stability Study of p(SS-*co*-PEGMA)-*b*-VS 77

2.2.6 FGF2-p(SS-*co*-PEGMA)-*b*-VS Receptor Binding Assays 77

2.2.7 Cell Proliferation Study with FGF2-p(SS-*co*-PEGMA)-*b*-VS 80

2.2.8 In-vitro Migration and Angiogenesis Assays with FGF2-p(SS-*co*-PEGMA)-*b*-VS 81

2.3 Conclusions 86

2.4 Experimental 87

2.4.1 Materials 87

2.4.2 Analytical Techniques 88

2.4.3 Experimental 89

2.5 Appendix to Chapter 2 – Supplemental Figures 101

2.6 References 108

Chapter 3. Structure Activity Relationship of Heparin Mimicking Polymer p(SS-*co*-PEGMA): Effect of Sulfonation and Polymer Size on FGF2 Receptor Binding 115

3.1 Introduction 116

3.2 Results and Discussion 118
3.2.1 Polymerization of p(SS-*co*-PEGMA) to Yield Library of Polymers with Varying Degrees of Sulfonation 118
3.2.2 Evaluation of Polymer Kinetics 120
3.2.3 Effect of Degree of Sulfonation on Receptor Binding with Excipients.....121
3.2.4 Preparation of FGF2-p(SS-co-PEGMA) conjugates 124
3.2.5 Effect of Degree of Sulfonation on Receptor Binding with Conjugates 125
3.2.6 Verification on Conjugate Activity.....126
3.2.7 Effect of Polymer Size on Receptor Binding.....127
3.3 Conclusions and Future Directions.....131
3.4 Experimental.....132
3.4.1 Materials 132
3.4.2 Analytical Techniques 133
3.4.3 Methods.....133
3.5 Appendix to Chapter 3 – Supplementary Figures.....136
3.6 References.....150
Chapter 4. Dimerization of FGF2 with Heparin-Mimicking Polymer p(SS-*co*-PEGMA) .154
4.1 Introduction.....155
4.2 Results and Discussion 157
4.2.1 In-Vitro Angiogenesis Assay of FGF2-PEG2k-FGF2.....157
4.2.2 Effect of Adding Heparin to FGF2-PEG2k-FGF2.....159
4.2.3 Synthesis of Heparin-Mimicking Polymer for Linker in FGF2 Dimerization 160

4.2.4 Synthesis of Maleimide Terminated Polymer for FGF2 Dimerization 164

4.2.5 Dimerization of FGF2 with MAL-p(SS-*co*-PEGMA)-MAL.....166

4.3 Conclusions and Future Directions.....167

4.4 Experimental.....167

4.4.1 Materials 167

4.4.2 Analytical Techniques 168

4.4.3 Methods.....168

4.5 Appendix to Chapter 4 – Supplementary Figures.....176

4.6 References.....185

Chapter 5. Degradable Oxime and Hydrazone Based PEG-Like Polymers 189

5.1 Introduction.....190

5.2 Results and Discussion 193

5.2.1 Synthesis of Monomers for Oxime and Hydrazone Polymers.....193

5.2.2 Step-Growth Polymerization of Oxime and Hydrazone Polymers.....196

5.2.3 Degradation Study of Polymers.....200

5.3 Conclusions and Future Directions.....202

5.4 Experimental.....203

4.4.1 Materials 203

4.4.2 Analytical Techniques 203

4.4.3 Methods.....204

5.5 Appendix to Chapter 5 – Supplementary Figures.....209

5.6 References.....223

LIST OF FIGURES

Figure 1-1. Chemical structure of a heparin pentasaccharide showing various repeats containing sulfate (red), sulfamate (green), and carboxylate (blue) groups 2

Figure 1-2. Examples of heparin mimicking polymers discussed in this chapter, including modified dextrans, sulfated glycopolymers, polysulfonated compounds, sulfonated ionomers, and polyaromatic anionic compounds 7

Figure 1-3. Chemical structure of carboxymethyl benzylamide sulfonate dextrans (CMDBS).....8

Figure 1-4. Syntheses of heparin mimicking glycopolymers. (a) Poly glucosyloxyethyl methacrylate-sulfate p(GEMA)-sulfate synthesized by Akashi and co-workers via free radical polymerization. (b) Hexamethylene diisocyanate-based isocyanates polymerized by step growth polymerization by Ayres and co-workers. (c) Heptasulfate lactose-based glycopolymers polymerized by cyanoxal mediated polymerization by Chaikof and co-workers. (d) Heparin mimicking polymers by ROMP to contain pendant disaccharides with three sulfates fabricated by Hsieh-Wilson and co-workers. (e) 3,4,6-sulfo glucosamines copolymerized by free radical polymerization by Miura and co-workers.....21

Figure 1-5. Heparin mimicking sulfonated polymers. (a) Chemical structures of the various sulfonated polymers tested by Liekens et. al and (b) molecular modeling showing heparin and pAMPS interacting with the heparin binding domain of FGF2.....29

Figure 1-6. (a) Chemical structure of heparin mimicking terpolymers polymerized by Migonney and co-workers and (b) their ability to inhibit fibroblast adhesion (right) verses control (left) 38

Figure 1-7. Polysulfonated heparin-mimicking polymer, p(SS-*co*-PEGMA) and the stability profile of its conjugate to FGF2. (a) Chemical structure of the polymer. (b) Structure of the FGF2-

p(SS-*co*-PEGMA) conjugate. (c) Stability of the conjugate against various stressors, tested on human dermal fibroblast cells for stimulated cell proliferation.....39

Figure 1-8. Screening study of various sulfonated polymers. (a) Chemical structure of heparin mimicking polymers polymerization by free radical polymerization. (b) Cell proliferation studies in BaF3-FR1C cells showing the heparin mimicking nature of pVS. (c) FGFR based ELISA assay showing pVS increasing the binding of FGF2 to FGFR compared to heparin.....41

Figure 1-9. (a) Chemical structure of biodegradable sulfonated poly(glutamic acid) and GPC traces showing degradation of (b) non-sulfonated polyglutamic acid and (c) sulfonated poly(glutamic acid).....43

Figure 1-10. Sulfonated urethane ionomers used in development of new anticoagulants. (a) Chemical structure of polyurethane ionomers. (b) Degree of fibrinogen deposition on modified polyurethane materials showing an increase in fibrinogen accumulation with increasing degree of sulfonation. (c) Degree of platelet deposition on modified polyurethane materials showing a decrease in platelet accumulation with increasing degree of sulfonation.....48

Figure 2-1. Polymer p(SS-*co*-PEGMA) stabilizes FGF2 as a conjugate and pVS facilitates FGF2-receptor binding when added as an excipient. When combined into a block copolymer, p(SS-*co*-PEGMA)-*b*-VS, the new conjugate both stabilizes FGF2 and increases protein activity 70

Figure 2-2. Stability study of conjugates in human dermal fibroblasts at both 4 ºC and 23 ºC after 7 days 72

Figure 2-3. Polymer Cytotoxicity in (a) human umbilical vein endothelial cells and (b) human dermal fibroblasts. (c) Representative images of cells with live cells stained green and dead cells stained red 75

Figure 2-4. (a) SDS-PAGE of crude conjugate (stained with silver nitrate). Lane 1: Protein ladder; Lane 2: FGF2; Lane 3: p(SS-*co*-PEGMA)-*b*-VS; Lane 4: FGF2-p(SS-*co*-PEGMA)-*b*-VS in non-reducing conditions; Lane 5: FGF2-p(SS-*co*-PEGMA)-*b*-VS in reducing conditions. (b) Western blot of native-PAGE of purified conjugate. Lane 1: FGF2; Lane 2: FGF2-p(SS-*co*-PEGMA)-*b*-VS 76

Figure 2-5. Cell Growth of heparin-mimicking polymer conjugates in BaF3-FR1C cells 78

Figure 2-6. FGF Receptor based ELISA.....79

Figure 2-7. (a) HUVEC comparing cell growth when incubated with FGF2-p(SS-*co*-PEGMA-*b*-VS) and (b) HDF comparing cell growth when incubated with FGF2-p(SS-*co*-PEGMA-*b*-VS) .81

Figure 2-8. HUVEC migration after 18 hours. (a) Percent migration in the presence of FGF2, FGF2 plus 1 μg/mL of heparin, or FGF2-p(SS-*co*-PEGMA)-*b*-VS. (b) Representative images of HUVEC migration taken at 0 hours and 18 hours. (c) Cell growth measured after 18-hour incubation using CellTiter-Blue.....82

Figure 2-9. Coculture angiogenesis of HUVEC and HDF. (a) Node number, cord-like structure length, and cord-like structure number. (b) Representative images of cord-like structures stained for CD-31 85

Figure 2-10. ^{1}H NMR (400 MHz, $CDCl_3$) of (1): 2-(((neopentyloxy)carbonothioyl)thio)acetic acid 101

Figure 2-11. ^{13}C NMR (400 MHz, $CDCl_3$) of (1): 2-(((neopentyloxy)carbonothioyl)thio)acetic acid 102

Figure 2-12. ^{1}H NMR (400 MHz, $CDCl_3$) of (2): 2-(pyridin-2-yldisulfanyl)ethyl 2-(((neopentyloxy)carbonothioyl)thio)acetate 103

Figure 2-13. ^{13}C NMR (400 MHz, $CDCl_3$) of (2): 2-(pyridin-2-yldisulfanyl)ethyl 2-(((neopentyloxy)carbonothioyl)thio)acetate 104
Figure 2-14. ^{1}H NMR (400 MHz, $CDCl_3$) of (3): 2-((ethoxycarbonothioyl)thio)-2-methylpropanoic acid.....104
Figure 2-15. ^{13}C NMR (400 MHz, $CDCl_3$) of (3): 2-((ethoxycarbonothioyl)thio)-2-methylpropanoic acid.....105
Figure 2-16. ^{1}H NMR (400 MHz, $CDCl_3$) of CTA: 2-(pyridin-2-yldisulfanyl)ethyl 2-((ethoxycarbonothioyl)thio)-2-methylpropanoate 105
Figure 2-17. ^{13}C NMR (400 MHz, $CDCl_3$) of CTA: 2-(pyridin-2-yldisulfanyl)ethyl 2-((ethoxycarbonothioyl)thio)-2-methylpropanoate 106
Figure 2-18. ^{1}H NMR (400 MHz, D_2O/CD_3CN) of pVS 106
Figure 2-19. ^{1}H NMR (400 MHz, D_2O) of p(SS-co-PEGMA) macroCTA.....107
Figure 2-20. ^{1}H NMR (400 MHz, D_2O) of p(SS-*co*-PEGMA)-*b*-VS.....107
Figure 3-1. Polymer kinetics performed on p(SS-*co*-PEGMA) polymerizations. (a) Kinetic studies of the RAFT polymerization of $p(SS\text{-co-}PEGMA)_{81}$ at 70 ºC. Conversion, M_0, and M_t were calculated using ^{1}H NMR spectroscopy. (b) Percent styrene sulfonate incorporation over time. (c) Theoretical versus experimental M_n from right angle light scattering in aqueous running buffer. (d) F_{SS} versus f_{SS} curves 121
Figure 3-2. Examination of the ability of p(SS-*co*-PEGMA) to enhance FGF2 receptor binding. (a) FGF Receptor based ELISA. (b) Cell growth of heparin-mimicking polymers in BaF3-FR1C cells 123
Figure 3-3. SDS-PAGE with Western Blot of FGF-p(SS-*co*-PEGMA) conjugates in both (a) non-reducing conditions and (b) reducing conditions. Lane 1: FGF2, Lane 2: FGF2-p(SS-*co*-

PEGMA)$_{8.0}$, Lane 3: FGF2-p(SS-*co*-PEGMA)$_{28}$, Lane 5: FGF2-p(SS-*co*-PEGMA)$_{55}$, Lane 6: FGF2-p(SS-*co*-PEGMA)$_{81}$, Lane 7: FGF2-pPEGMA, Lane 8: FGF2-p(SS-*co*-PEGMA)$_{76}$, Lane 9: FGF2-p(SS-*co*-PEGMA)$_{95}$, Lane 10: FGF2-pSS 125

Figure 3-4. FGF2-p(SS-*co*-PEGMA) conjugates in FGF2 receptor binding assays. (a) FGF Receptor based ELISA. (b) Cell growth of heparin-mimicking polymer conjugates in BaF3-FR1C cells 126

Figure 3-5. Determination of FGF2-p(SS-*co*-PEGMA)$_{81}$ receptor binding in BaF3-FR1c with the addition of 1 μg/mL heparin 127

Figure 3-6. Light scattering GPC traces showing varying molecular weight polymers with 81% SS 129

Figure 3-7. Determining the ability of p(SS-*co*-PEGMA) with varying polymer sizes to enhance FGF receptor binding. (a) FGF receptor based ELISA. (b) Cell growth of heparin-mimicking polymers in BaF3-FR1C cells.....130

Figure 3-8. ^{1}H NMR (400 MHz, D_2O with CD_3CN) of p(SS-*co*-PEGMA)$_{8.0}$.....136

Figure 3-9. ^{1}H NMR (400 MHz, D_2O with CD_3CN) of p(SS-*co*-PEGMA)$_{28}$ 137

Figure 3-10. ^{1}H NMR (400 MHz, D_2O with CD_3CN) of p(SS-*co*-PEGMA)$_{55}$ 138

Figure 3-11. ^{1}H NMR (400 MHz, D_2O with CD_3CN) of p(SS-*co*-PEGMA)$_{63}$ 139

Figure 3-12. ^{1}H NMR (400 MHz, D_2O with CD_3CN) of p(SS-*co*-PEGMA)$_{76}$ 140

Figure 3-13. ^{1}H NMR (400 MHz, D_2O with CD_3CN) of p(SS-*co*-PEGMA)$_{81}$ 141

Figure 3-14. ^{1}H NMR (400 MHz, D_2O with CD_3CN) of p(SS-*co*-PEGMA)$_{95}$ 142

Figure 3-15. ^{1}H NMR (400 MHz, D_2O with CD_3CN) of pSS 143

Figure 3-16. ^{1}H NMR (400 MHz, D_2O with CD_3CN) of p(SS-*co*-PEGMA) DP 41 144

Figure 3-17. ^{1}H NMR (400 MHz, D_2O with CD_3CN) of p(SS-*co*-PEGMA) DP 78 145

Figure 3-18. ^{1}H NMR (400 MHz, D_2O with CD_3CN) of p(SS-*co*-PEGMA) DP 161 146

Figure 3-19. ^{1}H NMR (400 MHz, D_2O with CD_3CN) of p(SS-*co*-PEGMA) DP 22 147

Figure 3-20. ^{1}H NMR (400 MHz, D_2O with CD_3CN) of p(SS-*co*-PEGMA) DP 263 148

Figure 3-21. ^{1}H NMR (400 MHz, D_2O with CD_3CN) of p(SS-*co*-PEGMA) DP 296 149

Figure 3-22. ^{1}H NMR (400 MHz, D_2O with CD_3CN) of p(SS-*co*-PEGMA) DP 390 150

Figure 4-1. Co-culture angiogenesis assay showing the effect of FGF2-PEG2k-FGF2 on cord-like structure formation. (a) Representative images of cord-like structure growth stained for CD31. (b) Comparison of the number of node, (c) cord-like structure number, and (d) average total cord-like structure length per image. 158

Figure 4-2. Cell growth of FGF2-PEG2k-FGF2 dimer in BaF3-FR1C cells compared to FGF2 alone and FGF2 with excess heparin 160

Figure 4-3. SDS-PAGE in reducing conditions stained with coomassie showing FGF2-p(SS-*co*-PEGMA)-FGF2 conjugate as well as FGF2-DVS-FGF2 dimer. Lane 1: Protein ladder; Lane 2: FGF2; Lane 3: crude conjugation; Lane 4: FGF2 164

Figure 4-4. SDS-PAGE in reducing conditions with coomassie stain showing FGF2-p(SS-co-PEGMA)-FGF2 conjugate. Crude conjugation. Lane 1: Protein ladder; Lane 2: FGF2; Lane 3: crude conjugation 166

Figure 4-5. ^{1}H NMR (400 MHz, D_2O with CD_3CN) of p(SS-*co*-PEGMA) 176

Figure 4-6. ^{1}H NMR (400 MHz, $CDCl_3$) of **CTA1** 177

Figure 4-7. ^{13}C NMR (400 MHz, $CDCl_3$) of **CTA1** 177

Figure 4-8. ^{1}H NMR (400 MHz, D_2O with CD_3CN) of p(SS-*co*-PEGMA)$_{CTA1}$ 178

Figure 4-9. ^{1}H NMR (400 MHz, D_2O with CD_3CN) of PDS-p(SS-*co*-PEGMA)$_{CTA1}$-PDS 179

Figure 4-10. ^{1}H NMR (400 MHz, D_2O with CD_3CN) of DVS-p(SS-*co*-PEGMA)$_{CTA1}$-DVS 180

Figure 4-11. ^{1}H NMR (400 MHz, $CDCl_3$) of **CTA 2** 181

Figure 4-12. ^{13}C NMR (400 MHz, $CDCl_3$) of **CTA 2** 182

Figure 4-13. ^{1}H NMR (400 MHz, D_2O with CD_3CN) of FPM-p(SS-*co*-PEGMA)-FPM 183

Figure 4-14. ^{1}H NMR (400 MHz, D_2O with CD_3CN) of MAL-p(SS-*co*-PEGMA)-MAL.....184

Figure 5-1. Incorporation of polymers in therapeutics 191

Figure 5-2. ^{1}HNMR and IR data for the synthesis of oxime polymer, **6** 197

Figure 5-3. GPC traces showing the degradation of (a) PEG-hydrazone polymer **14** in DPBS, PB at pH 6, and serum free cell culture medium and (b) PEG-oxime polymer **13** in DPBS and PB at pH 6 after 12 month 201

Figure 5-4. Cell viability assay performed on both 3T3 fibroblasts and human dermal fibroblasts for both (a) PEG-AO monomers and (b) PEG-hydrazine monomers.....202

Figure 5-5. ^{1}H NMR (400 MHz, CD_2Cl_2) of TEG-phthalimide (**1**).....209

Figure 5-6. ^{13}C NMR (400 MHz, CD_2Cl_2) of TEG-phthalimide (**1**) 210

Figure 5-7. ^{1}H NMR (400 MHz, CD_2Cl_2) of PEG-phthalimide (**7**) 211

Figure 5-8. ^{13}C NMR (400 MHz, CD_2Cl_2) of PEG-phthalimide **(7)** 212

Figure 5-9. ^{1}H NMR (400 MHz, CD_2Cl_2) of TEG-AO (**2**).....213

Figure 5-10. ^{1}H NMR (400 MHz, CD_2Cl_2) of PEG-AO (**8**).....214

Figure 5-11. ^{13}C NMR (400 MHz, CD_2Cl_2) of PEG-AO (**8**).....215

Figure 5-12. ^{1}H NMR (400 MHz, CD_2Cl_2) of TEG-acetal (**4**) 216

Figure 5-13. ^{13}C NMR (400 MHz, CD_2Cl_2) of TEG-acetal (**4**) 217

Figure 5-14. ^{1}H NMR (400 MHz, CD_2Cl_2) of oxime polymer (**6**) 218

Figure 5-15. ^{1}H NMR (400 MHz, CD_2Cl_2) of PEG-hydrazide (**9**).....219

Figure 5-16. ^{13}C NMR (400 MHz, CD_2Cl_2) of PEG-hydrazide (**9**).....220

Figure 5-17. ^{1}H NMR (400 MHz, CD_2Cl_2) of oxime polymer (**13**) 221

Figure 5-18. ^{13}H NMR (400 MHz, D_2O) hydrazone polymer (**14**) 222

LIST OF TABLES

Table 1-1. Examples of some of the biological properties of heparin 3

Table 1-2. Structures and biological activities of polyaromatic anionic heparin-mimicking compounds 12

Table 1-3. Heparin mimicking glycopolymers and their biological applications.....23

Table 1-4. Heparin mimicking polysulfonated compounds and their biological applications 31

Table 1-5. Heparin mimicking ionomers and their biological applications.....46

Table 3-1. p(SS-*co*-PEGMA) library with varying styrene sulfonate monomer incorporation ..120

Table 3-2. p(SS-*co*-PEGMA) library with varying sizes and 81% SS incorporation.....128

Table 5-1. Degradation results comparing GPC of polymers in degradation study to polymers before degradation study.....200

LIST OF SCHEMES

Scheme 2-1. (a) Synthesis of xanthate CTA. (b) RAFT polymerization of pVS polymer and (c) protein polymer conjugation of pVS to FGF2 72

Scheme 2-2. (a) Synthesis of CTA, (b) RAFT polymerization of p(SS-*co*-PEGMA) to yield macro CTA, (c) subsequent RAFT polymerization to yield block copolymer p(SS-*co*-PEGMA)-*b*-VS, and (d) protein polymer conjugation to FGF2 conducted on a heparin column 74

Scheme 3-1. Synthesis of heparin mimicking polymer-protein conjugate, FGF2-p(SS-*co*-PEGMA). (a) Polymerization of p(SS-*co*-PEGMA) via RAFT polymerization. (b) Conjugation of p(SS-*co*-PEGMA) to FGF2 via disulfide exchange..... 119

Scheme 4-1. Modification of p(SS-*co*-PEGMA) to contain two divinyl sulfone end groups for protein conjugation. (a) Reduction of trithiocarbonate and capping with PDS-methacrylate followed by (b) TCEP reduction of disulfide bonds in the presence of excess divinyl sulfone .. 161

Scheme 4-2. Synthesis of symmetrical DVS-p(SS-*co*-PEGMA)-DVS. (a) Synthesis of a bis-trithiocarbonate CTA. (b) Polymerization of p(SS-*co*-PEGMA) by RAFT polymerization. (c) Reduction of trithiocarbonate and capping with PDS-methacrylate followed by (d) TCEP reduction of disulfide bonds in the presence of excess divinyl sulfone. (e) Conjugation of the bis-DVS polymer to FGF2 through disulfide exchange 163

Scheme 4-3. Synthesis of a bis-maleimide p(SS-*co*-PEGMA) and dimerization of FGF2. (a) Synthesis of bis-furan protected maleimide CTA. (b) RAFT polymerization of SS and PEGMA to yield FPM-p(SS-*co*-PEGMA)-FPM. (c) Deprotection of the maleimide to unveil a protein reactive polymer. (d) Dimerization of FGF2 using MAL-p(SS-*co*-PEGMA)-MAL 165

Scheme 5-1. Reversible formation of oxime and hydrazone bonds 194

Scheme 5-2. Synthesis of monomers for degradable PEG. (a) Synthesis of TEG-phthalimide, **2**, and PEG-phthalimide, **7**, by Mitsunobu reaction. (b) Deprotection to yield and TEG-aminooxy, 2, and PEG-aminooxy **8**.....194

Scheme 5-3. Attempted syntheses of TEG-aldehyde via (a) PCC oxidation (b) and Pfitzner-Moffat 195

Scheme 5-4. Synthesis of (a) TEG-acetal, **4**, and (b) deprotection to yield TEG-aldehyde, **5**....196

Scheme 5-5. Synthesis of oxime polymer **6** from TEG-aminooxy **2** and diacetyl 196

Scheme 5-6. Synthesis of PEG-dihydrazide 9 198

Scheme 5-7. Step-growth polymerization of (a) oxime polymer **10** and (b) hydrazone polymer **11**. 198

Scheme 5-8. Step-growth polymerization to synthesize oxime polymer (a) using TEG-AO or PEG-AO monomers to yield polymers **12** and **13**, respectively, and (b) synthesis of hydrazone polymer **14**.....199

LIST OF ABBREVIATIONS

AA	Acrylic acid
AD	Alzheimer's disease
AIBN	Azobis(isobutyronitrile)
AO	Aminooxy
apoE	Apolipoprotein E
APTT	Activated partial thromboplastin time
ATIII	Antithrombin III
ATRP	Atom-transfer radical polymerization
AU	Absorption units
BA	Butyl acrylate
BACE-1	B-site APP cleaving enzyme-1
BBE	Bovine brain extract
BDDS	4,4'-Diamino-2,2'-biphenyldisulfonicacid disodium salt
Bipy	2,2'-Bipyridine
BMA	Butyl methacrylate
BMP-2	Bone morphogenic protein-2
BSA	Bovine serum albumin
C NMR	Carbon nuclear magnetic resonance
CD31	Cluster of differentiation 31
CMDBS	Carboxymethyl benzylamide sulfonate dextrans
CMP	Cyanoxyl mediated polymerization

CTA	Chain transfer agent
D-PBS	Dulbecco's phosphate-buffered saline
DCM	Dichloromethane
DIAD	Diisopropyl azodicarboxylate
DMAP	Dimethyl aminopyridine
DMF	Dimethylformamide
DMSO	Dimethyl sulfoxide
DP	Degree of polymerization
DPBS	Dulbecco's phosphate buffered saline
DS	Degree of sulfonation
DS	Dextran sulfate
DTT	Dithiothreitol
ECM	Extracellular matrix
EDC	1-Ethyl-3-(3-dimethylaminopropyl) carbodiimide
EDL	Extensor digitorum longus
EDTA	Ethylenediaminetetraacetic acid
EGF	Epidermal growth factor
EGM	Endothelial growth medium
ELISA	Enzyme linked immunosorbent assay
EPR	Enhanced permeation and retention
ESI	Electron spray ionization
EtOH	Ethanol
FDA	Food and drug administration

FGF1	Fibroblast growth factor 1
FGF2	Fibroblast growth factor 2
FGFR	Fibroblast growth factor receptor
FPLC	Fast protein liquid chromatography
FPM	Furan protected maleimide
FRP	Free radical polymerization
f_{SS}	Mole fraction of SS in comonomer solution
F_{SS}	Mole fraction of SS in copolymer
GAG	Glycosaminoglycan
GEMA	Glucosyloxyethyl methacrylate
GPC	Gel permeation chromatography
H NMR	Proton nuclear magnetic resonance
HB-EGF	Heparin binding-epidermal growth factor
HCII	Heparin cofactor II
HDF	Human dermal fibroblasts
HDI	Hexamethylene diisocyanate
HMDI	Methylene bis(4-cyclohexyl isocyanate)
HPLC	High performance liquid chromatography
HS	Heparan sulfate
HUVEC	Human umbilical vein endothelial cells
IL-3	Interleukin 3
IPDI	Isophorone diisocyanate
IR	Infrared spectroscopy

kDa	KiloDalton
LMWH	Low molecular weight heparin
MA	Methacrylic acid
MADIX	Macromolecular design by interchange of xanthates
MAG	2-Methacrylamide glucopyranose
MAL	Maleimide
MDEAPS	N,N-bis (2-hydroxyethyl) methylamine ammonium propane sulfonate
MDI	Methylene bis(p-phenyl isocyanate)
MeOH	Methanol
mESCs	Mouse embryonic stem cells
MMA	Methyl methacrylate
M_n	Number average molecular weight
MW	Molecular weight
MWCO	Molecular weight cut off
NA	Not available/not reported
NIH	National institute of health
NMP	Nitroxide-mediation polymerization
p(SS-*co*-PEGMA)	poly(sodium 4-styrenesulfonate-c-poly(ethylene glycol) methyl ether methacrylate)
p(SS-*co*-PEGMA)-*b*-VS	poly(sodium 4-styrenesulfonate-c-poly(ethylene glycol) methyl ether methacrylate)-block-vinyl sulfonate
PAGE	polyacrylamide gel electrophoresis

pAHPS	poly(sodium 1-allyloxy-2-hydroxypropyl sulfonate)
pAMPS	poly(2-acrylamido-2-methyl-1-propanesulfonic acid
pAS	poly(anetholesulfonic acid)
PB	Phosphate buffer
PCC	Pyridinium chlorochromate
pCL	poly(caprolactone)
PDB	Protein database
PDGF	Platelet derived growth factor
PDS	Pyridyl disulfide
PDSMA	Pyridyl disulfide methacrylate
PECAM-1	Platelet endothelial cell adhesion molecule 1
PEG	poly(ethylene glycol)
PEGMA	poly(ethylene glycol) methyl ether methacrylate
PF4	Platelet factor 4
pGA	poly(glutamic acid)
PPO	poly(propylene glycol)
PPP	Platelet poor plasma
pSPM	poly(potassium 3-sulfopropyl methacrylate)
pSS	poly(styrene sulfonic acid)
PT	Prothrombin time
PTMO	poly(tetra-methylene oxide)
PVP	polyvinyl pyrrolidone
pVS	poly(vinyl sulfonic acid)

RAFT	Reversible addition-fragmentation chain transfer
RALS	Right angle light scattering
RANTES	Regulated on activation, normal T cell expressed and secreted
RGTA	ReGeneraTing Agents
ROMP	Ring-opening metathesis polymerization
ROP	Ring opening polymerization
r_{PEGMA}	Reactivity ratio for PEGMA
r_{SS}	Reactivity ratio for SS
SDS	Sodium dodecyl sulfate
SEM	Standard error of the mean
SG	Step growth
sLe^X	Sialyl Lewis X
SMC	Smooth muscle cell
SS	Styrene sulfonate
TCEP	Tris(2-carboxyethyl) phosphine hydrochloride
TDI	Toluene 2,4-diisocyanate
TEG	Triethylene glycol
TGF	Transforming growth factor
THF	Tetrahydrofuran
TMB	3,3',5,5'-tetramethylbenzidine
ULMWH	Ultralow molecular weight heparin
V501	4,4′-Azobis(4-cyanovaleric acid)

VEGF	Vascular endothelial growth factor
VP	Vinylpyrrolidone

ACKNOWLEDGEMENTS

Without the help and support from these people in some way, the completion of this dissertation would not have been possible. I would first like to thank Heather Maynard, for her invaluable support and encouragement over the past 5 years. Her creativity and innovative outlook propelled my research forward. Thank you, Heather, I am incredibly grateful for your one of a kind mentorship and will always be proud to call myself a Maynard Lab member. I would also like to thank the other members of my Doctoral Committee, Timothy Deming and Daniel Kamei, for their guidance, feedback, and involvement throughout this process. Additionally, I thank David Goode for his mentorship during my undergraduate studies and for helping to provide the foundation I needed to be successful in my graduate research. I also thank Adam Kiefer, Kevin Bucholtz, Kathryn Kloepper, and David Goode for sparking my interest in chemistry. Without you I would not be in this amazing field today.

In addition to the mentorship I received from faculty, I would like to thank Maynard Group members, past and present, for being amazing colleagues and offering advice and support throughout my journey. I thank Erhan Bat, whose guidance and dedication early in my graduate studies set me on a great path. I thank Natalie Boehnke, without whom my transition to grad school would not have been as easy. I thank Emma Pelegri-O'Day for being the best office mate I could ask for and whose friendship helped me through. I am grateful for the many insightful conversations we had in 4230 and will miss being able to simply turn around to ask questions. I thank Kathy Nguyen for her mentorship, friendship, and collaboration (Chapters 1 and 2). I thank Caitlin Decker for her collaboration on Chapter 4 as well as always keeping things fun around the office. I thank Jeong Hoon Ko (JK) for his knowledgeable advice and amazing friendship. I thank

Marco Messina for his input and ability to always provide a good laugh or a listening ear. I would also like to thank Kathryn Mansfield, Kyle Tamshen, and Priera Panescu for encouraging conversations and helpful advice. Additionally, I would like to thank June Lee, Nic Matsumoto, and En-Wei Lin for showing me the ropes and Maltish Lorenzo, Peter Nauka, Jonghan Lee (Chapter 2), Madeline Gelb, Doug Rose, and Neil Forsyth for being great colleagues.

Last but certainly not least I would like to thank my family. A special thanks to my mother, Natalie, and brother, Greg, for encouraging my interest in science at an early age (sorry about the many frogs). I thank the best father I could ask for, Peter, for his continued love and support throughout the duration of my education. I would also like to thank Eric, for his love and undying support throughout this process. Thank you for the countless late nights studying and for being there with me during the hardest parts of my graduate studies, and celebrating with me through my achievements. You are my rock. I also thank Gram and Pop for instilling educational discipline and skills for success at a very young age. I thank my brothers Peter and Brian for their encouragement and support and for providing me with a good laugh when it was needed most. Additionally, I would like to thank the Raftery's for taking an interest in my success and for their encouragement and support over the last few years.

The research described in this dissertation is supported by the National Institutes of Health (R01 EB136774). I also thank the NIH Chemistry Biology Interface Training Fellowship (T32 GM 008496) as well as the UCLA Chemistry and Biochemistry Department for funding.

[†]Chapter 1 is reproduced with permission from Paluck, S.J.; Nguyen, T.H.; Maynard, H.D. Heparin-Mimicking Polymers: Synthesis and Biological Applications. *Biomacromolecules* **2016**, *17*, 3417-3440. 10.1021/acs.biomac.6b01147. Copyright 2016 American Chemical Society. Chapter 2 is reproduced with permission from Paluck, S.J.; Nguyen, T.H.; Lee, J.P.; Maynard,

H.D. A Heparin-Mimicking Block Copolymer Both Stabilizes and Increases the Activity of Fibroblast Growth Factor 2 (FGF2). *Biomacromolecules* **2016**, *17*, 3386-3395. 10.1021/acs.biomac.6b01182. Copyright 2016 American Chemical Society. Portions of Chapter 3 are reproduced from the submitted manuscript Paluck, S.J.; Maynard, H.D. Structure Activity Relationship of Heparin Mimicking Polymer p(SS-*co*-PEGMA): Effect of Sulfonation and Polymer Size on FGF2-Receptor Binding. Portions of Chapter 4 are reproduced with permission from Decker, C.G.; Wang, Y.; Paluck, S.J.; Shen, L.; Loo, J.A.; Levine, A.J.; Miller, L.S.; Maynard, H.D. *Biomaterials* **2016**, *81*, 157-168.

VITA

Education

2012	B.S. Chemistry	Mercer University, Macon Georgia
2014	M.S. Chemistry	University of California, Los Angeles

Research Experience

2012-2017	Graduate Student Researcher: University of California, Los Angeles
2009-2012	Undergraduate Researcher: Mercer University, Macon, Georgia

Publications

Paluck, S.J.; Maynard, H.D. *Polym. Chem*. Structure Activity Relationship of Heparin-Mimicking Polymer p(SS-*co*-PEGMA): Effect of Sulfonation and Polymer Size on FGF2 Receptor Binding *Submitted*, **2017**.

Pelegri-O'Day, E.M.; Paluck, S.J.; Maynard, H.D. Substituted Polyesters by Thiol-ene Modification: Rapid Diversification for Therapeutic Protein Stabilization. *J. Am. Chem. Soc.* **2017**, *139*, 1145-1154.

Paluck, S.J.; Nguyen, T.H.; Lee, J.P.; Maynard, H.D. A Heparin-Mimicking Block Copolymer Both Stabilizes and Increases the Activity of Fibroblast Growth Factor 2 (FGF2). *Biomacromolecules*. **2016**, *17*, 3386–3395. *Paper chosen for the October 2016 cover of *Biomacromolecules*.

Paluck, S.J.; Nguyen, T.H.; Maynard, H.D. Heparin Mimicking Polymers and Their Biological Applications. *Biomacromolecules*. **2016**, *17*, 3417–3440.

Vanparijs, N.; Nuhn, L.; Paluck, S.J.; Maynard, H.D.; De Geest, B.G. Core and Shell Reactive Nanogels for Protein Conjugation via a Combination of RAFT Polymerization and Vinyl Sulfone Post-Modification. *Nanomedicine: Nanotechnology, Biology and Medicine.* **2016**, 20, 2631-2645.

Mancini, R.J.; Paluck, S.J.; Bat, E.; Maynard H.D. Encapsulated Hydrogels by E-Beam Lithography Used for Enzyme Cascade Reactions. *Langmuir*. **2016**, *32(16),* 4043-4051.

Lorenzo, L.M.; Decker, C.G.; Kahveci, M.U.; Paluck, S.J.; Maynard, H.D. Homodimeric Protein–Polymer Conjugates via the Tetrazine–*trans*-Cyclooctene Ligation. *Macromolecules*, **2016**, *49*, 30-37.

Decker, C.G.; Wang, Y.; Paluck, S.J.; Shen, L. Loo, J.A.; Levine, A.J.; Miller, L.S.; Maynard, H.D. Fibroblast Growth Factor 2 Dimer with Superagonist Activity Improves Wound Healing. *Biomaterials.* **2016**, 81, 157-168.

Nguyen, T.H.; Paluck, S.J.; McGahran, A.J.; Maynard, H.D. Poly(vinyl sulfonate) Facilitates bFGF Induced Cell Proliferation. *Biomacromolecules*, **2015**, *16(9),* 2684-2692.

Chapter 1

Heparin-Mimicking Polymers:

Synthesis and Biological Applications[†]

1.1 Introduction to Heparin

Heparin is a linear, highly sulfated glycosaminoglycan produced by mast cells. Its chemical structure consists of repeating monomeric disaccharides of uronic acid and glucosamine in a 1,4-linkage (Figure 1-1), and the three-dimensional structure exists primarily in a helical form.[1] On average, there are 2.7 sulfate groups per disaccharide monomer, which when combined gives heparin a total negative net charge of approximately -75.[2-4] Since heparin has an average molecular weight of 15 kDa, this property gives heparin the highest negative charge density of any known naturally-derived biomolecule.[3] The size of heparin varies greatly between tissues with molecular weights ranging from 5 – 40 kDa with structural variations such as amount of sulfation, epimerization and degree of acetylation. Heparin and heparan sulfate (HS) are similar due to their high degree of sulfation, however heparan sulfate differs from heparin in that it is a proteoglycan presented on the surface of virtually all native cells and is significantly less sulfated than heparin.[1]

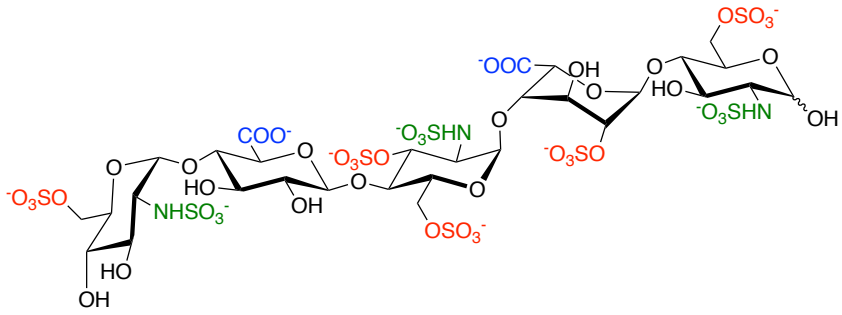

Figure 1-1. Chemical structure of a heparin pentasaccharide showing various repeats containing sulfate (red), sulfamate (green), and carboxylate (blue) groups.

Heparin is most well-known for its role in blood clotting, but also plays a role in other cellular functions such as cell adhesion, proliferation, differentiation, migration, and inflammation (Table 1-1).[5-7] Heparin interacts with proteins primarily through electrostatic interactions between its sulfate and carboxylate groups with clusters of positively charged amino acid residues, such as arginine and lysine, in the heparin binding sites of the biomolecules. In addition to electrostatic interactions, heparin-binding domains also contain amino acids such as asparagine and glutamine that can participate in hydrogen bonding with heparin. These interactions help stabilize proteins, regulate their affinity for cell receptors and aid in extracellular matrix (ECM) assembly.[8]

Table 1-1. Examples of some of the biological properties of heparin

Biological Property of Heparin	**Interactions Leading to Biological Outcome**
Anticoagulant	Binds fibrin, antithrombin, factor Xa, factor IXa, thrombin, heparin cofactor II, and protein C inhibitor
Protein Stabilizer	Forms strong electrostatic interactions with many heparin-binding proteins such as FGF1 and FGF2, protecting them from deactivation
Anti-Inflammatory	Binds to selectins on leukocytes, inhibiting their interaction with sialyl Lewis X (sLe^x), thus preventing interactions with endothelial cells Binds and neutralizes proteins, enzymes, chemokines, and cytokines that activate or are released from inflammatory cells
Alterations in cellular migration and proliferation	Binds various growth factors involved in cell growth and migration, such as FGFs, VEGF, and PDGF, thus, altering their ability to bind with receptors on the cell surface

While there are over 400 heparin binding proteins,[9] research has mainly focused on the serine protease inhibitor antithrombin III (ATIII), as well as proteins including acidic fibroblast growth factor (FGF1), basic fibroblast growth factor (FGF2), vascular endothelial growth factor (VEGF), heparin binding-epidermal growth factor (HB-EGF), platelet-derived growth factor

(PDGF), and transforming growth factor (TGF).[4,10] Heparin binding motifs, the clusters of positively charged amino acids called heparin binding domains, have been defined on these proteins by molecular modeling and crystallographic studies.[11-13] Other heparin binding proteins include adhesion proteins, chemokines like platelet factor 4 (PF4), and lipid or membrane binding proteins such as apolipoprotein E (apoE).[4]

Heparin itself is currently Food and Drug Administration (FDA) approved for clinical uses, such as for the treatment of deep vein thrombosis and pulmonary embolism, making it an attractive platform for new applications. Heparin-based materials are thus widely studied for use in tissue engineering, wound healing, cell replacement therapies, angiogenic treatments and encapsulation and release of proteins.[14] Since the realization of its importance and necessity as an anticoagulant a century ago, heparin has been exploited most heavily in the clinic for this purpose, yet the only sources of heparin are animal tissues. This raises the concern of the possible risk of virus contamination and adverse effects.[15,16] Heparin also has notable variable patient-dependent dose-response.[17-19] Another issue with using heparin in therapeutics is that heparin can be degraded or desulfated *in vivo* by heparinases and other enzymes, which is not necessarily harmful, but could result in unwanted loss of bioactivity. Researchers also found that patients prescribed longer-term treatments of unfractionated heparin were at increased risk for negative clinical effects of heparin induced thrombocytopenia (low platelet count).[20] At first, low molecular weight heparins (LMWH) with an average molecular weight of 6 kDa were used because of their more predictable pharmacokinetics as well as their ability to reduce unwanted side effects.[21] Oligomers of heparin, termed ultralow molecular weight heparins (ULMWH), were also utilized and preferred over unfractionated heparin. However, due to the high cost and difficult synthesis of producing ULMWH and LMWH new synthetic routes had to be explored as

alternatives to heparin therapies.[22] In addition, heparin is extremely heterogeneous in structure with different binding motifs leading to a broad range of biological activities which can lead to side effects.[8] All of the downfalls of heparin and oligoheparins, along with batch-to-batch variability, have inspired researchers to study synthetic alternatives. There are a range of synthetic mimics such as small molecules,[23,24] peptides,[25-28] polysaccharides[29,30] and polymers.[29,31] A few of these are even approved for clinical use, including small molecule heparin mimics Suramin® and Carafate®, the first of which is an antiparasitic and has also been studied as an anticancer drug; the latter is used to treat intestinal ulcers.[32,33] In this chapter, the main focus will be on synthetic polymer mimics.

1.2 Heparin Mimicking Polymers

1.2.1 Introduction to Heparin-Mimicking Polymers

Polymeric heparin-mimics can provide better control over structure, sulfation and purity. It is also possible to obtain narrow molecular weight dispersities. The ability to tune parameters such as molecular weight and sulfation percentage allows for controlled tuning of binding affinity and other factors. This can in turn provide for more specific interactions with receptors and proteins. In addition, heparin-mimicking polymers typically resist degradation/desulfation by heparinases, allowing for increased longevities in the body; this can be an advantage or a disadvantage depending on the application. Preparing heparin-mimics by synthetic means also permits incorporation of reactive handles, which allows for easier functionalization and conjugation of the polymers. Thus, many groups have focused on the synthesis of polymeric heparin mimics as a way to improve current heparin based therapies. Research has shown that some of these synthetic heparin-mimics are superior to heparin in terms of purity and resistance

to degradation, while still providing desired effects. This chapter provides an introduction for newcomers in the field of heparin-mimicking polymers. Heparin mimicking hydrogels have been reported elsewhere.[34] Surfaces and membranes modified with heparin and heparin mimicking polymers have recently been reviewed[29,35-38] and reviews on glycosaminoglycans (GAGs), in general, have been published.[29,39] In this chapter, an example of semisynthetic polymers and many examples of synthetic polymers are highlighted, focusing mostly on soluble mimics (overview provided in Figure 1-2). For the semisynthetic polymers, we focus on one class, derivatives of dextran, which have been the most extensively studied. Semi-synthetic polymers based on other naturally occurring polysaccharides such as alginate,[40-42] cellulose,[43,44] and chitosan[45-47] that have been sulfated for use as heparin mimics will not be reviewed here. Applications of the polymers are discussed where appropriate, as well as future directions for heparin mimicking polymers.

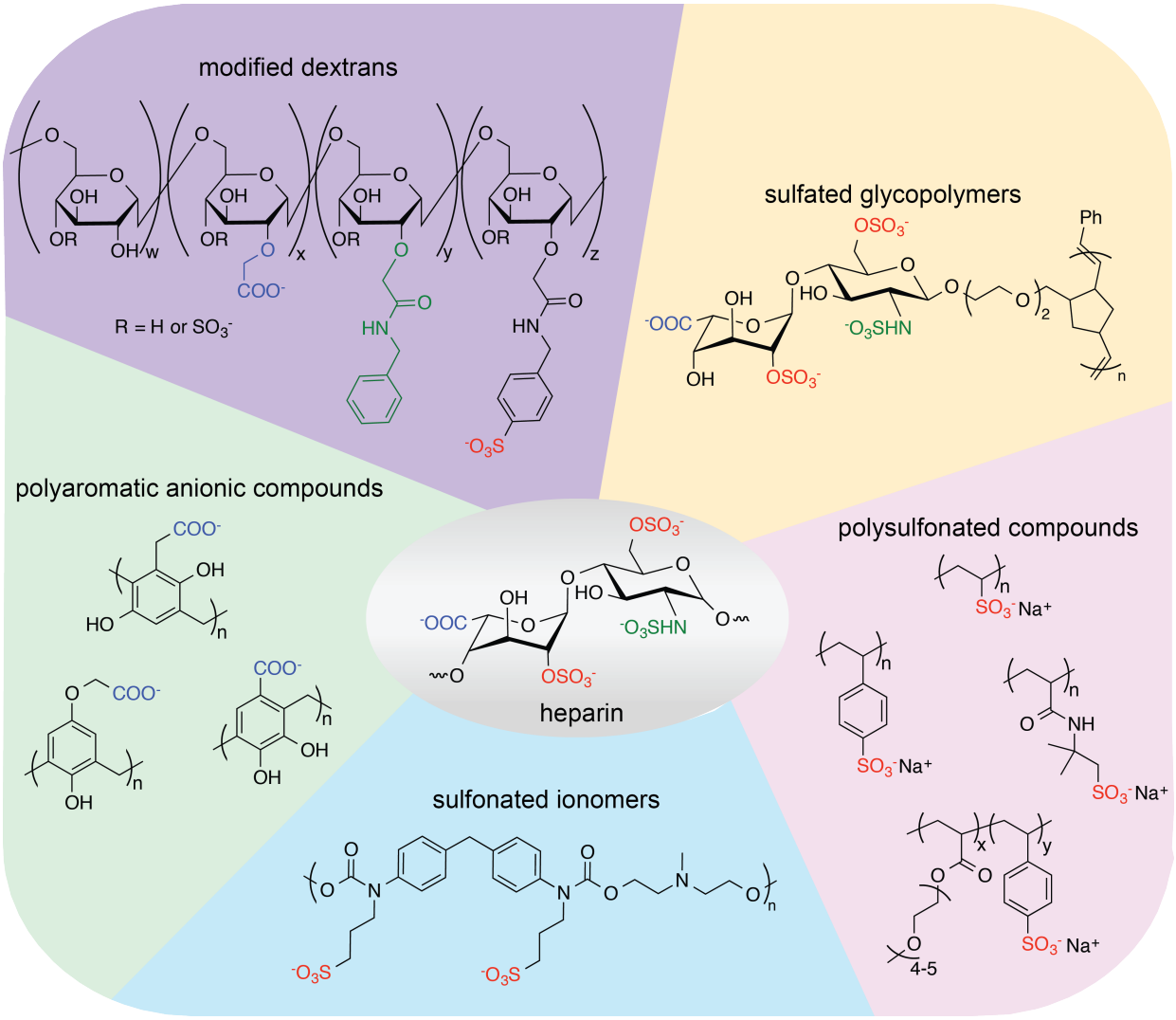

Figure 1-2. Examples of heparin-mimicking polymers discussed in this chapter, including modified dextrans, sulfated glycopolymers, polysulfonated compounds, sulfonated ionomers, and polyaromatic anionic compounds.

1.2.2 Carboxymethyl Benzylamide Sulfonate Dextrans (CMDBS)

The first semisynthetic heparin-mimicking polymers reported were functionalized dextrans, called carboxymethyl benzylamide sulfonate dextrans (CMDBS Figure 1-3).[48] Dextran, a complex branched glycan, was chosen as the polymeric base for these mimics for

many reasons including its approved used in the clinic as a plasma volume expander, as well as its ease of modification. Mauzac and Jozefonvics reported the modification of dextrans with the addition of benzyl sulfonates and benzyl amines to form soluble CMDBS polymers.[49] The synthesis of the CMDBS polymers was achieved by first carboxymethylating (CM) the hydroxyl groups on dextran (D). Next, benzylamidation (B) was performed and subsequent sulfonation (S) afforded the CMDBS polymers (Figure 1-3) in three reaction steps, and varying degrees of modification were achieved by repeating reaction steps multiple times. It is important to note that the dextrans can be modified at carbon 1 and/or carbon 6.

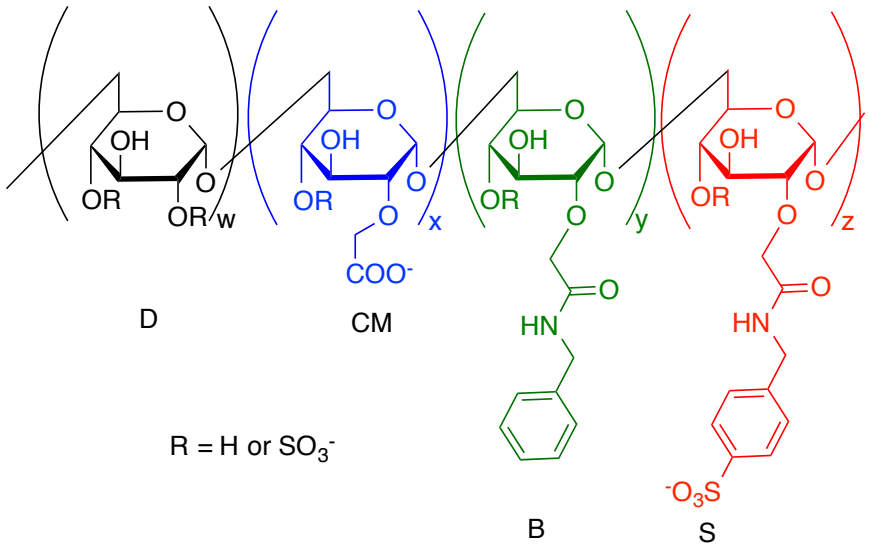

Figure 1-3. Chemical structure of carboxymethyl benzylamide sulfonate dextrans (CMDBS).

Initially, the polymers were studied for their anticoagulant activity by measuring the clotting time of platelet-poor plasma (PPP) in the presence of CMDBS polymers or heparin. The authors found that changes in the overall percentage of carboxylic and benzyl sulfonate groups had an effect on anticoagulant activity; specifically, CM content greater than 40% was required to exhibit anticoagulant activity. When the CM content was maintained at 47.5%, antithrombic

activity increased exponentially as S content increased.[49] The effect of molecular weight on anticoagulant activity was tested in CMDBS polymers with molecular weights ranging from 5.5 to 190 kDa. The anticoagulant activity of the dextran derivatives increased with increasing molecular weight up to 40 kDa.[50] Anticoagulation effects of these polymers are likely due to the distribution of carboxylic and sulfonate groups on the dextran backbone. It is important to note that, while the CMDBS polymers were able to induce clotting, they exhibited much lower antithrombic activity than heparin itself.

In addition to its study as an anticoagulant, the CMDBS family also attracted much attention for its potential as a heparin-mimicking material in other applications. Biological activities reported include anti-inflammatory activity, antibacterial and antiviral activities, regenerating activity, modulation of vascular cell proliferation, and anti-proliferative and anti-tumoral activity.[31] The capability of the functionalized dextrans to mimic the role of heparin in skin,[51,52] bone,[53-58] colon,[59] cornea,[60] and muscle[61-64] have also gained a lot of attention. CMDBS polymers were named "ReGeneraTing Agents" (RGTA) for their ability to help regenerate various types of tissues. The polymers were found to interact with heparin-binding growth factors; for example, in 1989 Tardieu and colleagues reported that a member of the CMDBS family with 82% CM, 6% B, and 5.6% S potentiated the mitogenic activity of FGF1 to Chinese hamster fibroblast cells similar to heparin when 20 times higher concentration of the CMDBS was used.[65] In terms of growth factor protection, a CMDBS polymer with 82% CM, 23% B, and 13% S was shown to protect FGF2 against pH and heat stressors more effectively than heparin.[66] However, the same CMDBS polymer was not as effective at stabilizing FGF1 compared to heparin. This is likely due to the polymer having different binding affinities for each individual protein.

CMDBS polymers have also been tested *in vivo* for functions in tissue regeneration. Meddahi *et al.* used RGTA11 polymer comprising of 110% CM, 2.5% B, and 36.5% S to promote rat extensor digitorum longus (EDL) muscle regeneration post crushing via a single systemic administration (where 200% modification signifies complete modification at both carbon 1 and carbon 6).[62] Mice receiving an injection of RGTA11 polymer displayed increased muscle regeneration compared to mice receiving no treatment. Furthermore, RGTA11 was found to promote enhanced proliferation and migration in endothelial cells as well as endothelialization of vascular prostheses in combination with FGF2 *in vitro* when compared to FGF2 alone.[67]

Papy-Garcia and co-workers reported an improved synthesis and characterization of another member of the family, RGTA OTR4120, in 2005.[68] The compound was prepared by carboxymethylation and subsequent *O*-sulfonation of T40 dextran in the presence of the acid scavenger 2-methyl-2-butene to reduce glycosidic bond cleavage. RGTA OTR4120 was shown to enhance VEGF-induced human umbilical vein endothelial cell (HUVEC) proliferation and migration *in vitro* and VEGF-induced angiogenesis in a chick embryo assay.[69] Additionally, the positive dermal effects of RGTA OTR4120 have been demonstrated in various animal models including necrotic skin ulcers in mice,[70] burn wounds in rats,[71] surgical excision wounds in rats,[72,73] dermal ischemia ulcers in rats,[74] and diabetes-impaired wounds in rats.[75] To summarize, RGTAs have been extensively utilized, and additional applications not discussed here have been recently reviewed elsewhere.[76] The polymers have also been employed in the clinic: for example, RGTA OTR4120 is marketed in France under the name CACIPLIQ20® to treat chronic wounds.

Dextran derived CMDBS polymers provided the initial groundwork toward new polymeric heparin mimics and also gained approval for use in humans. They have a wide range of bioactivities similar to heparin and also many biological applications. However, they do not

overcome the issue of heterogeneity unless fractionated. Also, the dextrans from which CMDBS polymers are derived are isolated from animal tissues or bacteria, and therefore are not purely synthetic heparin mimics. The modification of these materials can also be tedious and can introduce additional heterogeneity. Thus, researchers continued to look for alternative solutions.

1.2.3 Polyaromatic Anionic Compounds

Regan and colleagues reported a series of non-sulfated heparin-mimicking polymers (Table 1-2).[77] These polyaromatic compounds were synthesized from the acid-catalyzed polymerization of various anionic group-substituted phenols with formaldehyde. Unlike CMDBS polymers, the polyaromatic anionic compounds were not necessarily sulfated and some relied solely on carboxylic acids for their negative charge density. The group tested these polymers for their heparin-mimicking ability by using NIH3T3 mouse fibroblast cells transfected with FGF2 conjugated to a signal peptide sequence to afford so-called spFGF2 cells; these cells were studied because of their potential relation to cancer.[78] Specifically, the incorporation of cells with spFGF2 causes FGF2 to be secreted resulting in transformation of the cells in culture and tumorgenicity in animals.[79] However, molecules such as heparin that bind FGF2 had been shown to interfere with this process, thus, reverting the phenotype. Among the polymers tested, poly(4-hydroxyphenoxyacetic acid) named RG-13577 (Table 1-2) was first identified as the most worthy candidate of its class for its ability to revert the FGF2-mediated transformed phenotype of these tumorigenic cells.[78] Furthermore, Benezra and co-workers reported that RG-13577 mimicked heparin in many other aspects including its ability to inhibit proliferation of vascular smooth muscle cells (SMCs) induced by FGF2, efficiently releasing surface-bound FGF2, and inhibiting heparanase activity.[80,81] Additionally, the compound exhibited only 1-10% of the anticoagulant ability of heparin suggesting that the polymer can be utilized for specific biological

purposes when anticoagulation is not desired.[77] RG-13577 has a lower molecular weight than heparin, and although polydisperse (2.53 dispersity) is not as heterogeneous as heparin.

Table 1-2. Structures and biological activities of polyaromatic anionic heparin-mimicking compounds.* (Modified with permission from reference 81; Copyright 2002 Wiley-Liss, Inc., John Wiley and Sons)

Polymer		Antiproliferative activity of Smooth Muscle Cells stimulated with			Release of ECM-bound FGF2	Heparanase inhibitory activity
		Thrombin 10^{-7} M	FGF2 2 ng/ml	Serum 10%		
RG-13525	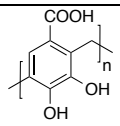	++	++	+++	+	++
RG-13527	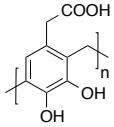	+++	++	+++	+++	+++
RG-13528	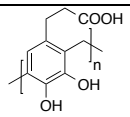	++	++	+	+++	++
RG-14444	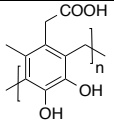	+	+	+	+	++++
RG-13576	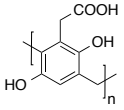	+++	++	++	+	+++

RG-13530	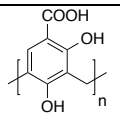	+++	++	+	+	++
RG-13519	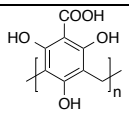	+++	++	+	+++	++
RG-13524	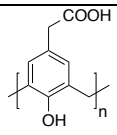	+	++	+	+	+
RG-13577	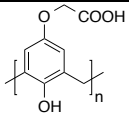	+++	+++	+++	++	+++

* The relative activity of each compound is presented as +, ++, +++, and ++++ representing a low (0–30%), medium (30–60%), high (60–90%), or almost complete (90–100%) inhibition of heparanase activity and SMC proliferation, or stimulated release of ECM-bound FGF2 expressed as percentage of the total ECM-bound FGF2. Note: In most cases, this polymerization will result in polymers with different structures and substitution patterns. Only one possible structure is drawn in each case.

Heparin and HS proteoglycan are well-known co-factors in growth factor-induced angiogenesis, a key event in cancer growth.[82] In contrast, heparin can also act as an anti-angiogenic factor depending on the concentration in HS-expressing cell lines by binding to growth factors such as FGF2 and preventing binding to FGFRs, thus, abrogating the vital formation of HS/FGF2/FGFR complex in many cell types.[83-85] Because of this, increasing interest has been focused on developing chemical structures that can turn off the angiogenic-promoting activity of heparin/HS in many diseases, including cancer. Miao et. al. found that

polyaromatic compounds, including RG-13577, inhibited heparin-mediated dimerization of FGF2 as well as binding of FGF2 to its receptor FGFR1, presumably by competitive binding.[86] RG-13577 completely inhibited FGF2-induced tyrosine phosphorylation of FGFR1 in cells where the heparan sulfate had been removed, compared to only partially in untreated cells, suggesting that the compound competed directly with HS for binding to FGF2. Furthermore, RG-13577 was shown to inhibit proliferation in both HS-expressing and HS-deficient cells in the presence of heparin. Microvessel formation was completely inhibited in the presence of 10-25 μg/mL of RG-13577, and this was reversible. Interestingly, the authors found that when up to 1 μg/mL of RG-13577 was incubated in the presence of 20 ng/mL of heparin, increased binding of FGF2 to its receptor was observed. Even though RG-13577 has received attention for its inhibitory activity in cells that cause angiogenesis, arteriosclerosis, glomerulosclerosis, and spinal chord inflammation,[87-91] these data at lower concentrations suggested that RG-13577 could be further investigated as candidate for regenerative therapy in combination with heparin.

Despite the many positive features of this class of materials, there are some drawbacks to these non-sulfated polyanionic polymers including lack of control over degree of negative charges. It is well-known that location of negative charges in heparin is important for its function and this kind of control cannot be obtained with these polymers. Additionally, the polymers are often chemically ill defined due to the use of acid catalyzed condensation polymerization, which can allow for functionalization at more than one position on the phenyl ring, and also, the polymers are typically polydisperse in molecular weight. Thus, researchers continued to explore other options.

1.2.4 Sulfated Synthetic Glycopolymers

The heterogeneous polysaccharide backbone in heparin provides specific structural motifs that have different interactions and bioactivities. Thus, the isolation of these oligosaccharide units is desirable. Total synthesis of these structural motifs is possible, but extremely cumbersome and low yielding.[92] Even though LMWH (average MW 6 kDa) and synthetic ultralow-molecular-weight heparin (average MW 1.5 kDa) have been developed to overcome problems associated with unfractionated heparin such as heparin-induced thrombocytopenia, their syntheses are also difficult and the structures are still heterogeneous.[20,93] Methods allowing for the assembly of minimal units to form multivalent heparin-mimicking glycopolymers are more straightforward and could be used for similar purposes. In fact, the minimal saccharide sequences required for heparin binding to proteins, such as ATIII, FGF1, and FGF2, are known and could be useful for rationally designing these heparin mimics.[94-96] Glycopolymers provide tunable multivalent interactions with proteins and other biological targets, and thus are a great starting point for GAG mimics. Indeed, glycopolymers with hydrocarbon backbones and pendant sulfated mono- or disaccharide units have been used as heparin-mimics. Sulfated glycopolymers have also been employed as mimics of other GAGs such as chondroitin sulfate and dermatan sulfate.[29] Glycopolymers can be synthesized through multiple polymerization methods including free radical polymerization (FRP), reversible addition-fragmentation chain transfer (RAFT) polymerization, ring-opening metathesis polymerization (ROMP), and nitroxide-mediated radical polymerization (NMP); some of these methods allow for specific control over polymer structure, end group, and molecular weight.[39,97] Pendant saccharides can be modified with sulfate groups either before or after polymerization. Other types of heparin-mimicking glycopolymers such as dendrimers and branched polymeric

glycopolymers have been studied; however, herein we will focus on synthetic and linear sulfated glycopolymers mimicking heparin specifically, as summarized in Table 1-3.

Initially, heparin-mimicking glycopolymers were synthesized by first polymerizing neutral glycomonomers, followed by post-polymerization functionalization with sulfate. For example, glucosyloxyethyl methacrylate (GEMA) was polymerized via free radical polymerization to form polymers and hydrogels.[98,99] Subsequent sulfation with N,N-dimethylformamide/sulfur trioxide afforded poly(GEMA)-sulfate with degrees of sulfation ranging from 1.91 to 3.75 out of 4 available hydroxyl groups per monomer depending on the reaction time (Figure 1-4a).[100] Increasing doses of poly(GEMA)-sulfate and increasing degrees of sulfation resulted in prolonged coagulation of human blood similar or better than heparin. Controls were also studied. Sulfated synthetic polymers poly(styrenesulfonic acid) (pSS) and poly(vinylsulfonic acid) (pVS) were minimally effective at prolonging clotting times, while dextran sulfate (DS) (degree of sulfation = 1.0) was better than sulfated poly(GEMA). The results suggest that sulfated glycopolymers are somewhere in between the anticoagulation ability of non-sugar containing synthetic polymers and sulfated polysaccharides. The results may also bode well for use of pSS and pVS in applications where anticoagulation is not desired (discussion of these types of polymers is the focus of section 1.2.5). Akashi and co-workers went on to study the mechanism of poly(GEMA)-sulfate anticoagulation and found that inhibition of coagulation was due to the polymer forming an insoluble complex with fibrinogen, thus slowing fibrin polymerization.[101] This mechanism is different than heparin, which binds to ATIII activating it to bind to thrombin and other proteases, thus, stopping the blood clotting cascade.[9] In subsequent studies, the authors found that the anticoagulation properties of poly(GEMA)-sulfate were also due to the polymer having heparin cofactor II (HCII)-mediated, but not ATIII-

mediated, thrombin inhibition.[102] In addition, the polymers inhibited Tenase (Factor IXa, Factor VIIIa, calcium, and phospholipid complex), which is an activator of Factor X similar to dextran sulfate, but to a lesser extent than heparin.

In another example of post-polymerization sulfation, Ayres and co-workers synthesized sulfated glycopolymers through step growth polymerizations.[103] To do this, isopropylidene protected saccharide tetramers were synthesized with secondary amines on each end. The tetramers were then copolymerized with hexamethylene diisocyanate (HDI) via step growth polymerization to yield polymers with saccharide side chains. After polymerization, the isopropylidene protecting groups were removed and the alcohols on the sugar groups were sulfated using SO_3/pyridine to obtain heparin-mimicking polymers with approximately 3.5 sulfates per saccharide (Figure 1-4b). To study the effects of differing saccharide groups, Ayres and coworkers synthesized the polymers containing sulfated glucose, mannose, lactose, and glucosamine pendant groups. The non-sulfated polymers did not exhibit any prolonged anticoagulation activity; however, the sulfated polymers did, with sulfated mannose and lactose polymers resulting in the longest anticoagulation times and the best blood compatibility.[104] To further study these polymers the authors varied the isocyanate monomer to determine the effects of backbone chemistry on anticoagulation times of lactose polymers and found that backbones made with isophorone diisocyanate (IPDI) and methylene bis(4-cyclohexyl isocyanate) (HMDI) provided better anticoagulation times than polymers made with HDI or toluene 2,4-diisocyanate (TDI).[105] This was hypothesized to be due to a higher degree of flexibility in the polymer backbone of HMDI and IPDI polymers. Furthermore, the authors varied the degree of sulfation on the lactose/HMDI polymers from 3 to 15% and saw a direct correlation between increasing degree of sulfation and increasing anticoagulation times. Yet, all of the polymers were

significantly lower in their ability to inhibit thrombin activity than heparin. The authors also showed they could prepare similar glycopolymers via RAFT polymerization, giving more well-defined polymers.[106]

To overcome the post-polymerization modification steps, the Chaikof group used cyanoxyl-mediated polymerization (CMP) of sulfonated glycomonomers to prepare the sulfated polymers directly.[107,108] This synthesis method also had the advantage of allowing control of the molecular weight and provided polymers with good to moderate control over molecular weight dispersity ($Đ$ between 1.1 and 1.6).[107-109] Sulfated 2-acrylamidoethyl β-lactosides were copolymerized with acrylamide yielding heptasulfate lactose-based glycopolymers (Figure 1-4c).[110,111] These copolymers were shown to have prolonged coagulation time compared to nonsulfated glycopolymers and homopolymers of the sulfated 2-acrylamidoethyl β-lactosides. None of the polymers were as effective as heparin; yet, the authors demonstrated that anticoagulant activity could be tuned to be increasingly heparin like by altering the ratios of acrylamide as a comonomer.[110] The copolymer was later demonstrated as a chaperon for FGF2 in protecting the protein from trypsin, acid, and heat-induced degradation.[111] The sulfated glycopolymer was able to replace heparin in facilitating binding of FGF2 to FGFRs, as well as in dimerization of FGF2 and FGFR, which are key events leading to cell proliferation in HS-deficient cell lines. To utilize these polymers in bioconjugations, Chaikof and co-workers copolymerized the sulfated lactose acrylamide monomers with acrylamide using functionalized arylamines as initiators in cyanoxyl mediated copolymerizations. This resulted in heparin-mimicking polymers with varying groups at the α-chain end and cyanate groups at the ω-functionalized chain ends, and the authors demonstrated the possibility of bioconjugation by conjugating biotin-functionalized heparin-mimicking polymers to streptavidin.[112] These well-

defined polymers have potential applications in proteins conjugations for protein delivery and protein stabilization.[113]

The Kiessling group has devoted much effort to preparing glycopolymers by ROMP and showed that the polymers, even sulfated ones, could be made with control.[114-116] These polymers were very effective at inhibiting L- and P-selectins. The Hsieh-Wilson group also reported the synthesis of glycopolymers via ROMP, in their case of norbornene functionalized tetrasulfated disaccharide of L-iduronic acid and glucosamine to target the anti-coagulation property of heparin.[117] In their studies they aimed to develop new heparinoids that improve upon the commercially available ultra low molecular weight heparin, Arixtra, a heparin pentasaccharide. The disaccharide moiety was rationally designed to include the iduronic acid moiety for flexibility and the glucosamine moiety due to its 3-O-sulfation, in order to improve the affinity of the polymer to antithrombin III. The disaccharide monomers were sulfated prior to polymerization, which allowed for homogeneous sulfation of the resulting glycopolymers. The glycopolymers were shown to have potent anticoagulant activity depending on the polymer size. For example, a minimum polymer size of 11.2 kDa (10 repeats of the disaccharide) was required to prolong the activated partial thromboplastin time (APTT) time in human blood, whereas a size of at least 32.7 kDa (30 repeats) was required to alter both APTT and the prothrombin time (PT). The results underscore the importance of being able to systematically alter the molecular weight to change the number of repeat units using a synthetic polymer.

In the above described report, the authors found an interesting effect whereby the glucosaminyl 3-*O*-sulfate was required for anticoagulant activity.[117] In a subsequent report, the same group studied the effects of varying the degree and position of the sulfate groups on the iduronic acid and glucosamine disaccharide polymerized via ROMP on the ability to mimic

heparin by binding to the proinflammatory chemokine RANTES (regulated on activation, normal T cell expressed and secreted).[118] Compared to disulfated and nonsulfated disaccharides, the trisulfated epitopes with one sulfate on the iduronic acid moiety and two sulfates on the glucosamine moiety were identified to be necessary to bind to most chemokines. Glycopolymers with these pendant groups were synthesized via ROMP (Figure 1-4d) and were shown to bind to and inhibit the activity of RANTES similar to heparin. Importantly, these heparin-mimicking glycopolymers did not exhibit anticoagulant activity; therefore, they have potential therapeutic value in treatment of inflammation since RANTES recruits leukocytes to inflammatory sites. Because of the synthetic methodology used, the sulfate groups can be moved around the disaccharide unit and be precisely controlled. The authors noted that this feature could allow for the preparation of other heparin mimics with activity relevant to diseases such atherosclerosis, cancer, and autoimmune disorders. The same group extended this ROMP based approach to synthesize mimics of other GAGs such as chondroitin sulfate.[119,120]

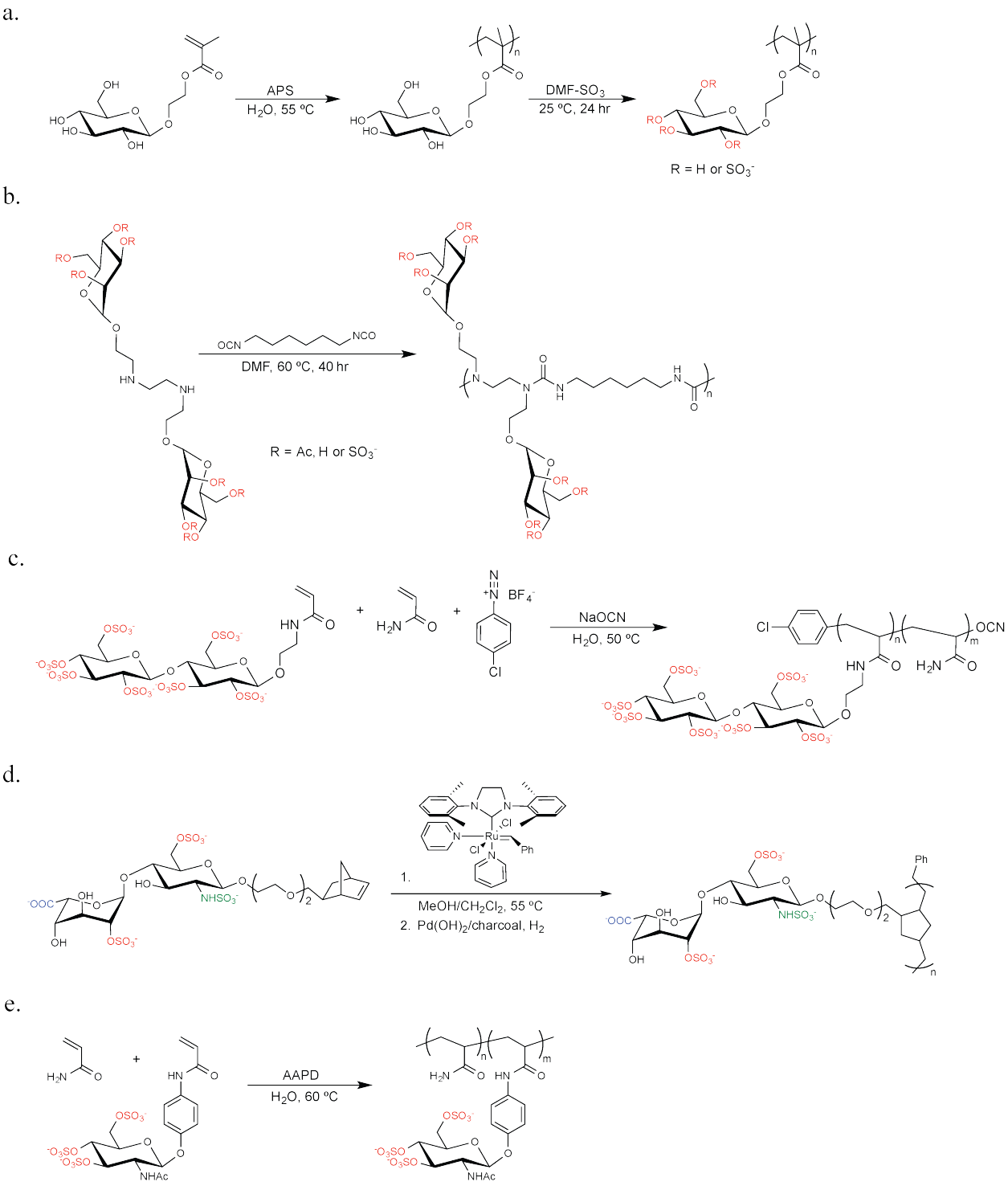

Figure 1-4. Syntheses of heparin-mimicking glycopolymers. (a) Poly glucosyloxyethyl methacrylate-sulfate p(GEMA)-sulfate synthesized by Akashi and co-workers via free radical polymerization.[100] (b) Hexamethylene diisocyanate-based isocyanates polymerized by step

growth polymerization by Ayres and co-workers.[103] (c) Heptasulfate lactose-based glycopolymers polymerized by cyanoxal mediated polymerization by Chaikof and co-workers.[111] (d) Heparin-mimicking polymers by ROMP to contain pendant disaccharides with three sulfates fabricated by Hsieh-Wilson and co-workers.[118] (e) 3,4,6-sulfo glucosamines copolymerized by free radical polymerization by Miura and co-workers.[121]

Other researchers investigated both location and number of sulfates, as well as the spacing between sugars as a factor. For example, Miura and co-workers synthesized heparin mimics containing glucosamine saccharides and acrylamide by free radical polymerization to bind to heparin binding proteins such as ß-Secretase (BACE-1) involved in Alzheimer's disease (AD). By varying the sulfation pattern on the pendant glucosamines from 3-sulfo, 4-sulfo, 6-sulfo and 3,4,6-sulfo, the authors found that polymers containing 3,4,6-sulfo pendant sugars significantly inhibited BACE-1 activity (a protease known to be involved in the pathogenesis of AD), while the 6-sulfo modestly inhibited (Figure 1-4e).[121] It was later shown that polymers containing 6-sulfo pendant sugars reduced amyloid fibril formation.[122] Interestingly, polymers with modest sugar contents inhibited amyloid ß fibril formation more effectively than polymers with high sugar contents. This could be due to spacing required in the sulfation pattern to obtain appropriate structure and binding relating to multivalency, and the flexibility of the polymer backbone. Miura and co-workers have also polymerized similar polymers through RAFT[123] polymerization to obtain more well-defined polymers. This allowed the group to study the influence of degree of polymerization (molecular weight) on amyloid ß fibril inhibition. Furthermore, the group showed the strongest inhibition was obtained from a terpolymer of acrylamide, 6-sulfo-glucosamine monomer, and glucuronic acid.

Table 1-3. Heparin-mimicking glycopolymers and their biological applications[a]

Polymer[1]	Polym. Tech.[2]	Mn (kDa)	*Đ*	Sulfation	Biological Properties	Ref.
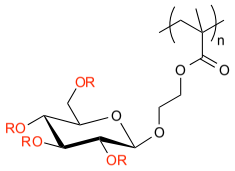 R = H or SO_3^- poly(GEMA)-sulfate	FRP	18.0	NA	Random sulfation post polymerization with DMF/SO_3^- (1.91-3.75 sulfates per saccharide)	Increases clotting time Polymer forms insoluble complex with fibrinogen, slowing fibrin polymerization	98,100
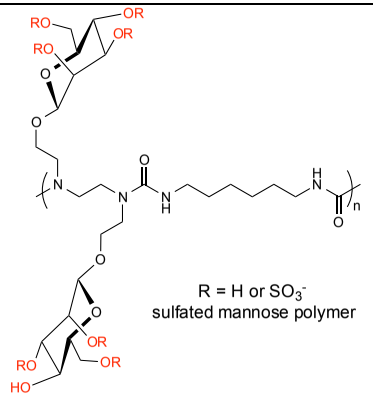 R = H or SO_3^- sulfated mannose polymer	SG	22.7	1.41	Random sulfation post polymerization with SO_3^-/pyridine (3.99 sulfates per saccharide)	Increases anticoagulation time Shows blood compatibility Exhibits anti-IIa activity in heparin's therapeutic range	103,104

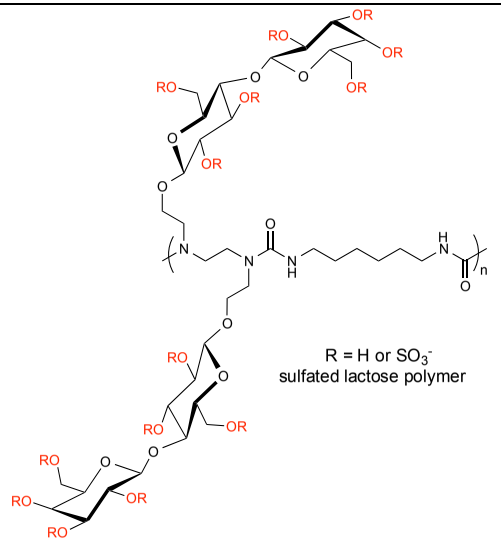	SG	27.0	1.75	Random sulfation post polymerization with SO_3^-/pyridine (6.88 sulfates per disaccharide)	Increases anticoagulation Prolongs blood clotting Shows blood compatibility	104
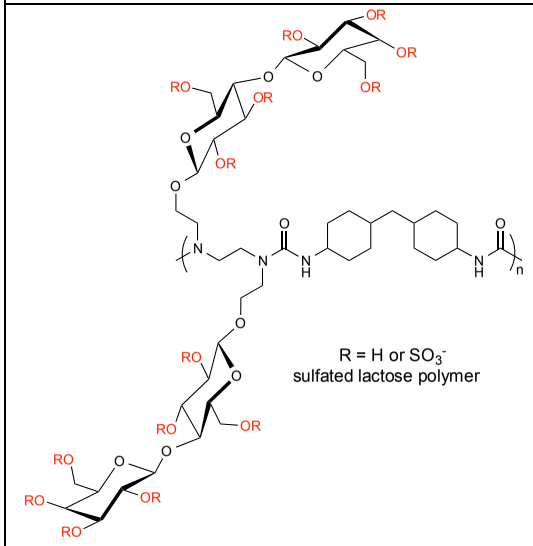	SG	11.0	1.42	Random sulfation post polymerization with SO_3^-/pyridine (5.97 sulfates per disaccharide)	Increases coagulation time Inhibits thrombin in the presence of ATIII	105

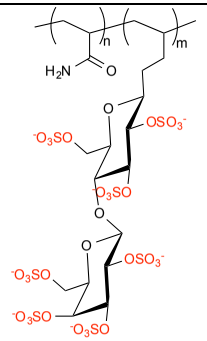	FRP	70.5	1.59	Heptasulfated at all available positions	Enhances FGF2 binding to FGFR1 (although not to the same extent as heparin)	110
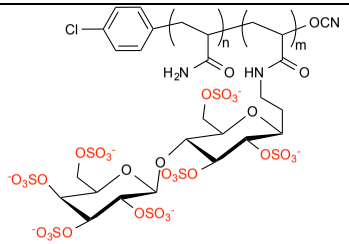	CMP	9.30 and 33.4	1.46 and 1.47	Heptasulfated at all available positions	Increases anticoagulant activity (higher than dermatan sulfate, but not as high as heparin) Protects FGF2 from degradation as efficiently as heparin	110,124
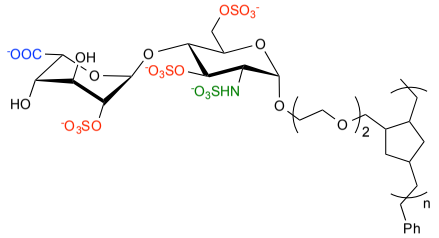	ROMP	11.2-43.0	1.25-1.41	Tetrasulfated at specific positions	Increases anticoagulant activity Prolong APTT (for polymers ranging from 11.2 kDa – 43.0 kDa) Prolong prothrombin time (for polymers ranging from 32.7 kDa to 43.0 kDa)	125
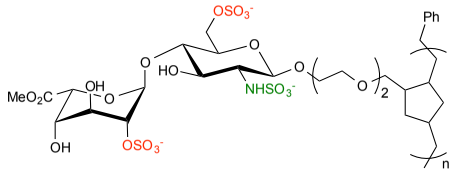	ROMP	27.9	1.22	Trisulfated at specific positions	Binds strongly with RANTES Inhibits migration of L1.2 cells similarly to heparin No anticoagulant activity	126

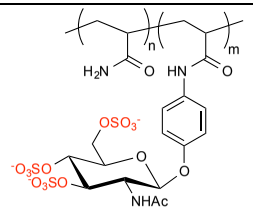	FRP	41.4	2.9	Trisulfated (3,4,6-sulfated)	Significantly inhibits BACE-1 activity	121
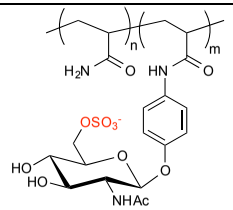	FRP	340-600	1.8-2.0	Monosulfated at the 6 position (11-28% sugar incorporation)	Inhibits amyloid-beta formation	122
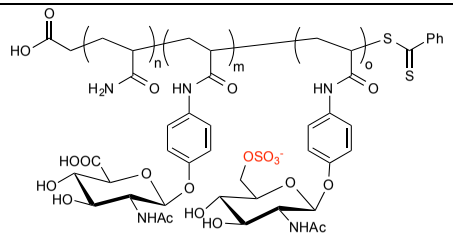	RAFT	7.6	1.4	Monosulfated at the 6 position (17.4% sugar incorporation)	Inhibits amyloid-beta formation	123

[a]Other acronyms: APTT, activated partial thromboplastin time; FGF2, fibroblast growth factor 2; FGFR1, fibroblast growth factor receptor 1; BACE-1, β-site APP cleaving enzyme-1.

[1]Location of sulfate is shown in red. If random all positions are highlighted in red.

[2]FRP, free radical polymerization; SG, step growth; CMP, cyanoxyl-mediated polymerization; ROMP, ring opening metathesis polymerization; RAFT, reversible addition-fragmentation chain transfer polymerization; NA, not available/not reported.

In many of the above examples, controlled polymerizations were utilized, resulting in polymers with well-defined molecular weight dispersities. This is an important advance allowing one to control and target the molecular weight. The results also nicely showed that by taking components of heparin and controlling the sugar identity and location of sulfates, the heterogeneity in biological activity could be reduced, thereby targeting particular biological paths over others. Great progress has been made in this regard by Hsieh-Wilson, and further use of minimal oligosaccharide sequences known to be required for binding to particular proteins would be advantageous to the field. In addition, the results showed the importance of spacing the sugars for certain applications. However, a drawback of these polymers is the need to prepare sulfated glycomonomers. Sugar chemistry can be tedious and the sulfate groups can still be desulfated under acidic conditions. Thus, some researchers have explored non-saccharide synthetic polymers that mimic the negative charge of the sulfate, rather than sugar structure itself.

1.2.5 Polysulfonated Compounds

Polysulfonated polymers are fully synthetic polymers that make up another large class of heparin-mimicking polymers (Table 1-4). These often rely on the negative charge from sulfonate groups on side chains of polymers for their heparin-mimicking properties and do not contain any sugars. Liekens and co-workers studied the salt forms of various sulfonated polymers (Figure 1-5a) including poly(2-acrylamido-2-methyl-1-propanesulfonic acid) (pAMPS), poly(anetholesulfonic acid) (pAS), poly(4-styrenesulfonic acid) (pSS), and poly(vinylsulfonic acid) (pVS) for their ability to inhibit cell proliferation similar to heparin at higher concentrations.[127] The polymers were prepared by free radical polymerization and, thus, were polydisperse. pAMPS, pAS, and pSS were found to have potent anti-proliferative activity in

fetal bovine aortic endothelial GM7373 cells by inhibiting binding of FGF2, and anti-angiogenic effects in an *in vitro* rat aorta ring assay.[128] Therefore, the polymers had promising therapeutic value in treating angiogenesis-promoted cancers. All of the polymers protected FGF2 to proteolytic enzymes, but none protected against heat degradation. For the former, the protein was incubated with polymers as excipients in a trypsin digestion assay and, in the presence of sulfonated polymers, showed an increase in undigested FGF2, with pSS and pAMPS performing better than pAS or pVS. To understand the interactions with FGF2, computational molecular modeling was performed and showed that the sulfonate groups in pAMPS are able to adopt a low-energy conformation (the polymer is likely helical) to interact with the heparin-binding domain of FGF2 (Figure 1-5b).[127] Of the sulfonated polymers that were tested, pSS was found to be the most effective in its ability to inhibit cell-cell adhesion and most potent in stabilization of FGF2. In later studies performed by Varghese and co-workers, pSS was tested for its ability to mimic heparin and effect FGF2 signaling in muscle progenitor cells, where addition of heparin promotes myogenesis. When incubated with muscle progenitor cells, the polymer facilitated an increase in myogenic differentiation and myotube formation similar to heparin.[129] Later studies showed that the hydrophobicity of polyanions also effects the complexation between proteins and sulfated polymers such as pSS.[130]

a.

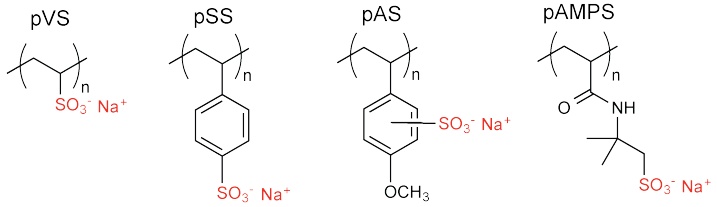

b.

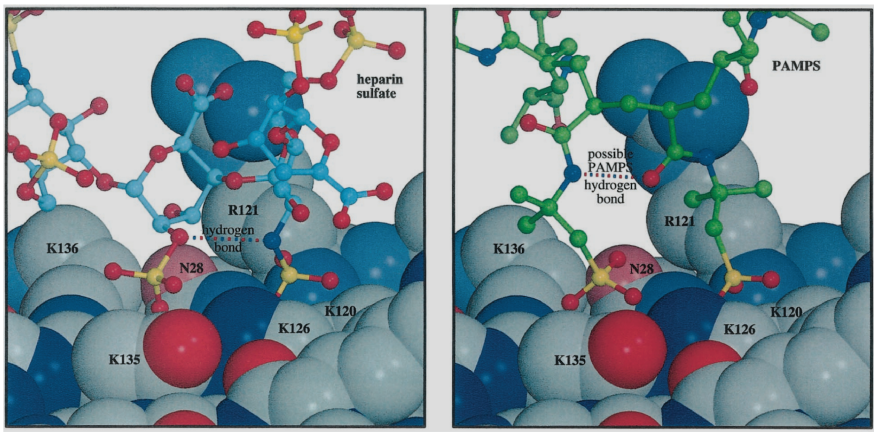

Figure 1-5. Heparin-mimicking sulfonated polymers. (a) Chemical structures of the various sulfonated polymers tested by Liekens et. al and (b) molecular modeling showing heparin and pAMPS interacting with the heparin-binding domain of FGF2. Reprinted with permission from reference 127. Copyright 1999 American Society for Pharmacology and Experimental Therapeutics.

Due to the promising biological activities of these sulfated/sulfonated polymers, work was done on determining the effect of incorporating these monomers in copolymer systems. Considering what was discussed in the glycopolymer section above (section 1.2.4), spacing the sulfonate groups may be an important factor. Rather than synthesizing a simple polysulfonated polymer, Chen and co-workers developed a new heparin-mimicking polymer that incorporated both non-sulfated glycomonomers for saccharide incorporation and SS for sulfonate incorporation. SS was copolymerized with 2-methacrylamido glucopyranose (MAG) by RAFT polymerization to yield polymers p(SS-*co*-MAG) between 8 and 9 kDa with SS incorporation

ranging from 35 to 64%.[131] The polymers were well-defined, with molecular weight dispersities between 1.17 and 1.20. They found that when cultured with FGF2, copolymers with 50% SS incorporation promoted cell proliferation in fibroblasts better than heparin. Additionally, the copolymer exhibited higher proliferation of mouse embryonic stem cells (mESCs) after 20 days better than either pSS or the MAG homopolymer, suggesting that both components are important for the increase in activity; the mESCs also proliferated better with the copolymer than heparin itself. The authors also looked at the ability of the polymers to promote neural differentiation in mESCs and found that pSS performed the same as heparin, pMAG did not promote neural differentiation, and p(SS-*co*-MAG) performed significantly better than pSS or heparin. These results suggest that there are synergistic effects between the sulfonate units and the sugar units in the copolymer and that both contribute to the high biological activity of this new polymer.

Table 1-4. Heparin-mimicking polysulfonated compounds and their biological applications[2a]

Polymer	Polym Tech.[1]	Mn (kDa)	*Đ*	Degree of sulfation	Biological Properties	Ref.
pSS 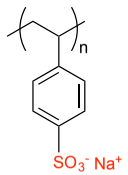	FRP	70.0	NA	100% of monomers contain 1 sulfonate	Inhibits FGF2 binding to FGFRs and HSPGs on endothelial GM 7373 cells Inhibits mitogenic activity of FGF2 in GM 7373 cells Inhibits FGF2 mediated cell-cell adhesion of HSPG-deficient CHO cells as effectively as heparin Protects FGF2 from proteolytic degradation Inhibits FGF2-induced cell proliferation and angiogenesis in endothelial cells	127,128
pVS 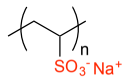	FRP	2.0	NA	100% of monomers contain 1 sulfonate	Inhibits FGF2 binding to FGFRs and HSPGs on endothelial GM 7373 cells Inhibits FGF2 mediated cell-cell adhesion of HSPG-deficient CHO cells Protects FGF2 from proteolytic cleavage No antiangiogenic activity in a rat aorta-ring assay or CAM assay	127,128

pAMPS 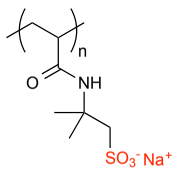	FRP	7.0-10.0	NA	100% of monomers contain 1 sulfonate	Inhibits FGF2 binding to FGFRs and HSPGs on endothelial GM 7373 cells Protects FGF2 from proteolytic degradation more efficiently than other sulfonated polymers Inhibits FGF2 mediated cell-cell adhesion of HSPG-deficient CHO cells Inhibits mitogenic activity of FGF2 in GM 7373 cells Inhibits FGF2-induced cell proliferation in endothelial cells Angiogenesis inhibitor	127,128
pAPS 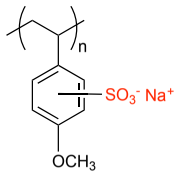	FRP	9.0-11.0	NA	100% of monomers contain 1 sulfonate	Inhibits FGF2 binding to FGFRs and HSPGs on endothelial GM 7373 cells Inhibits FGF2 mediated cell-cell adhesion of HSPG-deficient CHO cells Protects FGF2 from proteolytic cleavage Inhibits FGF2-induced cell proliferation in endothelial cells Angiogenesis inhibitor	127,128

pSS 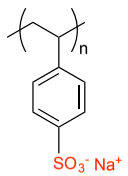	FRP	70.0	3-5	75% of monomers sulfonated	Promotes FGF2 induced myogenic differentiation and myotube formation in muscle progenitor cells	132
p(SS-*co*-MAG) 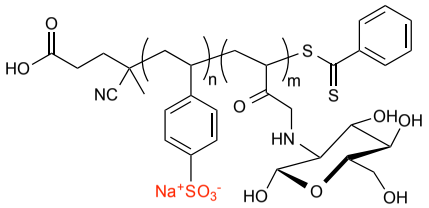	RAFT	8.0-9.0	1.17-1.20	35-64%	Promotes fibroblast proliferation better than heparin Stimulates mESC proliferation better than heparin Promotes neural differentiation of mESCs	131
p(MMA-*co*-MA-*co*-SS) 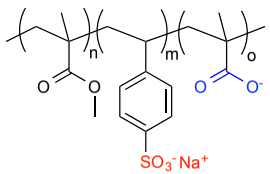	FRP	NA	NA	2-7%	Interacts with fibronectin to inhibit adhesion of bacteria onto surfaces	133,134
p(MMA-*co*-MA-*co*-SS) 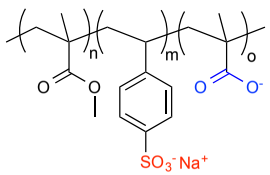	FRP	M_v = 75.2	NA	7.5% SO_3^- and 7.5% COO^-	Polymer films absorb fibronectin and inhibit fibroblast adhesion and proliferation	135

p(MMA-*co*-SS) 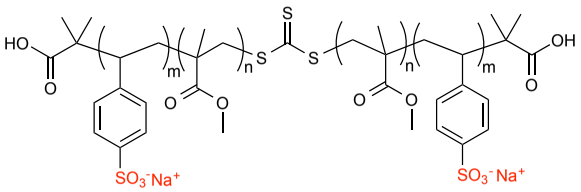	RAFT	27.3-31.0	1.69-1.75	20-80% SO_3^- incorporation	Increases APTT with increasing SO_3^- incorporation	136
p(AMPS-*co*-BA) 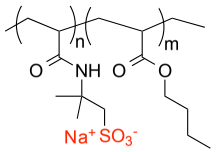	FRP	23.3-72.5	1.6-2.6	25-75%	Inhibits FGF1 induced mitogenic activity of fibroblasts (higher AMPS incorporation leads to greater inhibition at lower concentration)	137
p(SS-*co*-PEGMA) 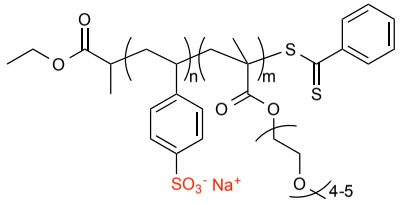	RAFT	24.0	1.17	69%	Strongly binds FGF2 and VEGF to high salt concentrations Binds FGF2 when immobilized on surfaces allowing endothelial cell spreading	138
p(SS-*co*-PEGMA) 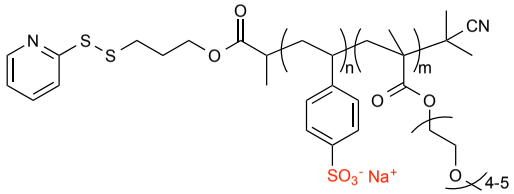	RAFT	26.1	1.16	68%	When conjugated to FGF2, polymer helps stabilize FGF2 to trypsin degradation, heat, storage and acidic pH	139

pVS 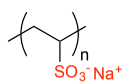	FRP	6.4	1.21	100%	Facilitates binding of FGF2 to FGFR Promotes FGF2-induced cell proliferation	140
pVS 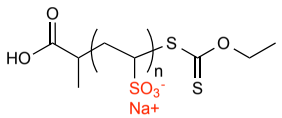	RAFT	6.6-80.3	1.14-1.40	100%	Promotes FGF2-induced cell proliferation in HSPG deficient cell lines	140
p(SS-*co*-PEGMA)-*b*-VS 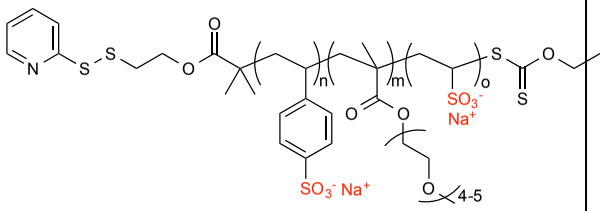	RAFT	57.2	1.46	86.5%	Facilitates binding of FGF2 to FGFR Conjugate promotes FGF2 induced endothelial cell migration and cord-like structure formation Conjugate stabilizes FGF2 from denaturation upon storage at room temperature or refrigeration	141
pGA-sulfonate 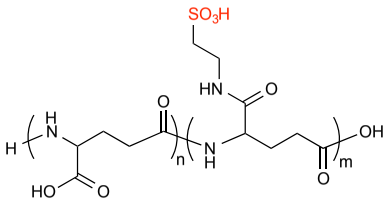	NA	1,230	1.20	13-81%	Increases blood coagulation time with increasing degree of sulfonation Degradable at pH 7.4 at 80 ºC over 48 hours	142

pGA-sulfonate 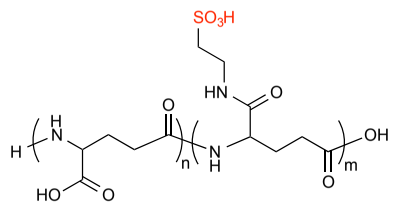	NA	310	1.20	72%	Promotes FGF2 induced fibroblast growth in cells lacking native HSPG (better than exogenous heparin) Slightly stabilizes FGF2 from heat and acidic environments	143
pCL-APS 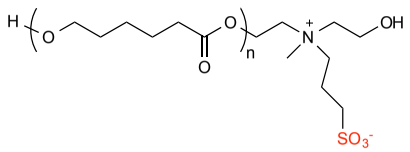	ROP	3.02-10.73	1.09-1.43	NA	Increased blood coagulation times Reduces platelet adhesion on surfaces coated with polymer	144

[2a]Other acronyms: HSPG, heparin sulfate proteoglycan; CHO cell, Chinese hamster ovarian cell; CAM, chick chorioallantoic membrane; FGF2, fibroblast growth factor-2; FGF1, fibroblast growth factor-1; FGFR, fibroblast growth factor receptor; APTT, activated partial thromboplastin time; VEGF, vascular endothelial growth factor; mESC, mouse embryonic stem cell;

[1]FRP, free radical polymerization; RAFT, reversible addition fragmentation chain transfer polymerization; ROP, ring opening polymerization. NA, not available/not reported.

The Migonney group investigated the incorporation of SS into terpolymers for use in materials that require heparin or heparin-mimics. They synthesized polymers by FRP using methyl methacrylate (MMA), methacrylic acid (MA) and sodium styrene sulfonate (SS) to obtain terpolymers containing both sulfonate and carboxylate moieties (Figure 1-6a), thus, incorporating the various components of heparin including hydrophobic domains.[133] Heparin coated surfaces are known to be antibacterial, and the authors found the terpolymer also inhibited *Staphylococcus aureus* bacterial adhesion.[134] It was found that the ratio of carboxylates to total negative charge mattered, and that values between 0.28 and 0.8 inhibited the bacteria from attaching. To further study the heparin-mimicking properties of these polymers, the group studied the ability of the polymers to inhibit fibroblast cell growth on films of the polymers (Figure 1-6b). They found that polymers containing 15% ionic groups (specifically 7.5% sulfonate and 7.5% carboxylate) had the highest inhibitory effects and that the total number of ionic groups could be altered as long as the number of carboxylates to sulfonates was equal.[135] Zhao and co-workers prepared similar polymers changing methyl acrylic acid for acrylic acid (AA) but varied the comonomers to yield p(SS-*co*-MMA), p(AA-*co*-MMA), and p(SS-*co*-AA-*co*-MMA) via RAFT polymerization. However, instead of polymerizing styrene sulfonate directly, the authors copolymerized with styrene, and then sulfonated the styrene moieties post polymerization with concentrated sulfuric acid. They found that increasing incorporation of AA or SS in the polymers increased coagulation time, and free polymers in solution prolonged coagulation time at 0.5 mg polymer/0.1 mL platelet-poor plasma (PPP) and the solutions were incoagulable at 2 mg/0.1 mL polymer/PPP.[136] The polymers were not directly compared to heparin in this assay.

a. b.

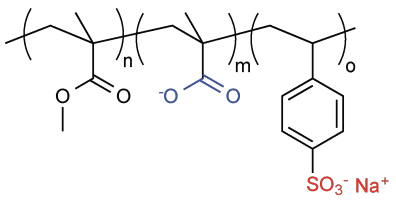

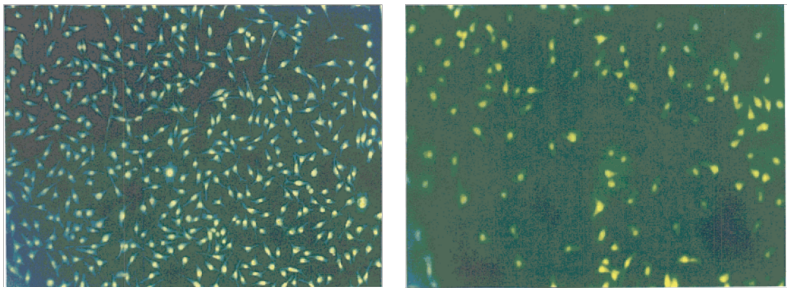

Figure 1-6. (a) Chemical structure of heparin-mimicking terpolymers polymerized by Migonney and co-workers and (b) their ability to inhibit fibroblast adhesion (right) verses control (left). Reprinted with permission from reference 135. Copyright 2002 American Chemical Society.

Copolymers of pAMPS have also been synthesized. Aguilar and co-workers copolymerized AMPS with either vinylpyrrolidone (VP) or butyl acrylate (BA) by FRP to yield p(AMPS-*co*-VP) and p(AMPS-*co*-BA). In this study they looked at the ability of the polymers to inhibit heparin-binding growth factor-induced cell mitogenic activity.[137] They found that polymers containing BA inhibited FGF1 stimulated mitogenic activity of mouse fibroblasts (Balb/c 3T3); however, none of the VP containing polymers had an effect on the mitogenic activity. Not surprisingly, the sulfonated concentration in the copolymers was the important factor with polymers containing a larger amount of AMPS (50% or greater) inhibiting at lower concentrations. The authors wrote that the differences in activity between VP and BA were likely due to the reactivity ratios of the two monomers with AMPS. Specifically, that BA/AMPS copolymers had BA-rich and AMPS-rich sequences allowing for a helical conformation of the pAMPS to interact with the FGF1, while the VP system had an alternating sequence, which prevented the helical type structural formation. pAMPS has also been used in the fabrication of core-shell particles by emulsion polymerization of butyl methacrylate (BMA) and studied for retention and release of heparin-binding growth factors important in wound healing. Rimmer and co-workers polymerized AMPS by RAFT to give both linear and hyperbranched core-shells and

chain extended with BMA during the emulsion polymerization.[145] Interestingly, they found that the release of VEGF from linear-grafted shells was slower in the first 200 hours compared to the branched shells; but after 200 hours the release from the branched shells stopped, while release from the linear shells continued out to at least 800 hours. For PDGF, the rate of release from the linear shells remained slower than from branched throughout the entire 800 hours.

a.

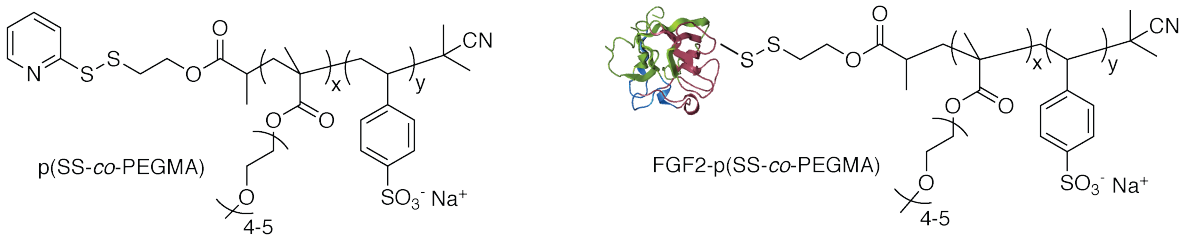

b.

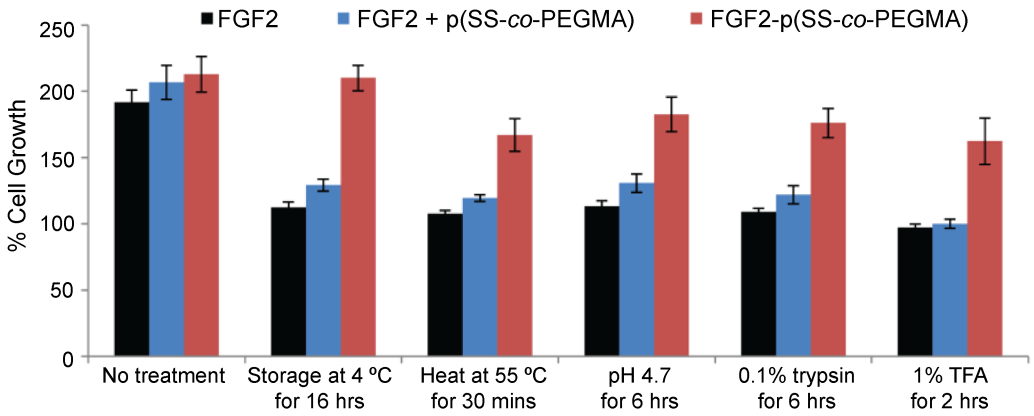

Figure 1-7. Polysulfonated heparin-mimicking polymer, p(SS-*co*-PEGMA) and the stability profile of its conjugate to FGF2. (a) Chemical structure of the polymer. (b) Structure of the FGF2-p(SS-*co*-PEGMA) conjugate. (c) Stability of the conjugate against various stressors, tested on human dermal fibroblast cells for stimulated cell proliferation. Modified with permission from reference 139. Copyright 2013 Nature Publishing Group.

Recently, we reported the synthesis of poly(sodium 4-styrenesulfonate-*co*-poly(ethylene glycol) methyl ether methacrylate) (p(SS-*co*-PEGMA)) via RAFT polymerization (Figure 1-7a)

and showed that the polymer bound to FGF2 to high salt concentrations and in cellular media.[146,147] Furthermore, the polymer immobilized on surfaces was able to present FGF2 in a manner that could be utilized by human endothelial cells, enlarging their area compared to integrin-binding peptide presenting surfaces alone. In a subsequent study, this heparin-mimicking polymer was conjugated to FGF2 through a disulfide linkage, resulting in a highly stable protein-heparin-mimicking polymer conjugate, FGF2-p(SS-*co*-PEGMA) (Figure 1-7b).[139] Heparin is a natural stabilizer for many heparin-binding proteins including FGF2, which is typically very unstable and denatures quickly.[148] FGF2-p(SS-*co*-PEGMA) was demonstrated to be stable to a variety of environmentally and therapeutically relevant stressors such as heat, mild and harsh acidic conditions, storage and proteolytic degradation (Figure 1-7c). The conjugate also induced proliferation of human dermal fibroblast cells, a critical cell line in wound healing, as effectively as the native protein. Interestingly, neither the polymer nor conjugate induced proliferation in cells lacking natural HS, suggesting that, in contrast to heparin, the polymer at the molecular weight explored did not bind to the receptor to help induce receptor mediated signaling.

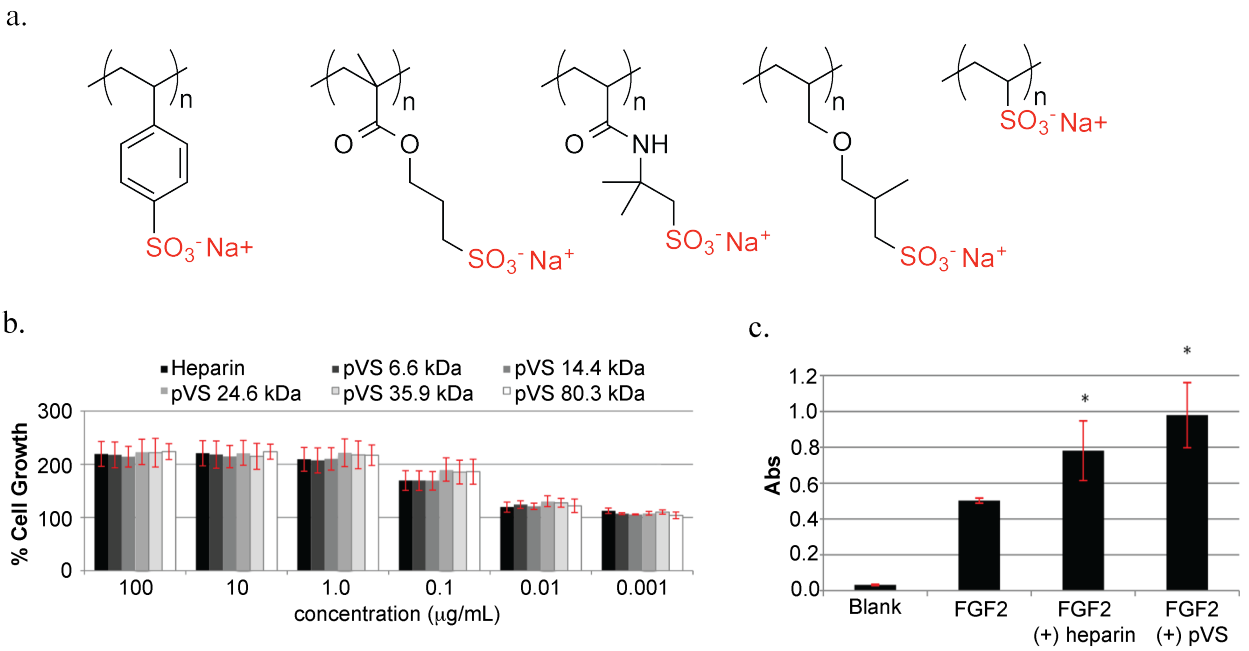

Figure 1-8. Screening study of various sulfonated polymers. (a) Chemical structure of heparin-mimicking polymers polymerized by free radical polymerization. (b) Cell proliferation studies in BaF3-FR1C cells showing the heparin-mimicking nature of pVS. (c) FGFR based ELISA assay showing pVS increasing the binding of FGF2 to FGFR compared to heparin. Reprinted with permission from reference 140. Copyright 2015 American Chemical Society.

To search for a new heparin-mimicking polymer that would stabilize FGF2 and activate the cell receptors, we screened a variety of sulfated and sulfonated polymers, including poly(potassium 3-sulfopropyl methacrylate) (pSPM), poly(sodium 1-allyloxy-2 hydroxypropyl sulfonate) (pAHPS), pSS, pVS, and pAMPS (Figure 1-8a) using a cell line that lacks native HS.[140] The polymers were added and cell proliferation in the presence of FGF2 was utilized as a readout (compared to cells with no FGF2 or FGF2 and no heparin as controls). In this assay it was found that pVS activated FGF2-induced cell proliferation at all concentrations tested. Figure 1-8b shows the results for different molecular weight pVS compared to heparin. The

results were verified by an ELISA based receptor assay (Figure 1-8c). Using these assays, it was determined that pVS enhanced FGF2 receptor binding when added as an excipient to the same extent as heparin, meaning that the polymer facilitated FGF2 binding to its receptor. This effect is likely due to the polymer binding to both the protein and receptor in the active tetrameric complex as does heparin. This was the first fully synthetic polymer reported to be as good as heparin in facilitating FGF2 binding to its receptor and subsequent activation. In Chapter 2 we report that by combining pVS in a block copolymer with p(SS-*co*-PEGMA), a new block copolymer conjugate was fabricated that both stabilized FGF2 and facilitated receptor binding, thus, leading to an increase in endothelial cell migration and tubulogenesis compared to unmodified FGF2.[141]

The backbone of all the polymers mentioned above are hydrocarbon based and not degradable. Additional backbones were also studied that completely degrade over time, which has advantages for many different biomedical applications of heparin-mimics. Akashi and co-workers utilized a poly(glutamic acid) (pGA) polymer backbone for biological degradation to form heparin-mimicking polymers.[142] The group functionalized pGA with sulfonate groups by reacting the amine of taurine with the carboxylic acids along the polymer chain (Figure 1-9a). They found that increasing polymer concentration and degree of sulfonation both impacted blood clotting by increasing coagulation time. While coagulation time was increased when compared to non-sulfonated pGA, the clotting time was significantly less than heparin. pGA-sulfonate was compared to well known heparin mimics, pVS and pSS, and delayed clotting longer than both of these polymers, while the clotting time was much less than dextran sulfate. The authors also showed that pGA-sulfonate was degradable by studying GPC over 48 hours in phosphate buffer at pH 7.4 at 80 ºC (Figure 1-9b and 1-9c). In a follow-up study, pGA with varying degrees of

sulfonation were analyzed in an FGF-2 dependent mouse fibroblast proliferation assay, and pGA with 72% of the carboxyl groups converted to sulfonates provided the maximal FGF2-induced proliferation, greater cell number compared to higher and lower percent sulfonation.[143] The 72% pGA sulfonate also increased cell proliferation above that of pSS, pVS and heparin itself. Additionally, pGA-sulfonate was able to slightly protect FGF2 from heat and acidic environments, but not to the extent of heparin. Molecular modeling studies showed that pGA-sulfonate with 72% sulfonation provided polymers with sulfonate groups in the right location to bind to the heparin binding site. Akashi and co-workers have gone on to use these polymers in hydrogels for growth factor delivery.[149,150]

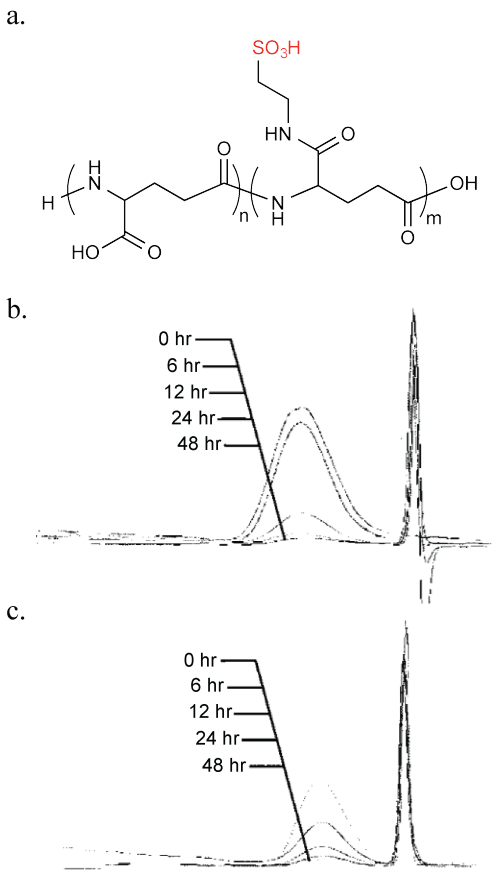

Figure 1-9. (a) Chemical structure of biodegradable sulfonated poly(glutamic acid) and GPC traces showing degradation of (b) non-sulfonated polyglutamic acid and (c) sulfonated

poly(glutamic acid). Reprinted with permission from reference 142. Copyright 2002 American Chemical Society.

Another biodegradable backbone utilized by Luo and co-workers was poly(caprolactone).[144] Polycaprolactone containing *N,N*-bis (2-hydroxyethyl) methylamine ammonium propane sulfonate (MDEAPS) was made via ring opening polymerization (ROP) to yield pCL-APS. First 1,3-propanesultone was opened with *N,N*-bis (2-hydroxyethyl) methylamine to give MDEAPS. Caprolactone was then polymerized in the presence of MDEAPS to give pCL polymers containing sulfobetaine. Reduced platelet adhesion was observed on surfaces with the pCL-sulfobetaine polymer, and the polymers showed prolonged coagulation times compared to analogous unsulfonated polymers.

In all of the above examples, stable sulfonated polymers were utilized. The polymers showed a wide range of activities including inhibiting and promoting cell proliferation and stabilizing growth factors. By utilizing the synthetic polymers, the amount and presentation of the negative charge could be altered, for example, by exploiting comonomers with different reactivity ratios. The results allow the community to start to understand the differences in biological activity depending on how the sulfonate is presented and what the backbone and side chain linkages are. Another advantage of this approach is that in many instances the monomers are commercially available. Employing controlled radical polymerization with specially designed chain transfer agents also allows for the synthesis of well-defined and near monodisperse polymers with targeted molecular weights. Furthermore, the polymers contain end groups that can easily be modified or covalently attached to proteins, surfaces and other materials. However,

a disadvantage of sulfonated synthetic polymers is that in many instances the activities were lower than that of heparin or sulfated polysaccharides such as dextran sulfate or the glycopolymers.

1.2.6 Polyionomers as Heparin-Mimics

Ionomers, which are copolymers consisting of both neutral and ionic monomers with an ionic incorporation of less than 15%, have also been studied for use as heparin-mimics. Most of the work done on heparin-mimicking ionomers has been focused on polyurethanes. Polyurethanes have been widely used as materials in biomedical devices such as stents and catheters because of their biocompatibility. To improve upon their blood compatibility, research on studying the effects of sulfonating polyurethane has been undertaken. While much work has been done on insoluble polyurethanes,[151] some groups have studied soluble forms to learn more about their heparin like properties. Heparin containing urethanes have been reviewed elsewhere;[151] here we focus on heparin-mimicking polyurethanes that are sulfonated and soluble (Table 1-5).

Table 1-5. Heparin-mimicking ionomers and their biological applications

Polymer	Polym Tech.	Mn (kDa)	*Đ*	Degree of sulfation	Biological Properties	Ref.
PEU-SO_3^- 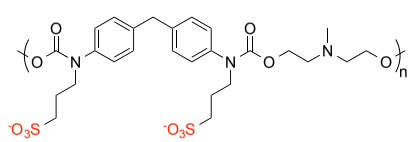	Step Growth	NA	NA	15-20%	Increased fibrinogen deposition compared to surfaces not coated with polymer Decreased platelet deposition on surfaces coated with polymer Inhibited thrombin and fibrin assembly	152,153
PEU-BES 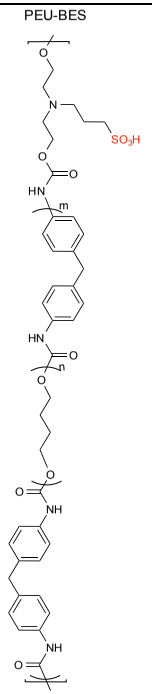	Step Growth	32.0-36.0	1.3-1.4	NA	Increased fibrinogen adsorption	154,155

Sulfonating polyurethanes can be accomplished by post-polymerization modification of the backbone with sulfonate side chains, or by polymerizing sulfonated segments on active isocyanate end groups after polymerization. For example, Grasel and Cooper synthesized polyurethanes from methylene bis(*p*-phenyl isocyanate) (MDI), poly(tetra- methylene oxide) (PTMO), and 1,4-butanediol.[152] After polymerization, the polyurethanes were reacted with NaH to remove the urethane hydrogen and then subsequent reaction with propane sultone afforded the sulfonated urethane (Figure 1-10a). The authors used these polymers to coat polyethylene and studied the blood compatibility in a canine ex vivo model. Tubes coated with sulfonated urethane showed a decrease in platelet deposition and an increase in fibrinogen deposition compared to the unsulfonated polyurethane (Figure 1-10b and 1-10c). To further study the properties of these polymers, Cooper and coworkers studied the mechanism by which these soluble polymers prolong blood coagulation.[153] They found that sulfated polyurethanes inhibited thrombin, likely via interaction with antithrombin III as does heparin. It was also found that the polymers directly inhibit fibrin assembly, rather than complexing free calcium or interfering with factor XIIIa.

Sulfonated polyurethanes can also be synthesized by using a sulfonated chain extender after polymerization. Brash and co-workers synthesized sulfonated urethanes by polymerizing MDI and poly(propylene glycol) (PPO) to yield urethanes with isocyanate end groups. The sulfonated segments were then added by reacting with 4,4'-diamino-2,2'-biphenyldisulfonicacid disodium or dipotassium salt (BDDS).[154] They found that thrombin times increased (i.e., plasma coagulation time was delayed) with increasing sulfonate content.[155] Kuo and co-workers also synthesized heparin-mimicking polyurethanes by adding a chain extender containing either sulfonate or carboxylate groups.[156] When anions were incorporated into the polyurethanes there was less platelet adhesion than on polyurethane alone; however, the carboxylate chain extenders

provided less platelet adhesion than the sulfonated ones.

a.

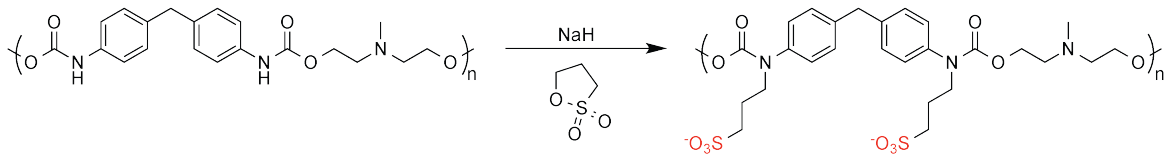

b.

c.

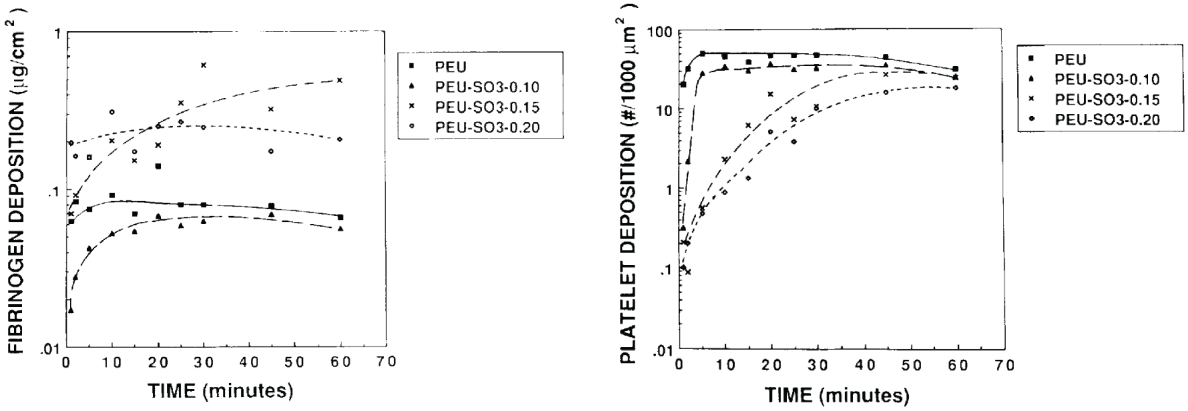

Figure 1-10. Sulfonated urethane ionomers used in development of new anticoagulants. (a) Chemical structure of polyurethane ionomers. (b) Degree of fibrinogen deposition on modified polyurethane materials showing an increase in fibrinogen accumulation with increasing degree of sulfonation. (c) Degree of platelet deposition on modified polyurethane materials showing a decrease in platelet accumulation with increasing degree of sulfonation. Reprinted with permission from reference 152. Copyright 1989 John Wiley and Sons.

Another example of heparin mimicking ionomers have been developed by Yui and co-workers consisting of sulfonated polyrotaxanes. To synthesize heparin-mimicking polyrotaxanes the authors first fabricated polyrotaxanes consisting of α-cyclodextrin around PEG (in a pluronic triblock copolymer) and then reacted the sodium salt with 1,3-propane sultone to form the sulfonated α-cyclodextrins.[157] They found that the sulfonated polyrotaxanes improved anticoagulation compared to the unsulfated version, which in turn was better than just the pluronic.

To further study these polymers, the authors synthesized polyrotaxanes with both sulfonate and carboxylate groups.[158] Carboxyethyl ester groups were conjugated to the α-cyclodextrins followed by taurine to afford mixed sulfonated and carboxylated polyrotaxanes. Importantly, the authors found that lower percentages of threaded α-cyclodextrin were better, likely because of charge spacing; for these polymers there was a maximal SO_3^-/COO^- ratio between 2 and 3. Shorter polymers also gave better anticoagulation properties. In a more recent study Yui and co-workers found that their sulfonated polyrotaxanes increased osteogenic differentiation when incubated with bone morphogenic protein-2 (BMP-2); this is similar to the positive effect of heparin complexed with this protein.[159] This class of sulfonated polyionomers provides new and interesting architectures with easy variability for use as heparin-mimics.

The development of polyionomers has advantages in that the polymers are wholly synthetic. In addition, ionomers with low incorporation of sulfonate can retain materials properties of the parent polymer, while imparting heparin-like activity. This means the materials can be used as biomedical devices (for example medical tubing), rather than serving as coatings. Thus, ionomers with post polymerization modification allows for the polymers to be easily functionalized after polymerization with widely varied structures. However, the polymerization technique used does not provide control over polymer molecular weight and post polymerization modification does not allow for easy control over the placement of negative charges.

1.3 Conclusions and Perspectives

Herein, we have summarized the synthesis and application of heparin-mimicking polymers and showed that they can be important in a wide range of applications, including protein protection, promoting cell differentiation, inhibiting cell adhesion, and anticoagulant activity. Polymeric synthetic mimics have addressed several disadvantages of heparin, including its heterogeneous structure. Recent advances in heparin-mimicking polymers offer opportunities for development of more structurally defined molecules that can target a specific biological interaction such as anticoagulant activity only. This can be useful when no cross-reactivity and low side reactions *in vivo* are desired. In addition, several examples have been shown to stabilize important heparin binding proteins to stressors that normally inactivate them. The ability of heparin-mimics to stabilize proteins opens a window for new therapeutics including new wound dressings produced by various techniques, such as electrospinning. Stabilization would also allow for administration of protein therapeutics through additional avenues and for easier storage of the drugs.

The synthetic polymers have the advantage compared to semi-synthetic or heparin itself of being stable, although desulfation of sulfates can still occur *in vivo*. However, there are many applications where a persistent heparin would not be desirable. While there are many advantages to synthetic heparin-mimics, FDA approval is often a lengthy process and extensive testing on safety and efficacy need to be undertaken for human use. Future directions that could improve the outlook for FDA approval include incorporation of degradable moieties in the backbones of heparin-mimicking polymers. A few sulfonated degradable polymers have been synthesized. For those non-degradable sulfated and sulfonated polymers prepared by radical polymerizations, this could be undertaken by incorporating cyclic ketene acetals into the polymerization mixtures, thus, providing points of degradation.[160-165] Use of heparin-mimics to even further modulate the activity

of native proteins, for example, to produce superagonists, would be significant in the fields of tissue regeneration, cell replacement therapies, and wound healing. Such approaches would be of value in further enhancing therapeutic efficacy and reducing side effects by fine-tuning the heparin binding motif and other molecular characteristics.

The examples thus far have shown that the spacing, sulfation presentation, addition of carboxylates or other chemical moieties, the molecular weight, the comonomers (i.e., reactivity ratios), and the backbone identity with regard to flexibility and degradability are all going to be important factors. Much work has been done to elucidate the minimal saccharide sequences required for heparin binding, which has helped inform researchers on oligosaccharides useful for glycopolymer mimics. However, little is known about the minimum units needed in synthetic heparin mimicking-polymers. Despite a lot work in this area, there are still no clear rules or extensive structure-property relationships on how the parameters above relate to resultant biological properties. Further systematic studies on type and presentation of sulfate and sulfonated groups and interactions with proteins coupled with computation and docking studies would be invaluable in this respect. Although this has been done on smaller scale, large-scale studies with many of these variables would be very useful. It could allow one to design a polymer that could interact with a specific domain of a heparin binding protein, thus, targeting a specific interaction/biological pathway. This could lead to further design optimization and target-based study versus empirical testing, which will be important to advance the field. In addition, the development of a broader range of heparin- and heparin-mimicking-based materials, tapping into new developments in polymer synthesis, such as precision control, would certainly further expand impact of these materials in the treatment of various diseases.

1.4 References

†Chapter 1 is reproduced with permission from Paluck, S.J.; Nguyen, T.H.; Maynard, H.D. Heparin-Mimicking Polymers: Synthesis and Biological Applications. *Biomacromolecules* **2016**, *17*, 3417-3440. 10.1021/acs.biomac.6b01147. Copyright 2016 American Chemical Society. http://pubs.acs.org/doi/abs/10.1021/acs.biomac.6b01147

(1) Sasisekharan, R.; Venkataraman, G. *Curr. Opin. Chem. Biol.* **2000**, *4*, 626-631.

(2) Hileman, R. E.; Fromm, J. R.; Weiler, J. M.; Linhardt, R. J. *Bioessays* **1998**, *20*, 156-167.

(3) Hirsh, J.; Warkentin, T. E.; Shaughnessy, S. G.; Anand, S. S.; Halperin, J. L.; Raschke, R.; Granger, C.; Ohman, E. M.; Dalen, J. E. *Chest* **2001**, *119*, 64S-95S.

(4) Capila, I.; Linhardt, R. J. *Angew. Chem. Int. Ed.* **2002**, *41*, 391-412.

(5) Khorana, A. A.; Sahni, A.; Altland, O. D.; Francis, C. W. *Arterioscler. Thromb. Vasc. Biol.* **2003**, *23*, 2110-2115.

(6) Quaranta, M.; Erez, O.; Mastrolia, S. A.; Koifman, A.; Leron, E.; Eshkoli, T.; Mazor, M.; Holcberg, G. *Peerj* **2015**, 2, 1-20.

(7) Olczyk, P.; Mencner, L.; Komosinska-Vassev, K. *Biomed. Res. Int.* **2015**, 1-7.

(8) Rosenberg, R. D.; Lam, L. *Proc. Nat. Acad. Sci. USA* **1979**, *76*, 1218-1222.

(9) Peysselon, F.; Ricard-Blum, S. *Matrix Biol.* **2014**, *35*, 73-81.

(10) Ornitz, D. M.; Yayon, A.; Flanagan, J. G.; Svahn, C. M.; Levi, E.; Leder, P. *Mol. Cell. Biol.* **1992**, *12*, 240-247.

(11) Li, Y.-C.; Ho, I. H.; Ku, C.-C.; Zhong, Y.-Q.; Hu, Y.-P.; Chen, Z.-G.; Chen, C.-Y.; Lin, W.-C.; Zulueta, M. M. L.; Hung, S.-C.; Lin, M.-G.; Wang, C.-C.; Hsiao, C.-D. *ACS Chem. Biol.* **2014**, *9*, 1712-1717.

(12) Schlessinger, J.; Plotnikov, A. N.; Ibrahimi, O. A.; Eliseenkova, A. V.; Yeh, B. K.; Yayon, A.; Linhardt, R. J.; Mohammadi, M. *Mol. Cell* **2000**, *6*, 743-750.

(13) Pellegrini, L.; Burke, D. F.; von Delft, F.; Mulloy, B.; Blundell, T. L. *Nature* **2000**, *407*, 1029-1034.

(14) Yingkai, L.; Kiick, K. L. *Acta Biomater.* **2014**, *10*, 1588-1600.

(15) Blossom, D. B.; Kallen, A. J.; Patel, P. R.; Elward, A.; Robinson, L.; Gao, G.; Langer, R.; Perkins, K. M.; Jaeger, J. L.; Kurkjian, K. M.; Jones, M.; Schillie, S. F.; Shehab, N.; Ketterer, D.; Venkataraman, G.; Kishimoto, T. K.; Shriver, Z.; McMahon, A. W.; Austen, K. F.; Kozlowski, S.; Srinivasan, A.; Turabelidze, G.; Gould, C. V.; Arduino, M. J.; Sasisekharan, R. *N. Engl. J. Med.* **2008**, *359*, 2674-2684.

(16) Guerrini, M.; Beccati, D.; Shriver, Z.; Naggi, A.; Viswanathan, K.; Bisio, A.; Capila, I.; Lansing, J. C.; Guglieri, S.; Fraser, B.; Al-Hakim, A.; Gunay, N. S.; Zhang, Z. Q.; Robinson, L.; Buhse, L.; Nasr, M.; Woodcock, J.; Langer, R.; Venkataraman, G.; Linhardt, R. J.; Casu, B.; Torri, G.; Sasisekharan, R. *Nat. Biotechnol.* **2008**, *26*, 669-675.

(17) Hirsh, J.; van Aken, W. G.; Gallus, A. S.; Dollery, C. T.; Cade, J. F.; Yung, W. L. *Circulation* **1976**, *53*, 691-695.

(18) Kroon, C.; ten Hove, W. R.; de Boer, A.; Kroon, J. M.; van der Pol, J. M.; Harthoorn-Lasthuizen, E. J.; Schoemaker, H. C.; van der Meer, F. J.; Cohen, A. F. *Circulation* **1992**, *86*, 1370-1375.

(19) Manson, L.; Weitz, J. I.; Podor, T. J.; Hirsh, J.; Young, E. *J. Lab. Clin. Med.* **1997**, *130*, 649-655.

(20) Warkentin, T. E.; Levine, M. N.; Hirsh, J.; Horsewood, P.; Roberts, R. S.; Gent, M.; Kelton, J. G. *N. Engl. J. Med.* **1995**, *332*, 1330-1335.

(21) Merli, G. J.; Groce, J. B. *P. T.* **2010**, *35*, 95-105.

(22) Linhardt, R. J.; Liu, J. *Curr. Opin. Pharmacol.* **2012**, *12*, 217-219.

(23) Middaugh, C. R.; Mach, H.; Burke, C. J.; Volkin, D. B.; Dabora, J. M.; Tsai, P. K.; Bruner, M. W.; Ryan, J. A.; Marfia, K. E. *Biochemistry* **1992**, *31*, 9016-9024.

(24) Hassan, H. H. A. M. *Mini Rev. Med. Chem.* **2007**, *7*, 1206-1235.

(25) Maynard, H. D.; Hubbell, J. A. *Acta Biomater.* **2005**, *1*, 451-459.

(26) Vazquez-Cameos, S.; St Hilaire, P. M.; Damgaard, D.; Meldal, M. *QSAR Comb. Sci.* **2005**, *24*, 923-942.

(27) Mammadov, R.; Mammadov, B.; Guler, M. O.; Tekinay, A. B. *Biomacromolecules* **2012**, *13*, 3311-3319.

(28) Kim, S. H.; Kiick, K. L. *Peptides* **2007**, *28*, 2125-2136.

(29) Miura, Y.; Fukuda, T.; Seto, H.; Hoshino, Y. *Polym. J.* **2016**, *48*, 229-237.

(30) Deirdre R. Coombe, W. C. K. Handb. Exp. Pharmacol. **2012**, *207*, 1-462.

(31) Logeart-Avramoglou, D.; Jozefonvicz, J. *J. Biomed. Mater. Res.* **1999**, *48*, 578-590.

(32) Alpsoy, E.; Er, H.; Durusoy, C.; Yilmaz, E. *Arch. Dermatol.* **1999**, *135*, 529-532.

(33) Stein, C. A.; Larocca, R. V.; Thomas, R.; McAtee, N.; Myers, C. E. *J. Clin. Oncol.* **1989**, *7*, 499-508.

(34) He, C.; Cheng, C.; Ji, H. F.; Shi, Z. Q.; Ma, L.; Zhou, M.; Zhao, C. S. *Polym. Chem.* **2015**, *6*, 7893-7901.

(35) Cheng, C.; Sun, S.; Zhao, C. *J. Mater. Chem. B* **2014**, *2*, 7649-7672.

(36) Tao Xiang, C.C.; Zhao, C. *J. Mem. Sep. Technol.* **2014**, *3*, 162-177.

(37) Ma, L.; Su, B. H.; Cheng, C.; Yin, Z. H.; Qin, H.; Zhao, J. M.; Sun, S. D.; Zhao, C. S. *J. Membr. Sci.* **2014**, *470*, 90-101.

(38) Deng, J.; Liu, X. Y.; Ma, L.; Cheng, C.; Shi, W. B.; Nie, C. X.; Zhao, C. S. *ACS Appl. Mater. Interfaces* **2014**, *6*, 21603-21614.

(39) Miura, Y. *Polym. J.* **2012**, *44*, 679-689.

(40) Arlov, O.; Aachmann, F. L.; Sundan, A.; Espevik, T.; Skjak-Braek, G. *Biomacromolecules* **2014**, *15*, 2744-2750.

(41) Ruvinov, E.; Freeman, I.; Fredo, R.; Cohen, S. *Nano Lett.* **2016**, *16*, 883-888.

(42) Ronghua, H.; Yumin, D.; Jianhong, Y. *Carbohydr. Polym.* **2003**, *52*, 19-24.

(43) Wang, Z.-M.; Xiao, K.-J.; Li, L.; Wu, J.-Y. *Cellulose* **2010**, *17*, 953-961.

(44) Groth, T.; Wagenknecht, W. *Biomaterials* **2001**, *22*, 2719-2729.

(45) Vikhoreva, G.; Bannikova, G.; Stolbushkina, P.; Panov, A.; Drozd, N.; Makarov, V.; Varlamov, V.; Gal'braikh, L. *Carbohydr. Polym.***2005**, *62*, 327-332.

(46) Suwan, J.; Zhang, Z.; Li, B.; Vongchan, P.; Meepowpan, P.; Zhang, F.; Mousa, S. A.; Mousa, S.; Premanode, B.; Kongtawelert, P.; Linhardt, R. J. *Carbohydr. Res.* **2009**, *344*, 1190-1196.

(47) Ding, K.; Wang, Y.; Wang, H.; Yuan, L.; Tan, M.; Shi, X.; Lyu, Z.; Liu, Y.; Chen, H. *ACS Appl. Mater. Interfaces* **2014**, *6*, 20043-20050.

(48) Mauzac, M.; Aubert, N.; Jozefonvicz, J. *Biomaterials* **1982**, *3*, 221-224.

(49) Mauzac, M.; Jozefonvicz, J. *Biomaterials* **1984**, *5*, 301-304.

(50) Crepon, B.; Maillet, F.; Kazatchkine, M. D.; Jozefonvicz, J. *Biomaterials* **1987**, *8*, 248-253.

(51) Meddahi, A.; Blanquaert, F.; Saffar, J. L.; Colombier, M. L.; Caruelle, J. P.; Josefonvicz, J.; Barritault, D. *Pathol. Res. Pract.* **1994**, *190*, 923-928.

(52) Meddahi, A.; Caruelle, J. P.; Gold, L.; Rosso, Y.; Barritault, D. *Diabetes Metab.* **1996**, *22*, 274-278.

(53) Albo, D.; Long, C.; Jhala, N.; Atkinson, B.; Granick, M. S.; Wang, T.; Meddahi, A.; Barritault, D.; Solomon, M. P. *J Craniofac. Surg.* **1996**, *7*, 19-22.

(54) Blanquaert, F.; Saffar, J. L.; Colombier, M. L.; Carpentier, G.; Barritault, D.; Caruelle, J. P. *Bone* **1995**, *17*, 499-506.

(55) Lafont, J.; Colombier, M. L.; Barritault, D.; Saffar, J. L. *J. Dent. Res.* **1998**, *77*, 1248-1248.

(56) Blanquaert, F.; Barritault, D.; Caruelle, J. P. *J. Biomed. Mater. Res.* **1999**, *44*, 63-72.

(57) Lafont, J.; Baroukh, B.; Berdal, A.; Colombier, M. L.; Barritault, D.; Caruelle, J. P.; Saffar, J. L. *Growth Factors* **1998**, *16*, 23-28.

(58) Lafont, J.; Blanquaert, F.; Colombier, M. L.; Barritault, D.; Carueelle, J. P.; Saffar, J. L. *Calcif. Tissue Int.* **2004**, *75*, 517-525.

(59) Meddahi, A.; Benoit, J.; Ayoub, N.; Sezeur, A.; Barritault, D. *J. Biomed. Mater. Res.* **1996**, *31*, 293-297.

(60) Fredjreygrobellet, D.; Hristova, D. L.; Ettaiche, M.; Meddahi, A.; Jozefonwicz, J.; Barritault, D. *Ophthalmic Res.* **1994**, *26*, 325-331.

(61) Desgranges, P.; Barbaud, C.; Caruelle, J. P.; Barritault, D.; Gautron, J. *FASEB J.* **1999**, *13*, 761-766.

(62) Meddahi, A.; Bree, F.; Papy-Garcia, D.; Gautron, J.; Barritault, D.; Caruelle, J. P. *J. Biomed. Mater. Res.* **2002**, *62*, 525-531.

(63) Papy-Garcia, D.; Barbosa, I.; Duchesnay, A.; Saadi, S.; Caruelle, J. P.; Barritault, D.; Martelly, I. *J. Biomed. Mater. Res.* **2002**, *62*, 46-55.

(64) Rouet, V.; Meddahi-Pelle, A.; Miao, H. Q.; Vlodavsky, I.; Caruelle, J. P.; Barritault, D. *J. Biomed. Mater. Res. Part A* **2006**, *78A*, 792-797.

(65) Tardieu, M.; Slaoui, F.; Josefonvicz, J.; Courty, J.; Gamby, C.; Barritault, D. *J. Biomater. Sci. Polym. Ed.* **1989**, *1*, 63-70.

(66) Tardieu, M.; Gamby, C.; Avramoglou, T.; Jozefonvicz, J.; Barritault, D. *J. Cell. Physiol.* **1992**, *150*, 194-203.

(67) Desgranges, F.; Barritault, D.; Caruelle, J. P.; Tardieu, M. *Int. J. Artif. Organs* **1997**, *20*, 589-598.

(68) Papy-Garcia, D.; Barbier-Chassefiere, V.; Rouet, V.; Kerros, M. E.; Klochendler, C.; Tournaire, M. C.; Barritault, D.; Caruelle, J. P.; Petit, E. *Macromolecules* **2005**, *38*, 4647-4654.

(69) Rouet, V.; Hamma-Kourbali, Y.; Petit, E.; Panagopoulou, P.; Katsoris, P.; Barritault, D.; Caruelle, J. P.; Courty, J. *J. Biol. Chem.* **2005**, *280*, 32792-32800.

(70) Barbier-Chassefiere, V.; Garcia-Filipe, S.; Yue, X. L.; Kerros, M. E.; Petit, E.; Kern, P.; Saffar, J. L.; Papy-Garcia, D.; Caruelle, J. P.; Barritault, D. *J. Biomed. Mater. Res. Part A* **2009**, *90A*, 641-647.

(71) Garcia-Filipe, S.; Barbier-Chassefiere, V.; Alexakis, C.; Huetl, E.; Ledoux, D.; Kerros, M. E.; Petit, E.; Barritault, D.; Caruelle, J. P.; Kern, P. *J. Biomed. Mater. Res. Part A* **2007**, *80A*, 75-84.

(72) Tong, M.; Tuk, B.; Hekking, I. M.; Vermeij, M.; Barritault, D.; van Neck, J. W. *Wound Repair Regen.* **2009**, *17*, 840-852.

(73) Tong, M.; Zbinden, M. M.; Hekking, I. J. M.; Vermeij, M.; Barritault, D.; van Neck, J. W. *Wound Repair Regen.* **2008**, *16*, 294-299.

(74) Tong, M.; Tuk, B.; Hekking, I. M.; Pleumeekers, M. M.; Boldewijn, M. B.; Hovius, S. E. R.; van Neck, J. W. *Wound Repair Regen.* **2011**, *19*, 505-514.

(75) Tong, M.; Tuk, B.; Shang, P.; Hekking, I. M.; Fijneman, E. M. G.; Guijt, M.; Hovius, S. E. R.; van Neck, J. W. *Diabetes* **2012**, *61*, 2633-2641.

(76) van Neck, J.; Tuk, B.; Barritault, D.; Tong, M. In *Tissue regeneration - From Basic Biology to Clinical Application*; Davies, J., Ed.; InTech: 2012, 1-520.

(77) Regan, J. R.; Bruno, J. G.; Chang, M. N.; Sabatino, R.; Dalisa, R.; Bensasson, S. A.; Eilat, D. *J. Bioact. Compat. Polym.* **1993**, *8*, 317-337.

(78) Benezra, M.; Vlodavsky, I.; Yayon, A.; Bar-Shavit, R.; Regan, J.; Chang, M.; Ben-Sasson, S. *Cancer Res.* **1992**, *52*, 5656-5662.

(79) Rogelj, S.; Weinberg, R. A.; Fanning, P.; Klagsbrun, M. *Nature* **1988**, *331*, 173-175.

(80) Benezra, M.; Bensasson, S. A.; Regan, J.; Chang, M.; Barshavit, R.; Vlodavsky, I. *Arterioscler., Thromb., Vasc. Biol.* **1994**, *14*, 1992-1999.

(81) Benezra, M.; Ishai-Michaeli, R.; Ben-Sasson, S. A.; Vlodavsky, I. *J. Cell. Physiol.* **2002**, *192*, 276-284.

(82) Yayon, A.; Klagsbrun, M.; Esko, J. D.; Leder, P.; Ornitz, D. M. *Cell* **1991**, *64*, 841-848.

(83) Ferrao, A. V.; Mason, R. M. *Biochim. Biophys. Acta Mol. Basis Dis.* **1993**, *1180*, 225-230.

(84) Ishihara, M.; Tyrrell, D. J.; Stauber, G. B.; Brown, S.; Cousens, L. S.; Stack, R. J. *J. Biol. Chem.***1993**, *268*, 4675-4683.

(85) Cariou, R.; Harousseau, J. L.; Tobelem, G. *Cell Biol. Int. Rep.* **1988**, *12*, 1037-1047.

(86) Miao, H. Q.; Ornitz, D. M.; Aingorn, E.; BenSasson, S. A.; Vlodavsky, I. *J. Clin. Invest.***1997**, *99*, 1565-1575.

(87) Katz, A.; Vlodavsky, I.; Davies, M.; Miao, H. Q.; BenSasson, S. A.; Darmon, D.; Hurwitz, H.; Borgel, H.; Benezra, M. *J. Am. Soc. Nephrol.* **1997**, *8*, 1688-1697.

(88) Schmidt, A.; Vlodavsky, I.; Volker, W.; Buddecke, E. *Atheroscler.* **1999**, *147*, 387-397.

(89) Benezra, M.; Vogel, T.; Ben-Sasson, S. A.; Panet, A.; Sehayek, E.; Al-Haideiri, M.; Decklbaum, R. J.; Vlodavsky, I. *J. Cell. Biochem.* **2001**, *81*, 114-127.

(90) Neuger, L.; Ruge, T.; Makoveichuk, E.; Vlodavsky, I.; Olivecrona, G. *Atheroscler.* **2001**, *157*, 13-21.

(91) Irony-Tur-Sinai, M.; Vlodavsky, I.; Ben-Sasson, S. A.; Pinto, F.; Sicsic, C.; Brenner, T. *J. Neurol. Sci.* **2003**, *206*, 49-57.

(92) Dulaney, S. B.; Huang, X. F. In *Adv. Carbohydr. Chem. Biochem.* **2012***, 67,* 95-136.

(93) Junqueira, D. R. G.; Perini, E.; Penholati, R. R. M.; Carvalho, M. G. *Cochrane Database Syst. Rev.* **2012**, *9*, CD007557-CD007557.

(94) Kusche, M.; Oscarsson, L. G.; Reynertson, R.; Roden, L.; Lindahl, U. *J. Biol. Chem.* **1991**, *266*, 7400-7409.

(95) Faham, S.; Hileman, R. E.; Fromm, J. R.; Linhardt, R. J.; Rees, D. C. *Science* **1996**, *271*, 1116-1120.

(96) Mach, H.; Volkin, D. B.; Burke, C. J.; Middaugh, C. R.; Linhardt, R. J.; Fromm, J. R.; Loganathan, D.; Mattsson, L. *Biochemistry* **1993**, *32*, 5480.

(97) Vazquez-Dorbatt, V.; Lee, J.; Lin, E. W.; Maynard, H. D. *Chem. Bio. Chem.* **2012**, *13*, 2478.

(98) Kitazawa, S.; Okumura, M.; Kinomura, K.; Sakakibara, T. *Chem. Lett.* **1990**, 1733-1736.

(99) Fukudome, N.; Suzuki, K.; Yashima, E.; Akashi, M. *J. Appl. Polym. Sci.* **1994**, *52*, 1759-1763.

(100) Akashi, M.; Sakamoto, N.; Suzuki, K.; Kishida, A. *Bioconjugate Chem.* **1996**, *7*, 393-395.

(101) Sakamoto, N.; Kishida, A.; Maruyama, I.; Akashi, M. *J. Biomater. Sci. Polym. Ed.* **1997**, *8*, 545-553.

(102) Onishi, M.; Miyashita, Y.; Motomura, T.; Yamashita, S.; Sakamoto, N.; Akashi, M. *J. Biomater. Sci. Polym. Ed.* **1998**, *9*, 973-984.

(103) Huang, Y.; Taylor, L.; Chen, X.; Ayres, N. *J. Polym. Sci. A* **2013**, *51*, 5230-5238.

(104) Huang, Y.; Shaw, M. A.; Mullins, E. S.; Kirley, T. L.; Ayres, N. *Biomacromolecules* **2014**, *15*, 4455-4466.

(105) Huang, Y.; Shaw, M. A.; Warmin, M. R.; Mullins, E. S.; Ayres, N. *Polym. Chem.* **2016**, *7*, 3897-3905.

(106) Taylor, L.; Chen, X.; Ayres, N. *Polym. Int.* **2014**, *63*, 127-135.

(107) Grande, D.; Baskaran, S.; Baskaran, C.; Gnanou, Y.; Chaikof, E. L. *Macromolecules* **2000**, *33*, 1123-1125.

(108) Grande, D.; Baskaran, S.; Chaikof, E. L. *Macromolecules* **2001**, *34*, 1640-1646.

(109) Baskaran, S.; Grande, D.; Sun, X. L.; Yayon, A.; Chaikof, E. L. *Bioconjugate Chem.* **2002**, *13*, 1309-1313.

(110) Sun, X. L.; Grande, D.; Baskaran, S.; Hanson, S. R.; Chaikof, E. L. *Biomacromolecules* **2002**, *3*, 1065-1070.

(111) Guan, R.; Sun, X. L.; Hou, S. J.; Wu, P. Y.; Chaikof, E. L. *Bioconjugate Chem.* **2004**, *15*, 145-151.

(112) Hou, S. J.; Sun, X. L.; Dong, C. M.; Chaikof, E. L. *Bioconjugate Chem.* **2004**, *15*, 954-959.

(113) Sun, X. L.; Faucher, K. M.; Houston, M.; Grande, D.; Chaikof, E. L. *J. Am. Chem. Soc.* **2002**, *124*, 7258-7259.

(114) Sanders, W. J.; Gordon, E. J.; Dwir, O.; Beck, P. J.; Alon, R.; Kiessling, L. L. *J. Biol. Chem.* **1999**, *274*, 5271-5278.

(115) Manning, D. D.; Strong, L. E.; Hu, X.; Beck, P. J.; Kiessling, L. L. *Tetrahedron* **1997**, *53*, 11937-11952.

(116) Manning, D. D.; Hu, X.; Beck, P.; Kiessling, L. L. *J. Am. Chem. Soc.***1997**, *119*, 3161-3162.

(117) Oh, Y. I.; Sheng, G. J.; Chang, S.-K.; Hsieh-Wilson, L. C. *Angew. Chem. Int. Ed.* **2013**, *52*, 11796-11799.

(118) Sheng, G. J.; Oh, Y. I.; Chang, S. K.; Hsieh-Wilson, L. C. *J. Am. Chem. Soc.* **2013**, *135*, 10898-10901.

(119) Lee, S.-G.; Brown, J. M.; Rogers, C. J.; Matson, J. B.; Krishnamurthy, C.; Rawat, M.; Hsieh-Wilson, L. C. *Chem. Sci.* **2010**, *1*, 322-325.

(120) Rawat, M.; Gama, C. I.; Matson, J. B.; Hsieh-Wilson, L. C. *J. Am. Chem. Soc.* **2008**, *130*, 2959-2961.

(121) Nishimura, Y.; Shudo, H.; Seto, H.; Hoshino, Y.; Miura, Y. *Bioorg. Med. Chem. Lett.* **2013**, *23*, 6390-6395.

(122) Miura, Y.; Yasuda, K.; Yamamoto, K.; Koike, M.; Nishida, Y.; Kobayashi, K. *Biomacromolecules* **2007**, *8*, 2129-2134.

(123) Miura, Y.; Mizuno, H. *Bull. Chem. Soc. Jpn.* **2010**, *83*, 1004-1009.

(124) Guan, R.; Sun, X.-L.; Hou, S.; Wu, P.; Chaikof, E. L. *Bioconjugate Chem.* **2004**, *15*, 145-151.

(125) Oh, Y. I.; Sheng, G. J.; Chang, S. K.; Hsieh-Wilson, L. C. *Angew. Chem. Int. Ed.* **2013**, *52*, 11796-11799.

(126) Sheng, G. J.; Oh, Y. I.; Chang, S.-K.; Hsieh-Wilson, L. C. *J. Am. Chem. Soc.* **2013**, *135*, 10898-10901.

(127) Liekens, S.; Leali, D.; Neyts, J.; Esnouf, R.; Rusnati, M.; Dell'Era, P.; Maudgal, P. C.; De Clercq, E.; Presta, M. *Mol. Pharmacol.* **1999**, *56*, 204-213.

(128) Liekens, S.; Neyts, J.; Degreve, B.; DeClercq, E. *Oncology Res.* **1997**, *9*, 173-181.

(129) Sangaj, N.; Kyriakakis, P.; Yang, D.; Chang, C. W.; Arya, G.; Varghese, S. *Biomacromolecules* **2010**, *11*, 3294-3300.

(130) Sedlak, E.; Fedunova, D.; Vesela, V.; Sedlakova, D.; Antalik, M. *Biomacromolecules* **2009**, *10*, 2533-2538.

(131) Wang, M.; Lyu, Z.; Chen, G.; Wang, H.; Yuan, Y.; Ding, K.; Yu, Q.; Yuan, L.; Chen, H. *Chem. Commun.* **2015**, *51*, 15434-15437.

(132) Sangaj, N.; Kyriakakis, P.; Yang, D.; Chang, C.-W.; Arya, G.; Varghese, S. *Biomacromolecules* **2010**, *11*, 3294-3300.

(133) Belleney, J.; Helary, G.; Migonney, V. *Eur. Polym. J.* **2002**, *38*, 439-444.

(134) Berlot, S.; Aissaoui, Z.; Pavon-Djavid, G.; Belleney, J.; Jozefowicz, M.; Helary, G.; Migonney, V. *Biomacromolecules* **2002**, *3*, 63-68.

(135) El Khadali, F.; Hélary, G.; Pavon-Djavid, G.; Migonney, V. *Biomacromolecules* **2002**, *3*, 51-56.

(136) Ran, F.; Nie, S.; Yin, Z.; Li, J.; Su, B.; Sun, S.; Zhao, C. *Int. J. Biol. Macromol.* **2013**, *55*, 269-275.

(137) Garcia-Fernandez, L.; Aguilar, M. R.; Fernandez, M. M.; Lozano, R. M.; Gimenez, G.; San Roman, J. *Biomacromolecules* **2010**, *11*, 626-634.

(138) Christman, K. L.; Vázquez-Dorbatt, V.; Schopf, E.; Kolodziej, C. M.; Li, R. C.; Broyer, R. M.; Chen, Y.; Maynard, H. D. *J. Am. Chem. Soc.* **2008**, *130*, 16585-16591.

(139) Nguyen, T. H.; Kim, S.-H.; Decker, C. G.; Wong, D. Y.; Loo, J. A.; Maynard, H. D. *Nat. Chem.* **2013**, *5*, 221-227.

(140) Nguyen, T. H.; Paluck, S. J.; McGahran, A. J.; Maynard, H. D. *Biomacromolecules* **2015**, *16*, 2684-2692.

(141) Paluck, S. J.; Nguyen, T. H.; Lee, J. P.; Maynard, H. D. *Biomacromolecules* **2016**.

(142) Matsusaki, M.; Serizawa, T.; Kishida, A.; Endo, T.; Akashi, M. *Bioconjugate Chem.* **2002**, *13*, 23-28.

(143) Matsusaki, M.; Serizawa, T.; Kishida, A.; Akashi, M. *Biomacromolecules* **2005**, *6*, 400-407.

(144) Cao, J.; Chen, Y.-W.; Wang, X.; Luo, X.-L. *J. Biomed. Mater. Res. Part A* **2011**, *97A*, 472-479.

(145) Platt, L.; Kelly, L.; Rimmer, S. *J. Mater. Chem. B* **2014**, *2*, 494-501.

(146) Christman, K. L.; Vazquez-Dorbatt, V.; Schopf, E.; Kolodziej, C. M.; Li, R. C.; Broyer, R. M.; Chen, Y.; Maynard, H. D. *J. Am. Chem. Soc.* **2008**, *130*, 16585-16591.

(147) Kolodziej, C. M.; Kim, S. H.; Broyer, R. M.; Saxer, S. S.; Decker, C. G.; Maynard, H. D. *J. Am. Chem. Soc.* **2012**, *134*, 247-255.

(148) Gospodarowicz, D.; Cheng, J. *J. Cell. Physiol.* **1986**, *128*, 475-484.

(149) Matsusaki, M.; Serizawa, T.; Kishida, A.; Akashi, M. *J. Biomed. Mater. Res. Part A* **2005**, *73A*, 485-491.

(150) Matsusaki, M.; Akashi, M. *Biomacromolecules* **2005**, *6*, 3351-3356.

(151) Zia, F.; Zia, K. M.; Zuber, M.; Tabasum, S.; Rehman, S. *Int. J. Biol. Macromol.* **2016**, *84*, 101-111.

(152) Grasel, T. G.; Cooper, S. L. *J. Biomed. Mater. Res.* **1989**, *23*, 311-338.

(153) Silver, J. H.; Hart, A. P.; Williams, E. C.; Cooper, S. L.; Charef, S.; Labarre, D.; Jozefowicz, M. *Biomaterials* **1992**, *13*, 339-344.

(154) Santerre, J. P.; Brash, J. L. *Macromolecules* **1991**, *24*, 5497-5503.

(155) Santerre, J. P.; Tenhove, P.; Vanderkamp, N. H.; Brash, J. L. *J. Biomed. Mater. Res.* **1992**, *26*, 39-57.

(156) Chen, K. Y.; Kuo, J. F.; Chen, C. Y. *Biomaterials* **2000**, *21*, 161-171.

(157) Dal Park, H.; Lee, W. K.; Ooya, T.; Park, K. D.; Kim, Y. H.; Yui, N. *J. Biomed. Mater. Res.* **2002**, *60*, 186-190.

(158) Joung, Y. K.; Sengoku, Y.; Ooya, T.; Park, K. D.; Yui, N. *Sci. Technol. Adv. Mater.* **2005**, *6*, 484-490.

(159) Terauchi, M.; Ikeda, G.; Nishida, K.; Tamura, A.; Yamaguchi, S.; Harada, K.; Yui, N. *Macromol. Biosci.* **2015**, *15*, 953-964.

(160) Bailey, W. J.; Ni, Z.; Wu, S. R. *Macromolecules* **1982**, *15*, 711-714.

(161) Lutz, J.-F.; Andrieu, J.; Uezguen, S.; Rudolph, C.; Agarwal, S. *Macromolecules* **2007**, *40*, 8540-8543.

(162) Siegwart, D. J.; Bencherif, S. A.; Srinivasan, A.; Hollinger, J. O.; Matyjaszewski, K. *J. Biomed. Mater. Res. Part A* **2008**, *87A*, 345-358.

(163) Delplace, V.; Tardy, A.; Harrisson, S.; Mura, S.; Gigmes, D.; Guillaneuf, Y.; Nicolas, J. *Biomacromolecules* **2013**, *14*, 3769-3779.

(164) Decker, C. G.; Maynard, H. D. *Eur. Polym. J.* **2015**, *65*, 305-312.

(165) Hedir, G. G.; Bell, C. A.; O'Reilly, R. K.; Dove, A. P. *Biomacromolecules* **2015**, *16*, 2049-2058.

Chapter 2

A Heparin-Mimicking Block Copolymer Stabilizes and Increases the Activity of Fibroblast Growth Factor 2 (FGF2)[†]

2.1 Introduction

There is growing interest in biomaterials capable of treating ischemic conditions and promoting healing in burned and wounded tissues. Approximately 0.15% of Americans suffer from limb ischemia each year (2011),[1] 1-2% from chronic wounds (2004),[2,3] and 450,000 from acute burn injuries (2014).[4] Together, treatments for chronic wounds cost over 35 billion dollars annually as of 2007 in the United States alone.[2,5] One important factor to consider in the successful development of biomaterials for treatment of ischemia and wound repair is the promotion of vascularization. Cellular proliferation, migration, and angiogenesis are crucial for formation of new vasculature and are key processes in tissue repair. In normal healing processes, growth factors are typically produced in wounds and act as signaling molecules to stimulate growth and new tissue formation.[6] In ischemic, burned, and chronically wounded tissues, these processes are impaired.[7] Many biomaterials have been developed to promote angiogenesis. These include hydrogels, topical creams, growth factors, small molecules, and polymers.[8,9] Yet, there is still interest in developing new options for successful treatment of ischemic and chronic wounds.

Fibroblast growth factor 2, or FGF2, is a 17 kDa heparin-binding protein that promotes a variety of cellular processes including cell proliferation, migration, vasculogenesis, cell differentiation, and stem cell self-renewal.[10,11] Additionally, FGF2 has been shown to play a crucial role in tissue repair, angiogenesis, bone growth, and neuroregeneration.[12] Decreased concentrations of growth factors including FGF2 in chronic wounds and ischemic conditions are known to inhibit these cellular processes, thereby preventing healing and angiogenesis.[7,13] This decrease in FGF2 combined with the advantageous effects of FGF2 in tissue regeneration have led to new biomaterials and

topical applications of FGF2 and other growth factors for treatment of chronic wounds.[14,15] For example, it has been shown that delivery of various growth factors such as FGF and VEGF increases the amount of angiogenesis, and thus pro-angiogenic treatments involving these proteins have been widely studied.[16] However, while these treatments have shown improved angiogenesis and tissue healing *in vitro*, their efficacy in clinical trials has been limited.[17] To overcome this obstacle, superagonists of FGF2 and other growth factors have been studied to increase the mitogenic response in chronic wounds. These agonists have shown improved cellular response when compared to FGF2 alone and therefore, can be used to make up for the lower receptor count and lower growth factor concentrations due to growth factor degradation in diabetic patients.[18] There are several known superagonists of FGF2 including protein mutants,[19-21] protein dimers,[22,23] FGF2 oligomers,[24] peptide sequences,[25,26] and protein conjugates.[27] Additionally, growth factor combination therapies have been employed to improve the activity of exogenously applied growth factors.[28,29]

Heparinoid complexes and heparin have also been employed to increase the activity of FGF2.[30] Heparin, a highly sulfated glycosaminoglycan, stabilizes FGF2[31] and promotes protein dimerization resulting in receptor dimerization and triggering of phosphorylation and eventual cell growth, migration, and angiogenesis.[32] Heparinoids are derivatives of heparin and typically are sulfated oligoheparin fragments, often well defined in length. Due to the important role of heparin in FGF2 activity, both heparin and heparinoids have been used to stabilize[33] or alter the activity of FGF2.[34] In addition, heparin has been employed in many other Food and Drug Administration (FDA) approved therapeutics including treatment of angina,[35] thrombosis[36] and myocardial infarction.[37] Heparin has also been shown to be efficacious in the treatment of chronic wounds and burns,[38,39] prevention of

metastatic cancer,[40] reduction of inflammation,[41] and is FDA approved as an antithrombotic and anticoagulant.[42]

Growth factor superagonists are helpful in increasing cellular response for new therapeutics; however, another obstacle in the successful use of FGF2 as a therapeutic protein drug is its instability.[43,44] FGF2 is quickly degraded during storage and upon delivery *in vivo*. Covalent protein-polymer conjugates have been used as a means of protein stabilization in the past and many conjugation chemistries have been explored. The covalent conjugation of poly(ethylene glycol) (PEG) to proteins (PEGylation) has become a popular means to stabilize proteins, with 10 FDA approved PEGylated proteins on the market.[45] While PEGylation provides increased stability, decreased immunogenicity, and increased blood half life, moving toward biomimetic polymers for use in protein conjugates could improve biological function and provide better stability.

In vivo, FGF2 is stabilized by heparin, allowing the protein to reach its target. While heparin and heparinoids provide many desirable therapeutic effects, they are susceptible to *in vivo* degradation and desulfation by heparinases.[46] Additionally, heparin is isolated from animal tissues and is susceptible to high batch-to-batch variability.[47] Fractionating the biomolecule has circumvented some negative effects of heparin, but this process is often costly.[48] Because of the downsides of heparin, there have been many reports of heparin mimics designed to provide the desired effects of heparin while minimizing heterogeneity and desulfation *in vivo*.[49] These include various polysacharides,[50] sulfonated dextrans,[51,52] sulfonated and sulfated polymers,[53,54] anionic polymers,[55] peptides,[56] sulfated glycopolymers,[57] and ionomers.[58,59] These alternatives have been used for protein stabilization,[60] anticoagulation,[57] and stimulation of cellular processes.[61] We previously

reported that conjugating a heparin-mimicking polymer, poly(sodium 4-styrenesulfonate-*co*-poly(ethylene glycol) methyl ether methacrylate) p(SS-*co*-PEGMA) (molecular weight 23.0 kDa), stabilized FGF2 to various stressors including heat and long-term storage.[60] Although stabilization of FGF2 improves the outlook for its therapeutic use, we found that unlike heparin, the conjugate was not able to facilitate the dimerization of FGF receptors (FGFRs) in cells lacking heparan sulfate proteoglycans.[60] As a result, we subsequently screened various sulfonated polymers to identify other heparin-mimicking polymers that could facilitate receptor binding and dimerization.[54] We identified that poly(vinylsulfonate) (pVS) exhibited heparin-like activity by enabling the binding of FGF2 to its high affinity receptors when added as an excipient.[54] Herein, we describe the combination of these two polymer types into a block copolymer containing both stabilizing and FGF2 binding sequences, namely FGF2-p(SS-*co*-PEGMA)-*b*-VS (Figure 2-1). The conjugation of this new heparin-mimicking block copolymer to FGF2 and evidence of resulting increased stability and growth factor activity is discussed herein.

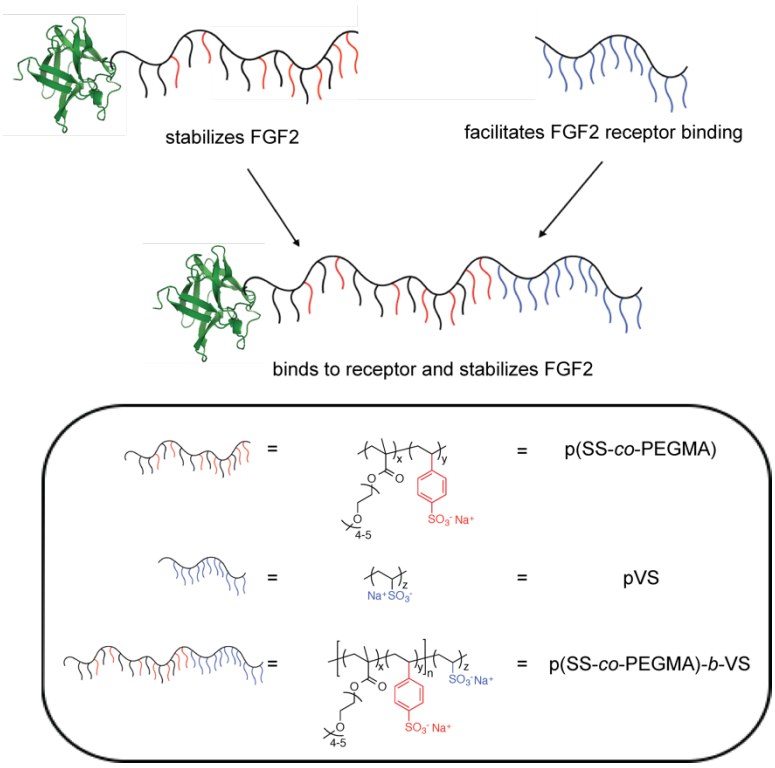

Figure 2-1. Polymer p(SS-*co*-PEGMA) stabilizes FGF2 as a conjugate and pVS facilitates FGF2-receptor binding when added as an excipient. When combined into a block copolymer, p(SS-*co*-PEGMA)-*b*-VS, the new conjugate both stabilizes FGF2 and increases protein activity. Protein structure modified from PDB 1CVS using PyMOL software.

2.2 Results and Discussion

2.2.1 Stability Study of FGF2-pVS Conjugate

In our recent report, pVS was added (not conjugated) to FGF2 and promoted proliferation in cells lacking native heparan sulfate proteoglycans; remarkably, the activity of FGF2 with pVS was the same as the positive control with added heparin.[54] We then wanted to investigate whether conjugating pVS to FGF2 would additionally stabilize the protein to storage. To explore this, a protein-reactive pVS polymer was prepared (Scheme

2-1). This was accomplished by synthesizing a chain transfer agent containing a cysteine-reactive pyridyl disulfide (PDS) group for protein conjugation and a xanthate functionality to accommodate the polymerization of deactivated VS monomer (Scheme 2-1a). Reversible addition-fragmentation chain-transfer (RAFT) polymerization of vinyl sulfonate (VS) was performed with the xanthate CTA, 2, to yield PDS end functionalized pVS (Scheme 2-1b). VS monomer was added with a feed ratio of [VS]:[CTA]:[V501] = 300:1:0.5 to yield a polymer with a degree of polymerization of 135 and molecular weight dispersities (*Đ*) of 1.16. Next, covalent conjugates were prepared through disulfide exchange of the PDS-pVS with a surface exposed cysteine on FGF2 (Scheme 2-1c). The conjugations were performed on a heparin resin column to prevent active site conjugations as previously described, and then used for subsequent studies after centrifugal filtration.[60] The FGF2-pVS conjugate was examined for its ability to stabilize FGF2 to storage. The conjugate or FGF2 was incubated at a concentration of 0.05 ng/μL at either 4 ºC or 23 ºC for 7 days. After 7 days, protein activity was evaluated through a cell proliferation assay in human dermal fibroblasts (HDFs). The results were compared to FGF2-p(SS-*co*-PEGMA) and pristine FGF2 as positive controls (Figure 2-2). Although FGF2-pVS showed stabilization effects, it was not to the same extent as our previously reported conjugate, FGF2-p(SS-*co*-PEGMA); the pVS conjugate exhibited statistically higher proliferation when compared to stressed FGF2, however it did not maintain activity as high as pristine FGF2, especially at 23 ºC.

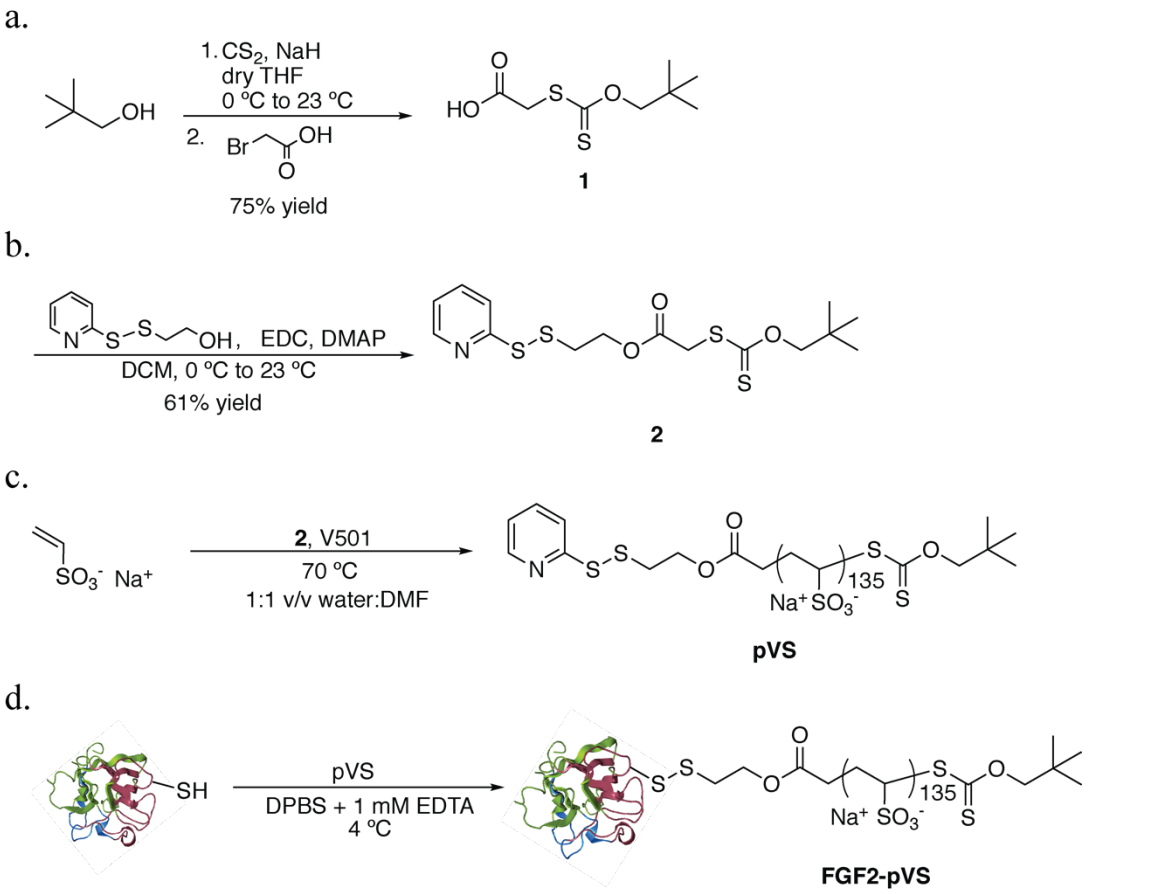

Scheme 2-1. (a) Synthesis of xanthate CTA. (b) RAFT polymerization of pVS polymer and (c) protein polymer conjugation of pVS to FGF2. Protein structure modified from PDB 1CVS using PyMOL software.

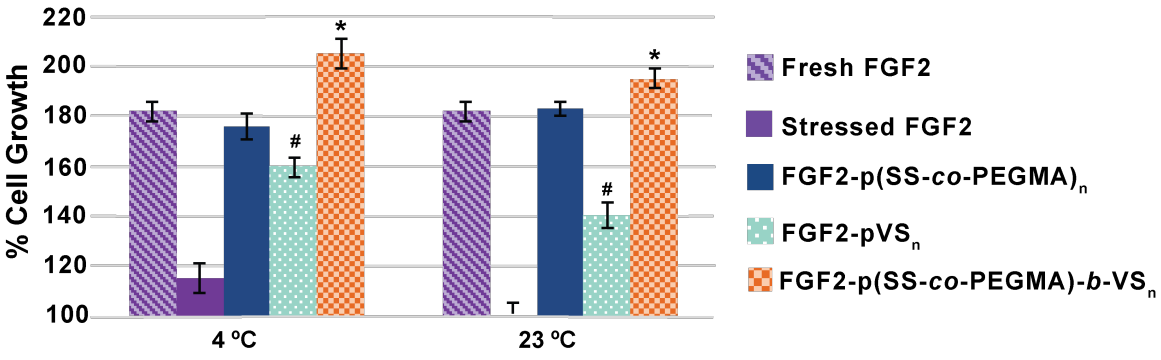

Figure 2-2. Stability study of conjugates in human dermal fibroblasts at both 4 ºC and 23 ºC after 7 days. Protein and conjugates were stressed at 0.5 ng/µL and plated for

proliferation study in HDFs at 1 ng/mL. Each sample was plated with six repeats. Error bars represent standard deviation. Statistical analysis was done using Student's t-test. * $p < 0.01$ compared to fresh FGF2. # $p < 0.005$ compared to fresh FGF2.

2.2.2 Synthesis of p(SS-*co*-PEGMA)-*b*-VS

To overcome this issue, we hypothesized that by combining the stabilizing polymer, p(SS-*co*-PEGMA) and the receptor activating polymer, pVS, into a single block copolymer conjugate, we could fabricate a new conjugate that would not only stabilize FGF2, but also facilitate protein-receptor binding, thus increasing protein activity. One of the difficulties with this approach was that the first block contains activated monomers and the second block deactivated monomers. Thus, a new CTA was designed to balance the requirements of both activated (styrene sulfonate and PEGMA) and deactivated (vinyl sulfonate) monomers (Scheme 2-2a). Specifically, the CTA contained dimethyl substituents at the fragmentation site (R group) to better match the rate of addition and fragmentation during SS and PEGMA polymerization, and the xanthate group was retained to accommodate the deactivated VS monomer through a RAFT/MADIX type mechanism.[62] The CTA was first used in the RAFT polymerization of styrene sulfonate and PEGMA with initial feed ratio of [SS]:[PEGMA]:[CTA]:[AIBN] = 35:10:1:0.2 to afford the p(SS-*co*-PEGMA) macro-CTA with a ratio of monomer incorporation of 2.2:1 SS:PEGMA (Scheme 2-2b). This macro-CTA was used in a subsequent RAFT polymerization with VS monomer to afford p(SS-*co*-PEGMA)-*b*-VS (50.7 kDa by ^{1}H NMR, $Đ$ = 1.20) as shown in Scheme 2-2c. Incorporation of the VS monomer was observed by ^{1}H NMR by an increase in backbone hydrogens between 0-2.8 ppm when compared to styrene sulfonate protons. ^{1}H NMR analysis also revealed a loss in PDS end group (approximately 30% overall), most likely

due to hydrolysis of the ester linkage during polymerization. Yet, the remaining end group was still sufficient for conjugation since an excess of polymers was utilized in the reaction. Additional evidence for VS incorporation was obtained through GPC analysis, which showed a molecular weight increase from 15.1 kDa for the macro-CTA to 28.3 kDa for the block copolymer.

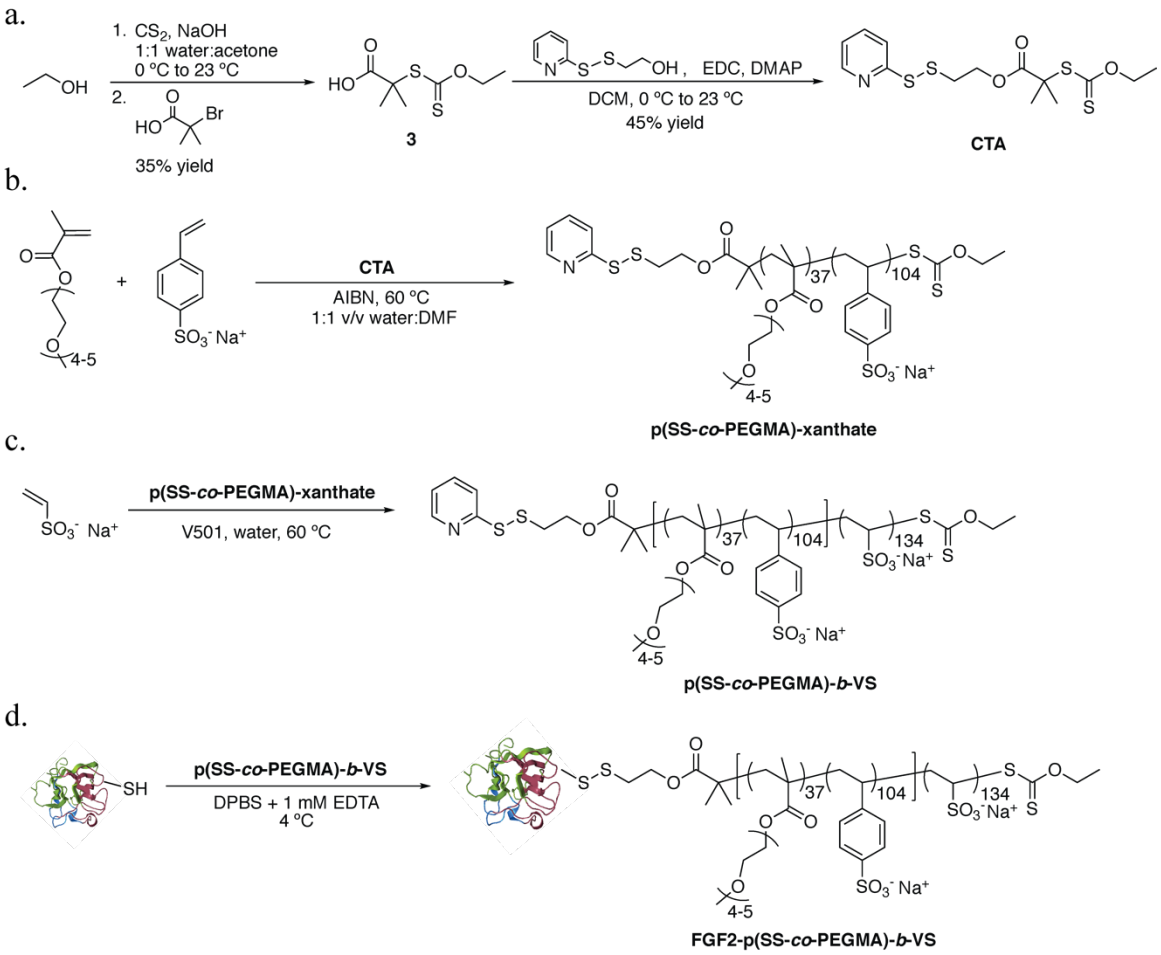

Scheme 2-2. (a) Synthesis of **CTA**, (b) RAFT polymerization of p(SS-*co*-PEGMA) to yield macro CTA, (c) subsequent RAFT polymerization to yield block copolymer p(SS-*co*-PEGMA)-*b*-VS, and (d) protein polymer conjugation to FGF2 conducted on a heparin column. Protein structure modified from PDB 1CVS using PyMOL software.

2.2.3 Cytotoxicity Study of p(SS-*co*-PEGMA)-*b*-VS

Toxicity tests of the polymer revealed that the block resulted in no loss of cell viability up to 1 mg/mL in both HDFs and HUVEC lines, with a slight loss in activity above that concentration (Figure 2-3). However, even 1 mg/mL is more than 1000 times over the concentration that the polymer would be used in the conjugate.

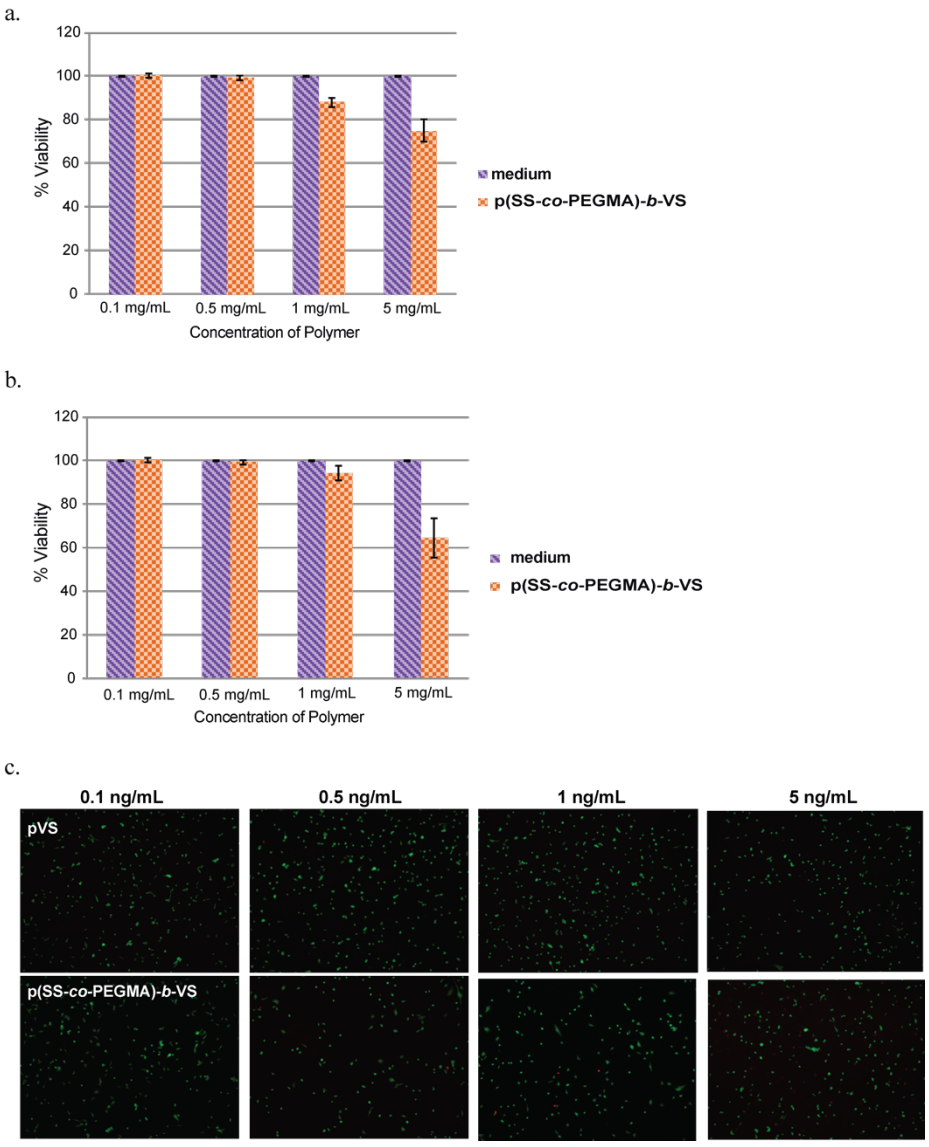

Figure 2-3. Polymer Cytotoxicity in (a) human umbilical vein endothelial cells and (b) human dermal fibroblasts (100% represents value for blank media). (c) representative

images of cells with live cells stained green and dead cells stained red.

2.2.4 Conjugation of p(SS-*co*-PEGMA)-*b*-VS to FGF2

The resulting polymer was then conjugated to FGF2 by incubation on a heparin resin column as previously described, in phosphate buffer at pH 7.4 (Scheme 2-2d). Successful conjugation was confirmed by sodium dodecyl sulfate-polyacrylamide gel electrophoresis (SDS-PAGE) (Figure 2-4a). The conjugate then was purified by centrifugation filtration to yield FGF2-p(SS-*co*-PEGMA)-*b*-VS conjugate. Western Blot of the native-PAGE confirmed that the conjugate was still intact and immunologically active (Figure 2-4b). There are two surface exposed cysteines in FGF2, and we have found that by performing polymer conjugation on heparin resin, only one of the two cysteines is modified.[60] Elman's assay was employed to determine the amount of free thiols and confirmed that approximately one cysteine was modified.

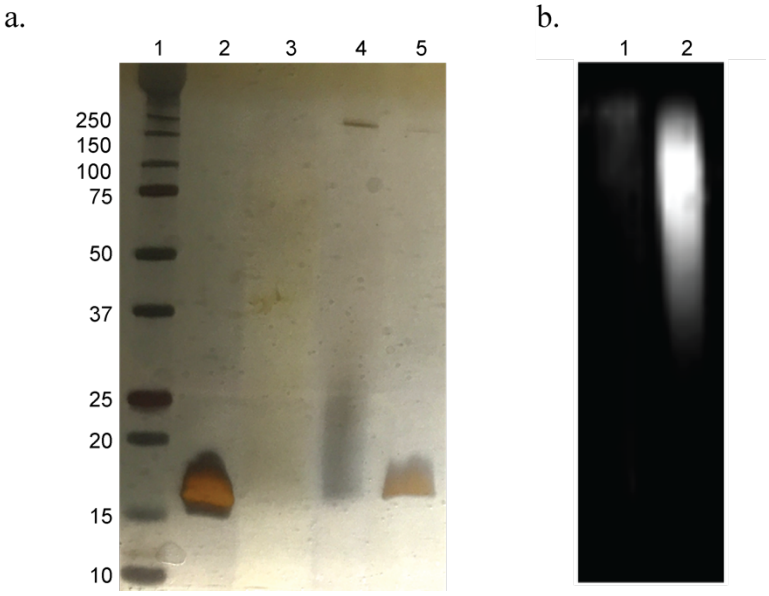

Figure 2-4. (a) SDS-PAGE of crude conjugate (stained with silver nitrate). Lane 1: Protein ladder; Lane 2: FGF2; Lane 3: p(SS-*co*-PEGMA)-*b*-VS; Lane 4: FGF2-p(SS-*co*-PEGMA)-

b-VS in non-reducing conditions; Lane 5: FGF2-p(SS-*co*-PEGMA)-*b*-VS in reducing conditions. (b) Western blot of native-PAGE of purified conjugate. Lane 1: FGF2; Lane 2: FGF2-p(SS-*co*-PEGMA)-*b*-VS.

2.2.5 Stability Study of p(SS-*co*-PEGMA)-*b*-VS

After successfully making the FGF2-p(SS-*co*-PEGMA)-*b*-VS conjugate, stability studies were performed to determine whether the new block copolymer conjugate could stabilize FGF2 at a concentration of 0.05 ng/μL at either 4 ºC or 23 ºC for 7 days. As shown in Figure 2.5, FGF2-p(SS-*co*-PEGMA)-*b*-VS completely stabilized FGF2. In fact, there appeared to be a slight, but significant increase in cell growth, which indicated an enhancement of activity, suggesting that the polymer may increase growth factor activity. It should be noted that the conjugate linkages during storage in buffer at 4 ºC were observed by native PAGE to be intact out to at least 1 year and 9 months. However, if in the future greater chemical stability is required for in vivo use, the polymer end group could be readily altered to contain an amide rather than an ester, and a thiol ether rather than a disulfide bond.

2.2.6 FGF2-p(SS-*co*-PEGMA)-*b*-VS Receptor Binding Assays

To investigate whether FGF2-p(SS-*co*-PEGMA)-*b*-VS facilitated receptor binding, we first tested the conjugate for its effects on cell proliferation in BaF3-FR1C cells. This cell line lacks native heparan sulfate proteoglycans on the cell surface and requires added heparin to observe significant FGF2-induced proliferation.[63] Thus, this cell line allows for indirect determination of the effect of heparin-mimicking polymers on FGF/FGFR binding. The conjugate was compared to FGF2 alone, as well as FGF2 plus an excess of

heparin. At a protein concentration of 0.5 ng/mL, the FGF2-p(SS-*co*-PEGMA)-*b*-VS conjugate increased cell growth more than native FGF2, with percent proliferation values of 352 ± 45% for the block copolymer and 151 ± 9% for FGF2, (Figure 2-5). Furthermore, the block copolymer conjugate, FGF2-p(SS-*co*-PEGMA)-*b*-VS, increased cell proliferation to the same extent as the positive control sample incubated with added 1 μg/mL heparin. The same trend was observed with protein concentrations of 1.5 ng/mL and 10 ng/mL. These data suggest that the FGF2-p(SS-*co*-PEGMA)-*b*-VS conjugate successfully bound to and activated the FGF receptors. This further suggested that the block copolymer could facilitate binding of FGF to its receptors.

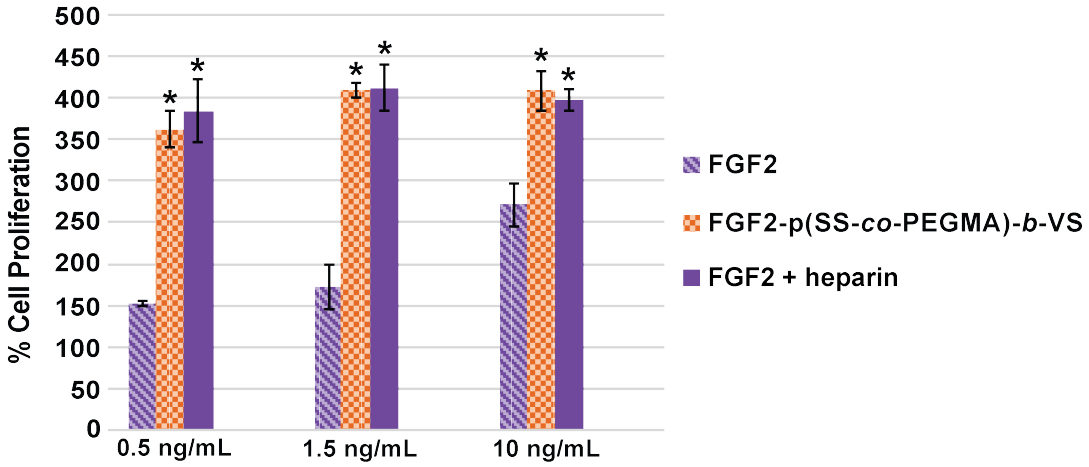

Figure 2-5. Cell Growth of heparin-mimicking polymer conjugates in BaF3-FR1C cells. Incubation of 20,000 cells/well in a 96-well plate with FGF2 or the heparin-mimicking polymer conjugates in the absence or presence of 1 μg/mL of heparin was carried out for 48 hours. CellTiter®-Blue assay was performed to quantify the extent of cell growth. Data was normalized to the blank medium group, which was set at 100%. Each sample contained four replicates and the experiment was repeated three times. Error bars represent standard error of the mean (SEM). Statistical analysis was done using Student's t-test. * $p < 0.01$ compared to FGF2.

To verify that the block copolymer in FGF2-p(SS-*co*-PEGMA)-*b*-VS was capable of facilitating binding of FGF2 to the receptor, we performed a receptor based enzyme linked immunosorbent assay (ELISA). In this assay, FGF receptor 1α was plated in the wells of a 96 well plate and then either free protein (negative control) or conjugate were plated to assay degree of binding. Since heparin is known to facilitate receptor binding, 1 ng/mL FGF2 plus excess heparin (1 μg/mL) was used as a benchmark positive control to determine desired binding. As shown in Figure 2-6, p(SS-*co*-PEGMA)-*b*-VS in the conjugate facilitated FGF2/FGFR binding similarly to heparin. The results for the block copolymer conjugate correlate to the cell-based results above and demonstrate that the polymer facilitates FGF2 binding to the receptor.

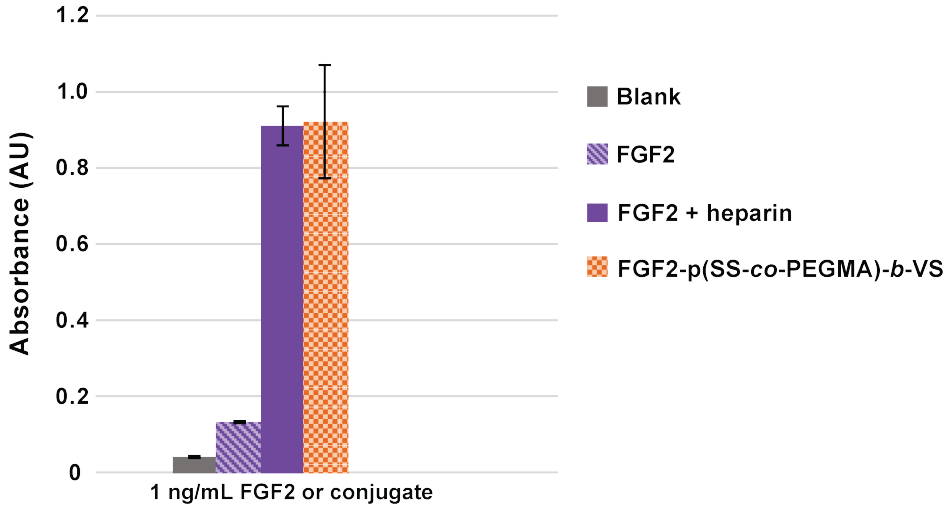

Figure 2-6. FGF Receptor based ELISA. Samples were incubated with 1 ng/mL FGF2, 1 ng/mL conjugate, or 1 ng/mL FGF2 plus 1 μg/mL heparin added as excipient. The experiment was repeated twice with n = 3. Error bars represent standard deviation.

2.2.7 Cell Proliferation Study with FGF2-p(SS-*co*-PEGMA)-*b*-VS

Since the conjugate was active in the BaF3-FR1C cell line, FGF2-p(SS-*co*-PEGMA)-*b*-VS was also tested in normal human cell lines for the effect on proliferation. In human dermal fibroblasts the conjugates were tested at increasing concentrations and were compared to FGF2 alone. FGF2-p(SS-*co*-PEGMA)-*b*-VS performed marginally better than FGF2 at concentrations of 1.5 ng/mL, 3 ng/mL and 5 ng/mL (Figure 2-7a). At lower concentrations of 0.5 ng/mL and 1 ng/mL, the protein-polymer conjugate and FGF2 exhibited statistically similar proliferation. The experiment was repeated in human umbilical vein endothelial cells (HUVECs) and the results showed that FGF2-p(SS-*co*-PEGMA)-*b*-VS conjugate stimulated cell proliferation only slightly better than FGF2 alone at all concentrations tested, 0.5 ng/mL, 1.0 ng/mL, 1.5 ng/mL, 3 ng/mL and 5 ng/mL (Figure 2-7b). These experiments suggest that FGF2-p(SS-*co*-PEGMA)-*b*-VS does not greatly increase cell proliferation in normal cell lines containing heparin sulfate proteoglycans. In our previous study whereby FGF2 was dimerized by PEG, we noticed that cell migration and angiogenesis were significantly affected by the architecture, greater than HUVEC proliferation.[23] Thus, we went on to further examine the effects of FGF2-p(SS-*co*-PEGMA)-*b*-VS on *in vitro* migration and tubulogenesis assays.

a.

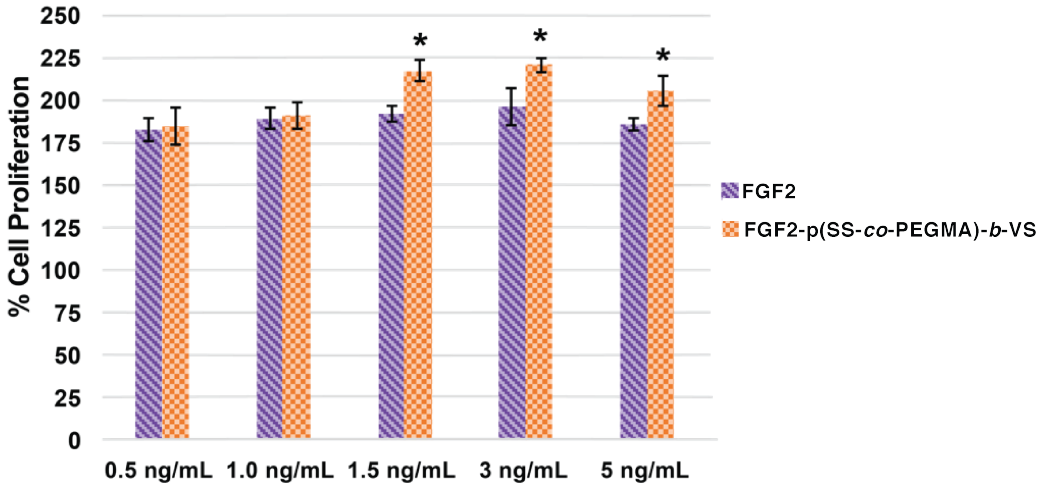

b.

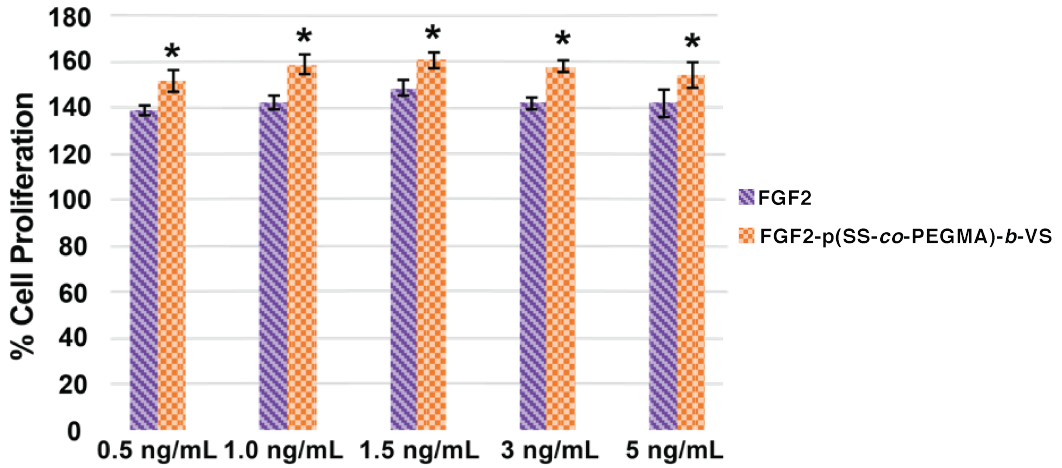

Figure 2-7. a) HUVEC comparing cell growth when incubated with FGF2-p(SS-*co*-PEGMA-*b*-VS) and c) HDF comparing cell growth when incubated with FGF2-p(SS-*co*-PEGMA-*b*-VS). Data was normalized to cells incubated with medium alone (set to 100%). Six replicates per sample, error bars represent standard deviation. Statistical analysis was done using Student's t-test. * $p < 0.01$ compared to FGF2.

2.2.8 In-Vitro Migration/Angiogenesis Assays with FGF2-p(SS-*co*-PEGMA)-*b*-VS

FGF2 is known to stimulate both migration and vasculogenesis of endothelial

cells.[64-66] First we performed a scratch migration assay to determine if FGF2-p(SS-*co*-PEGMA)-*b*-VS stimulates endothelial cell migration. As shown in Figure 2-8a and 2-8b, 10 ng/mL FGF2-p(SS-*co*-PEGMA)-*b*-VS induced migration of endothelial cells better than 10 ng/mL FGF2 after 18 hours, with a migration percentage of 214 ± 6% for the conjugate compared to 139 ± 4% for the native protein (blank media set at 100%). It also induced migration better than the addition of 1 μg/mL of heparin to FGF2. The heparin control did not induce cell migration, which was not unexpected, since it has been previously reported that added heparin at high concentrations has little effect on endothelial cell migration in combination with FGF2, and sometimes even displays inhibitory effects.[67] To ensure the observed effect of migration was not due to the ability of the conjugate to induce greater HUVEC proliferation, we quantified cell proliferation after the 18-hour incubation period. The percent of cell growth induced by the conjugate was not statistically different than native protein (Figure 2.8c) because of the shorter incubation period (18 hours versus 73 hours in Figure 2.7a) as has been previously reported.[65]

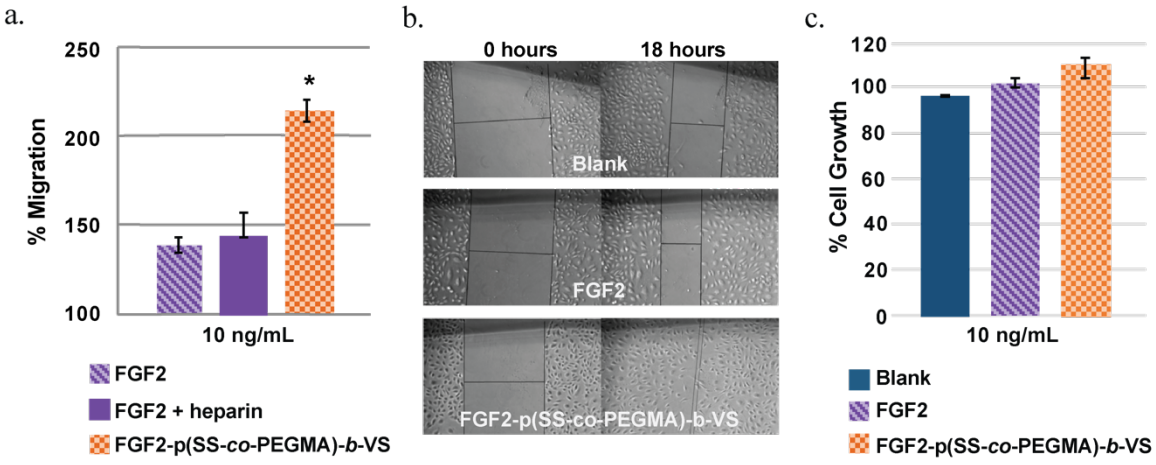

Figure 2-8. HUVEC migration after 18 hours. (a) Percent migration in the presence of FGF2, FGF2 plus 1 μg/mL of heparin, or FGF2-p(SS-*co*-PEGMA)-*b*-VS. Percent

migration was calculated using the formula: 100% − (distance at T0 /distance at T18) and blank medium was set at 100%. Each sample contained four to six replicates and the experiment was repeated three times, with each repeat being blinded. Error bars represent SEM. (b) Representative images of HUVEC migration taken at 0 hours and 18 hours. Statistical analysis was done using Student's t-test. * $p < 0.01$ compared to FGF2. (c) Cell growth measured after 18-hour incubation using CellTiter-Blue®. Data was normalized to blank medium (0%). Error bars represent SEM.

FGF2 also induces angiogenesis.[66] To begin to determine if the diblock copolymer conjugate had similar effects on angiogenesis as FGF2, a simple *in vitro* co-culture assay was performed.[68-70] In this assay, fibroblasts are first grown to confluency. During this incubation period, the fibroblasts produce a layer of collagen, which provides a matrix for endothelial cells to burrow in. After the fibroblasts reach confluency, a layer of endothelial cells are plated along with sample solutions in starvation medium. This assay provides information on the two-dimensional aspects of angiogenesis, but does not provide any information about the three-dimensional aspects, such as tubular structure and perfusion of vessels.

The endothelial cells were allowed to grow over 14 days with medium/sample changes every 2-3 days. Cord-like structures could be observed after antibody staining for CD-31 (or PECAM-1), a glycoprotein present at cell-cell junctions of vascular endothelial

cells.[71] In wells incubated with starvation medium alone, no cord-like structures were formed; however, when FGF2 was added to the starvation medium, cord-like structures became apparent at concentrations as low as 0.5 ng/mL. Samples were measured for an increase in length of cord-like structures, total number of cord-like structures, and the number of nodes compared to FGF2 alone. In wells containing the FGF2-p(SS-*co*-PEGMA)-*b*-VS conjugate, the number and length of cord-like structures, as well as the nodes were significantly increased compared to FGF2 alone (Figure 2-9a), suggesting that the protein-polymer conjugate induced cord-like structures better than the native protein. Control wells containing FGF2 plus 1 μg/mL heparin induced cord-like structure formation to a significantly lesser extent than FGF2-p(SS-*co*-PEGMA)-*b*-VS, and in some cases even showed a slight inhibitory effect. It has previously been reported that large concentrations of heparin have an inhibitory effect on angiogenesis; thus these data are not unexpected.[72] In order to determine whether excess polymer as an excipient would act similarly to heparin, control wells containing FGF2 plus 1 μg/mL free polymer were tested, and indeed the results were similar to added heparin. These results highlight the benefits of conjugating the polymer to the protein, and thus using the polymer at a small concentration, rather than as an additive in excess. Representative images of cord like structure formation are shown in Figure 2-9b. These results also indicate that the block copolymer conjugate could potentially induce angiogenesis better than FGF2 alone. In the future, more in depth three-

dimensional assays will be carried out to fully determine the success of FGF2-p(SS-*co*-PEGMA)-*b*-VS as an inducer of angiogenesis.

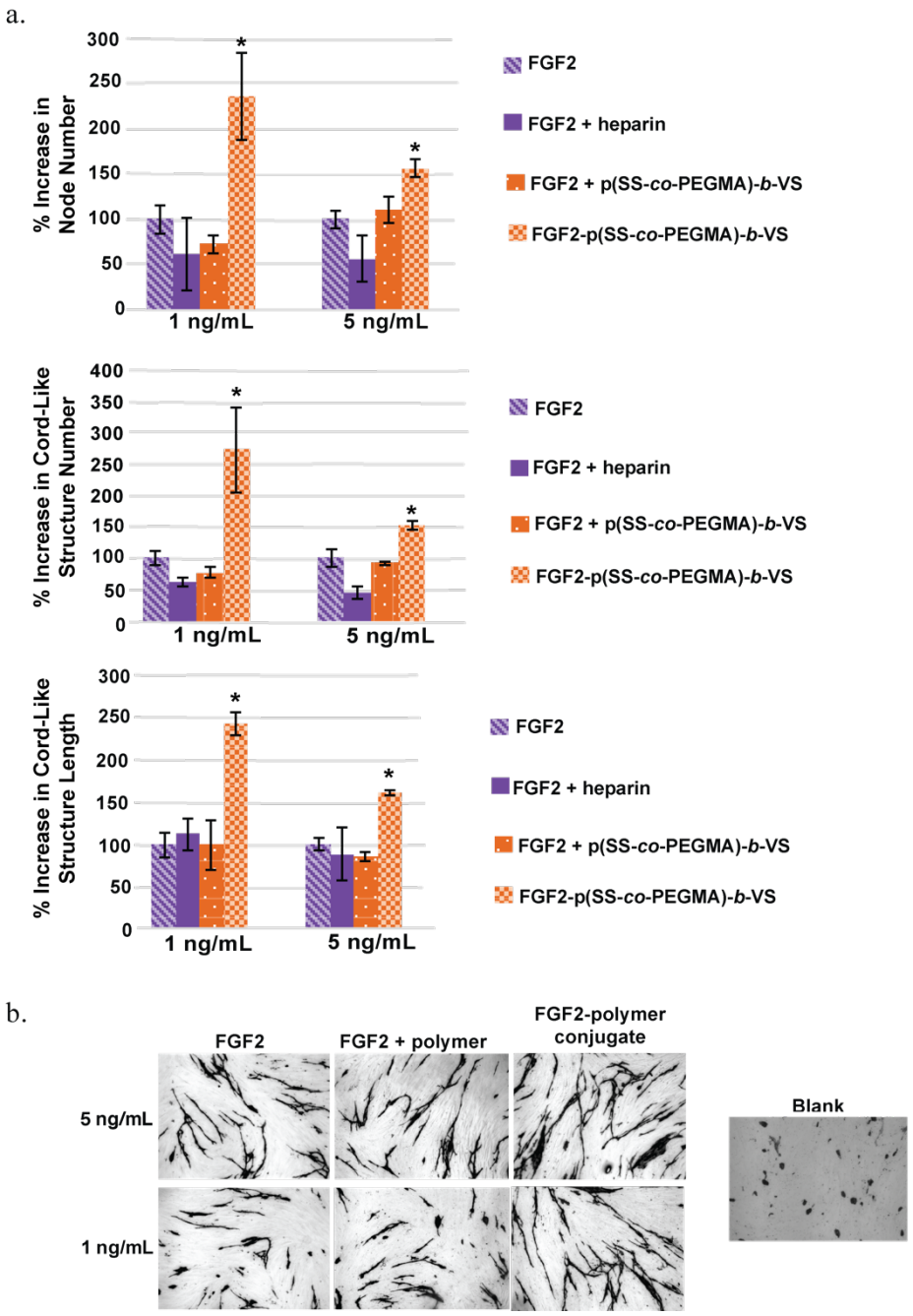

Figure 2-9. Coculture angiogenesis of HUVEC and HDF. (a) Node number, cord-like structure length and cord-like structure number. (b) Representative images of cord-like

structures stained for CD31. Three replicates per sample, error bars represent SEM. Statistical analysis was done using Student's t-test. * $p<0.01$ compared to FGF2.

Taken together these data suggest that FGF2-p(SS-*co*-PEGMA)-*b*-VS is a promising candidate for new wound healing and pro-angiogenic treatments. Besides an increase in cellular proliferation, migration, two dimensional angiogenesis, and stability, the growth factor polymer conjugate presented here has potential advantages over heparin added to growth factors in treatments. Lower FGF2 polymer conjugate concentration is needed to achieve similar cellular response compared to when just FGF2 is added. In addition, the use of a heparin-mimicking polymer allows for well-defined biomaterials for more predictable cell response. The conjugate is more stable to storage in the refrigerator and at room temperature than the native protein.

2.3 Conclusion

We have developed a novel protein-polymer conjugate, FGF2-p(SS-*co*-PEGMA)-*b*-VS that is composed of a heparin-mimicking polymer that imparts superagonist activity and stability to FGF2. This new polymer, containing both stabilization and receptor binding segments was conjugated to FGF2 through disulfide exchange with a pyridyl disulfide end group on the polymer and a surface exposed cysteine on the protein. The FGF2-p(SS-*co*-PEGMA)-*b*-VS conjugate was tested in multiple *in vitro* cell based assays and compared to FGF2 alone and addition of heparin. FGF2-p(SS-*co*-PEGMA)-*b*-VS facilitated receptor binding in both cellular and ELISA assays similar to addition of heparin. Additionally, FGF2-p(SS-*co*-PEGMA)-*b*-VS accelerated migration and endothelial cell cord-like

structure formation when compared to native FGF2 and addition of heparin. It also completely stabilized the protein to standard storage conditions, both refrigeration and room temperature. Together, these data suggest that this conjugate is promising and should be studied further for applications in tissue regeneration and wound healing. In the future, a switchable RAFT agent similar to the one described by Rizzardo and co-workers may be utilized to prepare these types of sulfonated block copolymers with better control, which is important for biomedical applications.[73] Additionally, *in vitro* and *in vivo* studies and further optimization of polymer design will be carried out to further determine the efficacy and potential of FGF2-p(SS-*co*-PEGMA)-*b*-VS as a therapeutic for healing chronic and ischemic wounds.

2.4 Experimental

2.4.1 Materials

Chemicals and reagents were purchased from Sigma-Aldrich and used as received unless otherwise indicated. Silica gel column chromatography was performed using Merck 60 (230-400 mesh) silica gel. Prior to polymerizations 4-styrene sulfonic acid and vinyl sulfonic acid monomers were pretreated with Na^+ and dried to produce the sodium salt. Before polymerization azobis(isobutyronitrile) (AIBN) was recrystallized twice from ethanol and dried, and V501 initiator was dried prior to use. Protein was expressed and purified from the plasmid pET29c(+)hFGF-2, which was kindly provided by Professor Thomas Scheper from the Helmholtz Centre for Infection Research (Braunschweig, Germany) according to Chen et. al.[74] HiTrap™ Heparin HP columns were purchased from GE Healthcare. ELISA was performed using the ELISA Development DuoSet® kit purchased from R&D Systems. Recombinant human FGFR1α(IIIc) Fc chimera, and

ELISA Development DuoSet kits were purchased from R&D Systems. Blot antibodies were purchased from CALBIOCHEM (rabbit anti-fibroblast growth factor basic) and Bio-Rad (goat anti-rabbit IgG-HRP conjugate). Normal human dermal fibroblasts and human umbilical vein endothelial cells were purchased from ATCC. BaF3-FR1C expressing FGFR1 were kindly provided by Professor David Ornitz (Washington University, Saint Louis).[75] Cell medium was purchased from ATCC or Invitrogen unless otherwise indicated. CellTiter-Blue® Cell Viability Assay was purchased from Promega. Polystyrene standards for GPC calibration were purchased from Polymer Laboratories.

2.4.2 Analytical Techniques

^{1}H NMR and ^{13}C NMR spectroscopy was performed on Avance DRX 400 or 500 MHz instruments. UV-Vis spectrophotometry was performed on a Biomate 5 Thermo Spectronic spectrometer. Dimethylformamdide (DMF) GPC was conducted in DMF containing 0.10 M LiBr (40 °C, 0.6 mL/min) on a Shimadzu HPLC system equipped with a refractive index detector RID-10A, one Polymer Laboratories PLgel guard column, and two Polymer Laboratories PLgel 5 μm mixed D columns. Calibration was performed using near-monodisperse polystyrene standards from Polymer Laboratories. Chromatograms were processed using the EZStart 7.2 chromatography software. Fast protein liquid chromatography (FPLC) was performed on a Bio-Rad BioLogic DuoFlow chromatography system equipped with a GE Healthcare Life Sciences Superdex 75 10/300 column and was run in Dulbecco's phosphate-buffered saline (D-PBS) + 1 mM ethylenediaminetetraacetic acid (EDTA). Gel electrophoresis was performed using Any kDTM Mini-PROTEAN® TGXTM precast gels with tris-glycine as running buffer (Bio-Rad, Hercules). ELISA assays were read on an ELX800 Universal Microplate Reader (Bio-Tek Instrument Inc.,

Winooski) with λ = 450 nm for signal and 630 nm for background. Western blot was developed on a FluorChem® FC2 System version 3.2 (Cell Biosciences, Santa Clara). CellTiter-Blue® assays were read on a SpectraMax M5 microplate reader (Molecular Devices, Sunnyvale). Cell images for cell viability/cytotoxicity, cell migration and angiogenesis were taken on an Axiovert 200 microscope equipped with an AxioCam MRm camera and FluoArc mercury lamp (Carl Zeiss, Thornwood). NIH ImageJ software was used to assist cell counting, to measure distances of cell-free paths and to measure degree of cord-like structure formation according to literature.[23]

2.4.3 Experimental

*Synthesis of 2-(((neopentyloxy)carbonothioyl)thio)acetic acid, (**1**).* A three-neck round bottom flask was purged with argon and dry THF (35 mL) was added. The round bottom was submerged in an ice bath and cooled to 0 °C. Sodium hydride, 60% in mineral oil (1.90 g, 47.5 mmol NaH) was added to the reaction flask and then neopentyl alcohol (3.13 mL, 28.8 mmol) was added drop-wise over 10 minutes. Following hydrogen evolution, the reaction was stirred for 10 minutes and then carbon disulfide was added (1.95 mL, 32.4 mmol); the reaction turned yellow. After 20 minutes, 2-bromoacetic acid (1.00 g, 7.20 mmol) was added and the reaction was slowly warmed to 23 °C over 5 hours. The reaction was quenched with 30 mL of methanol followed by 15 mL of water. THF was removed *in vacuo* and the crude mixture was washed twice with dichloromethane. The aqueous layer was acidified with 1 M HCl and then extracted three times with dichloromethane. The combined organic layer was dried over $MgSO_4$, filtered and concentrated, *in vacuo*. The product was further purified by recrystallization in warm water. The crystals were washed with cold water and lyophilized to dryness (1.2 g, 75% yield). δ ^{1}H NMR (400 MHz,

$CDCl_3$): 9.95 (1H, br. s, COO**H**), 4.26 (2H, s), 3.97 (2H, s), 1.01 (9H, s). δ ^{13}C NMR (400 MHz, $CDCl_3$): 212.11, 174.24, 84.22, 37.44, 31.84, 26.50. FT- IR (cm^{-1}): 2955, 2868, 2701, 2594, 1717, 1467, 1419, 1398, 1357, 1303, 1273, 1228, 1173, 1066, 1028, 955, 933, 913, 880, 793, 665. HRMS-ESI (expected, observed): $[M-H]^-$ = (221.0305, 221.0306).

Synthesis of 2-(pyridin-2-yldisulfanyl)ethyl 2 (((neopentyloxy)carbonothioyl)thio)acetate, ***(2)***. A three-neck round bottom flask was purged with argon and 2-pyridyl disulfide ethanol (0.40 g, 2.13 mmol) and (**1**) (0.31 g, 1.40 mmol) were added and dissolved in 14 mL of dry dichloromethane (DCM). The reaction flask was submerged in an ice bath and cooled to 0 °C. 1-Ethyl-3-(3'dimethylaminopropyl)-carbodiimide hydrochloride (EDC) (0.27 g, 1.39 mmol) and DMAP (0.034 g, 0.28 mmol) were added to the reaction flask and the reaction allowed to warm to 23 °C over 2 hours. The reaction was washed twice with saturated sodium bicarbonate and then twice with water. The organic layer was dried over anhydrous magnesium sulfate and the solvent was removed in *vacuo*. The product was purified by silica gel chromatography in 2:1 hexane:ethyl acetate (Rf = 0.4) to give a yellow oil (329 mg, 61% yield). δ ^{1}H NMR (400 MHz, $CDCl_3$): 8.49-8.48 (1H, d, J = 4.68 Hz), 7.71-7.65 (2H, m), 7.14-7.11 (1H, m), 4.44-4.41 (2H, t, J = 6.44 Hz), 4.26 (2H, s), 3.93 (2H, s), 3.09-3.05 (2H, t, J = 6.44 Hz), 0.99 (9H, s). δ ^{13}C NMR (400 MHz, $CDCl_3$): 212.51, 167.62, 159.59, 149.75, 137.15, 120.97, 119.93, 84.04, 63.55, 37.57, 37.12, 31.85, 26.55. FT- IR (cm^{-1}): 2959, 2871, 1739, 1572, 1446, 1416, 1365, 1273, 1225, 1147, 1116, 1059, 1029, 986, 950, 931, 906, 880, 759, 716, 616, 555, 529, 508, 486, 479, 462. HRMS-ESI (expected, observed): $[M_{H+}]$ = (392.0482, 392.0439).

Synthesis of 2-((ethoxycarbonothioyl)thio)-2-methylpropanoic acid, ***(3)***. A three-neck round-bottom was purged with argon followed by 40 mL of 1:1 water:acetone v:v. The

solvents were degassed with argon for 1 hour prior to use. The round-bottom was submerged in an ice bath to cool to 0 °C and then NaOH (1.26 g, 31.5 mmol) was added to the round-bottom and the mixture was stirred for 20 minutes. Degassed EtOH (1.24 g, 27.0 mmol) was added dropwise over 10 minutes followed by the dropwise addition of carbon disulfide (1.90 mL, 31.4 mmol). The reaction turned yellow and was stirred for 30 minutes at 0 °C. After 30 minutes, 2-bromo-2-methylpropanoic acid (1.50 g, 8.98 mmol) was added and the reaction was slowly warmed to 23 °C and stirred for 48 hours, over which time the reaction turned orange. After 48 hours the acetone was removed *in vacuo,* and the aqueous layer was checked for basicity, then extracted three times with DCM. The aqueous layer was then acidified using 1M HCl and extracted three times with DCM. The combined DCM layers were dried over $MgSO_4$, filtered, and the solvent was removed *in vacuo*. Next, 3 mL of water were added to the orange oil, and then the mixture was heated until all solid dissolved. The mixture was slowly cooled to room temperature over 12 hours. Light yellow to white crystals were observed in the water and were filtered and rinsed with cold water. The crystals were dried *in vacuo* (538 mg, 35 % yield). δ ^{1}H NMR (400 MHz, $CDCl_3$): 9.21-10.64 (1H, br s, COO**H**), 4.63-4.58 (2H, q, J = 8 Hz), 1.63 (6H, s), 1.41-1.37 (3H, t, J = 7.12 Hz). δ ^{13}C NMR (400 MHz, $CDCl_3$): 210.32, 118.43, 70.01, 53.86, 25.51, 13.32. FT- IR (cm^{-1}): 2986, 2867, 2653, 2553, 1704, 1466, 1416, 1362, 1284, 1249, 1175, 1108, 1037, 999, 922, 850, 806, 691, 631, 610, 590, 561, 538, 519, 509, 485, 471, 458. HRMS-ESI (expected, observed): $[M_{H+}]$ = (209.0307, 209.0289).

Synthesis of 2-(pyridin-2-yldisulfanyl)ethyl 2-((ethoxycarbonothioyl)thio)-2-methylpropanoate, ***CTA***. A two-neck round-bottom flask was purged with argon, and pyridyl disulfide (PDS)-alcohol (670 mg, 3.61 mmol) and **(3)** (500 mg, 2.40 mmol) were

added and dissolved in 5 mL of dry DCM. The round-bottom was submerged in an ice bath for 20 minutes. EDC (450 mg, 2.36 mmol) and 4-dimethylaminopyridine (DMAP) (58.7 mg, 0.48 mmol) were added to the reaction mixture, and the reaction was yellow. The reaction was slowly warmed to room temperature and stirred for 6 hours. After 6 hours, the solvent was removed *in vacuo* and a silica gel column was run in 2:1 hexane:EtOAc. Fractions were collected and solvent removed to obtain a yellow oil (407 mg, 45% yield). δ ^{1}H NMR (400 MHz, $CDCl_3$): 8.45- 8.43 (1H, dq, J = 4.85, 0.92 Hz), 7.68-7.60 (2H, m), 7.08-7.05 (1H, ddd, J = 6.61, 4.82, 1.32 Hz), 4.56-4.51 (2H, q, J = 7.15 Hz), 4.36-4.33 (2H, t, J = 6.42 Hz), 3.02-2.99 (2H, t, J = 6.40 Hz), 1.58 (6H, s), 1.34-1.30 (3H, t, J = 7.08 Hz). δ ^{13}C NMR (400 MHz, $CDCl_3$): 210.80, 172.82, 159.53, 149.74, 137.15, 120.94, 119.88, 69.84, 63.18, 54.08, 37.11, 25.74, 13.42. FT- IR (cm^{-1}): 2960, 2870, 1736, 1572, 1447, 1416, 1366, 1274, 1224, 1154, 1116, 1056, 1029, 986, 950, 931, 905, 806, 759, 731, 716, 616, 579, 565, 529, 508, 497, 492, 487, 471, 457. HRMS-ESI (expected, observed): [M_{H+}] = (377.0248, 377.0301).

Synthesis of pVS. RAFT polymerizations were performed with feed ratios of [VS]:[CTA1]:[V501] = 300:1:0.5 with a monomer concentration of 2.2 M. Vinyl sulfonate (VS) monomer (996 mg, 7.66 mmol) and V501 (3.6 mg, 0.013 mmol) were added to a Schlenk tube and dissolved in 1.5 mL of Milli-Q water (degassed prior to use). Next, **2** (10 mg, 0.026 mmol) was dissolved in 1.5 mL of DMF (degassed prior to use) and transferred to the Schlenk tube. The Schlenk tube was sealed and subjected to four freeze-pump-thaw cycles before immersion in an oil bath set to 70 °C. After 17 hours the polymerization was stopped by bubbling air through the Schlenk tube. The polymer was purified by dialysis in 1000 MWCO tubing against 1:1 v/v water:acetonitrile followed by 100% Milli-Q water.

The resulting contents of the dialysis were lyophilized to dryness. δ ^{1}H NMR 500 MHz (D_2O): 8.82-8.81 (1H, d, J = 5.67 Hz), 8.50-8.46 (1H, td, J = 8.04, 1.67), 8.36-8.34 (1H, d, J = 8.36), 7.90-7.88 (1H, ddd, J = 7.06, 5.71, 0.95), 4.52 (2H, s), 4.19 (2H, s), 4.2-2.9 ($CH_2C\mathbf{H}SO_3Na$ polymer backbone), 3.41-3.39 (2H, t, J = 5.83), 2.9-1.4 ($C\mathbf{H_2}CHSO_3Na$ polymer backbone), 1.20 (9H, s) . IR (cm^{-1}): 3419, 2957, 2878, 1725, 1642, 1448, 1366, 1148, 1027, 710, 610, 508. The M_n = 8.2, 10.2, and 17.9 kDa by NMR. The NMR spectrum of each polymer was calibrated to the peak at 8.82-8.81 ppm, and the M_n of the polymers were calculated using the formula: [(polymer integrals 4.2-2.9 ppm)-4] * MW monomer * MW CTA. The polymer was synthesized with M_n by ^{1}H NMR of 17.9 kDa and a degree of polymerization 135. The GPC trace in water showed M_n of 6.2 kDa with $Đ$ of 1.16.

Synthesis of p(SS-co-PEGMA) macroCTA: RAFT polymerization was performed with initial feed ratio of [SS]:[PEGMA]:[CTA]:[AIBN] = 35:10:1:0.2 and a monomer concentration of 1.0 M. Styrenesulfonate (382 mg, 1.85 mmol) and PEGMA M_n 300 (159 mg, 0.53 mmol) were dissolved in 1.2 mL of degassed water in a Schlenk tube. CTA (20 mg, 0.053 mmol) was dissolved in 1.2 mL of degassed DMF along with AIBN (1.74 mg, 0.011 mmol) and then transferred to the Schlenk tube. The Schlenk tube was sealed and subjected to four freeze-pump-thaw cycles before immersion in an oil bath set to 60 °C. After 4 hours the polymerization was stopped by cooling to room temperature (23 ºC) and bubbling air through the Schlenk tube. The polymer was purified by dialysis in 1000 MWCO tubing against 1:1 v/v water:MeOH followed by 100% Milli-Q water. The resulting contents of the dialysis tubing were lyophilized to dryness to give a fluffy light yellow solid. ^{1}H NMR 500 MHz (D_2O) δ: 8.40 (1H, s), 8.0-6.2 ($NaSO_3C_6\mathbf{H4}$ side chains), 4.2-2.8 (PEGMA side chains), 2.8-0.0 (polymer backbone). The ^{1}H NMR spectrum of the

resulting polymer was calibrated to the peak at 8.40 ppm, and the M_n of the polymers were calculated using the formula: M_n = [(integral of 8.2 – 6.2 ppm /4)*MW SS monomer]+[(integral of 4.2-2.8 ppm /20.4)*MW PEGMA monomer]+MW CTA. The M_n = 33.0 kDa by NMR. M_n = 15.1 kDa by GPC, $Đ$ of 1.13.

Synthesis of p(SS-co-PEGMA)-b-VS: RAFT polymerization was performed with initial feed ratio of [VS]:[CTA]:[V501] = 200:1:0.5 and a monomer concentration of 1 M. The CTA (50 mg, 0.003 mmol), VS monomer (65 mg, 0.50 mmol) and V501 (0.4 mg, 0.001 mmol) were weighed and added to a 1 mL Schlenk tube and dissolved in 0.5 mL of degassed water. The Schlenk tube was sealed and subjected to four freeze-pump-thaw cycles before immersion in an oil bath set to 60 °C. After 3 hours the polymerization was stopped by cooling to room temperature and opening the Schlenk tube to atmosphere. The polymer was purified by dialysis in 6000 MWCO tubing against water over 72 hours. The resulting contents of the dialysis were lyophilized to dryness. ^{1}H NMR 500 MHz (D_2O) δ: 8.72 (1H, s), 8.2-6.0 (SS side chains), 4.3-2.8 (PEGMA side chains and $CH_2C\mathbf{H}SO_3Na$ polymer backbone), 2.8-0.0 (SS and PEGMA polymer backbone and $C\mathbf{H_2}CHSO_3Na$ polymer backbone). The M_n = 50.7 kDa by NMR, 28.3 kDa by GPC (DMF), with $Đ$ = 1.20.

Synthesis of p(SS-co-PEGMA): RAFT polymerization was performed with initial feed ratios of [SS]:[PEGMA]:[CTA]:[AIBN] = 35:10:1:0.2 and a monomer concentration of 1.0 M. Styrene sulfonate (382 mg, 1.85 mmol) was dissolved in 1.2 mL of degassed DMF in a Schlenk tube. CTA 3 (20 mg, 0.053 mmol) was dissolved in 1.2 mL of degassed water along with PEGMA M_n 300 (159 mg, 0.53 mmol) and AIBN (1.74 mg, 0.011 mmol) and then transferred to the Schlenk tube. The Schlenk tube was sealed and subjected to four

freeze-pump-thaw cycles before immersion in an oil bath set to 70 °C. After 4 hours the polymerization was stopped by bubbling air through the Schlenk tube. The polymer was purified by dialysis in 1000 MWCO tubing against 1:1 v/v water:MeOH followed by 100% Milli-Q water. The resulting contents of the dialysis tubing were lyophilized to dryness. ^{1}H NMR 500 MHz (D_2O) δ: 8.40 (1H, s), 8.2-6.2 ($NaSO_3C_6\mathbf{H_4}$ side chains), 4.2-2.8 (PEGMA side chains), 2.8-0.0 (polymer backbone). The ^{1}H NMR spectrum of the resulting polymer was calibrated to the peak at 8.40 ppm, and the M_n of the polymers were calculated using the formula: M_n = [(integral of 8.2 – 6.2 ppm /4)*MW SS monomer]+[(integral of 4.2-2.8 ppm /20.4)*MW PEGMA monomer]+MW CTA. The M_n by NMR was 17.2 kDa. GPC was performed in DMF and M_n was calculated to be 19.8 kDa with $Đ$ of 1.21.

Preparation of FGF2 conjugates: FGF2 (100 μg, 5.9 x 10^{-3} μmol) was diluted in 500 μl of D-PBS + 1mM EDTA and loaded onto a hand-packed 0.5ml-heparin Sepharose column. Next, 100 equivalents of PDS-p(SS-*co*-PEGMA), PDS-VS or PDS-p(SS-*co*-PEGMA-*b*-VS) were dissolved in 500 μL of D-PBS + 1mM EDTA and loaded onto the column. The column was incubated at 4 °C for 16 hours. After the incubation, the column was first washed with 5 column volumes of D-PBS + 1 mM EDTA to remove unreacted polymer. Next, the column was washed with 10 column volumes of D-PBS + 2M NaCl to remove conjugated protein. Conjugate was purified using a CentriPrep® centrifugal membrane MWCO 3,000 against D-PBS 10 times at 12.0 rcf for 10 minutes/cycle. The collected conjugate was then characterized by gel electrophoresis and the concentration was determined by ELISA prior to *in vitro* studies.

BaF3 Cell Proliferation: BaF3-FR1C cells were grown in RPMI1640 medium containing 2 mM L-glutamine, 10% newborn bovine calf serum, 0.5 ng/mL IL-3, 50 nM 2-mercaptoethanol, 600 μg/mL G418, 100 μg/mL penicillin and 100 μg/mL streptomycin. Before seeding cells for experiments the cells were collected and washed twice with culture medium without IL-3. Cells were plated at a concentration of 20,000 cells/well/50 μL in the internal wells of a 96 well plate in culture medium without IL-3. Samples were prepared in culture medium without IL-3 to contain double the final concentration and then 50 μL of each sample was added to the corresponding well. The external wells were blocked in 100 μL of DPBS and then incubated at 37 °C and 5% CO_2. After 48 hours of incubation CellTiter-Blue assay was performed to determine extent of cell growth. All samples were normalized to the control group, which contained only culture medium without IL-3. Each group contained six replicates.

ELISA Based FGFR Binding Assay: A 96 well-plate was incubated with rhFGFR1α(IIIc) (100 μL per well at a concentration of 0.5 μg/mL in D-PBS) for 16 hours at 23 ºC. After 16 hours the wells were blocked with 1% bovine serum albumin (BSA) in D-PBS (2 hours). Next, solutions of protein or conjugates were prepared at a concentration of 1 ng/mL and 100 μL was plated in the wells and then incubated for 2 hours. After 2 hours 100 μL of FGF2 antibody-biotin conjugate was added and incubated for an additional 2 hours before streptavidin-horseradish peroxidase solution was incubated for 20 minutes. The plate was developed by incubating with 100 μL of 1-Step Ultra 3,3',5,5'-tetramethylbenzidine (TMB) solution (Pierce Biotechnology, Rockford) for 8 minutes. The assay was terminated by the addition of 50 μL of 1 M H_2SO_4. Absorbance was read at $\lambda = 450$ nm. Each sample

was plated in triplicate.

Stability Study: Samples of protein and conjugates were prepared at a concentration of 0.05 ng/μL in sterile D-PBS and then stored at either 4 ºC or 23 ºC for 7 days. After 7 days an aliquot was removed from each sample and diluted to 1 ng/mL in Ultraculture cell medium. Fresh FGF2 samples were prepared the day of each cell experiment at 1 ng/mL in Ultraculture medium. Each sample was used in the HDF proliferation assay described below. Plates were prepared with 6 repeats per sample.

Fibroblast Proliferation: Normal human dermal fibroblasts (HDFs) were grown in ATCC Fibroblast Basal Medium with 100 μg/mL penicillin and 100 μg/mL streptomycin supplemented. Cells were trypsinized and resuspended in Lonza UltraCULTURE™ serum-free medium supplemented with 2 mM L-Glutamine, 100 unit/ml penicillin, and 100 μg/ml streptomycin, then plated in the internal wells of a 96 well plate at a concentration of 2,000 cells/well/100 μL. The external wells were blocked with D-PBS and the plate was incubated at 37 °C, 5% CO_2 for 16 hours to allow cells to adhere. After the 16-hour incubation period the medium was aspirated out of the wells and replaced with 100 μL of samples diluted in the supplemented UltraCULTURE™ medium. The cells with samples were incubated for 72 hours at 37 °C, 5% CO_2 and then CellTiter-Blue assay was performed to determine extent of cell proliferation. All groups were normalized to the control, which contained only UltraCULTURE™ medium. Each group contained six repeats.

Endothelial Cell Proliferation: Human umbilical vein endothelial cells (HUVECs) were grown in ATCC endothelial cell medium supplemented with 100 unit/mL penicillin and

100 μg/mL streptomycin. Cells were trypsinized and resuspended in the growth medium without bovine brain extract (-BBE) then plated in the internal wells of a 96 well plate at a concentration of 1,000 cells/well/100 μL. The external wells were blocked with D-PBS and the plate was incubated at 37 °C, 5% CO_2 for 16 hours to allow cells to adhere. After the 16-hour incubation period the medium was aspirated out of the wells and replaced with 100 μL of samples diluted in the supplemented UltraCULTURE™ medium. The cells with samples were incubated for 72 hours at 37 °C, 5% CO_2 and then CellTiter-Blue assay was performed to determine extent of cell proliferation. All groups were normalized to the control, which contained only growth medium without BBE. Each group contained six repeats.

Cell Migration Assay: HUVECs were seeded in the internal wells of a 24 well plate and grown to 90-95% confluency. After reaching confluency the cell monolayers were washed once with D-PBS, and then the medium was replaced with starvation medium (endothelial growth medium (EGM) (-) BBE (-) rhEGF). The cells were starved for 24 hours at 37 °C, 5% CO_2. The medium was then aspirated out of the wells and replaced with D-PBS. A scratch was made in the center of each well using a standard P1000 pipette tip, and a marker line perpendicular to the scratch was drawn on the bottom of each well. The D-PBS was aspirated out of the wells and the wells were washed once more with D-PBS to remove cell debris. The cell monolayers were allowed to incubate with 400 μL of starvation medium or samples in starvation medium at 37 °C, 5% CO_2. Immediately after treatment (T = 0), two pictures of the scratch/well (one above and one below the marker) were obtained using a 5X objective on the Axiovert 200 microscope equipped with an AxioCam MRm camera, n = 4 - 6. At the end of the 18- hour incubation (T = 18), pictures of the scratches were

taken again in the same manner. CellTiter-Blue® assay was then used to quantify the extent of cell growth. The NIH ImageJ software was used to analyze the cell images: two parallel lines were drawn to outline each scratch, then the distance between them was measured using the "Measure Length" option. Percent migration was calculated using the formula: 100% − (distance T=18/distance T=0) x 100. The experiment was blinded and repeated three times.

Coculture Angiogenesis Assay: Experimental for co-culture angiogenesis assay and staining of cord-like structures were adapted from known literature procedures.[68,70] HDFs were trypsinized and resuspended in endothelial growth medium then plated at a concentration of 12,500 cells/well/250 μL in the internal 48-well plate. The external wells were blocked and the cells were incubated at 37 °C, 5% CO_2 for 72 hours or until cells reached confluency. The fibroblasts were then starved for 18 hours in EGM (-) BBE (-) rhEGF. After the starvation period, the starvation medium was replaced with HUVECs at a concentration of 10,000 cells/well/125 μL in EGM (-) BBE (-)EGF. Samples were prepared in EGM (-) BBE (-) rhEGF to contain double the concentration and then 125 μL of each sample was placed in the wells containing HUVECs. Sample solutions were refreshed after 72 and 144 hours by aspirating out the medium and replacing with sample solutions prepared fresh. Ten days after the addition of HUVECs the medium was removed from each well and the cells were fixed with 70% EtOH for 30 minutes at room temperature (the ethanol was previously cooled to -20 °C and used straight out of the freezer). The wells were then rinsed with 0.5 mL of 1% BSA in D-PBS three times. Endogenous alkaline phosphatase was removed by incubating the cells in 0.3% H_2O_2 in MeOH for 15 minutes at room temperature before washing the wells again with 1% BSA. The wells were

incubated with mouse anti-human PECAM1/CD31 (R&D Systems) at a concentration of 1 μg/mL in 1% BSA for 1 hour at 37 °C, 5% CO_2. The wells were again rinsed 3 times with 1% BSA and then incubated with goat anti-mouse IgG alkaline phosphatase (Sigma Aldrich) at 3 μg/mL in 1% BSA for 1 hour at 37 °C, 5% CO_2. The wells were then washed 3 times with MilliQ water and then incubated with BCIP/NBT solution (1 tablet in 10 mL MilliQ water, sterile filtered) for 15 minutes at room temperature. The cord-like structures were visually stained and the wells were rinsed 3 times with MilliQ water and allowed to dry. Images were taken using 5X magnification (five images per well). Plates were stored for up to 2 months at -80 °C. Cord-like structures were analyzed using NIH ImageJ Software while blinded. The values for each of the five images per well were summed and the sums from each well were averaged (a total of three wells per sample).

Cell Viability/Cytotoxicity: HUVECs or HDFs were trypsinized and resuspended in growth medium. The cells were plated at a concentration of 2,000 cells/well/100 μL and were incubated at 37 °C, 5% CO_2 over 16 hours to allow cells to adhere. After incubation the medium was replaced with 100 μL of polymer solutions in growth medium and incubated for another 24 hours at 37 °C, 5% CO_2. Extent of cell viability was assessed using a LIVE/DEAD® viability/cytotoxicity assay. The cells were washed with D-PBS then incubated with 1 μM calcein AM and 4 μM ethidium homodimer-1 in D-PBS at 37 °C, 5% CO_2. Fluorescent images were captured using red and green channels. NIH ImageJ Software was utilized to count the number of live and dead cells. Each sample assay was performed with six repeats.

2.5 Appendix to Chapter 2 – Supplementary Figures

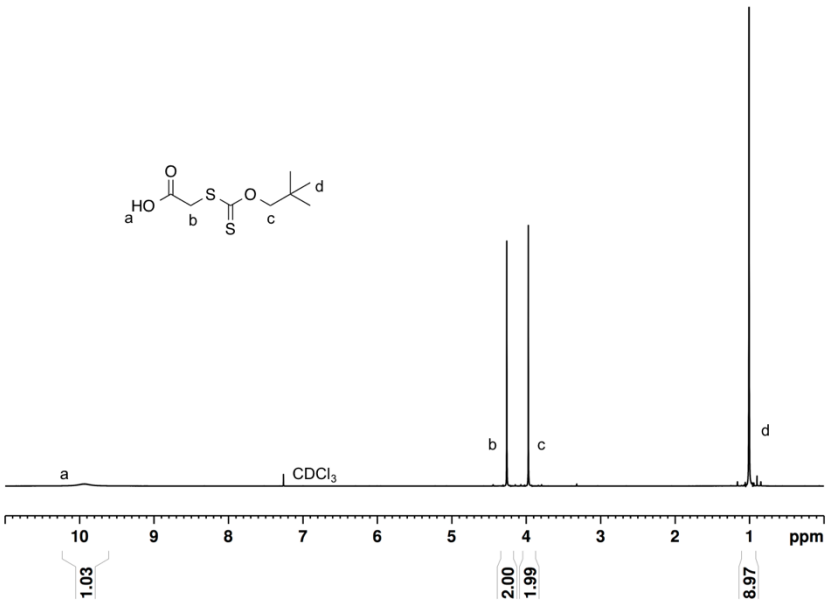

Figure 2-10. ^{1}H NMR (400 MHz, $CDCl_3$) of (1): 2-(((neopentyloxy)carbonothioyl)thio)acetic acid

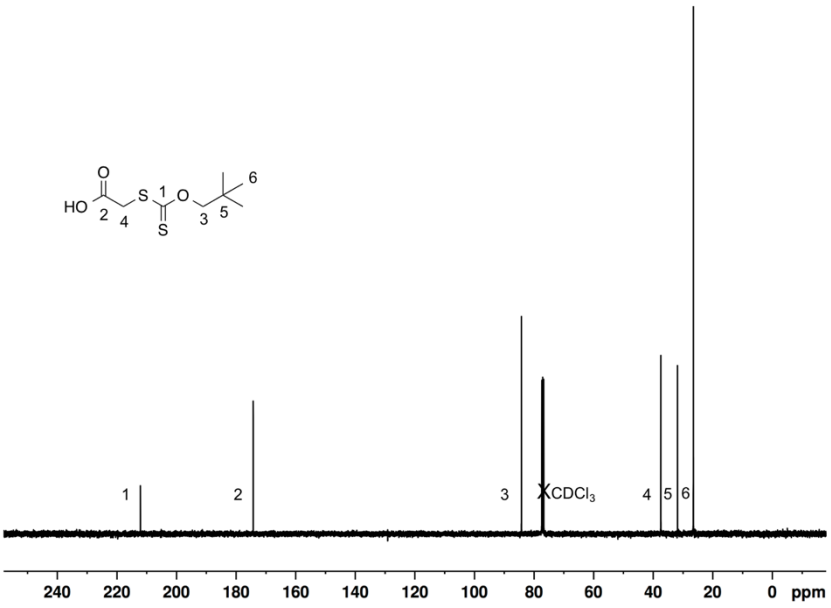

Figure 2-11. ^{13}C NMR (400 MHz, $CDCl_3$) of (1): 2-(((neopentyloxy)carbonothioyl)thio)acetic acid

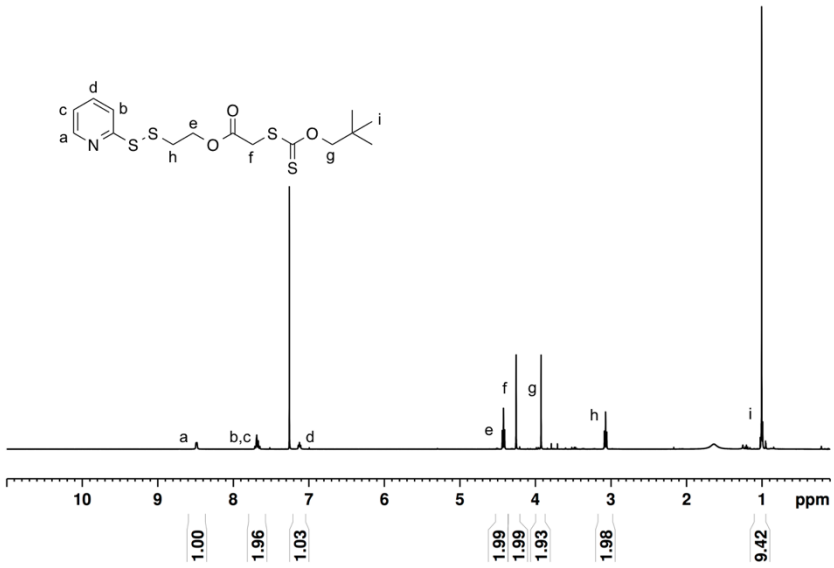

Figure 2-12. ^{1}H NMR (400 MHz, $CDCl_3$) of (2): 2-(pyridin-2-yldisulfanyl)ethyl 2-(((neopentyloxy)carbonothioyl)thio)acetate

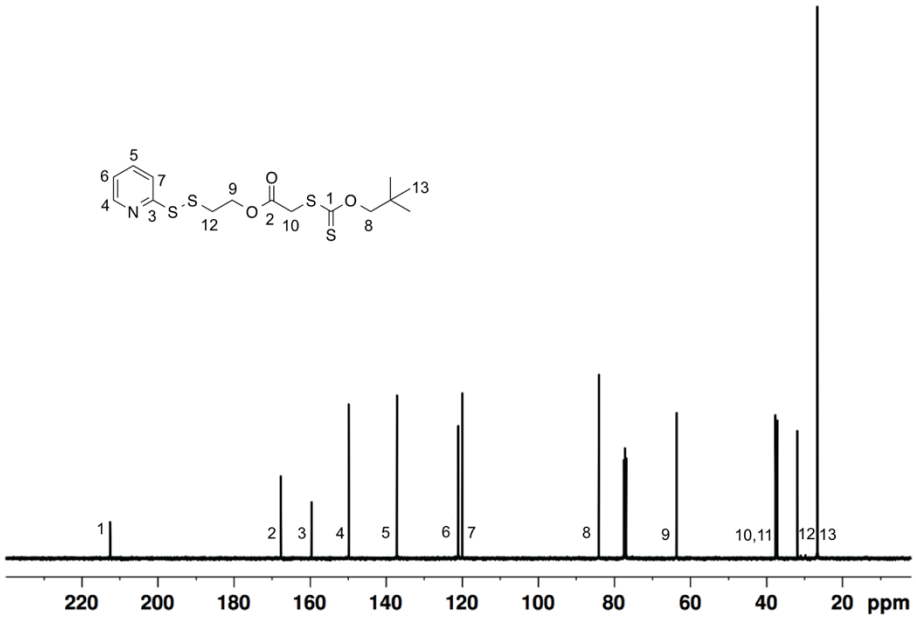

Figure 2-13. ^{13}C NMR (400 MHz, $CDCl_3$) of (2): 2-(pyridin-2-yldisulfanyl)ethyl 2-(((neopentyloxy)carbonothioyl)thio)acetate

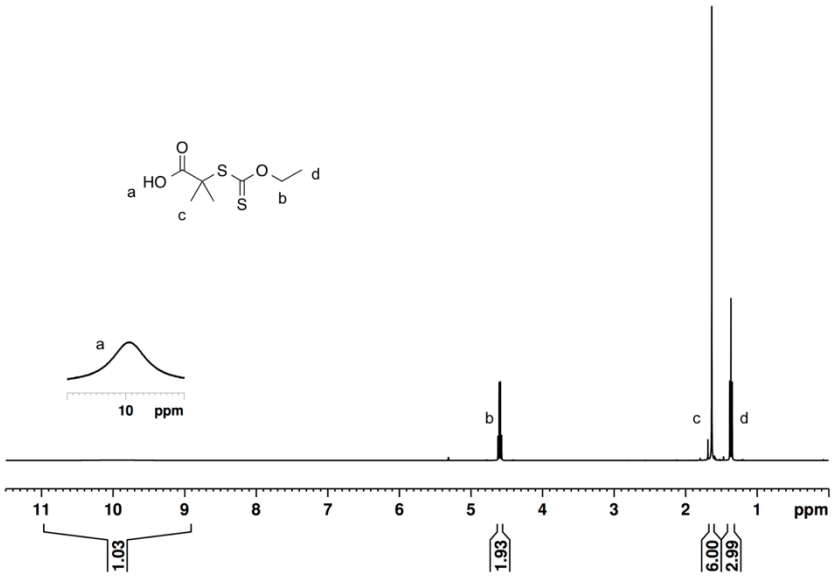

Figure 2-14. ^{1}H NMR (400 MHz, $CDCl_3$) of (3): 2-((ethoxycarbonothioyl)thio)-2-methylpropanoic acid

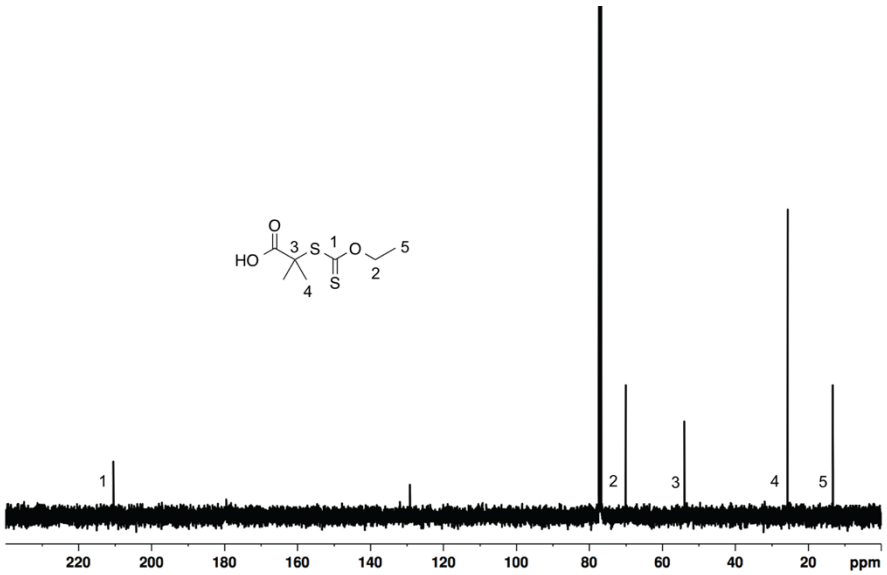

Figure 2-15. ^{13}C NMR (400 MHz, $CDCl_3$) of (3): 2-((ethoxycarbonothioyl)thio)-2-methylpropanoic acid

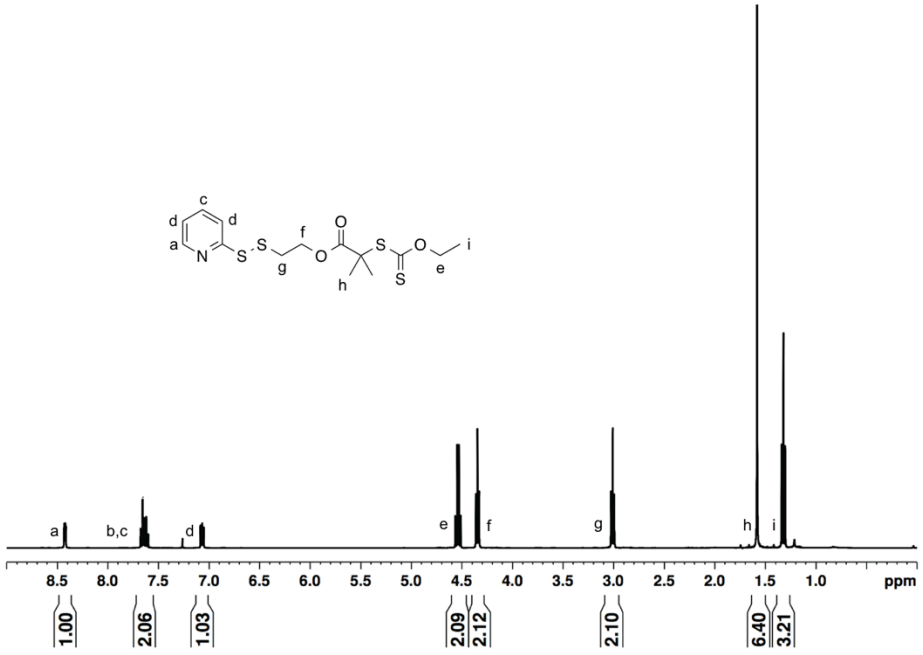

Figure 2-16. ^{1}H NMR (400 MHz, $CDCl_3$) of CTA: 2-(pyridin-2-yldisulfanyl)ethyl 2-((ethoxycarbonothioyl)thio)-2-methylpropanoate

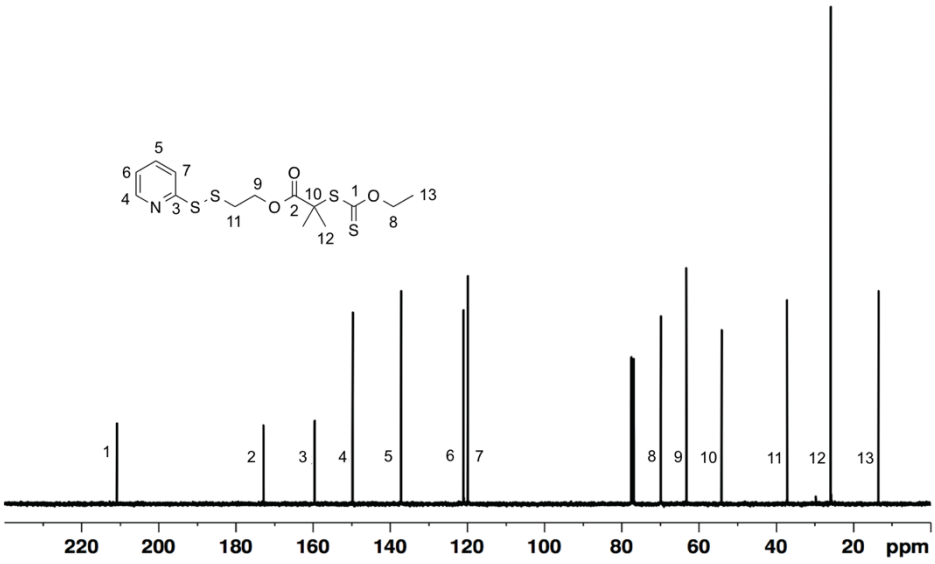

Figure 2-17. ^{13}C NMR (400 MHz, $CDCl_3$) of CTA: 2-(pyridin-2-yldisulfanyl)ethyl 2-((ethoxycarbonothioyl)thio)-2-methylpropanoate

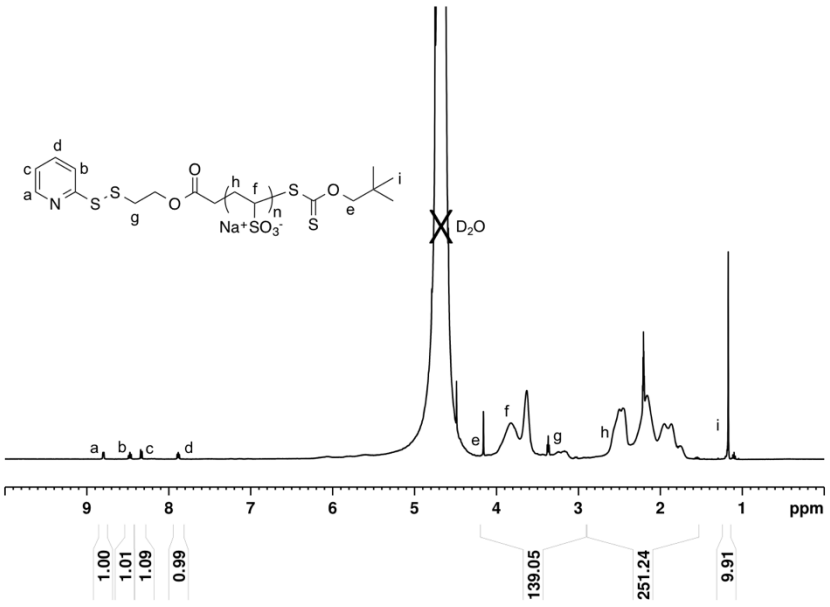

Figure 2-18. ^{1}H NMR (400 MHz, D_2O/CD_3CN) of pVS

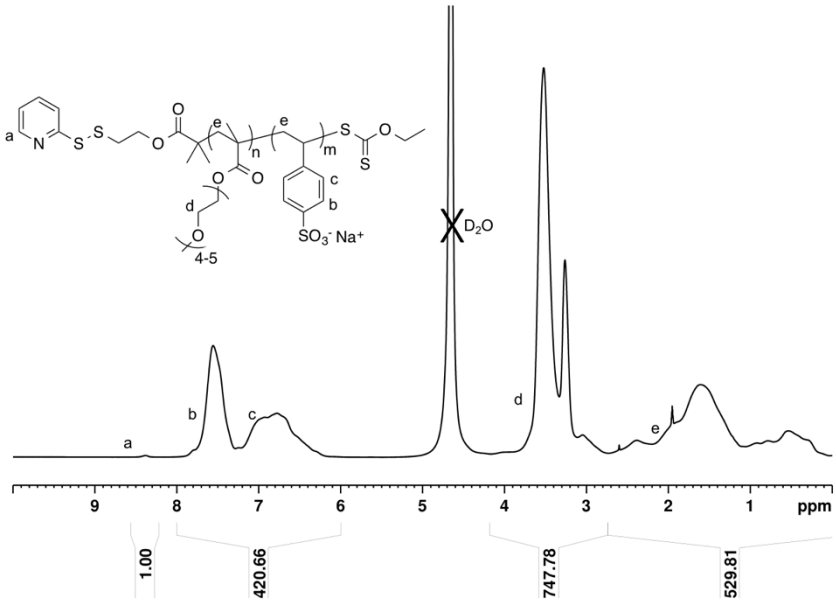

Figure 2-19. ^{1}H NMR (400 MHz, D_2O) of p(SS-co-PEGMA) macroCTA

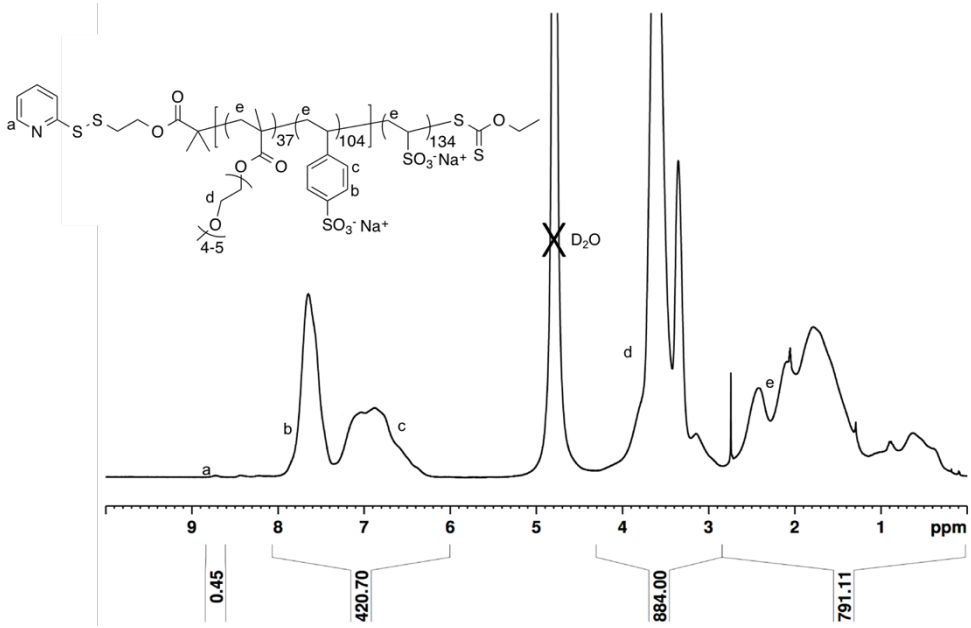

Figure 2-20. ^{1}H NMR (400 MHz, D_2O) of p(SS-*co*-PEGMA)-*b*-VS

2.6 References

†Chapter 2 is reproduced with permission from Paluck, S.J.; Nguyen, T.H.; Lee, J.P.; Maynard, H.D. A Heparin-Mimicking Block Copolymer Both Stabilizes and Increases the Activity of Fibroblast Growth Factor 2 (FGF2). *Biomacromolecules* **2016**, *17*, 3386-3395. 10.1021/acs.biomac.6b01182. Copyright 2016 American Chemical Society. http://pubs.acs.org/doi/abs/10.1021/acs.biomac.6b01182

(1) Agarwal, S.; Sud, K.; Shishehbor, M. H. *J. Am. Coll. Cardiol.* **2016,** *67*, 1901.

(2) Sen, C. K.; Gordillo, G. M.; Roy, S.; Kirsner, R.; Lambert, L.; Hunt, T. K.; Gottrup, F.; Gurtner, G. C.; Longaker, M. T. *Wound Repair Regen.* **2009**, *17*, 763.

(3) Singer, A. J.; Clark, R. A. F. *N. Engl. J. Med.* **1999**, *341*, 738.

(4) Doctor, N.; Yang, S.; Maerzacker, S.; Watkins, P.; Dissanaike, S. *J. Burn Care Res.* **2016**, *37*, E56.

(5) Driver, V. R.; Fabbi, M.; Lavery, L. A.; Gibbons, G. *J. Am. Podiatr. Med. Assoc.* **2010**, *100*, 335.

(6) Greenhalgh, D. G. *J. Trauma Injury Infect. Crit. Care* **1996**, *41*, 159.

(7) Demidova-Rice, T. N.; Hamblin, M. R.; Herman, I. M. *Adv. Skin Wound Care* **2012**, *25*, 304.

(8) Wells, L. A.; Valic, M. S.; Lisovsky, A.; Sefton, M. V. *Isr. J. Chem.* **2013**, *53*, 637.

(9) Rufaihah, A. J.; Seliktar, D. *Adv. Drug Delivery Rev.* **2016**, *96*, 31.

(10) Itoh, N.; Ornitz, D. M. *J. Biochem.* **2011**, *149*, 121.

(11) Ornitz, D. M.; Itoh, N. *Genome biology* **2001**, *2*, 3005.

(12) Bikfalvi, A.; Klein, S.; Pintucci, G.; Rifkin, D. B. *Endocr. Rev.* **1997**, *18*, 26.

(13) Werner, S.; Grose, R. *Physiol. Rev.* **2003**, *83*, 835.

(14) Fu, X. B.; Shen, Z. Y.; Guo, Z. R.; Zhang, M. L.; Sheng, Z. Y. *Chin. Med. J.* **2002**, *115*, 331.

(15) Whitaker, M. J.; Quirk, R. A.; Howdle, S. M.; Shakesheff, K. M. *J. Pharm. Pharmacol.* **2001**, *53*, 1427.

(16) Presta, M.; Dell'Era, P.; Mitola, S.; Moroni, E.; Ronca, R.; Rusnati, M. *Cytokine Growth Factor Rev.* **2005**, *16*, 159.

(17) Richard, J. L.; Bringer, J.; Parerrichard, C.; Rodier, M.; Daures, J. P.; Jacob, C.; Clouet, S.; Comtebardonnet, M.; Vannereau, D. *Diabetes Care* **1995**, *18*, 64.

(18) Frykberg, R. G.; Banks, J. *Adv. Wound Care* **2015**, *4*, 560.

(19) Springer, B. A.; Pantoliano, M. W.; Sharp, C. M. Analogs of human basic fibroblast growth factor mutated at one or more of the positions glutamate 89, aspartate 101 or leucine 137. U.S. Patent US 6274712 B1, Aug. 14, 2001.

(20) Bogin, O.; Yayon, A.; Fgf variants and methods for use thereof. WIPO Patent WO 2003094835 A3, Nov. 20, 2003.

(21) Yayon, A.; Rom, E.; Chumakov, I.; Blumenstein, S. FGF-2 variants having N-terminal deletions and increased receptor selectivity and uses thereof. U.S. Patent US 8962556 B2. Feb. 24, 2015.

(22) Kwan, C. P.; Venkataraman, G.; Shriver, Z.; Raman, R.; Liu, D. F.; Qi, Y. W.; Varticovski, L.; Sasisekharan, R. *J. Biol. Chem.* **2001**, *276*, 23421.

(23) Decker, C. G.; Wang, Y.; Paluck, S. J.; Shen, L.; Loo, J. A.; Levine, A. J.; Miller, L. S.; Maynard, H. D. *Biomaterials* **2016**, *81*, 157.

(24) Safran, M.; Eisenstein, M.; Aviezer, D.; Yayon, A. *Biochem. J.* **2000**, *345*, 107.

(25) Rudenko, O.; Tkach, V.; Berezin, V.; Bock, E. *Neurosci. Res.* **2010**, *68*, 35.

(26) Anderson, A. A.; Kendal, C. E.; Garcia-Maya, M.; Kenny, A. V.; Morris-Triggs, S. A.; Wu, T.; Reynolds, R.; Hohenester, E.; Saffell, J. L. *J. Neurochem.* **2005**, *95*, 570.

(27) Nur-E-Kamal, A.; Ahmed, I.; Kamal, J.; Babu, A. N.; Schindler, M.; Meiners, S. *Mol. Cell. Biochem.* **2008**, *309*, 157.

(28) Choi, K.-C.; Yoo, D.-S.; Cho, K.-S.; Huh, P.-W.; Kim, D.-S.; Park, C.-K. *J. Korean Neurosurg. Soc.* **2008**, *44*, 375.

(29) Richardson, T. P.; Peters, M. C.; Ennett, A. B.; Mooney, D. J. *Nat. Biotechnol.* **2001**, *19*, 1029.

(30) Wu, J.; Mao, Z.; Hong, Y.; Han, L.; Gao, C. *Bioconjugate Chem.* **2013**, *24*, 1302.

(31) Gospodarowicz, D.; Cheng, J. *J. Cell. Physiol.* **1986**, *128*, 475.

(32) Plotnikov, A. N.; Schlessinger, J.; Hubbard, S. R.; Mohammadi, M. *Cell* **1999**, *98*, 641.

(33) Caldwell, M. A.; Garcion, E.; terBorg, M. G.; He, X. L.; Svendsen, C. N. *Exp. Neurol.* **2004**, *188*, 408.

(34) Ishihara, M.; Ono, K. *Trends Glycosci Glycotechnol.* **1998**, *10*, 223.

(35) Theroux, P.; Ouimet, H.; McCans, J.; Latour, J. G.; Joly, P.; Levy, G.; Pelletier, E.; Juneau, M.; Stasiak, J.; Deguise, P.; Pelletier, G. B.; Rinzler, D.; Waters, D. D. *N. Engl. J. Med.* **1988**, *319*, 1105.

(36) Fareed, J.; Hoppensteadt, D. A.; Bick, R. L. *Clin. Appl. Thromb./Hemostasis* **2003**, *9*, 101.

(37) Carter, N. J.; McCormack, P. L.; Plosker, G. L. *Drugs* **2008**, *68*, 691.

(38) Saliba, M. J. *Burns* **2001**, *27*, 349.

(39) Serra, R.; Buffone, G.; Molinari, V.; Montemurro, R.; Perri, P.; Stillitano, D. M.; Amato, B.; de Franciscis, S. *Int. Wound J.* **2015**, *12*, 150.

(40) Niers, T. M. H.; Klerk, C. P. W.; DiNisio, M.; Van Noorden, C. J. F.; Buller, H. R.; Reitsma, P. H.; Richel, D. J. *Crit. Rev. Oncol. Hematol.* **2007**, *61*, 195.

(41) Tyrrell, D. J.; Horne, A. P.; Holme, K. R.; Preuss, J. M. H.; Page, C. P. *Adv. Pharmacol.* **1999**, *46*, 151.

(42) Shafiq, N.; Malhotra, S.; Pandhi, P.; Sharma, N.; Bhalla, A.; Grover, A. *Pharmacology* **2006**, *78*, 136.

(43) Edelman, E. R.; Mathiowitz, E.; Langer, R.; Klagsbrun, M. *Biomaterials* **1991**, *12*, 619.

(44) Whalen, G. F.; Shing, Y.; Folkman, J. *Growth Factors* **1989**, *1*, 157.

(45) Pelegri-O'Day, E. M.; Lin, E.-W.; Maynard, H. D. *J. Am. Chem. Soc.* **2014**, *136*, 14323.

(46) Sasisekharan, R.; Moses, M. A.; Nugent, M. A.; Cooney, C. L.; Langer, R. *Proc. Nat. Acad. Sci. USA* **1994**, *91*, 1524.

(47) Shriver, Z.; Capila, I.; Venkataraman, G.; Sasisekharan, R. *Handb. Exp. Pharmacol.* **2012**, 159.

(48) Cohen, M.; Demers, C.; Gurfinkel, E. P.; Turpie, A. G. G.; Fromell, G. J.; Goodman, S.; Langer, A.; Califf, R. M.; Fox, K. A. A.; Premmereur, J.; Bigonzi, F. *N. Engl. J. Med.* **1997**, *337*, 447.

(49) Paluck, S. J.; Nguyen, T. H.; Maynard, H. D. *Biomacromolecules* **2016**, *17*, 3417.

(50) Papy-Garcia, D.; Barbier-Chassefiere, V.; Rouet, V.; Kerros, M. E.; Klochendler, C.; Tournaire, M. C.; Barritault, D.; Caruelle, J. P.; Petit, E. *Macromolecules* **2005**, *38*, 4647.

(51) Mauzac, M.; Jozefonvicz, J. *Biomaterials* **1984**, *5*, 301.

(52) Tardieu, M.; Gamby, C.; Avramoglou, T.; Jozefonvicz, J.; Barritault, D. *J. Cell. Physiol.* **1992**, *150*, 194.

(53) Liekens, S.; Leali, D.; Neyts, J.; Esnouf, R.; Rusnati, M.; Dell'Era, P.; Maudgal, P. C.; De Clercq, E.; Presta, M. *Mol. Pharmacol.* **1999**, *56*, 204.

(54) Nguyen, T. H.; Paluck, S. J.; McGahran, A. J.; Maynard, H. D. *Biomacromolecules* **2015**, *16*, 2684.

(55) Regan, J. R.; Bruno, J. G.; Chang, M. N.; Sabatino, R.; Dalisa, R.; Bensasson, S. A.; Eilat, D. *J. Bioact. Compat. Polym.* **1993**, *8*, 317.

(56) Mammadov, R.; Mammadov, B.; Guler, M. O.; Tekinay, A. B. *Biomacromolecules* **2012**, *13*, 3311.

(57) Sun, X. L.; Grande, D.; Baskaran, S.; Hanson, S. R.; Chaikof, E. L. *Biomacromolecules* **2002**, *3*, 1065.

(58) Grasel, T. G.; Cooper, S. L. *J. Biomed. Mater. Res.* **1989**, *23*, 311.

(59) Ito, Y.; Iguchi, Y.; Imanishi, Y. *Biomaterials* **1992**, *13*, 131.

(60) Nguyen, T. H.; Kim, S.-H.; Decker, C. G.; Wong, D. Y.; Loo, J. A.; Maynard, H. D. *Nat. Chem.* **2013**, *5*, 221.

(61) Benezra, M.; Ishai-Michaeli, R.; Ben-Sasson, S. A.; Vlodavsky, I. *J. Cell. Physiol.* **2002**, *192*, 276.

(62) Perrier, S.; Takolpuckdee, P. *J. Polym. Sci., Part A:Polym. Chem.* **2005**, *43*, 5347.

(63) Ornitz, D. M.; Yayon, A.; Flanagan, J. G.; Svahn, C. M.; Levi, E.; Leder, P. *Mol. Cell. Biol.* **1992**, *12*, 240.

(64) Yoshida, A.; AnandApte, B.; Zetter, B. R. *Growth Factors* **1996**, *13*, 57.

(65) Seghezzi, G.; Patel, S.; Ren, C. J.; Gualandris, A.; Pintucci, G.; Robbins, E. S.; Shapiro, R. L.; Galloway, A. C.; Rifkin, D. B.; Mignatti, P. *J. Cell Biol.* **1998**, *141*, 1659.

(66) Montesano, R.; Vassalli, J. D.; Baird, A.; Guillemin, R.; Orci, L. *Proc. Natl. Acad. Sci. USA* **1986**, *83*, 7297.

(67) Giraux, J. L.; Matou, S.; Bros, A.; Tapon-Bretaudiere, J.; Letourneur, D.; Fischer, A. M. *Eur. J. Cell Biol.* **1998**, *77*, 352.

(68) Hetheridge, C.; Mavria, G.; Mellor, H. *Biochem. Soc. Trans.* **2011**, *39*, 1597.

(69) Donovan, D.; Brown, N. J.; Bishop, E. T.; Lewis, C. E. *Angiogenesis* **2001**, *4*, 113.

(70) Bishop, E. T.; Bell, G. T.; Bloor, S.; Broom, I. J.; Hendry, N. F.; Wheatley, D. N. *Angiogenesis* **1999**, *3*, 335.

(71) DeLisser, H. M.; ChristofidouSolomidou, M.; Strieter, R. M.; Burdick, M. D.; Robinson, C. S.; Wexler, R. S.; Kerr, J. S.; Garlanda, C.; Merwin, J. R.; Madri, J. A.; Albelda, S. M. *Am. J. Pathol.* **1997**, *151*, 671.

(72) Jung, S. P.; Siegrist, B.; Wade, M. R.; Anthony, C. T.; Woltering, E. A. *Angiogenesis* **2001**, *4*, 175.

(73) Benaglia, M.; Chiefari, J.; Chong, Y. K.; Moad, G.; Rizzardo, E.; Thang, S. H. *J. Am. Chem. Soc.* **2009**, *131*, 6914.

(74) Chen, R.; John, J.; Lavrentieva, A.; Mueller, S.; Tomala, M.; Zhao, Y.; Zweigerdt, R.; Beutel, S.; Hitzmann, B.; Kasper, C.; Martin, U.; Rinas, U.; Stahl, F.; Scheper, T. *Eng. Life Sci.* **2012**, *12*, 29.

(75) Ornitz, D. M.; Leder, P. *J. Biol. Chem.* **1992**, *267*, 16305.

Chapter 3

Structure Activity Relationship of Heparin Mimicking Polymer p(SS-*co*-PEGMA): Effect of Sulfonation and Polymer Size on FGF2 Receptor Binding[†]

3.1 Introduction

Fibroblast growth factor 2 (FGF2) is a widely studied growth factor with important roles in cell growth, migration, and angiogenesis.[1-3] In its active form, fibroblast growth factor 2 (FGF2) is part of a pentameric complex that is required for mitogenic activity.[4,5] This complex is comprised of two FGF2 proteins, two FGF receptors (FGFRs) and heparan sulfate, a naturally occurring glycosaminoglycan. The two FGF2 proteins dimerize and dock on the FGFRs with heparan sulfate threaded through the binding pocket, interacting with amino acids on both the protein and receptor.[4] Heparin is required for receptor binding to occur and helps to facilitate protein dimerization and receptor binding, as well as stabilization of the protein.[5-7]

Because of its important biological role, heparin is an attractive therapy for treatment of diseases.[8] However, as discussed in Chapter 1, heparin is very heterogeneous in nature.[9,10] Polysaccharide size is one of the factors that contributes to its heterogeneity, with naturally occurring molecular weights ranging from 5 to 40 kDa.[9] Another factor is its sulfation pattern. The placement and degree of sulfation varies widely between saccharide units, and the structure and charge density of heparin play a large role in modulating binding.[11,12] Due to its heterogeneity, synthetic heparin mimics have been prepared as therapies to replace heparin for the purposes of either enhancing or preventing FGF2 receptor binding.[9,13] In applications where angiogenesis and cell growth are not desired, mimics have been designed to hinder receptor binding and are intended for use in cancer therapeutics.[14-16] Conversely, mimics that enhance receptor binding have been useful in applications where protein activity is required, such as in treatments for wound healing and ischemic conditions.[13,17]

The ability to modulate the heparin mimicking nature of polymers is attractive for applications in therapeutics where fine-tuning of heparin mimicking properties is desired. For

instance, recent work has demonstrated that changing the degree of sulfonation can affect heparin-mimicking polymer properties. Chen and coworkers found that cell growth could be tuned by manipulating styrene sulfonate (SS) incorporation in poly(styrene sulfonate-*co*-methacrylamido glucopyranose) (p(SS-*co*-MAG)).[18] Maximum embryonic stem cell proliferation was obtained when the ratio of SS:MAG was approximately 1:1, and this polymer enhanced cell growth to a greater extent than heparin itself. Cell growth was also tuned to have cell proliferation lower than added heparin, in the case of higher SS incorporation, and to have cell proliferation profiles similar to that of heparin, in the case of higher MAG incorporation. Additionally, changing the degree or location of sulfonation has been shown to influence protein binding[19] and increase blood coagulation times.[20,21] Location of sulfate moieties also plays a role in biological activity. By altering the placement and number of sulfates on sugar side chains in glycopolymers, certain biological pathways can be targeted.[22,23]

Another factor that influences the biological properties of heparin is polymer size. To assess how size affects function, Hsieh-Wilson and coworkers polymerized heparin mimicking glycopolymers by ROMP.[24] They found that anticoagulant activity could be modulated by changing polymer size. Specifically, increasing glycopolymer chain length increased blood coagulation times. Smaller heparin mimics can also display useful properties. Miura and coworkers found that lower molecular weight heparin mimics were able to inhibit amyloid-beta aggregation better than the higher molecular weight heparin mimics.[25]

We previously found that the heparin mimicking polymer poly(styrene sulfonate-*co*-poly(ethylene glycol) methyl ether methacrylate) (p(SS-*co*-PEGMA)) with a number average molecular weight (M_n) of 26 kDa could stabilize FGF2, but not activate it for receptor binding.[26] We also demonstrated that poly(vinyl sulfonate) (pVS) could facilitate FGF2 binding to its

receptor,[17] but did not stabilize FGF2 well.[13] We then showed that a block copolymer containing both segments could facilitate receptor binding in the absence of heparin, stabilize FGF2, and the FGF2-p(SS-*co*-PEGMA)-*b*-VS conjugate had superagonist activity compared to the unmodified protein.[13] However, the block copolymer is difficult to make with controlled end groups, mostly due to the complex polymerization of activated and deactivated monomers. In order to explore potential receptor binders, we decided to further examine the stabilizing block, p(SS-*co*-PEGMA), to determine if it could be structurally manipulated to enhance FGF2-receptor binding. To accomplish this, we investigated how varying the degree of SS monomer incorporation and polymer chain length would affect the polymers ability to facilitate receptor binding. The data and results are described in detail below.

3.2 Results and Discussion

3.2.1 Polymerization of p(SS-*co*-PEGMA) to Yield Library of Polymers with Varying Degrees of Sulfonation

To understand the structure activity relationship of our p(SS-*co*-PEGMA) heparin-mimicking polymer, we first investigated how varying the degree of sulfonated monomer incorporation would affect receptor binding. Reversible addition fragmentation chain transfer (RAFT) polymerization was utilized to synthesize a small p(SS-*co*-PEGMA) library with varying degrees of styrene sulfonate (SS) monomer incorporation. A previously reported trithiocarbonate chain transfer agent, **CTA 1** was used to copolymerize SS and PEGMA monomers with varying initial feed ratios (Scheme 1a).[27] This chain transfer agent containing a pryidyl disulfide group was chosen so that the polymers could be conjugated to the protein, which presents two free cysteines (Scheme 1b).

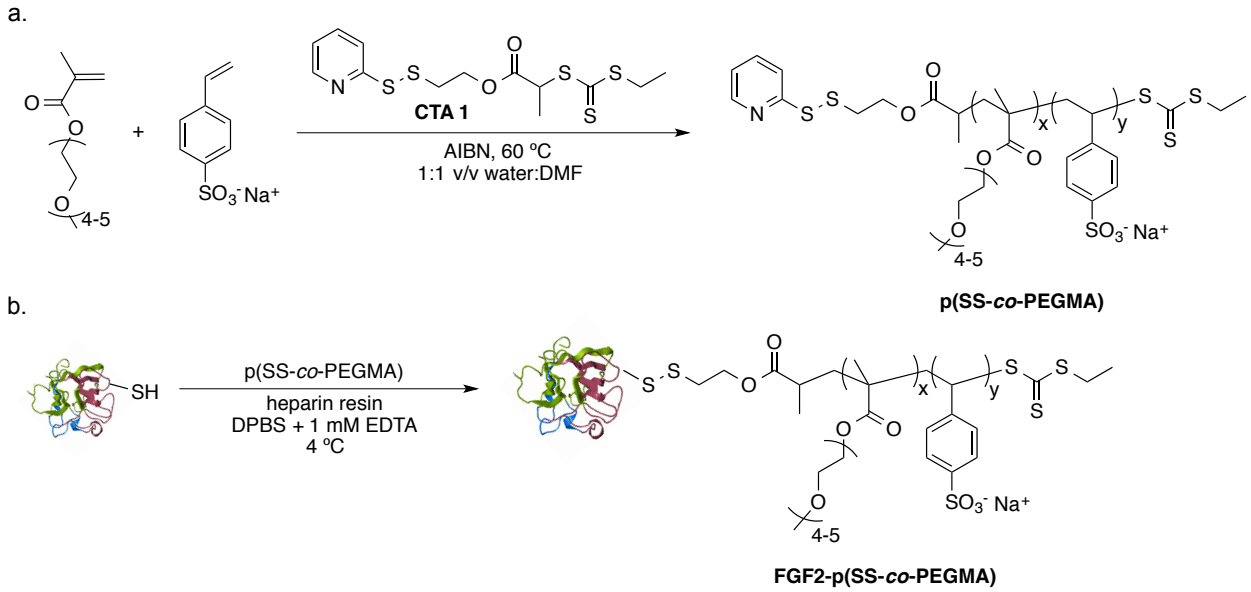

Scheme 3-1. Synthesis of heparin mimicking polymer-protein conjugate, FGF2-p(SS-*co*-PEGMA). (a) Polymerization of p(SS-*co*-PEGMA) via RAFT polymerization. (b) Conjugation of p(SS-*co*-PEGMA) to FGF2 via disulfide exchange. Protein structure modified from PDB 1CVS using PyMOL software.

Eight polymers were synthesized by RAFT polymerization with degrees of sulfonation ranging from 8.0% to 100% (Table 3-1). Polymer DP was maintained at approximately 135 monomer units in order to verify that any receptor binding observed was due to changes in degree of sulfonation and not polymer chain length. In addition, pPEGMA was homopolymerized so the library would contain 0% SS and 100% SS controls. Initially, RAFT polymerization was attempted to polymerize pPEGMA, however the polymerizations gelled even after manipulation of concentration and feed ratios. Therefore, atom-transfer radical polymerization (ATRP) was utilized to successfully polymerize pPEGMA as previously reported.[26]

Table 3-1. p(SS-*co*-PEGMA) library with varying styrene sulfonate monomer incorporation.

Polymer	Feed Ratio [SS]:[PEGMA]:[CTA 1]:[AIBN]	[SS]:[PEGMA] in Polymer	SS%	DP (NMR)	M_n (NMR)	M_n (GPC)[b]	$Đ$
pPEGMA	66:1:4.3:8.3[a]	0:1	0%	129	43.6	53.2	1.16
P(SS-*co*-PEGMA)$_{8.0}$	20:142:1:0.5	1:11.5	8.0%	141	41.6	51.0	1.20
P(SS-*co*-PEGMA)$_{28}$	38:118:1:0.5	1:2.5	28.4%	124	34.1	43.4	1.24
P(SS-*co*-PEGMA)$_{55}$	117:63:1:0.5	1.2:1	54.5%	136	34.2	34.8	1.26
P(SS-*co*-PEGMA)$_{63}$	148:42:1:0.5	1.7:1	62.9%	135	33.4	24.8	1.26
P(SS-*co*-PEGMA)$_{76}$	155:41:1:0.5	3.2:1	76.3%	135	31.3	23.6	1.24
P(SS-*co*-PEGMA)$_{81}$	166:30:1:0.5	4.4:1	81.4%	139	31.4	23.2	1.26
P(SS-*co*-PEGMA)$_{95}$	195:10:1:0.5	18:1	94.7%	139	29.7	22.5	1.29
pSS	205:0:1:0.5	1:0	100%	114	23.0	14.4	1.31

[a][PEGMA]:[Initiator]:[CuBr]:[bipy]
[b]GPC values calculated in DMF using an RI detector with polystyrene standards

3.2.2 Evaluation of Polymer Kinetics

Polymer kinetics were monitored for p(SS-*co*-PEGMA)$_{81}$ by taking time points throughout the duration of the polymerization. The plot of $\ln(M_0/M_t)$ in relation to reaction time was found to be linear, which confirms that the polymerization is first order and controlled, as we previously reported for the copolymerization of SS and PEGMA with a similar CTA (Figure 3-1a).[26] Additionally, the percentage of SS incorporation was maintained between 79.1% and 82.4% throughout the duration of the polymerization (Figure 3-1b). Furthermore, the molecular weight dispersity remained below 1.28 for all timepoints taken (Figure 3-1c). Reactivity ratios were calculated using the curve fitting method with time points of all polymers from Table 3-1 taken at 10-20% conversion. The data was similar when using ~50% of ~70% conversion (data not shown). The mole fraction of SS in the copolymer (F_{SS}) was plotted against the mole fraction of SS in the monomer solution (f_{SS}) (Figure 3-1d). The reactivity ratios for SS (r_{SS}) and PEGMA

(r_{PEGMA}) were both found to be below 1.0 (r_{SS} = 0.57 and r_{PEGMA} = 0.46), and are similar to reactivity ratios previously reported using the Fineman-Ross method (rSS = 0.70 rPEGMA = 0.50).[28] The azeotropic point was determined to be 55% SS monomer incorporation. Above the azeotropic point the compositional drift tended to prefer to add less SS than PEGMA and below the azeotropic point compositional drift tended to prefer to add more SS than PEGMA.

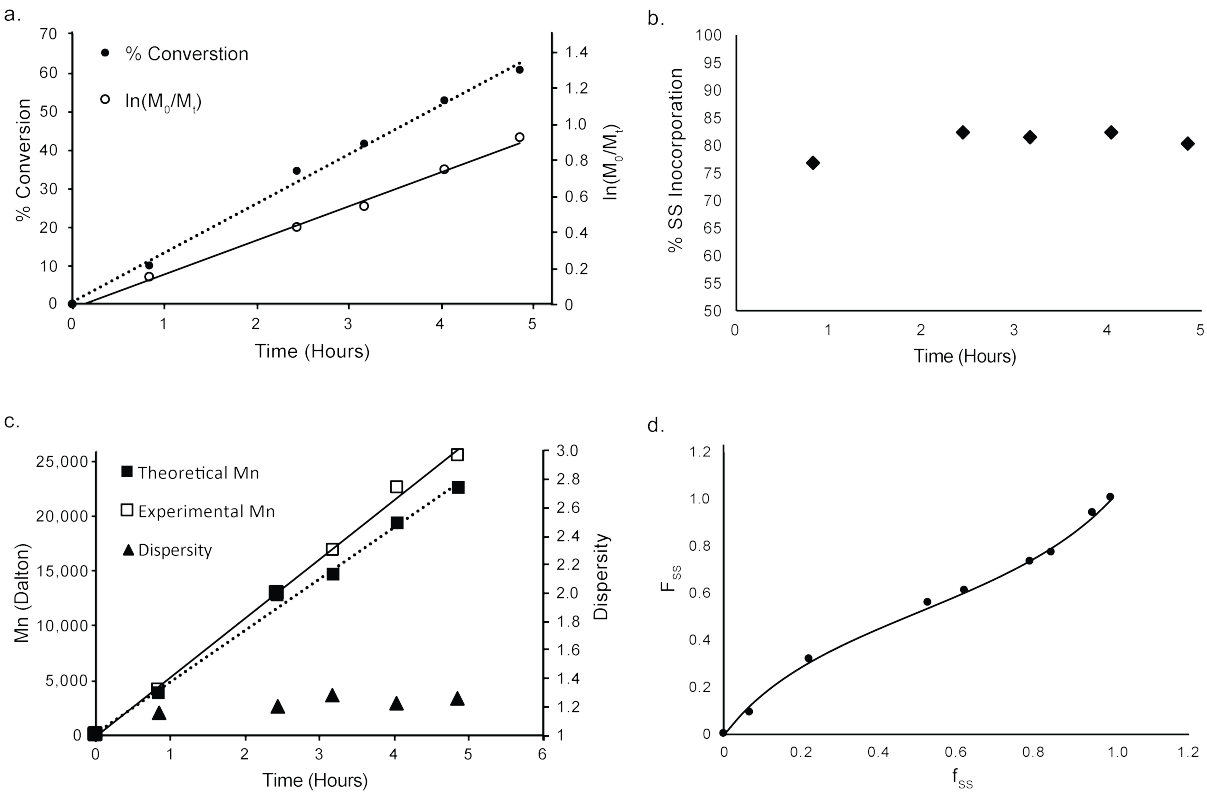

Figure 3-1. Polymer kinetics performed on p(SS-*co*-PEGMA) polymerizations. (a) Kinetic studies of the RAFT polymerization of $p(SS\text{-}co\text{-}PEGMA)_{81}$ at 70 ºC. Conversion, M_0, and M_t were calculated using ^1H NMR spectroscopy. (b) Percent styrene sulfonate incorporation over time. (c) Theoretical versus experimental M_n from right angle light scattering in aqueous running buffer. (d) F_{SS} versus f_{SS} curves.

3.2.3 Effect of Degree of Sulfonation on Receptor Binding with Excipients

After the library of polymers was obtained, the effect of SS monomer incorporation on receptor binding was examined using a FGF-receptor enzyme linked immunosorbent assay

(ELISA). In this assay, the FGF receptor FGF1α was immobilized in the wells of a 96 well plate. The receptor was then incubated with 1 ng/mL of FGF2 with 1μg/mL of either heparin or each of the polymers from Table 3-1. After washing away unbound FGF2, remaining receptor-bound FGF2 was monitored through the use of a secondary antibody. Without heparin, the binding to FGF2 to FGF1α was minimal, and as expected, the addition of heparin induced a large increase in receptor binding (Figure 3-2a). Additionally, we found that there was an increase in receptor binding for p(SS-*co*-PEGMA)$_{81}$. Even though there was an increase in receptor binding, it was not to the same extent as heparin. It is possible for the polymer to conjugate to FGF2 via disulfide exchange with the pyridyl disulfide end group on the polymer during sample incubation. This conjugation could occur at cysteines in the heparin binding domain or on the outside of the protein, altering receptor binding. Furthermore, we found that pSS inhibited FGF2 binding to its receptor. This was not surprising since similar results have been previously reported and is speculated to be due to the conformation of the polymer in the heparin binding pocket, which allows tight binding to the protein, but not to the receptor.[16,17,29] It is important to note that due to the high concentration of polymer added and the disulfide end group on the polymer, it is possible for the polymer to conjugate to the protein via disulfide exchange during sample incubation. Conjugation could alter receptor binding observed.

To evaluate the ability of the polymers to assist in FGF receptor binding in a more complex system, a cell-based assay was performed using BaF3 FR1c cells. This cell line was engineered to express FGF receptors on the cell surface, but lack native heparan sulfate proteoglycans.[30,31] For cell growth to be observed, exogenous heparin or heparin mimics are required. Therefore, this cell line is useful for assessing the ability of heparin mimics to facilitate receptor binding. Cells were incubated with 1 ng/mL of FGF2 and either 1 μg/mL of heparin or

heparin mimicking polymers. As shown in Figure 3.2b, when 1 µg/mL of heparin is added there was a large increase in cell proliferation up to 401.7±10% compared to 190±13% for FGF2 alone. When p(SS-*co*-PEGMA)$_{81}$ was incubated with the cells an increase in proliferation of 255±9% was observed.

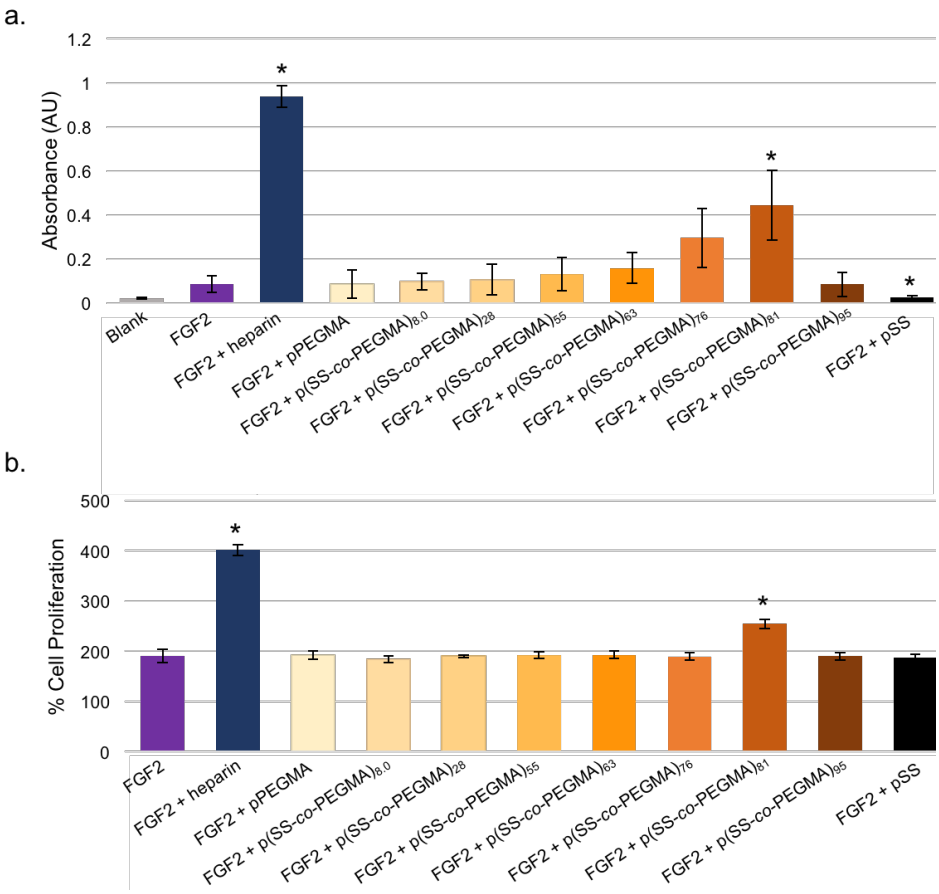

Figure 3-2. Examination of the ability of p(SS-*co*-PEGMA) to enhance FGF2 receptor binding. (a) FGF Receptor based ELISA. The experiment was repeated 3 times with n = 3 for each experiment. Error bars represent the standard deviation. (b) Cell growth of heparin-mimicking polymers in BaF3-FR1C cells. Data was normalized to the blank medium group, which was set at 100%. The experiment was repeated 3 times with n = 6 for each experiment. Error bars represent the standard deviation. Statistical analysis was done using Student's t test. * $p < 0.01$ compared to FGF2.

3.2.4 Preparation of FGF2-p(SS-*co*-PEGMA) conjugates

Next, covalent FGF2-polymer conjugates were prepared to determine if similar binding profiles could be observed. Protein-polymer conjugates can be preferable to excipients in that the polymer is used in much lower concentration as a conjugate. Thus, less polymer is required to achieve a similar biological response; likely due to attachment of the polymer near the binding site. The polymers from Table 3-1 all contain a protein reactive pyridyl disulfide (PDS) end group. This end group was used as a protein reactive handle to covalently attach the polymer to FGF2 through disulfide exchange, as shown in Scheme 3-1b. Conjugations were performed on heparin resin to prevent conjugation in the heparin binding site and conjugates were purified by centrifugation filtration. Conjugations were analyzed through sodium dodecyl sulfate poly(acrylamide) gel electrophoresis (SDS-PAGE) with protein detection by Western Blot (Figure 3-3a). Conjugates were observed as smears at slightly higher molecular weights than free protein (Figure 3-3a). Because the polymer conjugation was achieved through a disulfide bond, the addition of dithiothreitol (DTT) reduced the disulfide bond producing free protein, further verifying successful conjugation (Figure 3-3b). While conjugates are present in the gels and show up as higher molecular weight smears, there is still unconjugated FGF2 despite repeated purification. After analyzing conjugate concentration by ELISA receptor binding assays were used to determine extent of binding.

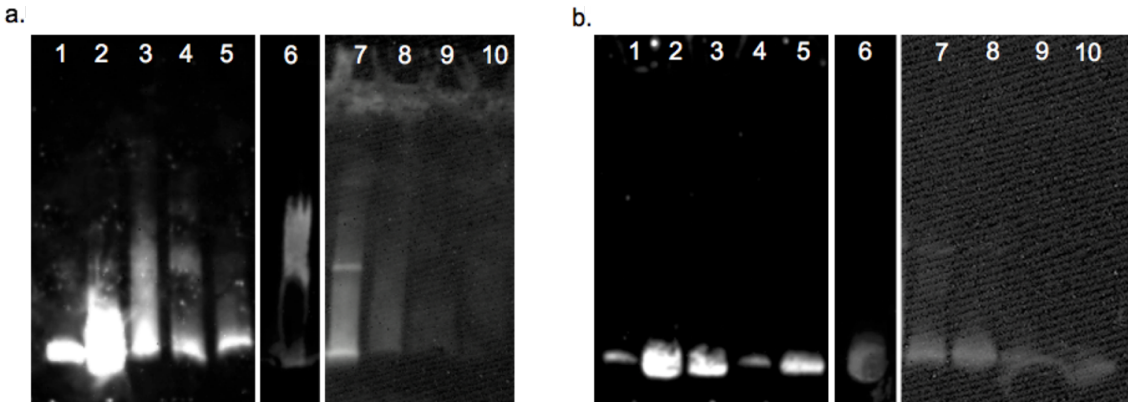

Figure 3-3. SDS-PAGE with Western Blot of FGF-p(SS-*co*-PEGMA) conjugates in both (a) non-reducing conditions and (b) reducing conditions. Lane 1: FGF2, Lane 2: FGF2-p(SS-*co*-PEGMA)$_{8.0}$, Lane 3: FGF2-p(SS-*co*-PEGMA)$_{28}$, Lane 5: FGF2-p(SS-*co*-PEGMA)$_{55}$, Lane 6: FGF2-p(SS-*co*-PEGMA)$_{81}$, Lane 7: FGF2-pPEGMA, Lane 8: FGF2-p(SS-*co*-PEGMA)$_{76}$, Lane 9: FGF2-p(SS-*co*-PEGMA)$_{95}$, Lane 10: FGF2-pSS.

3.2.5 Effect of Degree of Sulfonation on Receptor Binding with Conjugates

The conjugates were tested for extent of receptor binding in both ELISA and cell-based assays. Out of the polymer library tested, the FGF2-p(SS-*co*-PEGMA)$_{81}$ conjugate performed the best with an increase in absorbance of 0.29±0.08 AU when compared to FGF2 alone, which had an absorbance of 0.10±0.05 AU (Figure 3-4a). The conjugate did not facilitate receptor binding as well as heparin, which gave an absorbance of 1.01±0.10 AU. Similar results were observed in the BaF3-FR1c assay with FGF2-p(SS-*co*-PEGMA)$_{81}$ giving cell proliferation of 285±50% when compared to FGF2 alone, which gave cell proliferation of 203±12% (Figure 3-4b). Again the cell proliferation observed for FGF2-p(SS-*co*-PEGMA)$_{81}$ was not as high as FGF2 with added heparin (547±15%). Conjugates with higher degrees of sulfonation (pSS and p(SS-*co*-PEGMA)$_{95}$) exhibited statistically decreased binding when compared to FGF2 alone. This is consistent with what was observed for the excipient data.

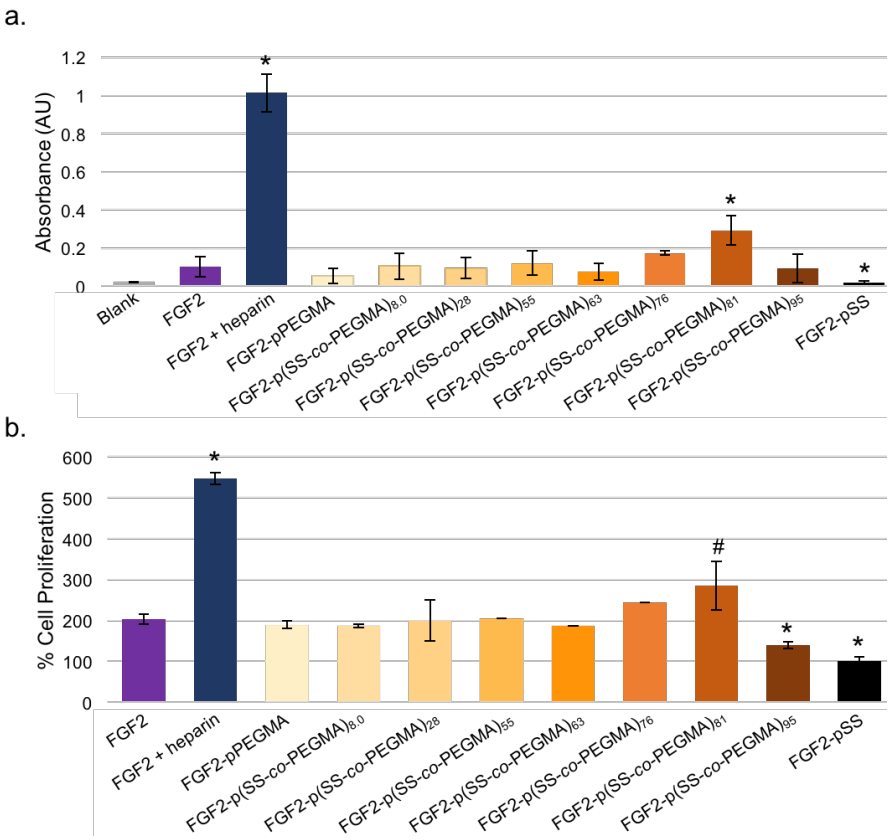

Figure 3-4. FGF2-p(SS-*co*-PEGMA) conjugates in FGF2 receptor binding assays. (a) FGF Receptor based ELISA. The experiment was repeated three times with n = 3 for each experiment. Error bars represent the standard deviation. (b) Cell growth of heparin-mimicking polymer conjugates in BaF3-FR1C cells. Data was normalized to the blank medium group, which was set at 100%. Each sample contained six replicates and the experiment was repeated three times. Error bars represent standard deviation. Statistical analysis was done using Student's t test. * $p < 0.01$ compared to FGF2, # $p < 0.03$ compared to FGF2.

3.2.6 Verification of Conjugate Activity

Since p(SS-*co*-PEGMA)$_{81}$ was not able to achieve full receptor binding, we wanted to ensure that the protein itself was not denatured during the conjugation reaction. To do this, 1 µg/mL of heparin was added to the conjugate and cell proliferation was monitored in BaF3-FR1c

cells. As shown in Figure 3-5, the conjugate plus 1 μg/mL heparin exhibited similar binding as FGF2 alone plus 1 μg/mL heparin.

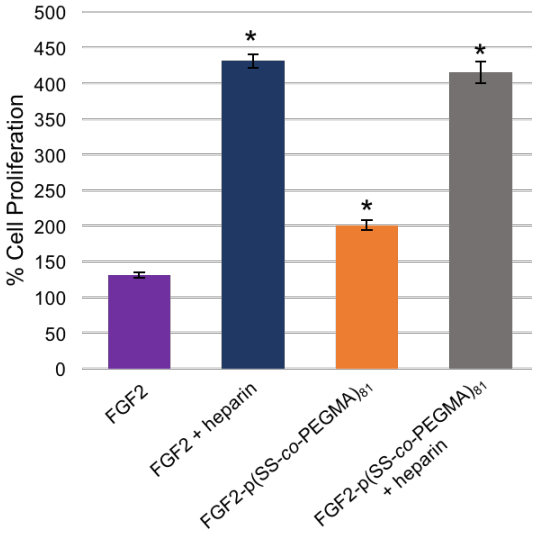

Figure 3-5. Determination of FGF2-p(SS-*co*-PEGMA)$_{81}$ receptor binding in BaF3-FR1c with the addition of 1 μg/mL heparin. Data was normalized to the blank medium group, which was set at 100%. Each sample contained six replicates. Error bars represent standard deviation. Statistical analysis was done using Student's t test. * $p < 0.01$ compared to FGF2.

Taken together these results demonstrate that 81% styrene sulfonate provided the best results out of the polymers tested. This was true whether conjugate was tested alone or with excess added polymer. Further when heparin was added to p(SS-*co*-PEGMA)$_{81}$, full cellular response was obtained as when heparin was added to FGF2. This demonstrates that the protein in the 81% conjugate is still bioactive and able to attain full efficacy with exogenous heparin. Thus, the conjugation procedure did not decrease FGF2 activity, but rather the polymer is not able to facilitate receptor binding to the same extent as heparin itself.

3.2.7 Effect of Polymer Size on Receptor Binding

It has previously been shown that polymer size can affect the therapeutic properties of heparin mimicking polymers.[24,25] Therefore, we wanted to determine if there was an optimal size

for receptor binding of FGF2-p(SS-*co*-PEGMA)$_{81}$. A small library of p(SS-*co*-PEGMA)$_{81}$ was polymerized by RAFT polymerization with **CTA 1** (Scheme 3-1a). The degree of sulfonation was maintained close to 80%, the best performing styrene sulfonate incorporation from the studies described above. DP was varied from 41 to 390 monomer units. This was done by maintaining the ratio of [SS]:[PEGMA] at approximately 5.5:1 in the initial feed ratio, but changing the ratio of total monomer concentration to CTA. Molecular weights of the polymers were calculated by ^{1}H NMR analysis relative to PDS end group (Table 3-2).

Table 3-2. p(SS-*co*-PEGMA) library with varying sizes and 81% SS incorporation.

Polymer	Feed Ratio [SS]:[PEGMA][a]	DS (^{1}H NMR)	M_n (^{1}H NMR)	DP (^{1}H NMR)	DP (GPC)[b]	M_n (GPC)[b]	$Đ$
p(SS-*co*-PEGMA) DP41	48:8	82.7%	8.8 kDa	38	41	9.3 kDa	1.15
p(SS-*co*-PEGMA) DP78	112:19	82.6%	16.6 kDa	73	78	17.5 kDa	1.37
p(SS-*co*-PEGMA) DP161	183:33	82.1%	31.7 kDa	141	161	35.4 kDa	1.13
p(SS-*co*-PEGMA) DP223	332:60	82.1%	53.1 kDa	236	223	49.7 kDa	1.14
p(SS-*co*-PEGMA) DP263	448:81	81.6 %	60.3 kDa	268	263	57.9 kDa	1.14
p(SS-*co*-PEGMA) DP295	608:109	80.9%	84.0 kDa	373	295	64.9 kDa	1.16
p(SS-*co*-PEGMA) DP390	767:138	82.0%	95.8 kDa	428	390	85.6 kDa	1.19

[a]Feed ratios of [CTA]:[AIBN] = 1:0.5 for all polymers
[b]GPC values calculated in aqueous buffer using a right angle light scattering detector

Additionally, right angle light scattering (RALS) GPC was utilized to determine accurate polymer molecular weight. All GPC traces were monomodal, except for p(SS-*co*-PEGMA)DP78, which contained a higher molecular weight shoulder (Figure 3-6). In general, the molecular weights by RALS-GPC and those calculated by ^{1}H NMR were similar. However, as molecular weight increased the difference between ^{1}H NMR M_n and GPC M_n increased. This is likely due to inaccuracies from calculating the molecular weights from the ^{1}H NMR spectra

when the concentrations of the end groups are relatively small. Therefore, molecular weights calculated by RALS-GPC are likely more accurate, and the DPs provided in the polymer names in Table 3-2 were based on the RALS-GPC data.

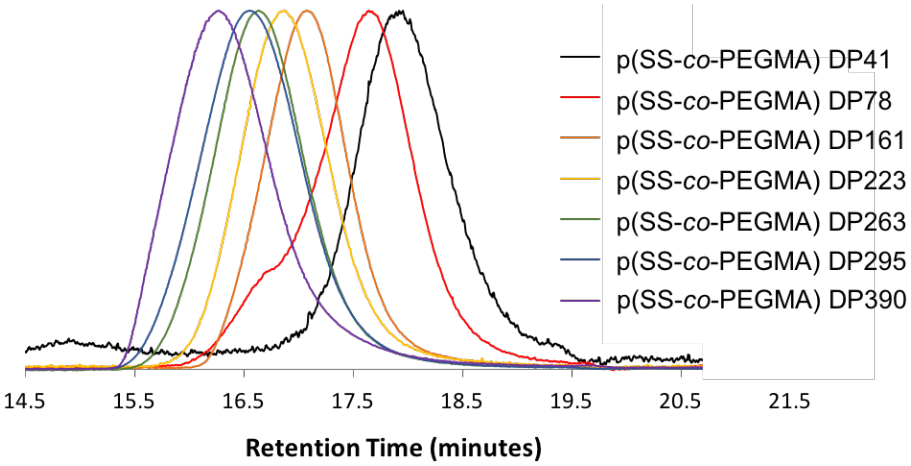

Figure 3-6. Light scattering GPC traces showing varying molecular weight polymers with 81% SS

The polymers from Table 3-2 were tested for receptor binding as excipients at a concentration of 1 µg/mL when added to 1 ng/mL of FGF2 as described above. No further increase in receptor binding was observed in relation to size. In the FGFR ELISA (Figure 3-7a) the polymers contributed to an increase in receptor binding up to 0.42±0.03 AU compared to FGF2 alone, which exhibited a response of 0.14±0.02 AU. FGF2 with 1 µg/mL of added heparin gave a response of 1.0±0.05 AU. The BaF3 receptor assay (Figure 3-7b) showed similar results with the polymers contributing to an increase in cell proliferation up to 215±12% when compared to FGF2, which had cell proliferation of 155±17%. These results were compared to heparin, which gave a cell response of 334±9%. Larger molecular weight polymers (DP295 and DP390) did not promote any receptor binding and were actually not statistically different from

FGF2. This data suggests that the size of the polymer does not matter, except for degrees of polymerization greater than or equal to 295.

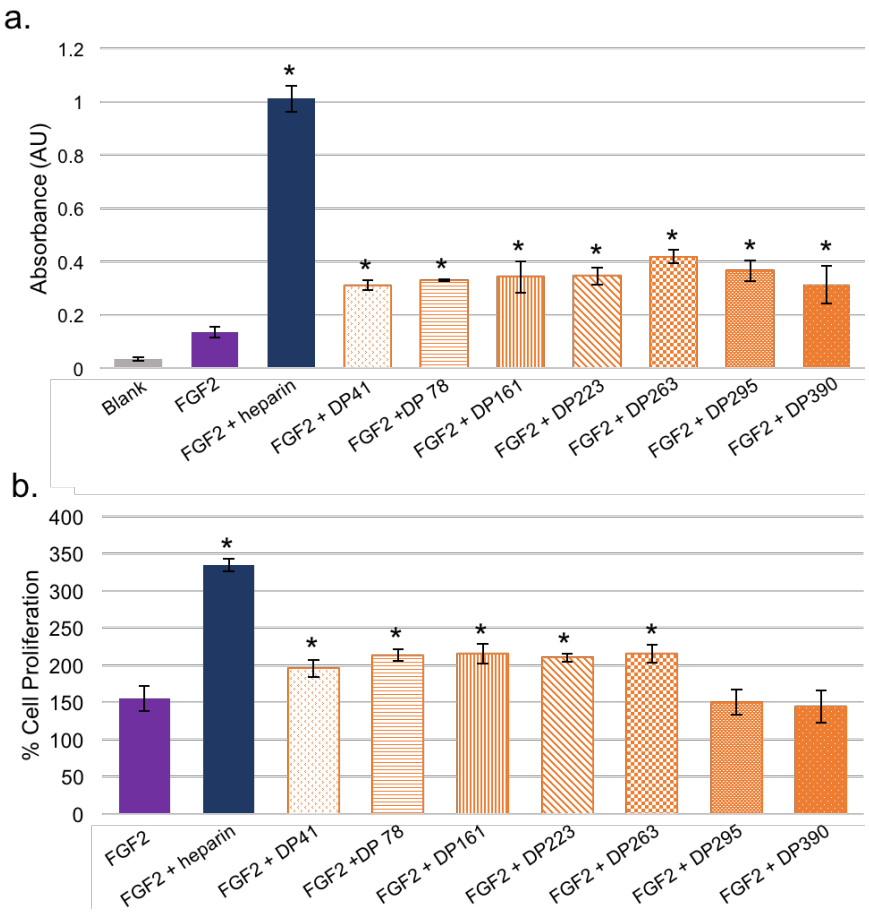

Figure 3-7. Determining the ability of p(SS-*co*-PEGMA) with varying polymer sizes to enhance FGF receptor binding. (a) FGF receptor based ELISA. The experiment was repeated 3 times with n = 3 for each experiment. Error bars represent standard deviation. (b) Cell growth of heparin-mimicking polymers in BaF3-FR1C cells. Data was normalized to the blank medium group, which was set at 100%. Each sample contained six replicates and the experiment was repeated three times. Error bars represent standard error of the mean (SEM). Statistical analysis was done using Student's t test. * $p < 0.01$ compared to FGF2.

While the heparin mimicking polymers did show a significant increase in receptor binding when compared to FGF2 alone, they were not able to facilitate receptor binding to the same extent as heparin. This observation may be due to the lowest energy conformation of the polymer. It could be that the p(SS-*co*-PEGMA) polymer is not able to display the sulfonates in the same locations that are necessary for receptor binding. Binding pockets are often specific in nature, so if the sulfonates are not displayed in the correct orientation then binding will not occur. While previous reports have shown that heparin-mimicking polymers can be tuned for receptor binding, this is the first report showing the tunable nature of p(SS-*co*-PEGMA) specifically. We have found that the degree of styrene sulfonate monomer incorporation is important for receptor binding, and thus, can likely influence other biological outcomes. Specifically, a degree of sulfonate monomer incorporation of approximately 81% is sufficient to increase protein activity in cells lacking heparin sulfate proteoglycans. Polymer size did not contribute to an increase in receptor binding, as all but the highest molecular weights facilitated FGF2 binding to its receptor to the same extent. These data together are important for understanding how to facilitate receptor binding of the known heparin mimicking polymer p(SS-*co*-PEGMA).

3.3 Conclusions and Future Directions

A small library of p(SS-*co*-PEGMA) polymers was polymerized by RAFT polymerization to contain polymers of similar sizes but varying degrees of styrene sulfonate incorporation. Polymers were conjugated to FGF2 and verified by SDS-PAGE stained with Western Blot. Both conjugates and FGF2 with polymers added in excess were assayed in ELISA based receptor binding assays and BaF3 cell based receptor binding assays. p(SS-*co*-PEGMA)$_{81}$

was identified to facilitate receptor binding of FGF2 to its receptors better than the other polymers, but not to the same extent as heparin. In order to determine the effect of degree of polymerization, another library of polymers was synthesized keeping degree of sulfonation the same at approximately 81% and altering the size of the polymer. Ultimately, changing the size of the polymers did not increase receptor binding. This information study shows that the heparin-mimicking nature of p(SS-*co*-PEGMA) can be increased, specifically by altering degree of sulfonated monomer incorporation rather than changing polymer size.

3.4 Experimental

3.4.1 Materials

Chemicals and reagents were purchased from Sigma Aldrich and used as received unless otherwise indicated. Prior to polymerizations 4-styrene sulfonic monomer was pretreated with Na^+ and dried to produce the sodium salt. Before polymerization azobis(isobutyronitrile) (AIBN) was recrystallized twice from ethanol and dried. Pyridyl disulfide pPEGMA (PDS-pPEGMA) was synthesized by ATRP as previously described.[32] Protein was expressed and purified from the plasmid pET29c(+)hFGF-2, which was kindly provided by Professor Thomas Scheper from the Helmholtz Centre for Infection Research (Braunschweig, Germany) according to Chen et al.[33] HiTrap Heparin HP columns were purchased from GE Healthcare. ELISA was performed using the ELISA Development DuoSet kit purchased from R&D Systems. Recombinant human FGFR1α(IIIc) Fc chimera, and ELISA Development DuoSet kits were purchased from R&D Systems. Blot antibodies were purchased from CALBIOCHEM (rabbit anti-fibroblast growth factor basic) and BioRad (goat anti-rabbit IgG-HRP conjugate). BaF3-FR1C expressing FGFR1 were kindly provided by Professor David Ornitz (Washington University, Saint Louis).[31] Cell medium was purchased from ATCC or Invitrogen unless otherwise indicated. Cell Titer Blue

Cell Viability Assay was purchased from Promega. Polystyrene standards for gel permeation chromatography (GPC) calibration were purchased from Polymer Laboratories.

3.4.2 Analytical Techniques

^{1}H NMR and ^{13}C NMR spectroscopy were performed on Avance DRX 400 MHz. Dimethylformamide (DMF) GPC was conducted in DMF containing 0.10 M LiBr (40 °C, 0.8 mL/min) on a Shimadzu HPLC system equipped with a refractive index detector RID-10A, one Polymer Laboratories PLgel guard column, and two Polymer Laboratories PLgel 5 μm mixed D columns. Calibration was performed using near-monodisperse polystyrene standards. Chromatograms were processed using the EZStart 7.2 chromatography software. Aqueous GPC was performed in 0.05 M Na_2SO_4 in MQ water with 10% MeOH on a Viscotek GPC_{max} VE 2001 GPC solvent/sample module equipped with Viscotek TDA 305 triple array detector. Gel electrophoresis was performed using Any kDTM Mini-PROTEAN TGXTM precast gels with SDS-Tris-glycine as running buffer (Biorad, Hercules). ELISA assays were read on an ELX800 Universal Microplate Reader (Bio-Tek Instrument Inc., Winooski) with λ = 450 nm for signal and 630 nm for background. Western blot was developed on a FluorChem FC2 System version 3.2 (Cell Biosciences, Santa Clara). CellTiter-Blue assays were read on a SpectraMax M5 microplate reader (Molecular Devices, Sunnyvale).

3.4.3 Methods

Polymerization of p(SS-co-PEGMA): RAFT polymerization was performed with varying feed ratios of [SS]:[PEGMA]:[CTA]:[AIBN] and a monomer concentration of 1.3 M. In an example polymerization, styrene sulfonate (382 mg, 1.85 mmol) was dissolved in 1.2 mL of degassed water in a Schlenk tube along with PEGMA M_n 300 (159 mg, 0.53 mmol). **CTA 1** (20 mg, 0.053 mmol) and AIBN (1.74 mg, 0.011 mmol) were dissolved in 1.2 mL of degassed DMF and then

transferred to the Schlenk tube. The Schlenk tube was sealed and subjected to four freeze-pump-thaw cycles before immersion in an oil bath set to 60 °C. After 4 hours the polymerization was stopped by cooling to room temperature and bubbling air through the Schlenk tube. The polymer was purified by dialysis in 3500 MWCO tubing against 1:1 v/v water:MeOH followed by 100% Milli-Q water. The resulting contents of the dialysis tubing were lyophilized to dryness. ^{1}H NMR 500 MHz (D_2O) δ: 8.40 (1H, s, PDS end group), 8.0-6.0 ($NaSO_3C_6\mathbf{H_4}$ side chains), 4.5-2.7 (PEGMA side chains), 2.7-0.0 (polymer backbone). The ^{1}H NMR spectrum of the resulting polymer was calibrated to the peak at 8.40 ppm, and the *Mn* of the polymer was calculated using the formula: M_n = [(integral of 8.0 – 6.0 ppm /4)*MW SS monomer]+[(integral of 4.5-2.7 ppm /20.4)*MW PEGMA monomer]+MW CTA. See ESI for ^{1}H NMR spectra with integrations for each polymer.

Conjugation of p(SS-co-PEGMA) to FGF2: FGF2 (100 μg, 5.9 x 10^{-3} μmol) was diluted in 400 μl of D-PBS + 1mM EDTA and loaded onto a column containing 0.5ml-heparin Sepharose resin. The resin was placed in a 4 ºC refrigerator for 30 minutes to allow the protein to bind to the resin. Next, 100 equivalents of PDS-p(SS-*co*-PEGMA) (various ratios or molecular weights) were dissolved in 400 μL of D-PBS + 1mM EDTA and loaded onto the column. The column was incubated at 4 °C for 16 hours. After incubation, the column was rinsed with 8 column volumes of D-PBS + 1 mM EDTA to remove unreacted polymer. Next, the column was rinsed with 10 column volumes of D-PBS + 2M NaCl to remove conjugates and protein. Conjugate was purified using a CentriPrep® centrifugal membrane MWCO 10,000 against D-PBS 10 times at 10.2 rcf for 10 minutes/cycle. The collected conjugate was then characterized by gel electrophoresis, and the concentration was determined by ELISA prior to *in vitro* studies.

FGFR ELISA Assay: A 96 well-plate was incubated with rhFGFR1α(IIIc) (100 μL per well at a

concentration of 0.5 μg/mL in D-PBS) for 12 hours at 23 ºC. After 16 hours the wells were washed and then blocked with 400 μL of 1% bovine serum albumin (BSA) in D-PBS (2 hours). Next, sample solutions were prepared at 1 ng/mL and aliquoted into Eppendorf tubes. After washing the wells, 100 μL of the sample solutions were added to each well. For protein solutions, heparin or polymer was added so that the final concentration of heparin or polymer was 1 μg/mL. After 2 hours the wells were washed and 100 μL of FGF2 antibody-biotin conjugate was added and incubated for an additional 2 hours before washing and incubating with streptavidin-horseradish peroxidase solution for 20 minutes. The plate was developed by incubating with 100 μL of 1-Step Ultra 3,3',5,5'-tetramethylbenzidine (TMB) solution (Pierce Biotechnology, Rockford) for 8 minutes. The assay was terminated by the addition of 50 μL of 1 M H_2SO_4. Absorbance was read at $\lambda = 450$ nm. Each sample was plated in triplicate.

BaF3-FR1C Binding Assay: BaF3-FR1C cells were grown in RPMI1640 medium containing 2 mM L-glutamine, 10% newborn bovine calf serum, and 0.5 ng/mL IL-3. Before seeding cells for experiments the cells were collected and washed twice with culture medium without IL-3. Cells were plated at a concentration of 20,000 cells/well/50 μL in the internal wells of a 96 well plate in culture medium without IL-3. Samples were prepared in culture medium without IL-3 to contain double the final concentration, and then 50 μL of each sample was added to the corresponding well. The external wells were blocked with 100 μL of DPBS and then incubated at 37 °C and 5% CO_2. After 48 hours of incubation CellTiter Blue assay was performed to determine the extent of cell growth. All samples were normalized to the control group, which contained only culture medium without IL-3. Each group contained six well replicates.

3.5 Appendix to Chapter 3 – Supplementary Figures

In the following ^{1}H NMR spectra of p(SS-*co*-PEGMA) 'g' refers to the methylene next to the ester group on the polymer side chain.

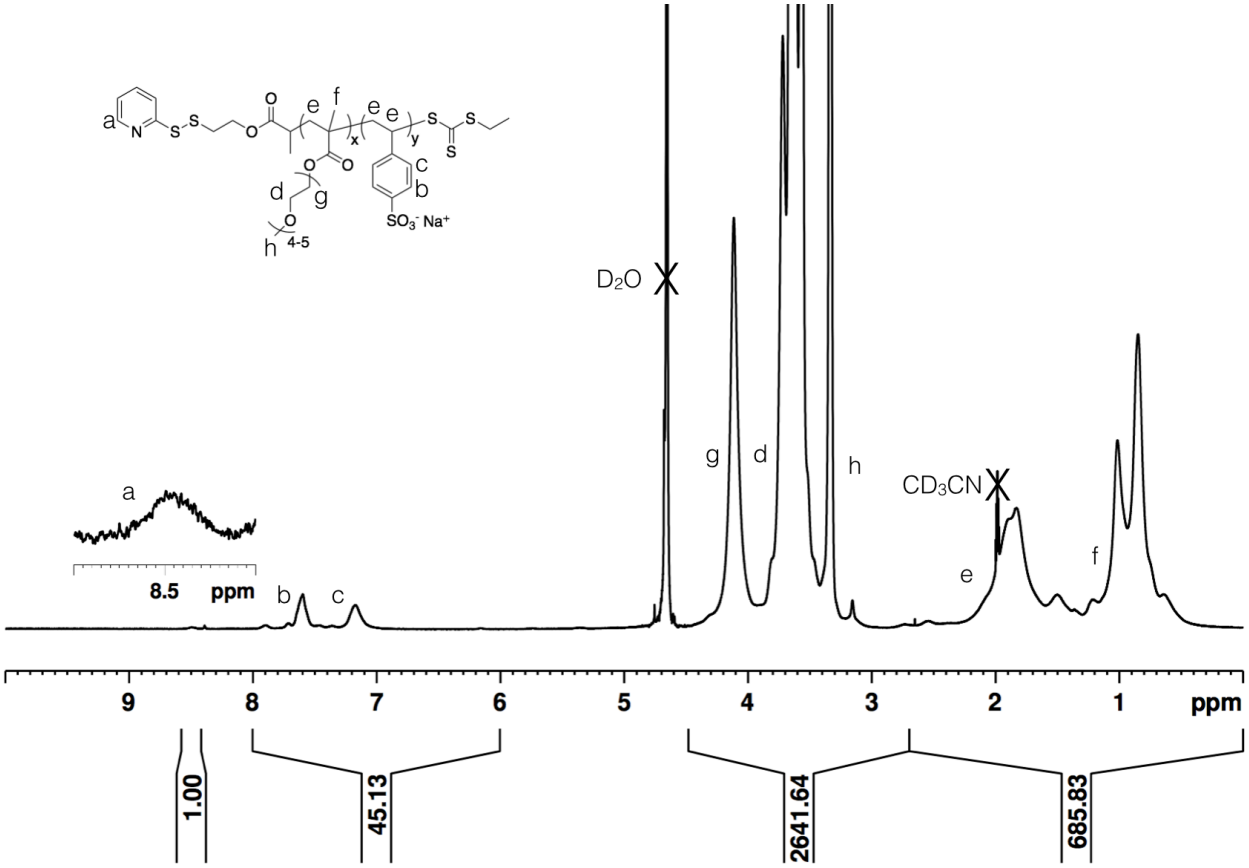

Figure 3-8. ^{1}H NMR (400 MHz, D_2O with CD_3CN) of p(SS-*co*-PEGMA)$_{8.0}$

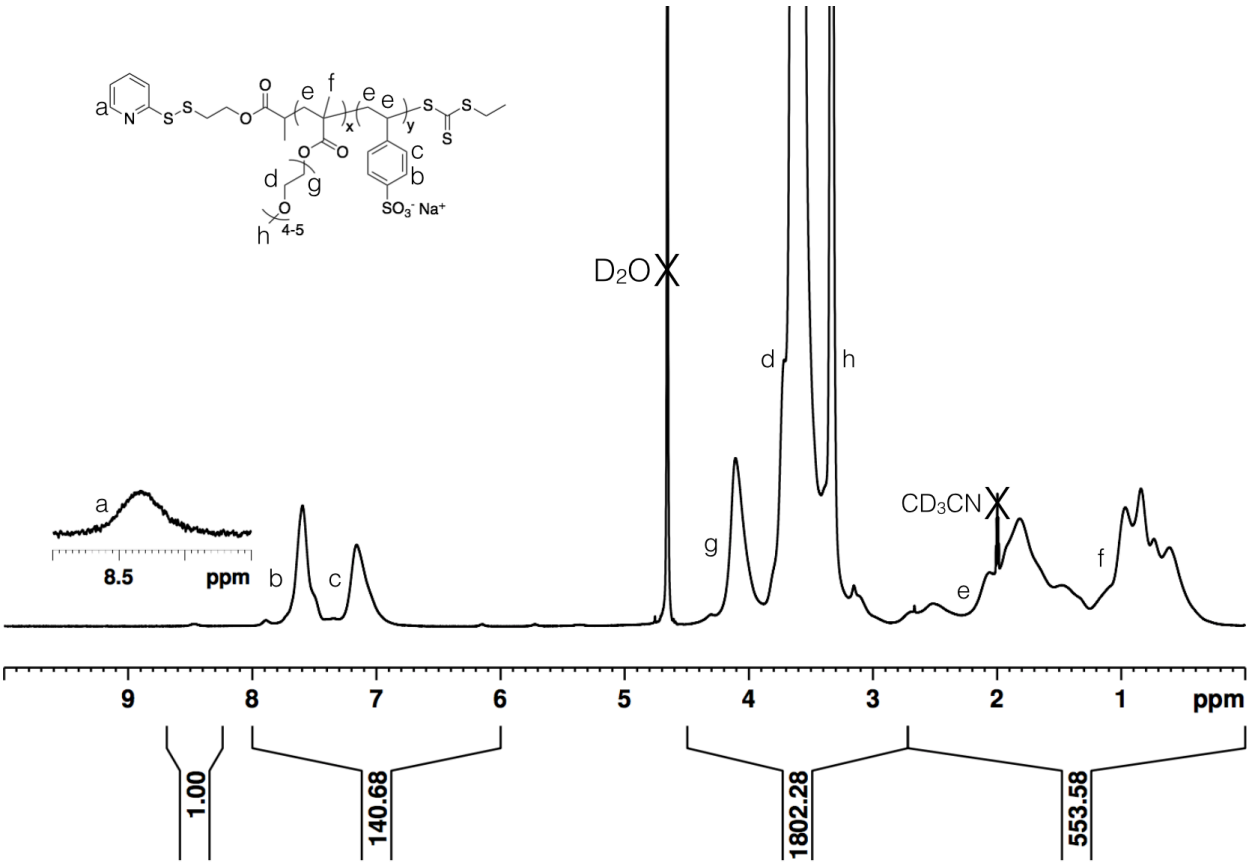

Figure 3-9. ^{1}H NMR (400 MHz, D_2O with CD_3CN) of p(SS-*co*-PEGMA)$_{28}$

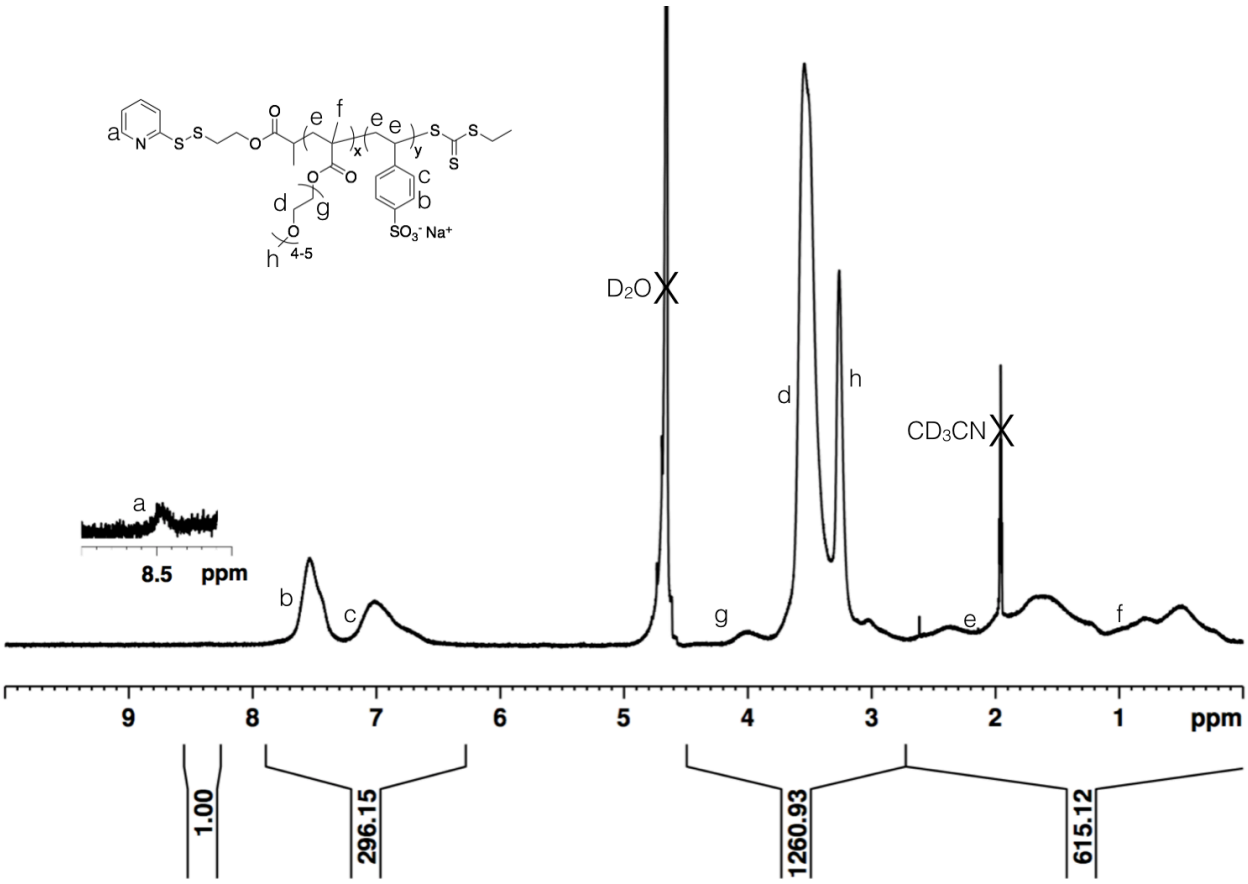

Figure 3-10. ^{1}H NMR (400 MHz, D_2O with CD_3CN) of p(SS-*co*-PEGMA)$_{55}$

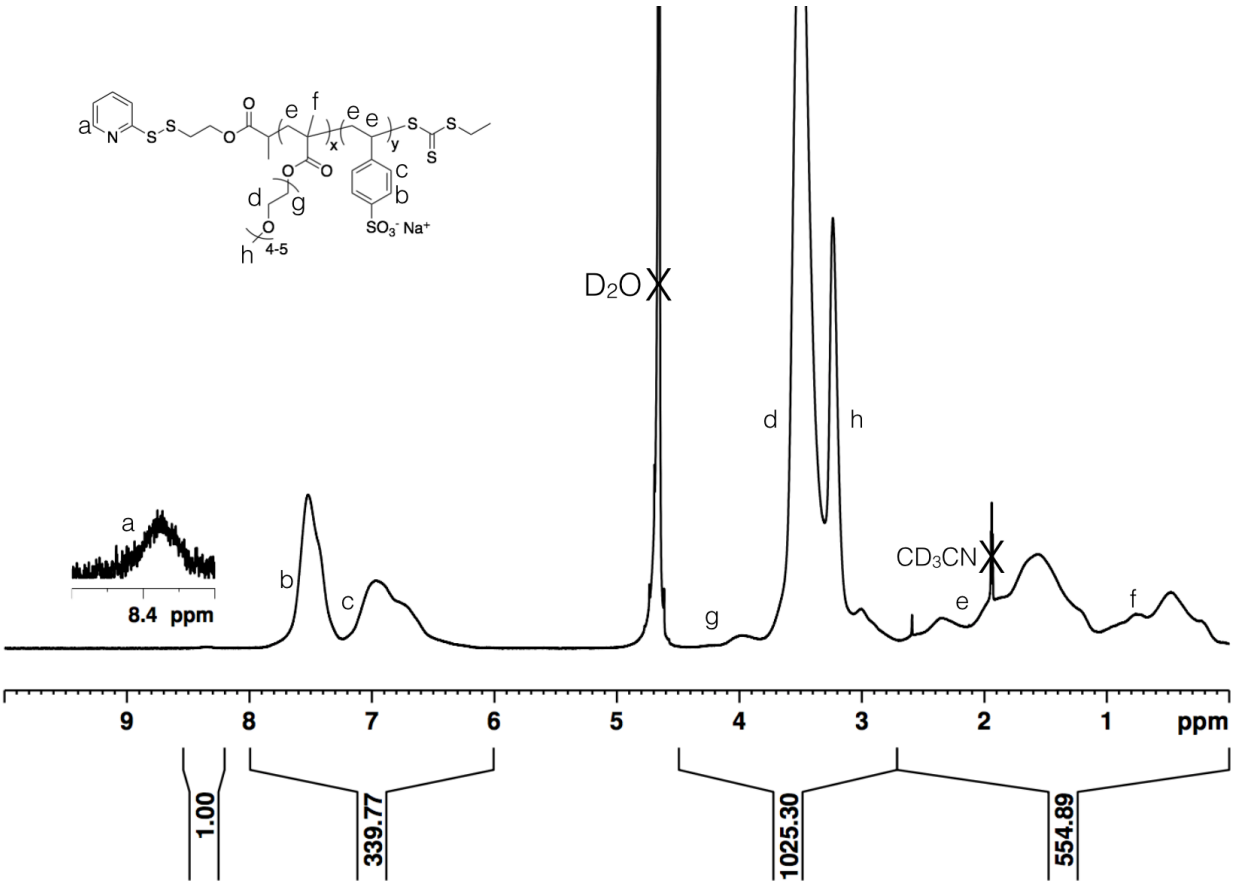

Figure 3-11. ^{1}H NMR (400 MHz, D_2O with CD_3CN) of p(SS-*co*-PEGMA)$_{63}$

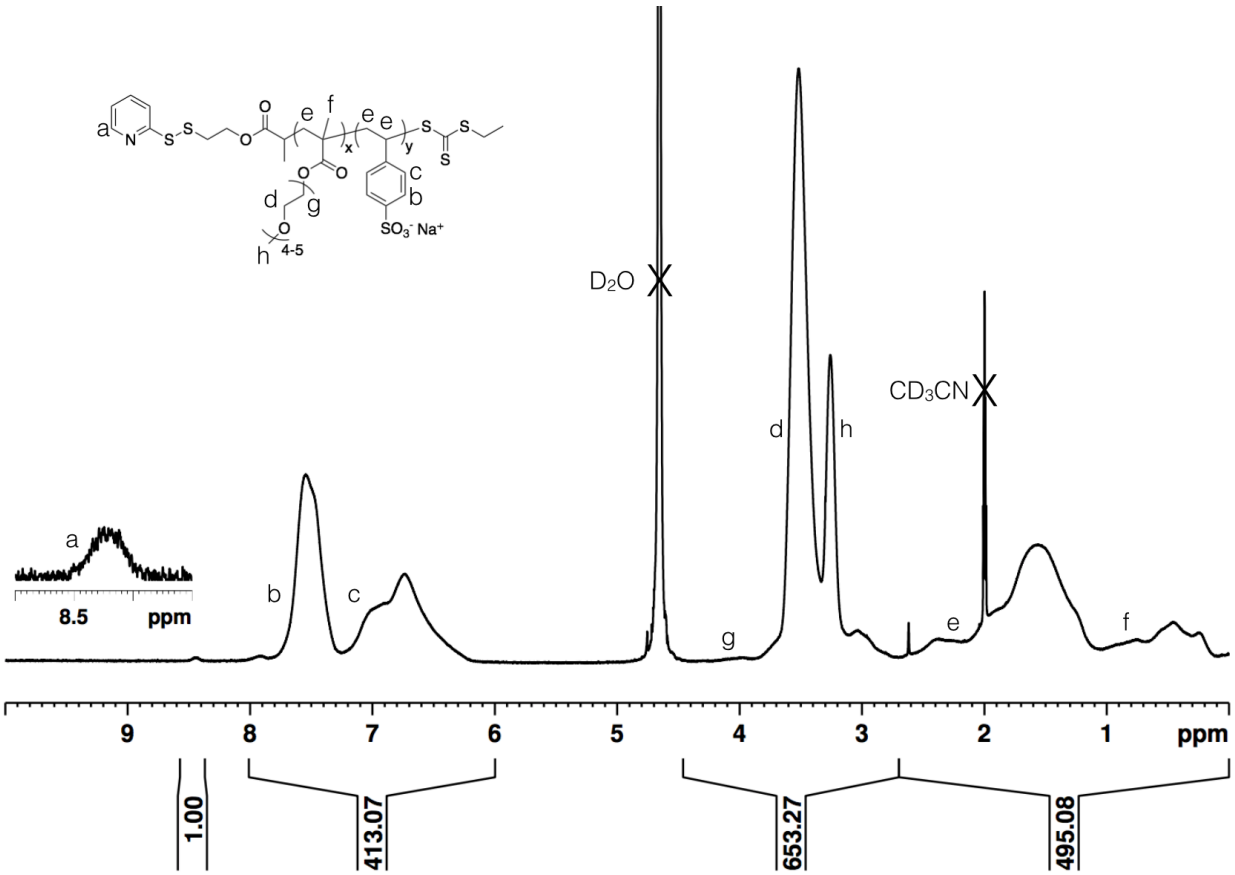

Figure 3-12. ^{1}H NMR (400 MHz, D_2O with CD_3CN) of p(SS-*co*-PEGMA)$_{76}$

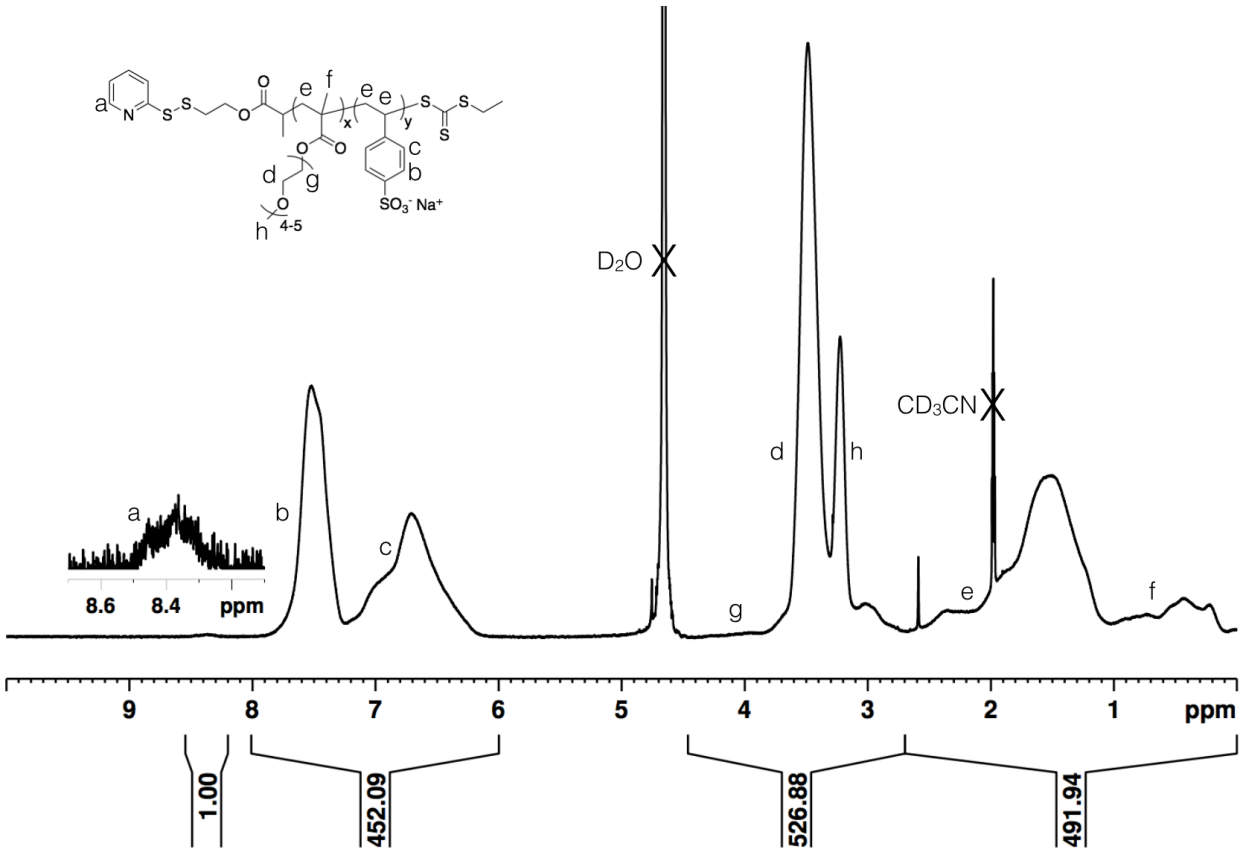

Figure 3-13. ^{1}H NMR (400 MHz, D_2O with CD_3CN) of p(SS-*co*-PEGMA)$_{81}$

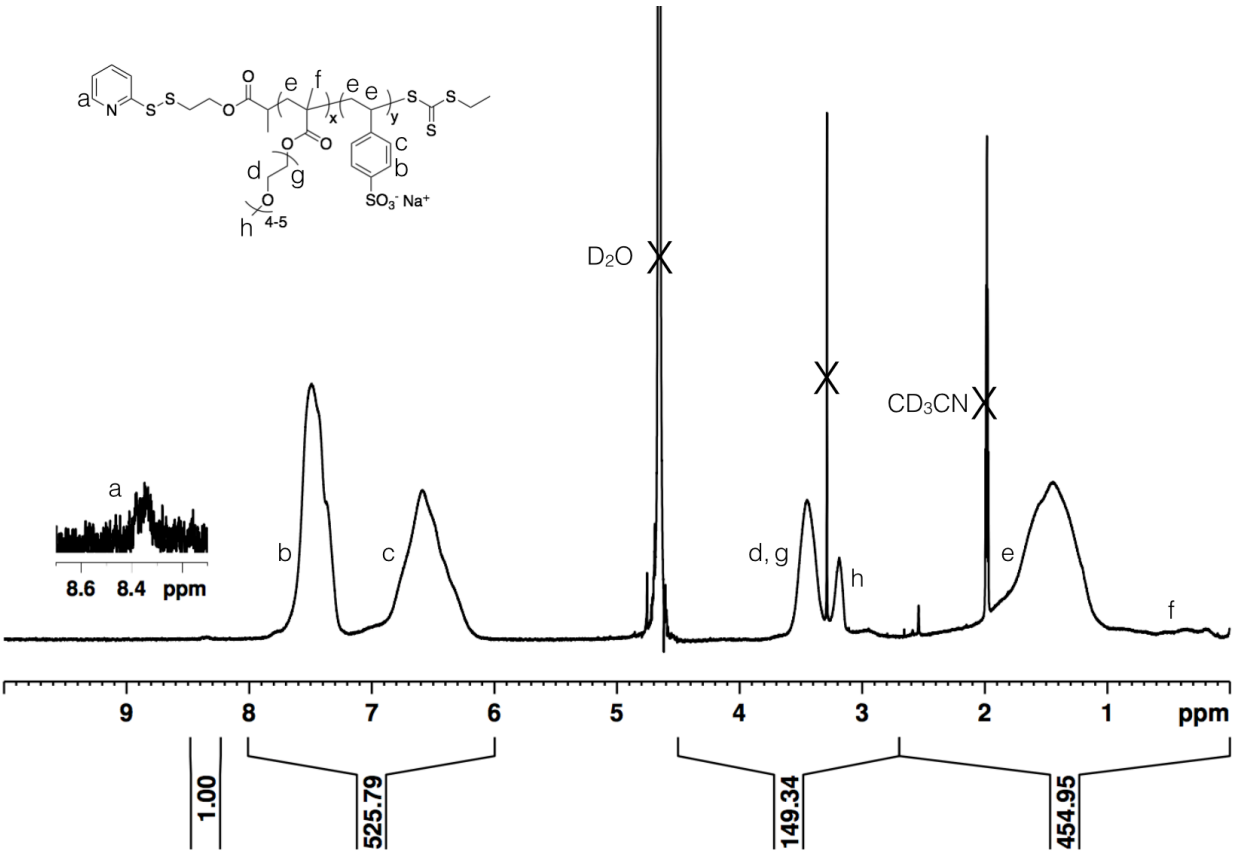

Figure 3-14. ^{1}H NMR (400 MHz, D_2O with CD_3CN) of p(SS-*co*-PEGMA)$_{95}$

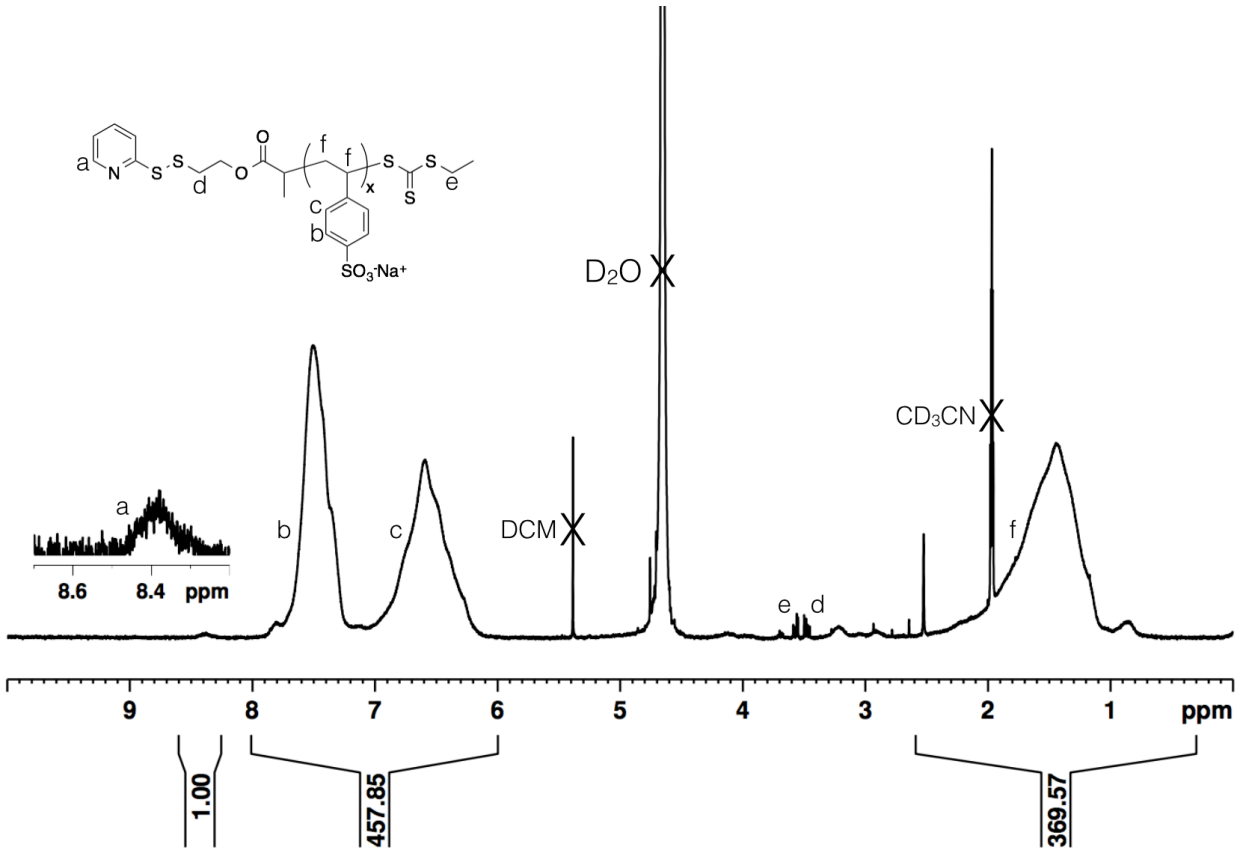

Figure 3-15. ^{1}H NMR (400 MHz, D_2O with CD_3CN) of pSS

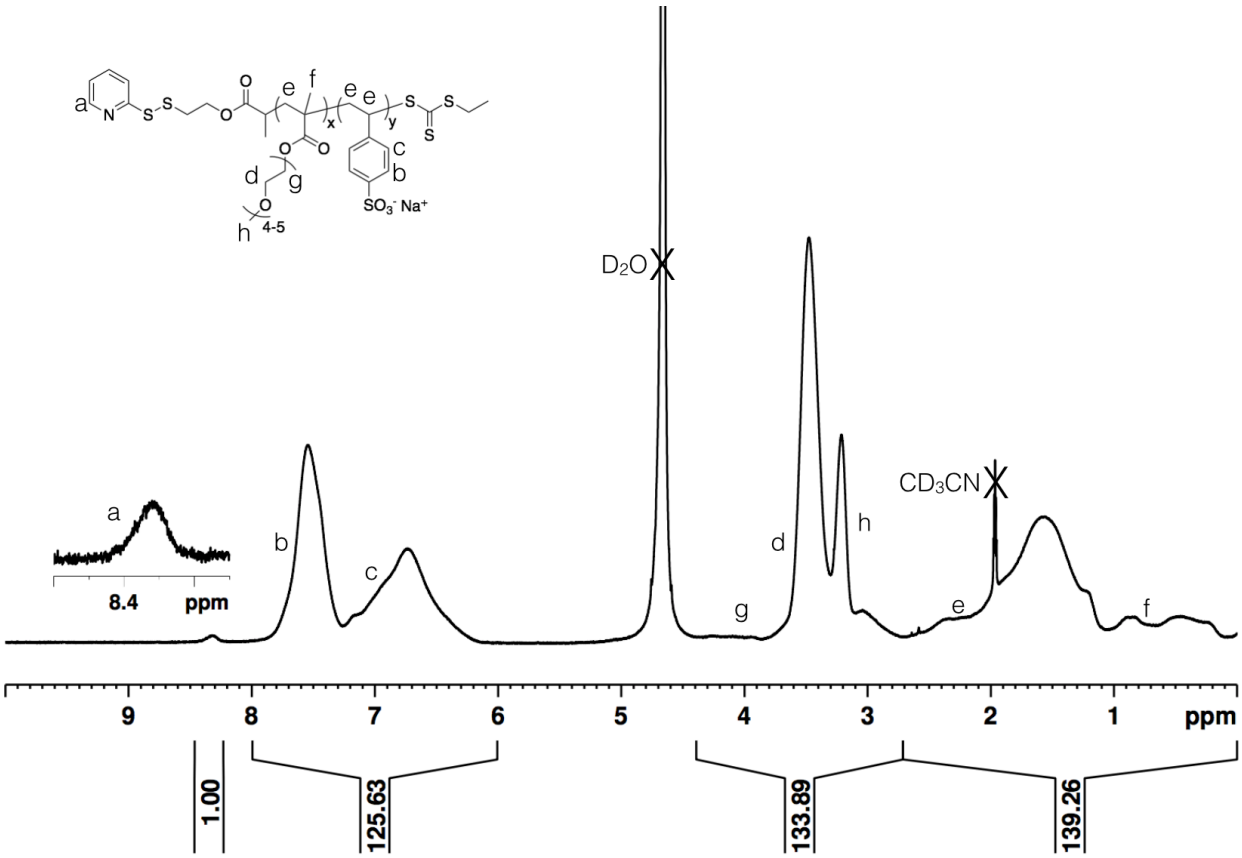

Figure 3-16. ^{1}H NMR (400 MHz, D_2O with CD_3CN) of p(SS-*co*-PEGMA) DP41

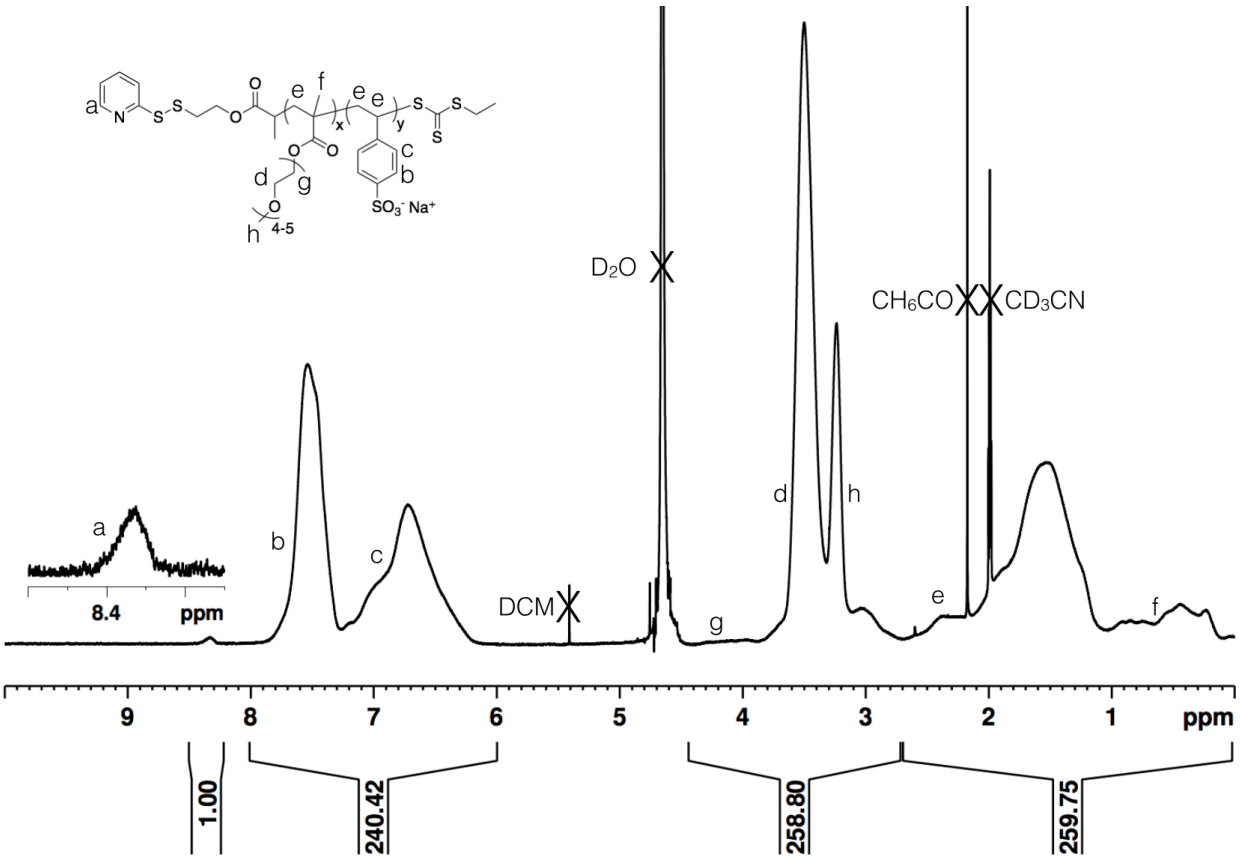

Figure 3-17. ^{1}H NMR (400 MHz, D_2O with CD_3CN) of p(SS-*co*-PEGMA) DP78

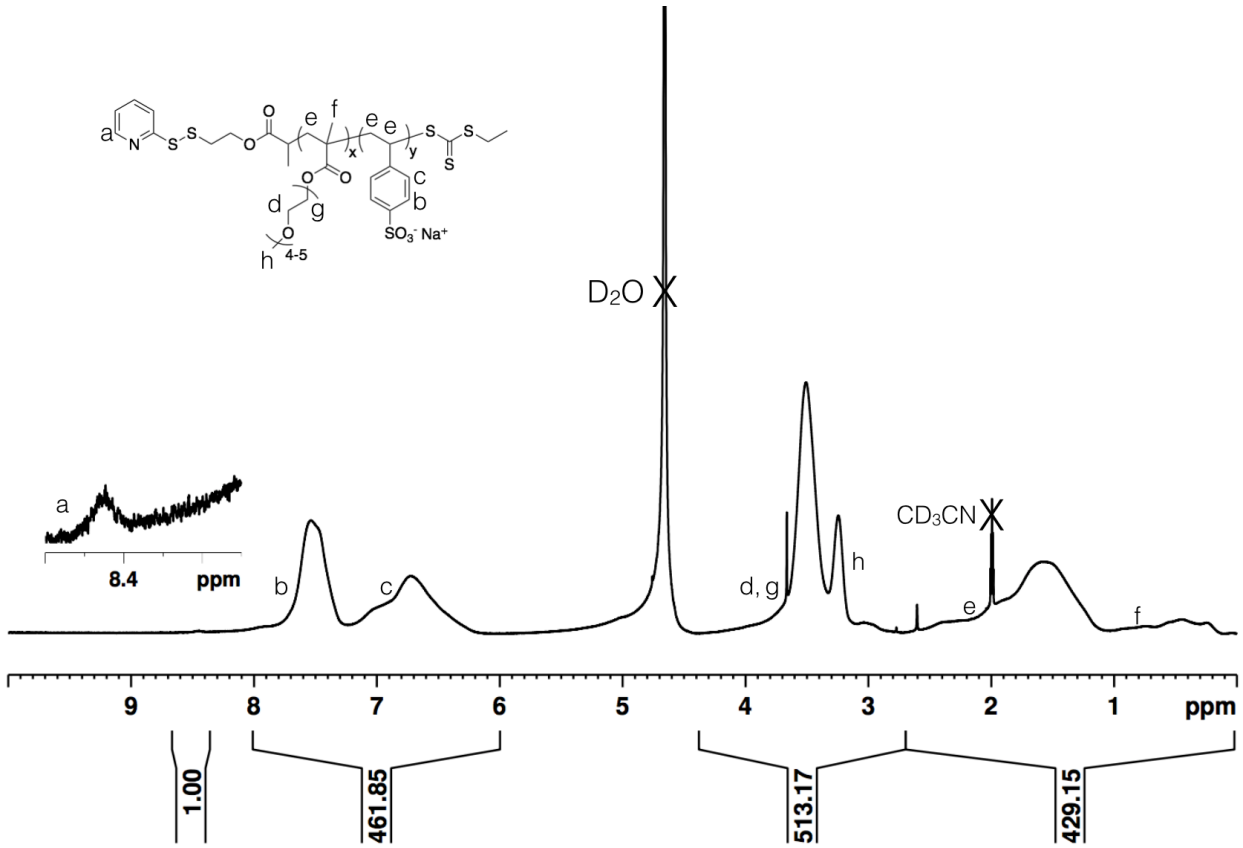

Figure 3-18. ^{1}H NMR (400 MHz, D_2O with CD_3CN) of p(SS-*co*-PEGMA) DP161

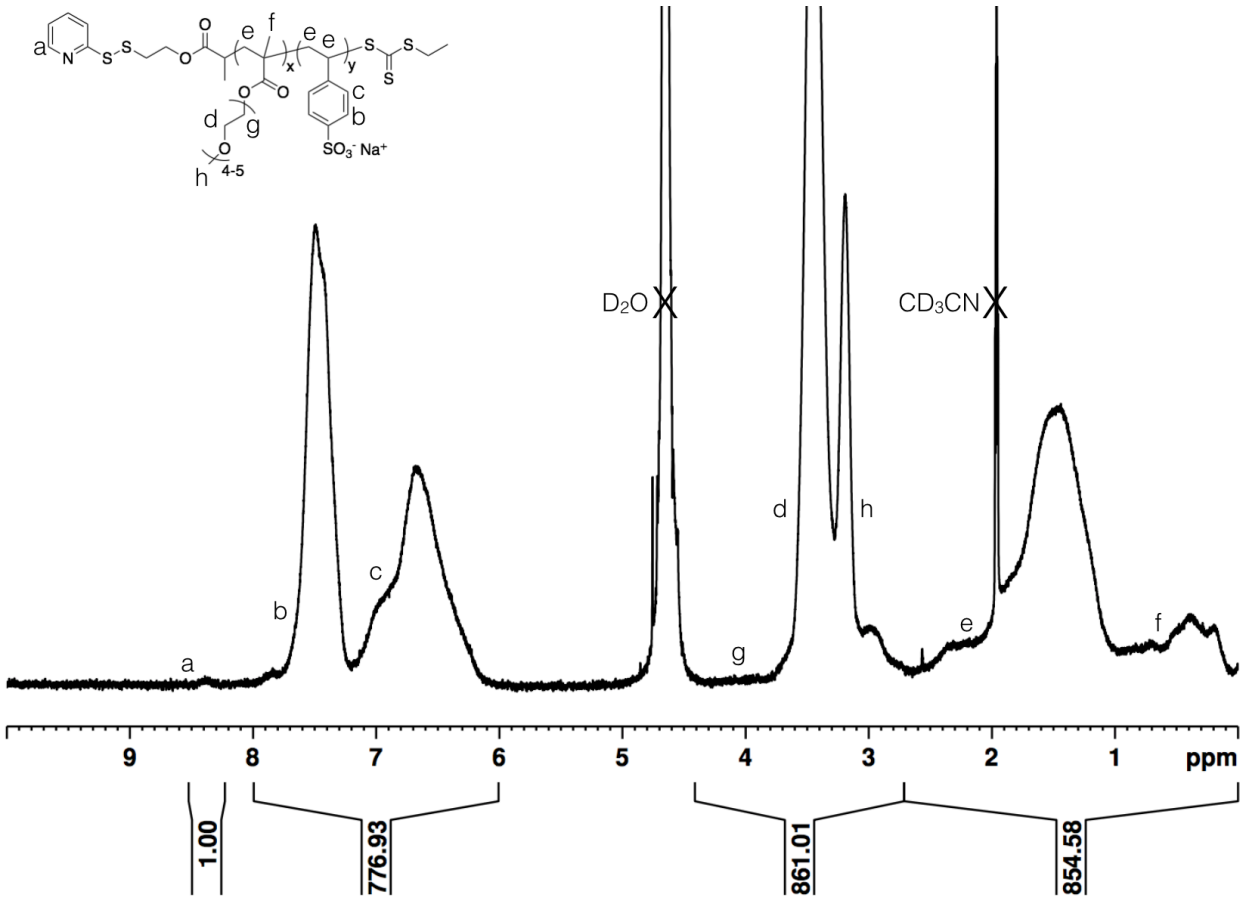

Figure 3-19. ^{1}H NMR (400 MHz, D_2O with CD_3CN) of p(SS-*co*-PEGMA) DP223

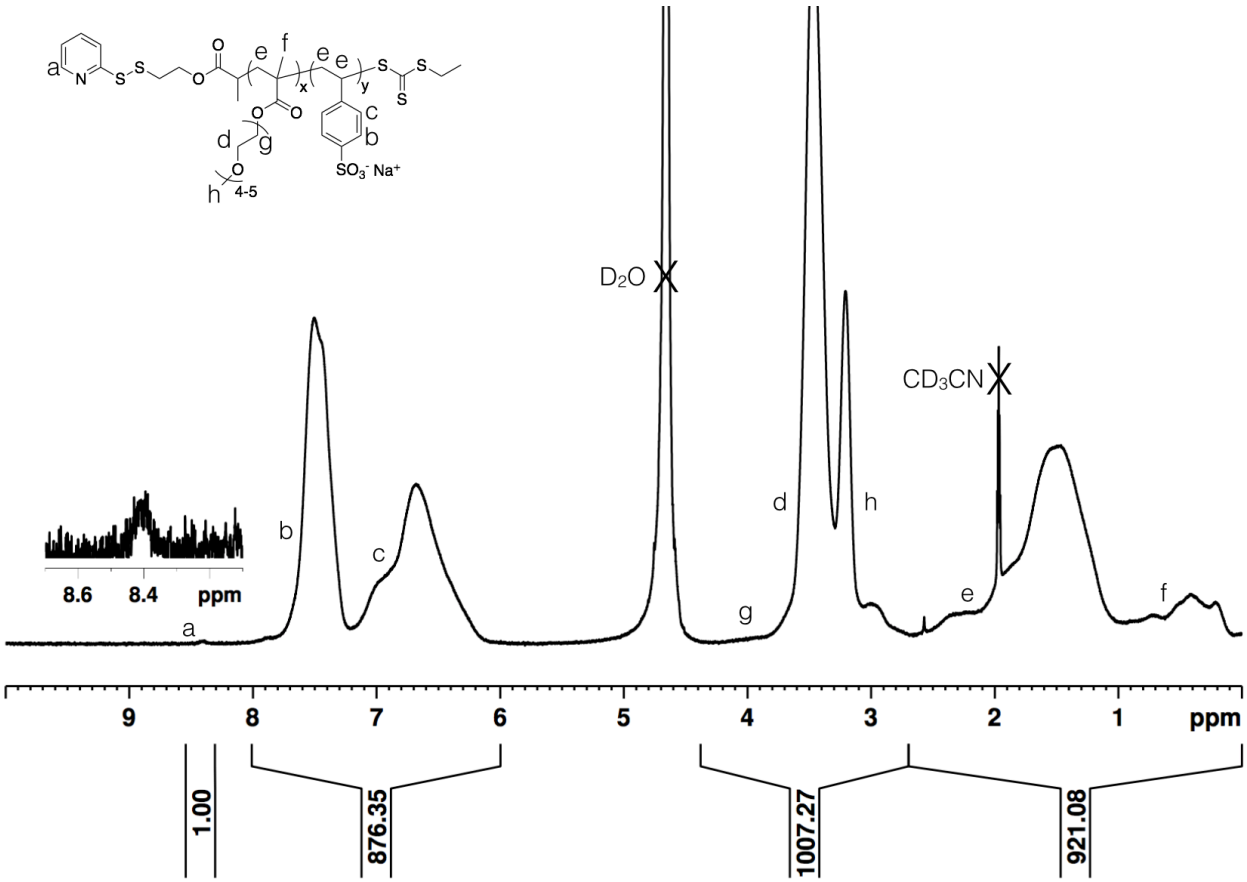

Figure 3-20. ^{1}H NMR (400 MHz, D_2O with CD_3CN) of p(SS-*co*-PEGMA) DP263

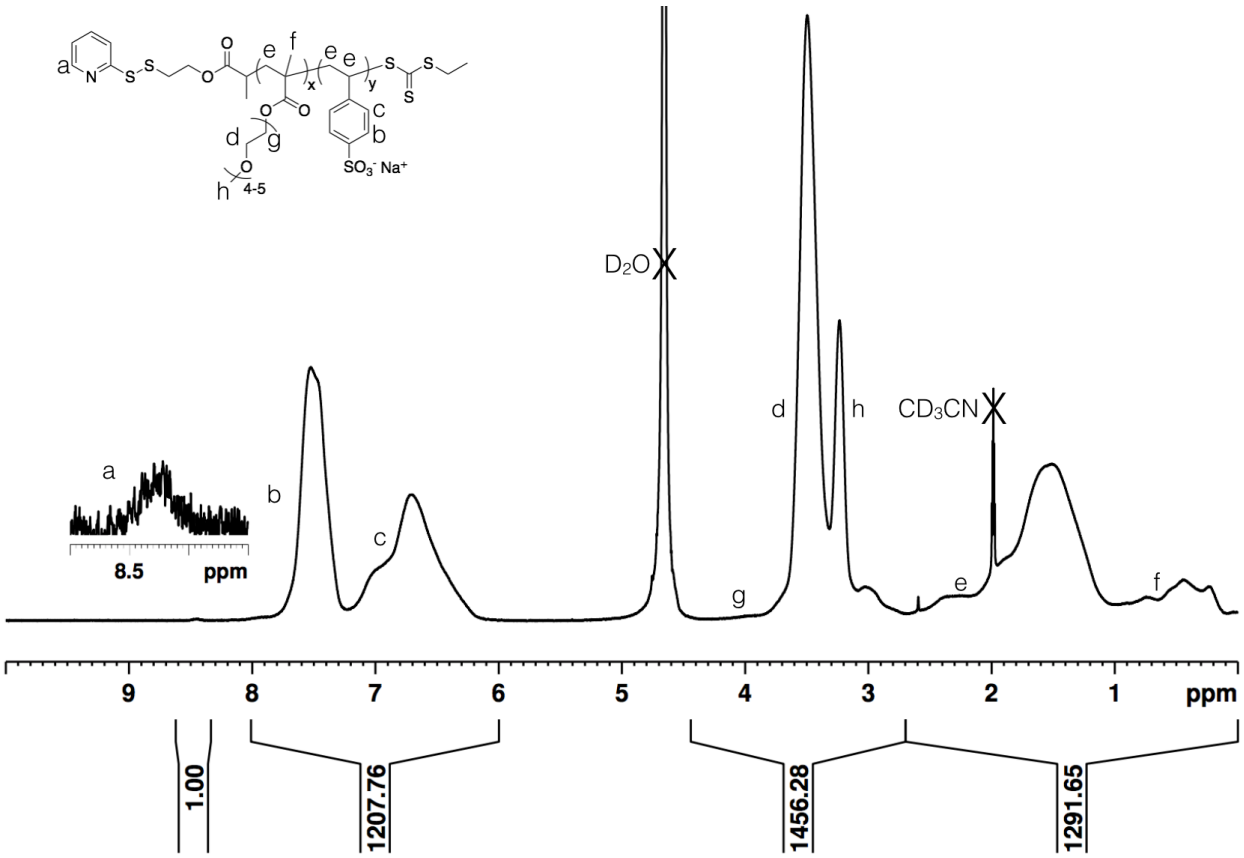

Figure 3-21. ^{1}H NMR (400 MHz, D_2O with CD_3CN) of p(SS-*co*-PEGMA) DP295

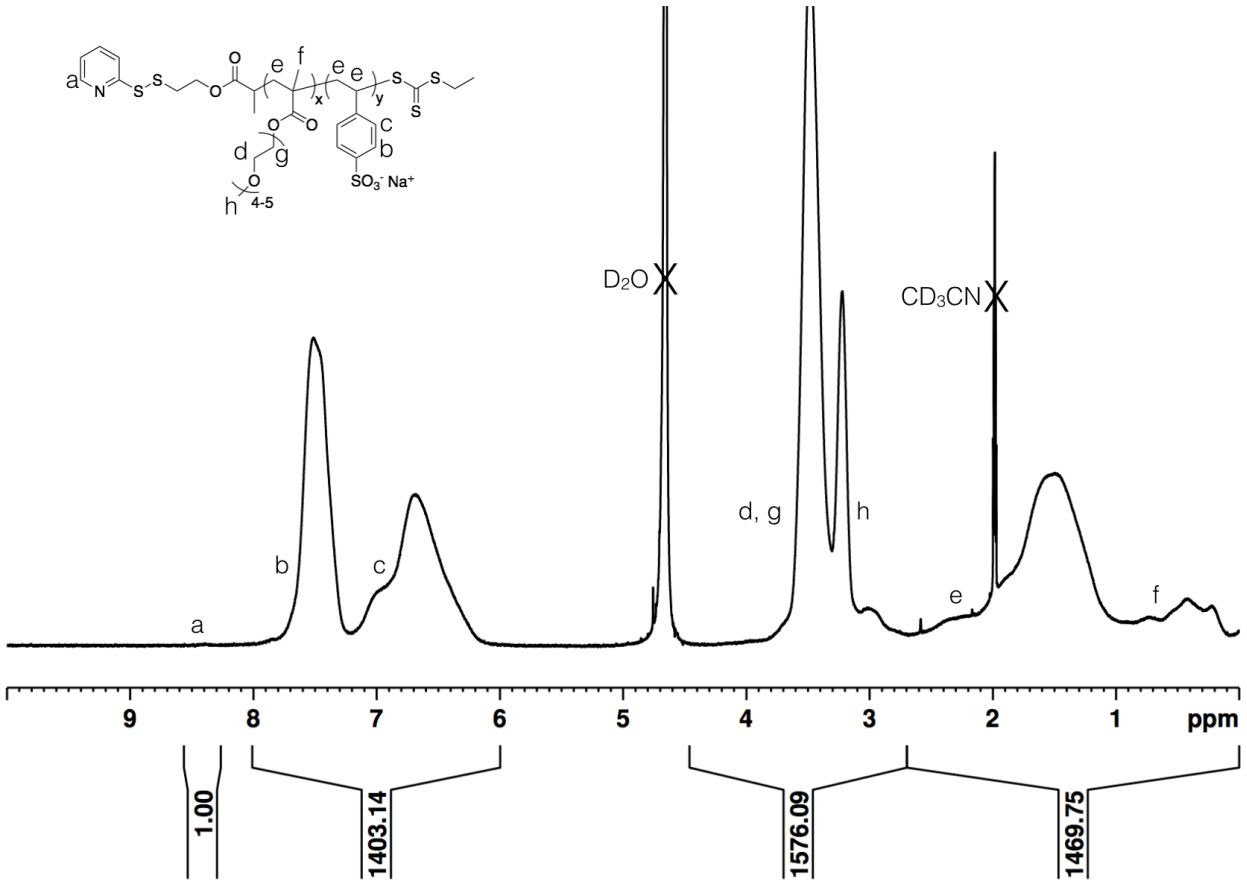

Figure 3-22. ^{1}H NMR (400 MHz, D_2O with CD_3CN) of p(SS-*co*-PEGMA) DP390

3.6 References

†Portions of Chapter 3 are reproduced from the submitted manuscript Paluck, S.J.; Maynard, H.D. Structure Activity Relationship of Heparin Mimicking Polymer p(SS-*co*-PEGMA): Effect of Sulfonation and Polymer Size on FGF2-Receptor Binding.

(1) Ornitz, D. M.; Itoh, N. *Genome Biol.* **2001**, *2*.

(2) Itoh, N.; Ornitz, D. M. *J. Biochem.* **2011**, *149*, 121.

(3) Seghezzi, G.; Patel, S.; Ren, C. J.; Gualandris, A.; Pintucci, G.; Robbins, E. S.; Shapiro, R. L.; Galloway, A. C.; Rifkin, D. B.; Mignatti, P. *J. Cell Biol.* **1998**, *141*, 1659.

(4) Plotnikov, A. N.; Schlessinger, J.; Hubbard, S. R.; Mohammadi, M. *Cell* **1999**, *98*, 641.

(5) Schlessinger, J.; Plotnikov, A. N.; Ibrahimi, O. A.; Eliseenkova, A. V.; Yeh, B. K.; Yayon, A.; Linhardt, R. J.; Mohammadi, M. *Mol. Cell* **2000**, *6*, 743.

(6) Waksman, G.; Herr, A. B. *Nat. Struct. Biol.* **1998**, *5*, 527.

(7) Gospodarowicz, D.; Cheng, J. *J. Cell. Physiol.* **1986**, *128*, 475.

(8) Tyrrell, D. J.; Kilfeather, S.; Page, C. P. *Trends Pharmacol. Sci.* **1995**, *16*, 198.

(9) Paluck, S. J.; Nguyen, T. H.; Maynard, H. D. *Biomacromolecules* **2016**, *17*, 3417.

(10) Capila, I.; Linhardt, R. J. *Angew. Chem. Int. Ed.* **2002**, *41*, 391.

(11) Meneghetti, M. C. Z.; Hughes, A. J.; Rudd, T. R.; Nader, H. B.; Powell, A. K.; Yates, E. A.; Lima, M. A. *J. Royal Soc. Int.* **2015**, *12*.

(12) Liu, J.; Pedersen, L. C. *Appl. Microbiol. Biotechnol.* **2007**, *74*, 263.

(13) Paluck, S. J.; Nguyen, T. H.; Lee, J. P.; Maynard, H. D. *Biomacromolecules* **2016**.

(14) Miao, H. Q.; Ornitz, D. M.; Aingorn, E.; BenSasson, S. A.; Vlodavsky, I. *J. Clin. Invest.* **1997**, *99*, 1565.

(15) Cassinelli, G.; Favini, E.; Dal Bo, L.; Tortoreto, M.; De Maglie, M.; Dagrada, G.; Pilotti, S.; Zunino, F.; Zaffaroni, N.; Lanzi, C. *Oncotarget* **2016**, *7*, 47848.

(16) Liekens, S.; Leali, D.; Neyts, J.; Esnouf, R.; Rusnati, M.; Dell'Era, P.; Maudgal, P. C.; De Clercq, E.; Presta, M. *Mol. Pharmacol.* **1999**, *56*, 204.

(17) Nguyen, T. H.; Paluck, S. J.; McGahran, A. J.; Maynard, H. D. *Biomacromolecules* **2015**, *16*, 2684.

(18) Wang, M.; Lyu, Z.; Chen, G.; Wang, H.; Yuan, Y.; Ding, K.; Yu, Q.; Yuan, L.; Chen, H. *Chem. Commun.* **2015**, *51*, 15434.

(19) Sheng, G. J.; Oh, Y. I.; Chang, S.-K.; Hsieh-Wilson, L. C. *J. Am. Chem. Soc.* **2013**, *135*, 10898.

(20) Huang, Y.; Shaw, M. A.; Warmin, M. R.; Mullins, E. S.; Ayres, N. *Polym. Chem.***2016**, *7*, 3897.

(21) Akashi, M.; Sakamoto, N.; Suzuki, K.; Kishida, A. *Bioconjugate Chem.* **1996**, *7*, 393.

(22) Nishimura, Y.; Shudo, H.; Seto, H.; Hoshino, Y.; Miura, Y. *Bioorg. Med. Chem. Letters* **2013**, *23*, 6390.

(23) Miura, Y.; Yasuda, K.; Yamamoto, K.; Koike, M.; Nishida, Y.; Kobayashi, K. *Biomacromolecules* **2007**, *8*, 2129.

(24) Oh, Y. I.; Sheng, G. J.; Chang, S. K.; Hsieh-Wilson, L. C. *Angew. Chem. Int. Ed.* **2013**, *52*, 11796.

(25) Miura, Y.; Mizuno, H. *Bull. Chem. Soc. Jpn.* **2010**, *83*, 1004.

(26) Nguyen, T. H.; Kim, S.-H.; Decker, C. G.; Wong, D. Y.; Loo, J. A.; Maynard, H. D. *Nature Chem.* **2013**, *5*, 221.

(27) Mancini, R. J.; Lee, J.; Maynard, H. D. *J. Am. Chem. Soc.* **2012**, *134*, 8474.

(28) Belleney, J.; Helary, G.; Migonney, V. *Euro. Polym. J.* **2002**, *38*, 439.

(29) Liekens, S.; Neyts, J.; Degreve, B.; DeClercq, E. *Oncology Res.* **1997**, *9*, 173.

(30) Ornitz, D. M.; Yayon, A.; Flanagan, J. G.; Svahn, C. M.; Levi, E.; Leder, P. *Mol. Cell. Biol.* **1992**, *12*, 240.

(31) Ornitz, D. M.; Leder, P. *J. Biol. Chem.* **1992**, *267*, 16305.

(32) Griffin, D. R.; Schlosser, J. L.; Lam, S. F.; Nguyen, T. H.; Maynard, H. D.; Kasko, A. M. *Biomacromolecules* **2013**, *14*, 1199.

(33) Chen, R.; John, J.; Lavrentieva, A.; Muller, S.; Tomala, M.; Zhao, Y. X.; Zweigerdt, R.; Beutel, S.; Hitzmann, B.; Kasper, C.; Martin, U.; Rinas, U.; Stahl, F.; Scheper, T. *Eng. Life Sci.* **2012**, *12*, 29.

Chapter 4

Dimerization of FGF2 with Heparin-Mimicking Polymer p(SS-*co*-PEGMA)[†]

4.1 Introduction

Growth factors play an important role in wound healing and function to modulate many cellular activities including cell recruitment and angiogenesis.[1,2] Because of their important role, growth factors, such as platelet derived growth factor (PDGF), fibroblast growth factor 2 (FGF2), epidermal growth factor (EGF), and vascular endothelial growth factor (VEGF) are studied for their ability to improve the wound healing process.[3] Currently, PDGF is the only growth factor that is approved by the Food and Drug Administration (FDA) for treatment of chronic wounds, and is formulated as a gel-based treatment under the trade name Regranex®.[4,5] Although therapeutics like Regranex show promise, the growth factor is needed in high concentrations in order to achieve therapeutic efficacy, which can lead to off-target effects. As a result, the FDA has placed a warning label on Regranex due to increased chances of malignancies.[6] Therefore, there is still a need for protein therapeutics that can be used in lower concentrations to obtain the same clinical efficacy.

One potential protein target is FGF2, a 17 kDa heparin binding growth factor that is primarily responsible for promoting cell growth, cell migration into the wound bed, and creation of new vasculature at the wound site.[7-9] Because of its many functions, FGF2 has been extensively studied to promote new growth in wounded tissue. However, its instability in storage and delivery as well as its limited efficacy in clinical trials have prevented FGF2 from achieving its full therapeutic potential.[10-12] New ways to stabilize and activate FGF2 are being explored to improve therapeutic outcomes.[13,14]

Chronic wounds contain low concentrations of growth factors, including FGF2, due to the harsh acidic environment and presence of proteolytic enzymes in the wound bed.[1,8] In order to overcome low concentrations, FGF2 superagonists have been prepared for the purposes of

increasing the effective local concentrations of FGF2. Typically, FGF2 superagonists work by increasing the affinity of FGF for its receptor or vice versa. There are three commonly employed methods for increasing the activity of FGF2. The addition of additives such as peptides, proteins and small molecules has been shown to help improve binding affinity between the protein and receptor.[15-19] The protein itself has also been modified through truncation or mutation of specific amino acids resulting in a more active protein.[20-22] Lastly covalent modification of the protein has also been shown to increase activity.[23-25]

One of these covalent modifications is achieved through chemical dimerization of FGF2 to form a homodimer. In its active form, FGF2 forms a homodimer with heparan sulfate threading through positively charged heparin-binding domain on both proteins.[26,27] This dimer is then docked on two FGF receptors (FGFRs), resulting in a pentameric complex that is required for receptor phosphorylation.[28] Since the dimerization of FGF2 plays a large role in receptor activation, some groups have investigated the affect of pre-forming similar protein structures. FGF2 has been oligomerized and dimerized by the addition of heparin,[29,30] the use of chemical cross-linkers,[23,24,26] or mutation of amino acids.[31] Some of these methods have even shown increased protein activity, which is likely due to the entropic benefit of pre-forming the dimer necessary for docking. We have shown that FGF2 can be covalently dimerized through the use of a poly(ethylene glycol) (PEG) linker.[32] A size study determined that there is an ideal linker length that gives higher mitogenic activity than larger and smaller linkers. This dimer was shown to increase angiogenesis in an *in vitro* assay and to increase blood vessel formation in a murine diabetic wound healing model. Not surprisingly, the dimer was not able to improve wound closure rate when compared to FGF2 alone because FGF2 alone does not typically increase wound closure.

Heparin, a highly sulfated glycosaminoglycan, is a naturally stabilizer of FGF2, and also aids in protein dimerization and receptor binding.[33-35] Even when FGF2 is pre-organized as a dimer, heparin is required for cell activity. We hypothesized that by using a heparin mimicking polymer in place of the PEG linker, we could further increase the mitogenic activity of the dimer. Additionally, the use of a heparin mimicking polymer should also stabilize the protein, allowing it to be stored and delivered for clinical treatments. We have previously shown that the heparin mimicking polymer p(SS-*co*-PEGMA) can influence FGF2-FGFR binding (Chapter 3). Therefore, this polymer was synthesized to contain protein reactive maleimide end groups that were used to dimerize FGF2 with exposed cysteines on each protein. We hypothesized that the resulting dimer will improve protein dimer stability and facilitate receptor activation.

4.2 Results and Discussion

4.2.1 In-Vitro Angiogenesis Assay of FGF2-PEG2k-FGF2

Before dimerizing FGF2 with a heparin mimicking polymer, we tested the ability of FGF2 dimerized with PEG to influence angiogenesis using an *in vitro* angiogenesis assay. FGF2 was dimerized with 2 kDa PEG to yield FGF2-PEG2k-FGF2.[32] The dimer was then tested for its ability to increase cord-like structure formation in a rudimentary co-culture assay.[36,37] Human dermal fibroblasts (HDFs) were grown to confluency followed by addition of human umbilical vein endothelial cells (HUVECs) and sample solution. Sample solutions were refreshed at 3 days and 6 days post HUVEC addition. After 10 days the cells were fixed and the cord-like structures were stained for the presence of CD31 (PECAM-1), a marker of angiogenesis found at endothelial cell junctions.[38] As shown in figure 4-1, the dimer performed as well as FGF2 at high concentrations (1.0, 5.0, and 10 ng/mL). At lower concentrations (0.1 and 0.5 ng/mL) FGF2-

PEG2k-FGF2 dimer induced a significant increase in the number of nodes, number of cord-like structures, and total length of cord-like structures when compared to FGF2 alone. Specifically, at 0.1 ng/mL, cells treated with FGF2-PEG2k-FGF2 increased the average number of nodes by 97, average number of cord-like structures by 186, and increased the total length of cord-like structures to 9 times that of FGF2. At 0.5 ng/mL, FGF2-PEG2k-FGF2 increased the average number of nodes by 120, cord-like structures by 229, and the total length of the cord-like structures was increased to 4 times that of FGF2. Thus at these low concentrations, FGF2-PEG2k-FGF2 improved all evaluated aspects of angiogenesis compared to free FGF2 as measured by this assay. Additionally, FGF2-PEG2k-FGF2 increased the number of blood vessels formed when compared to FGF2 in a diabetic mouse wound healing model.[32]

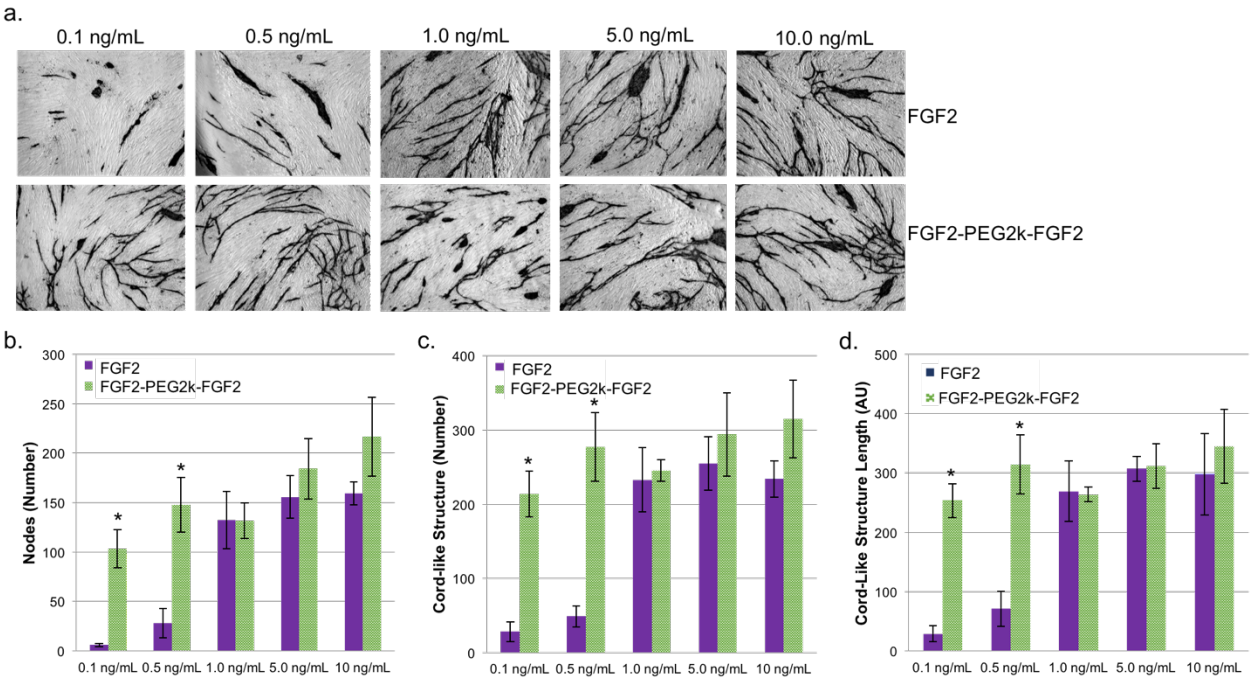

Figure 4-1. Co-culture angiogenesis assay showing the effect of FGF2-PEG2k-FGF2 on cord-like structure formation (n = 3). (a) Representative images of cord-like structure growth stained for CD31. (b) Comparison of the number of node, (c) cord-like structure number, and (d) average total cord-like structure length per image (pixels). (mean ± SD). Statistical analysis was carried

out using a student's t-test. * $p < 0.05$.

4.2.2 Effect of Adding Heparin to FGF2-PEG2k-FGF2

Previous work has concluded that heparin is necessary for receptor binding when free FGF2 is used.[33] To investigate whether heparin is necessary when the protein dimer is already pre-formed, FGF2-PEG2k-FGF2 was tested for receptor binding. BaF3-FR1c cells were used to assay receptor activation. This cell line was engineered by Ornitz and coworkers to express FGF receptors but lack native heparan sulfate,[33] making the addition of heparin necessary for cell proliferation. Therefore, BaF3 cells are useful for detecting receptor binding. FGF2-PEG2k-FGF2 was added to BaF3 cells at a concentration of 1 ng/mL with or without 1 μg/mL heparin. Additionally, FGF2 and FGF2 plus 1 μg/mL of heparin were used as positive and negative controls. As shown in Figure 4-2, FGF2-PEG2k-FGF2 was not capable of facilitating an increase in receptor binding without added heparin. However, the dimer retains activity and when heparin is added the conjugate is able to reach complete receptor binding. This is not surprising since it has been shown that the presence of heparin or heparin mimics is required for receptor binding. This experiment also verified that the increase in *in vitro* and *in vivo* activity observed with FGF2-PEG2k-FGF2 is due to the pre-organization of the dimer, since there is no receptor binding in the absence of heparin. In order to improve the receptor binding of the dimer, we explored the use of a heparin mimicking polymer in place of the PEG linker.

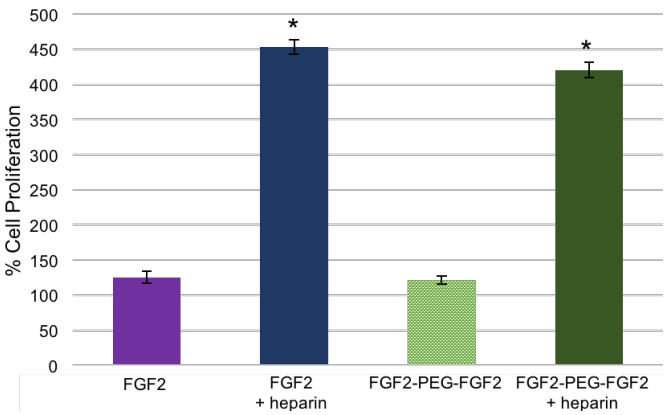

Figure 4-2. Cell growth of FGF2-PEG2k-FGF2 dimer in BaF3-FR1C cells compared to FGF2 alone and FGF2 with excess heparin. Data was normalized to the blank medium group, which was set at 100% (n = 6). Error bars represent standard deviation. Statistical analysis was done using Student's t test. * $p < 0.001$ compared to FGF2.

4.2.3 Synthesis of Heparin-Mimicking Polymer for Linker in FGF2 Dimerization

Heparin-mimicking polymer p(SS-*co*-PEGMA)-*b*-VS is able to facilitate receptor binding to the same extent as heparin (Chapter 2). This polymer was explored for use as a protein linker, however, the polymerization of p(SS-*co*-PEGMA)-*b*-VS is difficult and often leads to low end group retention. This precludes the polymer from being a good candidate for dimerization, because high end group retention is needed for appreciable dimer formation. Therefore, p(SS-*co*-PEGMA) with 81% SS incorporation was used. As shown in Chapter 3, p(SS-*co*-PEGMA)$_{81}$ facilitates an increase in receptor binding, though not to the same extent as heparin. We anticipated that the moderate binding of the polymer to the receptor should improve the FGF2 binding to its receptor when dimerized. The heparin-mimicking linker should also provide stability to a greater extent than the PEG linker, allowing for better activity after storage and delivery.

Initially the same divinyl sulfone-cysteine conjugation chemistry that was used for the preparation of FGF2-PEG2k-FGF2[32] was also attempted for the formation of FGF2-p(SS-*co*-PEGMA)-FGF2. First, p(SS-*co*-PEGMA) with 81% SS modification was synthesized with the α-PDS group as described in Chapter 3. The trithiocarbonate on the omega (ω) terminus was then reduced with n-butyl amine and the free thiol was capped with pyridyl disulfide methacrylate (PDSMA) to yield PDS-p(SS-*co*-PEGMA)-PDS (Scheme 4.1a). The PDS end groups were then reduced with tris(2-carboxyethyl)phosphine (TCEP) in the presence of divinyl sulfone to obtain the protein reactive polymer DVS-p(SS-*co*-PEGMA)-DVS (Scheme 4-1b). After purification, the dimerization of FGF2 with DVS-p(SS-*co*-PEGMA)-DVS was attempted, but without success. We found that some of the PDS end group was cleaved via ester hydrolysis during the reduction of the trithiocarbonate. This led to decreased end group retention, and thus no dimer formation.

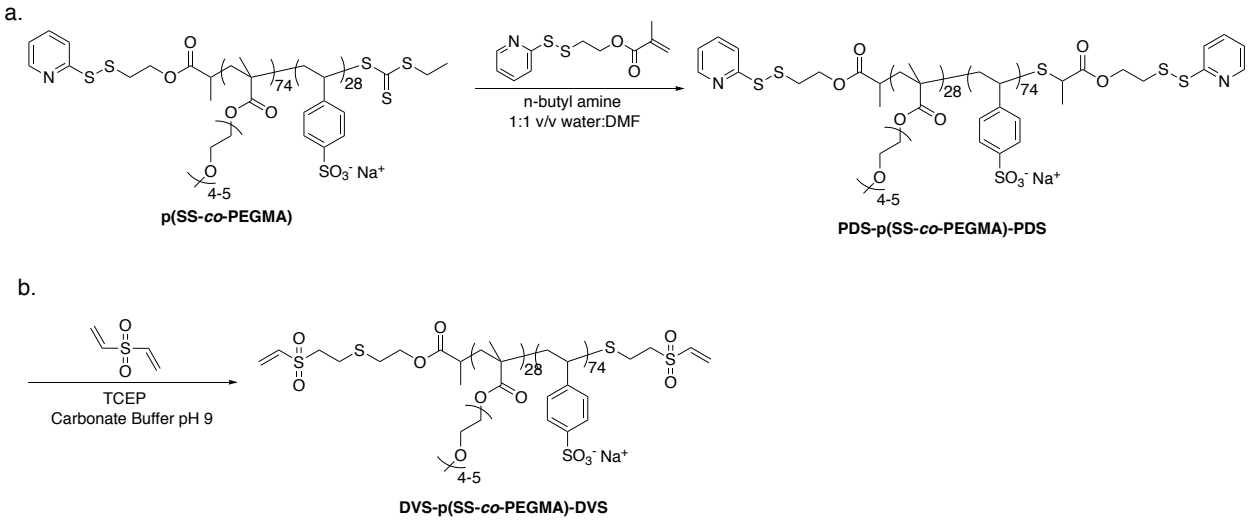

Scheme 4-1. Modification of p(SS-*co*-PEGMA) to contain two divinyl sulfone end groups for protein conjugation. (a) Reduction of trithiocarbonate and capping with PDS-methacrylate followed by (b) TCEP reduction of disulfide bonds in the presence of excess divinyl sulfone.

To attempt to improve the likelihood of dimerization **CTA 1** was designed to prevent hydrolysis during the reduction step by incorporating amide functional groups instead of esters (Scheme 4-2a). Additionally, **CTA 1** was synthesized to contain trithiocarbonate end groups on each side to maintain symmetry in the polymer leading to identical reactivity of the end groups. The CTA was synthesized in 68% yield, with some small impurities on the baseline of the ^{1}H NMR. These impurities did not seem to alter the controlled nature of the polymerization, and are likely dialyzed out during purification of the polymer. **CTA 1** was used to polymerize p(SS-*co*-PEGMA)$_{CTA1}$ by reversible addition fragmentation chain transfer (RAFT) polymerization (Scheme 4-2b). The number average molecular weight (M_n) of the polymer was determined by right angle light scattering gel permeation chromatography (RALS-GPC) to be 28.1 kDa with a dispersity ($Đ$) of 1.16. The trithiocarbonate end groups were then reduced with n-butyl amine in the presence of PDSMA to yield PDS-p(SS-*co*-PEGMA)-PDS (Scheme 4-2c). Finally, the disulfides were reduced with TCEP in the presence of DVS to yield DVS-p(SS-*co*-PEGMA)-DVS (Scheme 4-2d).

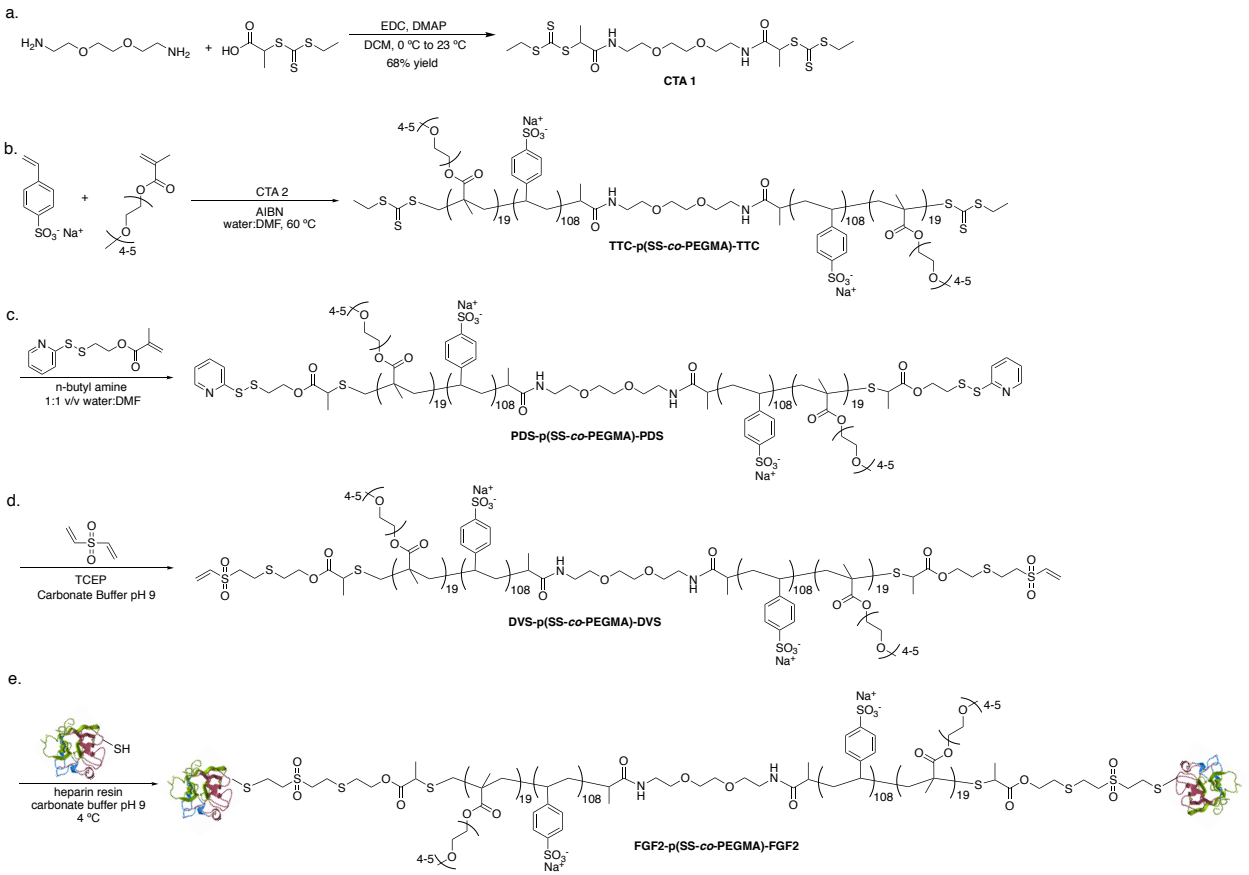

Scheme 4-2. Synthesis of symmetrical DVS-p(SS-*co*-PEGMA)-DVS. (a) Synthesis of a bis-trithiocarbonate CTA. (b) Polymerization of p(SS-*co*-PEGMA) by RAFT polymerization. (c) Reduction of trithiocarbonate and capping with PDS-methacrylate followed by (d) TCEP reduction of disulfide bonds in the presence of excess divinyl sulfone. (e) Conjugation of the bis-DVS polymer to FGF2 through disulfide exchange.

The DVS-p(SS-*co*-PEGMA)-DVS polymer was used to dimerize FGF2 through Michael addition with the exposed cysteine in FGF2 (Scheme 4-2e). Dimerizations were performed using a previously reported mutant FGF2.[32,39] In this mutant, one of the two surface exposed cysteines (C78) was mutated to a serine to prevent oligomerization during conjugation. It has previously been reported that the mutant retains all biological activity and therefore is still therapeutically relevant.[39] Conjugation was performed on a heparin resin to retain activity of the protein during

the reaction. The dimer was analyzed by sodium dodecyl sulfate poly(acrylamide) gel electrophoresis (SDS-PAGE) and compared to free FGF2. All gel electrophoresis was run in reducing conditions with an excess of DTT to prevent bands from naturally occurring disulfide dimer. Analysis indicated that FGF2-p(SS-*co*-PEGMA)-FGF2 dimer was successfully formed. However, the presence of residual DVS resulted in the formation of a FGF2-DVS-FGF2 dimer in greater yield (Figure 4-3). Further purification of the polymer was attempted by dialysis, centrifugation filtration, aqueous extraction, precipitation, and elution on activated charcoal with no success. Because of this undesired DVS conjugation and difficulty in purifying the polymer, maleimide chemistry was investigated instead.

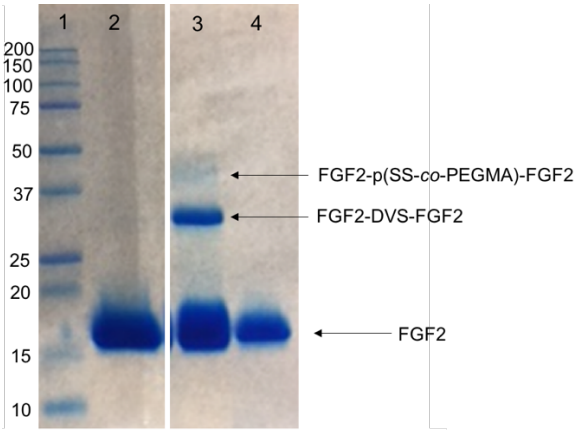

Figure 4-3. SDS-PAGE in reducing conditions stained with coomassie showing FGF2-p(SS-*co*-PEGMA)-FGF2 conjugate as well as FGF2-DVS-FGF2 dimer. Lane 1: Protein ladder; Lane 2: FGF2; Lane 3: crude conjugation; Lane 4: FGF2.

4.2.4 Synthesis of Maleimide Terminated Polymer for FGF2 Dimerization

Maleimides are readily conjugated to proteins via Michael addition with high specificity via free cysteines.[40] Attempts at post-polymerization modification of TTC-p(SS-*co*-PEGMA)-TTC with a furan protected maleimide (FPM) following previously reported procedures[41] led to only 30% end group conversion. Therefore, the CTA was modified to contain a FPM on each

end of the CTA, eliminating the need for post-polymerization modification. **CTA 2** was synthesized through 1-ethyl-3-(3-dimethylaminopropyl)carbodiimide (EDC) coupling of a bis carboxylic acid-trithiocarbonate with FPM-alcohol (Scheme 4-3a). Next, **CTA 2** was used to successfully polymerize FPM-p(SS-*co*-PEGMA)-FPM via RAFT polymerization (Scheme 4-3b). The polymer had a M_n of 14.7 kDa by ^{1}H NMR and 13.1 kDa by RALS with a $Đ$ of 1.20. Additionally, the polymer was confirmed to have a degree of sulfonate incorporation of 79%. Finally, reverse Diels-Alder was implemented to deprotect the maleimide by subjection of the polymer to heat while under vacuum (Scheme 4-3c).

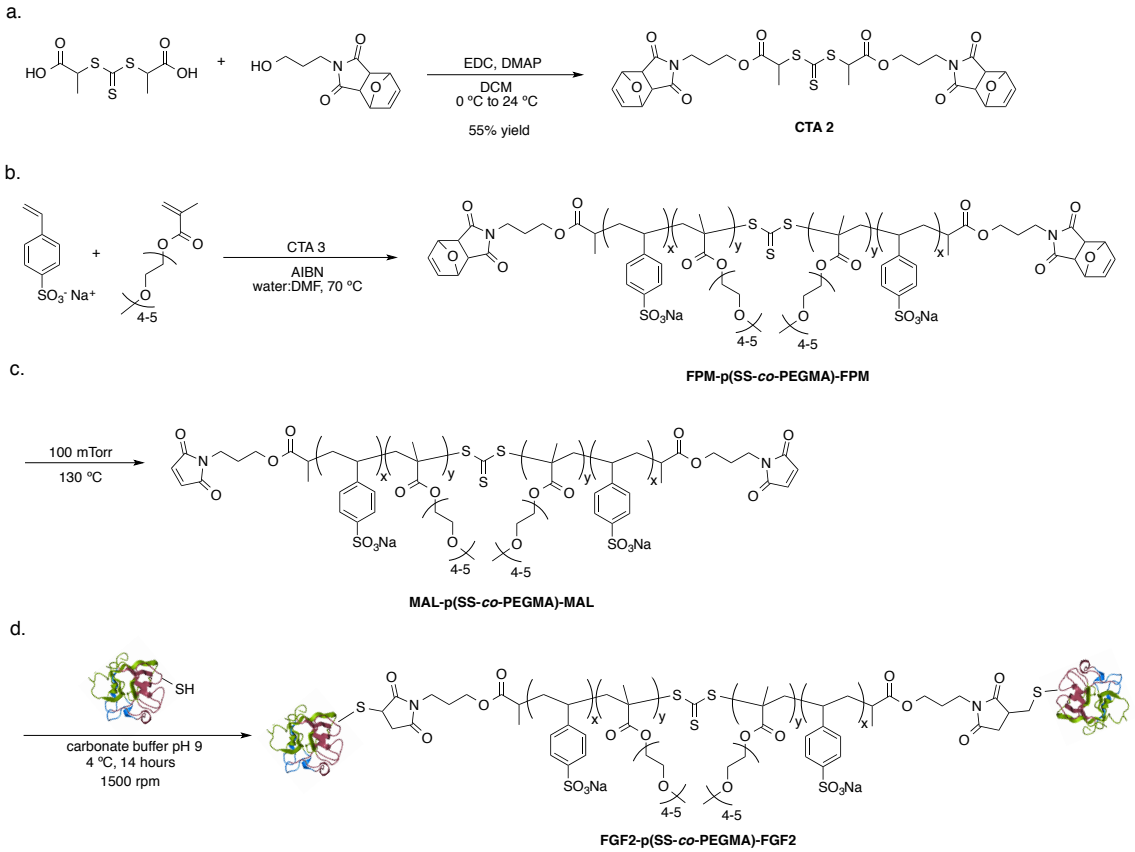

Scheme 4-3. Synthesis of a bis-maleimide p(SS-*co*-PEGMA) and dimerization of FGF2. (a) Synthesis of bis-furan protected maleimide CTA. (b) RAFT polymerization of SS and PEGMA to yield FPM-p(SS-*co*-PEGMA)-FPM. (c) Deprotection of the maleimide to unveil a protein reaction polymer. (d) Dimerization of FGF2 using MAL-p(SS-*co*-PEGMA)-MAL.

4.2.5 Dimerization of FGF2 with MAL-p(SS-*co*-PEGMA)-MAL

The MAL-p(SS-*co*-PEGMA)-MAL polymer was then used to dimerize FGF2. Dimerizations were attempted in both carbonate and tris buffers at pH 9 so that the conjugation solution was basic enough to deprotonate the cysteine. Although maleimides are degradable at pH 9, this pH was chosen due to much faster reaction rate than more neutral pH. Conjugations performed in carbonate buffer resulted in higher yields and therefore these conditions were used to scale up the dimerization. Conjugation was performed in lo-bind Eppendorf tubes at 4 ºC and mostly unreacted FGF2 was observed (Figure 4-4). It was therefore concluded that high yielding dimerization of FGF2 with a heparin mimicking polymer would be difficult to achieve. The low yielding conjugation is likely due to maleimide hydrolysis before dimerization or polymer to protein stoichiometry being slightly off due to transfer error.

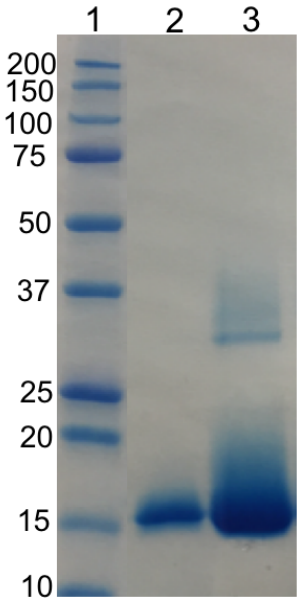

Figure 4-4. SDS-PAGE in reducing conditions with coomassie stain showing FGF2-p(SS-co-PEGMA)-FGF2 conjugate. Crude conjugation. Lane 1: Protein ladder; Lane 2: FGF2; Lane 3: crude conjugation.

4.3 Conclusions and Future Directions

FGF2 dimerized with a 2 kDa PEG linker showed increased cord-like structure and node formation in a co-culture angiogenesis assay. Although the dimer was active in *in vitro* angiogenesis assays FGF2-PEG2k-FGF2 was not able to facilitate receptor binding and required added heparin for receptor activation. A heparin mimicking polymer was utilized as a linker instead of PEG in hopes that it would help facilitate receptor binding and stabilize FGF2 to storage. The heparin mimicking polymer p(SS-*co*-PEGMA) was synthesized to contain protein reactive vinyl and maleimide end groups, which were then used in the dimerization of FGF2. However, the concentrations of FGF2 polymer dimer were minimal. In the future, conjugations could be performed at pH 7.4 with longer reaction times to improve the yield of the conjugation.

4.4 Experimental

4.4.1 Materials

Chemicals and reagents were purchased from Sigma-Aldrich and used as received unless otherwise indicated. Silica gel column chromatography was performed on a Biotage Isolera™ Spektra System with ACI™ and UV detector. Prior to polymerizations 4-styrene sulfonic acid was pretreated with Na^+ and dried to produce the sodium salt. Before polymerization azobis(isobutyronitrile) (AIBN) was recrystallized twice from ethanol and dried. Protein was mutated (C78S), expressed and purified from the plasmid pET29c(+)hFGF-2, which was kindly provided by Professor Thomas Scheper from the Helmholtz Centre for Infection Research (Braunschweig, Germany) according to Chen et. al.[42] HiTrap™ Heparin HP columns were purchased from GE Healthcare. ELISA was performed using the ELISA Development DuoSet® kit purchased from R&D Systems. ELISA Development DuoSet kits were purchased from R&D Systems. BaF3-FR1C expressing FGFR1 were kindly provided by Professor David Ornitz

(Washington University, Saint Louis).[43] Cell medium was purchased from ATCC or Invitrogen unless otherwise indicated. CellTiter-Blue® Cell Viability Assay was purchased from Promega. Polystyrene standards for GPC calibration were purchased from Polymer Laboratories.

4.4.2 Analytical Techniques

^{1}H NMR and ^{13}C NMR spectroscopy was performed on an Avance DRX 400 instrument. Aqueous GPC was performed in 0.05 M Na_2SO_4 in MilliQ (MQ) water with 10% MeOH on a Viscotek GPC_{MAX} VE 2001 GPC solvent/sample module equipped with Viscotek TDA 305 triple array detector. Gel electrophoresis was performed using Any kDTM Mini-PROTEAN® TGXTM precast gels with tris-glycine as running buffer (Bio-Rad, Hercules). ELISA assays were read on an ELX800 Universal Microplate Reader (Bio-Tek Instrument Inc., Winooski) with λ = 450 nm for signal and 630 nm for background. CellTiter-Blue® assays were read on a SpectraMax M5 microplate reader (Molecular Devices, Sunnyvale).

4.4.3 Methods

Modification of p(SS-co-PEGMA) with PDS: p(SS-*co*-PEGMA) (0.10 g, 0.004 mmol) was added to a vial with stir bar and dissolved in 2 mL of 1:1 water:DMF that had been degassed prior to use. Pyridyl disulfide methacrylate (PDSMA) (0.05 g, 0.192 mmol) was added and a T_0 was taken by UV-Vis to visualize the trithiocarbonate end group. n-Butyl amine (0.014 g, 0.192 mmol) was added and the reduction of the trithiocarbonate peak at 215 nm was monitored by UV-Vis. After 9 hours the reaction solution was filtered by centrifugal filtration in a 3.0 kDa filter against 2M NaCl to remove the n-butylamine. The remaining solution was dialyzed in a 3.5 kDa MWCO dialysis membrane against 1:1 water:MeOH for 2 days followed by 100% MQ water for 1 day. The contents of the dialysis tube were lyophilized to dryness to yield a light yellow solid. To determine the extent of PDS modification, a 1 mg/mL solution of PDS-p(SS-co-

PEGMA)-PDS was incubated with DTT for 16 hours. The cleavage of PDS was monitored by UV-Vis and compared to a 1mg/mL solution of PDS-p(SS-co-PEGMA) incubated with DTT. The amount of PDS in the modified polymer compared to unmodified polymer was found to be 171%.

Modification of PDS-p(SS-co-PEGMA)-PDS with DVS: PDS-p(SS-*co*-PEGMA)-PDS (0.10 g, 0.004 mmol) was added to a small vial containing tris(2-carboxyethyl)phosphine (TCEP) (0.01 g, 0.039 mmol). The contents of the vial were dissolved in 0.2 mL of tris buffer at pH 9.0. The polymer solution was added dropwise to a stirring solution of divinyl sulfone (2 mL, 19.92 mmol). The reaction was stirred vigorously over 16 hours. Next, the reaction mixture was diluted with 10 mL of deionized water and placed in a 3.0 kDa MWCO dialysis tube. The polymer was purified by dialysis against acetone for 24 hours, 1:1 water:MeOH for 2 days, then 100% water for 1 day. The contents of the dialysis tube were lyophilized to dryness to yield a white solid.

Synthesis of CTA 1: A 2-neck round bottom flask was purged with argon, and 2-((ethylthio)carbonothioyl) thio propanoic acid (0.30 g, 1.43 mmol) was added and dissolved in 30 mL of dry dichloromethane (DCM). The round bottom was submerged in an ice bath and 1-ethyl-3-(3-dimethylaminopropyl)carbodiimide (EDC) (0.658 g, 3.43 mmol) and 4-dimethylaminopyridine (DMAP) (0.43 g, 0.042 mmol) were added. The reaction was stirred for 20 minutes and changed from yellow to bright orange upon formation of the activated ester. Triethylene glycol amine (TEG-amine) (0.64 g, 0.095 mmol) was dissolved in 1 mL of dry DCM and added to the reaction dropwise over 10 minutes. The reaction was stirred for 6 hours and warmed slowly from 0 ºC to 19 ºC, the stirred until the reaction turned from dark red to light yellow. The solvent was evaporated *in vacuo* and a silica gel column was run in 3:1 ethyl acetate:hexanes on a biotage system. The product fractions were rotovapped to yield a yellow oil

in 68% yield. ^{1}H NMR (400 MHz, $CDCl_3$) δ: 6.71 (2H, br s), 4.70-4.77 (2H, q), 4.59 (4H, s), 4.52-4.56 (4H, t), 4.43-4.49 (4H, t), 3.30-3.38 (4H, q), 1.54-1.51 (6H, d), 1.30-1.35 (6H, t). ^{13}C NMR (400 MHz, $CDCl_3$) δ: 223.59, 170.43, 70.41, 69.70, 48.12, 39.59, 31.74, 16.40, 12.96. FT-IR (cm^{-1}): 3294, 2972, 2928, 2866, 1739, 1653, 1529, 1445, 1417, 1374, 1253, 1077, 1027, 877, 812.

Polymerization of p(SS-co-PEGMA)$_{CTA1}$: RAFT polymerization was performed with initial feed ratio of [SS]:[PEGMA]:[CTA]:[AIBN] = 166:30:1:0.5 and a monomer concentration of 0.92 M. Styrene sulfonate (322 mg, 1.56 mmol) and PEGMA M_n 300 (85 mg, 0.282 mmol) were dissolved in 1.0 mL of degassed water in a Schlenk tube. CTA 1 (5 mg, 0.009 mmol) and AIBN (0.77 mg, 0.005 mmol) were dissolved in 1.0 mL of degassed DMF and then transferred to the Schlenk tube. The Schlenk tube was sealed and subjected to three freeze-pump-thaw cycles before immersion in an oil bath set to 60 °C. After 4 hours the polymerization was stopped by cooling to room temperature (23 ºC) and bubbling air through the Schlenk tube. The polymer was purified by dialysis in 3.5 MWCO tubing against 1:1 v/v water:MeOH followed by 100% Milli-Q water. The resulting contents of the dialysis tubing were lyophilized to dryness to give a fluffy light yellow solid. ^{1}H NMR 400 MHz (D_2O with CD_3CN) δ: 6.15-7.77 (SS side chains), 2.60-3.90 (PEGMA side chains), 0.00-2.60 (polymer backbone). Degree of sulfonation was calculated to be 79.7% by ^{1}H NMR. The M_n = 28.1 kDa by RALS-GPC with $Đ$ of 1.16.

Synthesis of PDS-p(SS-co-PEGMA)$_{CTA1}$-PDS: p(SS-*co*-PEGMA)$_{CTA1}$ (100 mg, 0.004 mmol) was weighed and dissolved in 2 mL of 1:1 DMF:H2O (degassed for 1 hour prior to use) in a round bottom flask. PDSMA (46 mg, 0.179 mmol) was added to the polymer solution and a T_0 was taken by UV-Vis to visualize the trithiocarbonate peak at 215 nm. N-butylamine (18 µL, 0.179 mmol) was added and the reaction was stirred vigorously at 23 ºC. Reduction of the

trithiocarbonate was evaluated by reduction of the 315 nm peak by UV-Vis. After 5 hours the trithiocarbonate was mostly reduced. The reaction was let stir for an additional hour, and then reaction solution was filtered by centrifugal filtration 5 times in a 3.0 kDa filter against 2M NaCl to remove the n-butylamine. The remaining solution was dialyzed in a 3 kDa MWCO dialysis membrane against 1:1 water:MeOH for 2 days followed by 100% MQ water for 1 day. The contents of the dialysis tube were lyophilized to dryness to yield a light yellow solid. ^{1}H NMR 400 MHz (D_2O with CD_3CN) δ: 8.15-8.35 (1H, br s, PDS end groups), 6.15-7.98 (SS side chains), 2.60-4.12 (PEGMA side chains), 0.00-2.60 (polymer backbone).

Synthesis of DVS-p(SS-co-PEGMA)$_{CTA1}$-DVS: PDS-p(SS-*co*-PEGMA)$_{CTA1}$-PDS (0.10 g, 0.004 mmol) was placed in an Eppendorf tube along with TCEP (0.0096 g, 0.039 mmol). The solids were dissolved in 0.5 mL of tris buffer at pH 9.0. The polymer solution was added dropwise to a stirring solution of divinyl sulfone (1 mL, 9.96 mmol). The reaction was stirred vigorously over 11 hours. Next, reaction mixture was diluted with 10 mL of deionized water and placed in a 3.5 kDa MWCO dialysis tube. The polymer was purified by dialysis against acetone for 24 hours, 1:1 water:MeOH for 2 days, then 100% water for 1 day. The contents of the dialysis tube were lyophilized to dryness to yield a white solid. ^{1}H NMR 400 MHz (D_2O with CD_3CN) δ: 6.10-7.70 (SS side chains), 2.60-4.12 (PEGMA side chains), 0.00-2.60 (polymer backbone).

Synthesis of CTA 2: A 2-neck round bottom flask was purged with argon, and 2,2'-(thiocarbonylbis(sulfanediyl))dipropionic acid (0.50 g, 1.97 mmol) and 2-(3-hydroxypropyl)-3a,4,7,7a-tetrahydro-1*H*-4,7-epoxyisoindole-1,3(2*H*)-dione (1.1 g, 4.92 mmol) were added and dissolved in 20 mL of dry DCM. After 20 minutes EDC (0.74 g, 4.72 mmol) and DMAP (0.10 g, 0.79 mmol) were added and the reaction was allowed to warm from 0 ºC to 23 ºC over 16 hours.

After 16 hours the solvent was removed *in vacuo* and a silica gel column was run in 7:1 EtOAc:Hexane using a Biotage purification system. Product fractions were collected and *dried in vacuo* to provide the product as a sticky yellow solid in 55% yield. ^{1}H NMR (400 MHz, $CDCl_3$) δ: 6.46-6.52 (4H, s), 5.25-5.30 (4H, s), 4.76-4.82 (2H, q), 4.05-4.16 (4H, m), 3.52-3.61 (4H, m), 2.80-2.88 (4H, s), 1.89-2.01 (4H, t), 1.59-1.67 (6H, d). ^{13}C NMR (400 MHz, $CDCl_3$) δ: 219.97, 176.11, 170.71, 136.53, 80.97, 62.87, 48.35, 47.45, 35.69, 26.63, 16.92. FT-IR (cm^{-1}): 2965, 1774, 1733, 1693, 1446, 1402, 1376, 1350, 1310, 1247, 1175, 1153, 1075, 1023, 956, 917, 877, 854, 804.

Polymerization of FPM-p(SS-co-PEGMA)-FPM: RAFT polymerization was performed with initial feed ratio of [SS]:[PEGMA]:[CTA]:[AIBN] = 115:21:1:0.5 and a monomer concentration of 1.28 M. Styrene sulfonate (357 mg, 1.73 mmol) and PEGMA M_n 300 (95 mg, 0.316 mmol) were dissolved in 0.8 mL of degassed water in a Schlenk tube. **CTA 2** (10 mg, 0.015 mmol) and AIBN (1.24 mg, 0.008 mmol) were dissolved in 0.8 mL of degassed DMF and then transferred to the Schlenk tube. The Schlenk tube was sealed and subjected to three freeze-pump-thaw cycles before immersion in an oil bath set to 70 °C. After 4 hours the polymerization was stopped by immersion in liquid nitrogen and then bubbling air through the Schlenk tube. The polymer was purified by dialysis in 3500 MWCO tubing against 1:1 v/v water:MeOH followed by 100% Milli-Q water. The resulting contents of the dialysis tubing were lyophilized to dryness to give a fluffy white solid. ^{1}H NMR 400 MHz (D_2O with CD_3CN) δ: 6.10-7.90 (SS side chains), 5.05-5.12 (4H, br s), 2.7-4.1 (PEGMA side chains), 0.00-2.50 (polymer backbone). The M_n by ^{1}H NMR = 14.7 kDa with a degree of sulfonation of 79.0%. The M_n= 13.1 kDa by RALS-GPC with $Đ$ of 1.20.

Deprotection of FPM-p(SS-co-PEGMA)-FPM to yield MAL-p(SS-co-PEGMA)-MAL: FPM-p(SS-*co*-PEGMA)-FPM (25 mg, 0.002 mmol) was added to a Schlenk tube with stir bar. The Schlenk tube was place under vacuum (100 mTorr) and submerged in an oil bath set to 130 ºC. After 16 hours the Schlenk tube was cooled to 23 ºC. ^{1}H NMR 400 MHz (D_2O with CD_3CN) δ: 6.10-7.90 (SS side chains), 2.75-4.30 (PEGMA side chains), 0.00-2.75 (polymer backbone). Deprotection of the maleimide was monitored by disappearance of the ^{1}H NMR at 5.05-5.12 ppm. Polymer was 98.3% deprotected.

Dimerization and Purification of FGF2-p(SS-co-PEGMA)-FGF2: Dimerizations were performed in carbonate buffer at pH 9.0 with a molar ratio of FGF2:polymer of 2:1. In a typical dimerization FGF2 (400 μg, 23.53 nmol) was added to a 0.5 mL eppendorf tube containing 80 μL of heparin resin in carbonate buffer at pH 9.0. A 30 mg/mL polymer solution was prepared in carbonate buffer pH 9.0, and then 5.77 μL was added to the tube containing protein. For all conjugations the protein concentration was maintained between 2-3 mg/mL. The tube was placed on a shaker table set to 4 ºC and 1100 rpm. After 16 hours the solution was removed and a crude SDS-PAGE was run. For purification, the conjugation mixture was added to a 1 mL heparin resin column. The column was rinsed with 3 mL of DPBS to remove unconjugated polymer. Next, the resin was rinsed with 3 mL DPBS + 0.3 M NaCl. The salt fractions were increased by 0.1 M NaCl steps from concentrations of 0.3 M to 2.0 M. Fractions were concentrated by centrifugation filtration in a 10 kDa membrane at 10.2 rcf. Fractions were collected and analyzed for purity by SDS-PAGE.

Angiogenesis Co-Culture Assay: Methods for angiogenesis co-culture and cord-like structure staining were adapted from literature procedures.[36,37] HDFs (P3) were plated at 12,500 cells/well in a 48-well plate, in EGM with full supplement and incubated at 37 ºC for 72 hours or until cells

reached confluency. The cells were then starved for 18 hours with EGM without bovine brain extract or epidermal growth factor (-BBE) (-EGF). HUVECs (P4) were trypsinized and resuspended in EGM (-BBE) (-EGF). Starvation media was aspirated and HUVECs were plated on top of the HDF monolayer at 10,000 cells/well in EGM (-BBE) (-EGF) followed by sample (either FGF2 or FGF2-PEG2k-FGF2) diluted in EGM (-BBE) (-EGF). Final concentrations of FGF2 and FGF2-PEG2k-FGF2 were 10 ng/mL, 5 ng/mL, 1 ng/mL, 0.5 ng/mL, and 0.1 ng/mL. After 72 and 144 hours the sample solutions were refreshed with samples in EGM (-BBE) (-EGF) at the appropriate concentrations. Ten days after HUVEC and the first sample addition, the medium was removed and each well fixed with 70% EtOH (at 20 ºC) for 30 minutes. After fixing, the wells were rinsed with 0.5 mL of 1% BSA in D-PBS three times. Next, endogenous alkaline phosphatase was removed by incubation with 0.3% H_2O_2 in MeOH at 24 ºC for 15 minutes. The H_2O_2 solution was removed once the solution was cloudy. The wells were washed 3 times with 1% BSA. The wells were then incubated with primary antibody (mouse anti-human PECAM1/CD31, R&D Systems) at 1 mg/mL in 1% BSA for 60 min at 37 ºC. The wells were then rinsed 3 times with 1% BSA. The wells were then incubated with secondary antibody (goat anti-mouse IgG alkaline phosphatase, Sigma Aldrich) at 3 mg/mL in 1% BSA for 60 minutes at 37 ºC and then wells were rinsed 3-5 minutes with MilliQ water. Next, the wells were incubated with BCIP/NBT solution (one tablet dissolved in 10 mL MilliQ water, filtered) at 24 ºC for 6-15 min. After the cord-like structures were visually stained, the BCIP/NBT (Life Technologies) was removed and the wells were washed 3 times with MilliQ water and allowed to dry. Plates were stored for up to 60 days at -80 ºC. To assess the extent of angiogenesis, 5 bright field images were captured per well at 5X magnification. Number and length of the cord-like structures as well as number of nodes were calculated manually using NIH ImageJ Software. The values for

each of 5 images per well were summed and then the sums were averaged across 3 wells. The sample identities remained blinded during analysis and until after results were calculated.

BaF3-FR1C Receptor Assay: BaF3-FR1C cells were grown in RPMI1640 medium containing % newborn bovine calf serum, 0.5 ng/mL IL-3, 100 μg/mL penicillin, and 100 μg/mL streptomycin. Before seeding cells for experiments the cells were collected and washed twice with culture medium without IL-3. Cells were plated at a concentration of 20,000 cells/well/50 μL in the internal wells of a 96 well plate in culture medium without IL-3. Samples were prepared in culture medium without IL-3 to contain double the final concentration and then 50 μL of each sample was added to the corresponding well. The external wells were blocked in 100 μL of DPBS and then incubated at 37 °C and 5% CO_2. After 48 hours of incubation CellTiter-Blue assay was performed to determine extent of cell growth. All samples were normalized to the control group, which contained only culture medium without IL-3. Each group contained six replicates.

4.5 Appendix to Chapter 4 – Supplementary Information

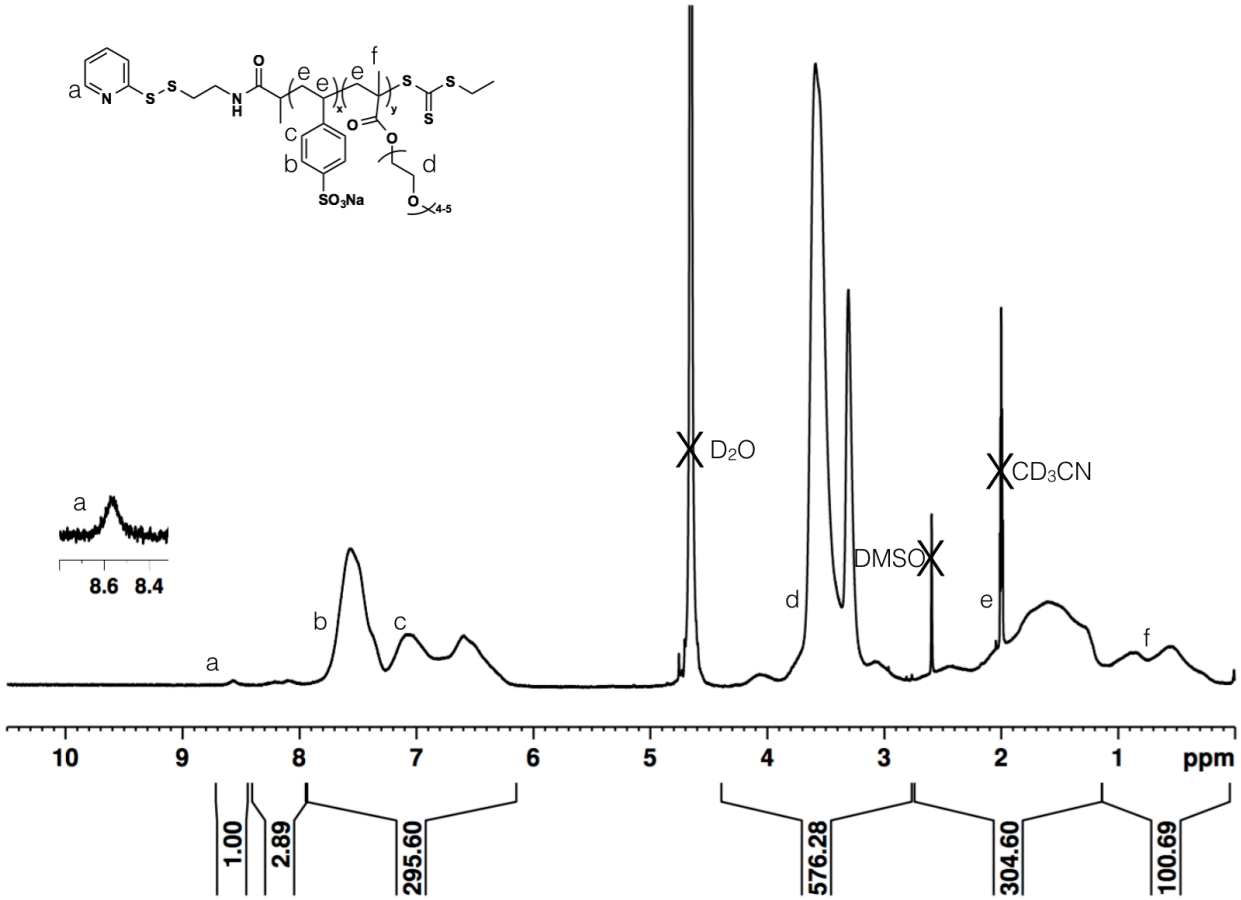

Figure 4-5. ^{1}H NMR (400 MHz, D_2O with CD_3CN) of p(SS-*co*-PEGMA)

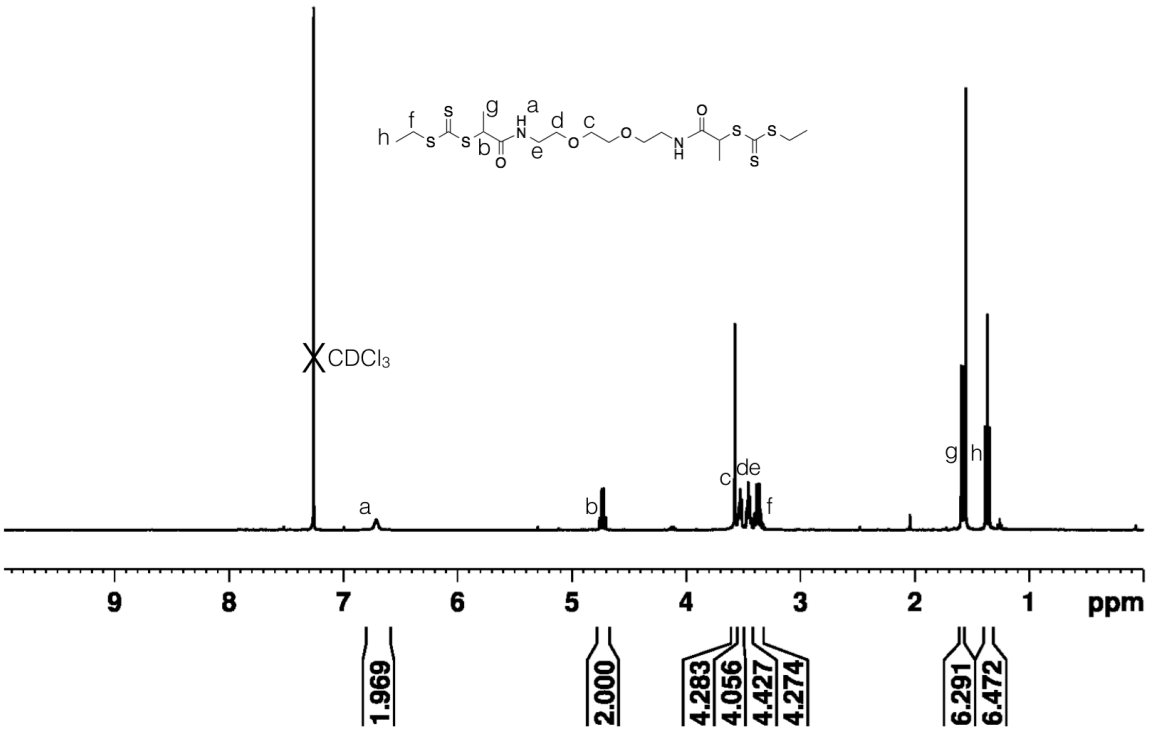

Figure 4-6. ^{1}H NMR (400 MHz, $CDCl_3$) of **CTA1**

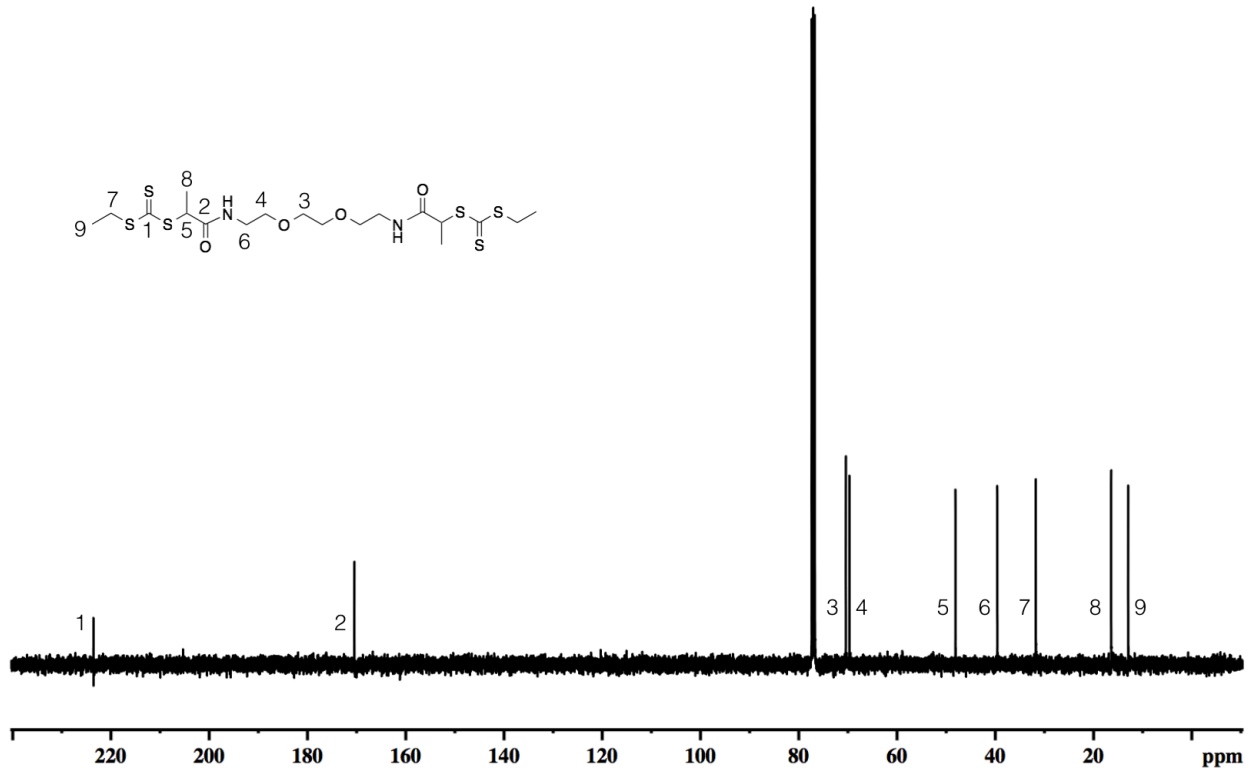

Figure 4-7. ^{13}C NMR (400 MHz, $CDCl_3$) of **CTA1**

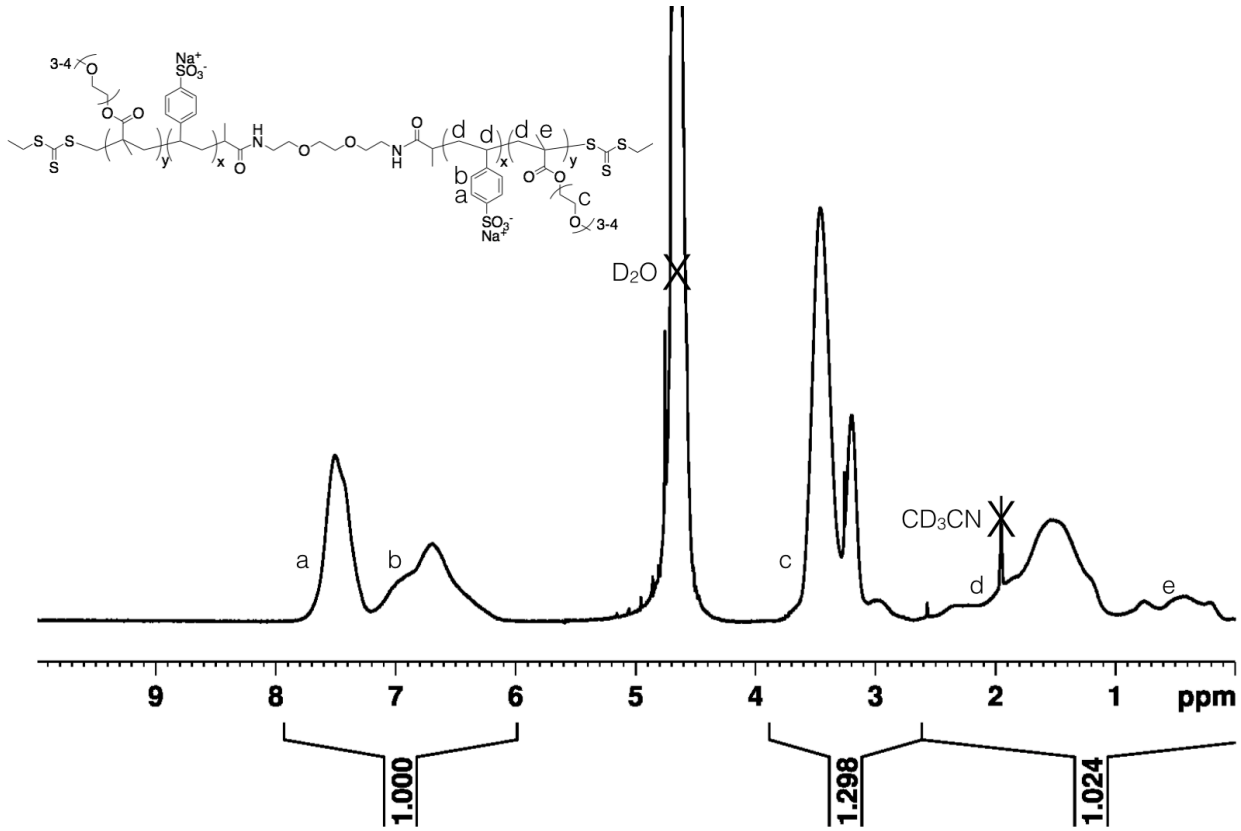

Figure 4-8. ^{1}H NMR (400 MHz, D_2O with CD_3CN) of p(SS-*co*-PEGMA)$_{CTA1}$

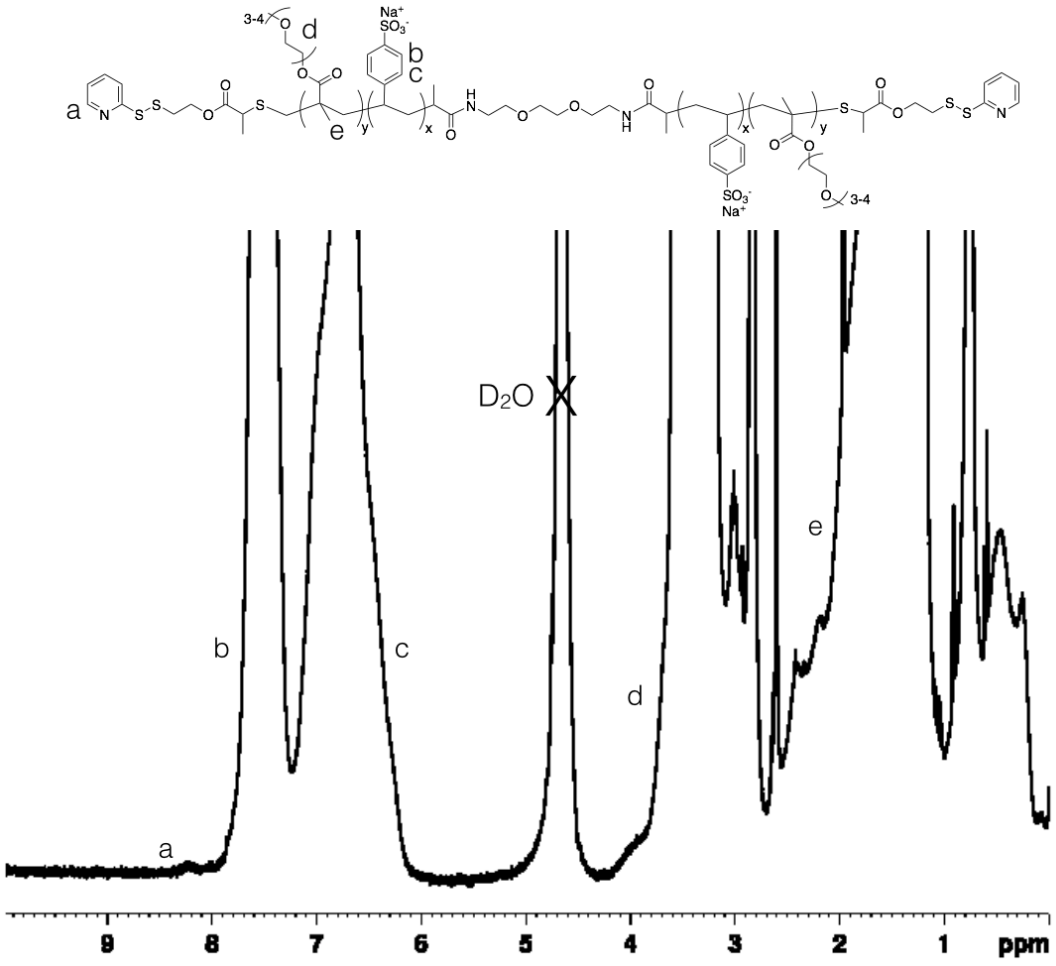

Figure 4-9. ^{1}H NMR (400 MHz, D_2O with CD_3CN) of PDS-p(SS-*co*-PEGMA)$_{CTA1}$-PDS

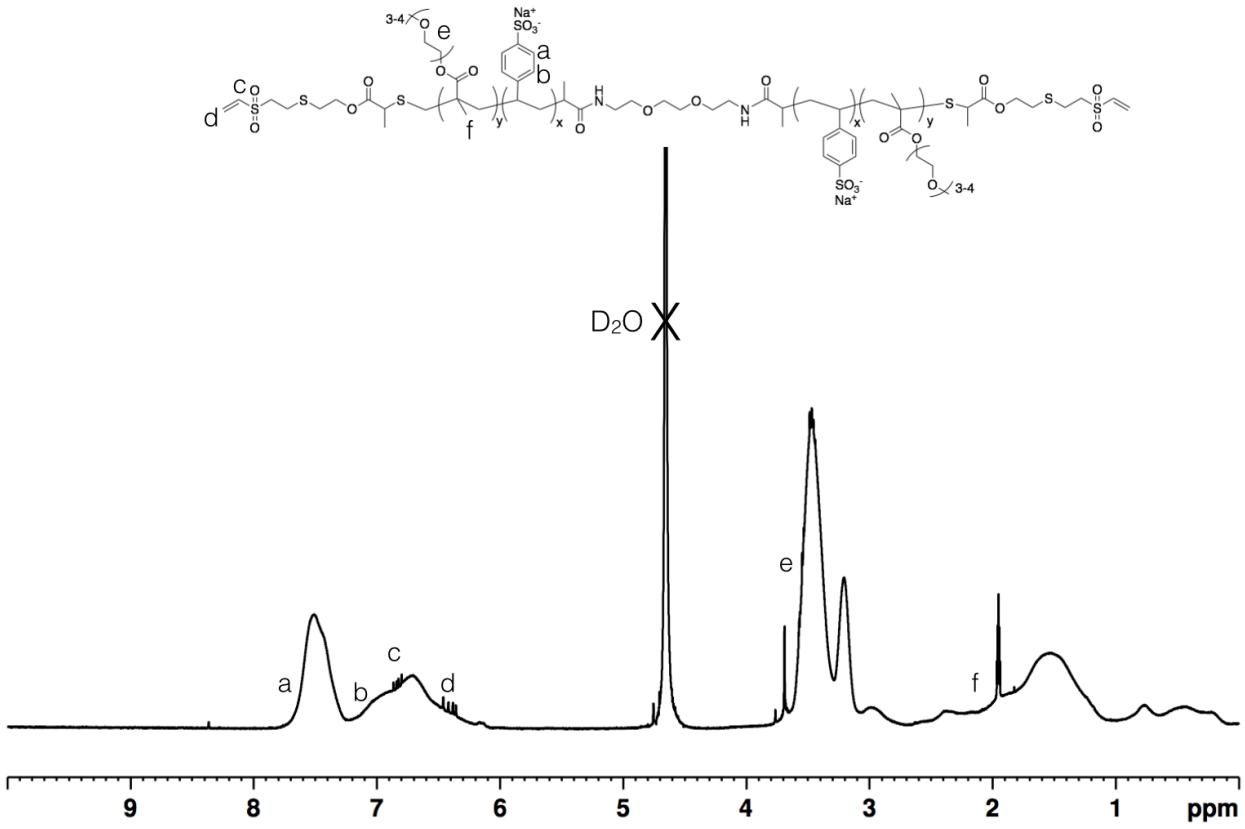

Figure 4-10. ^{1}H NMR (400 MHz, D_2O with CD_3CN) of DVS-p(SS-*co*-PEGMA)$_{CTA1}$-DVS

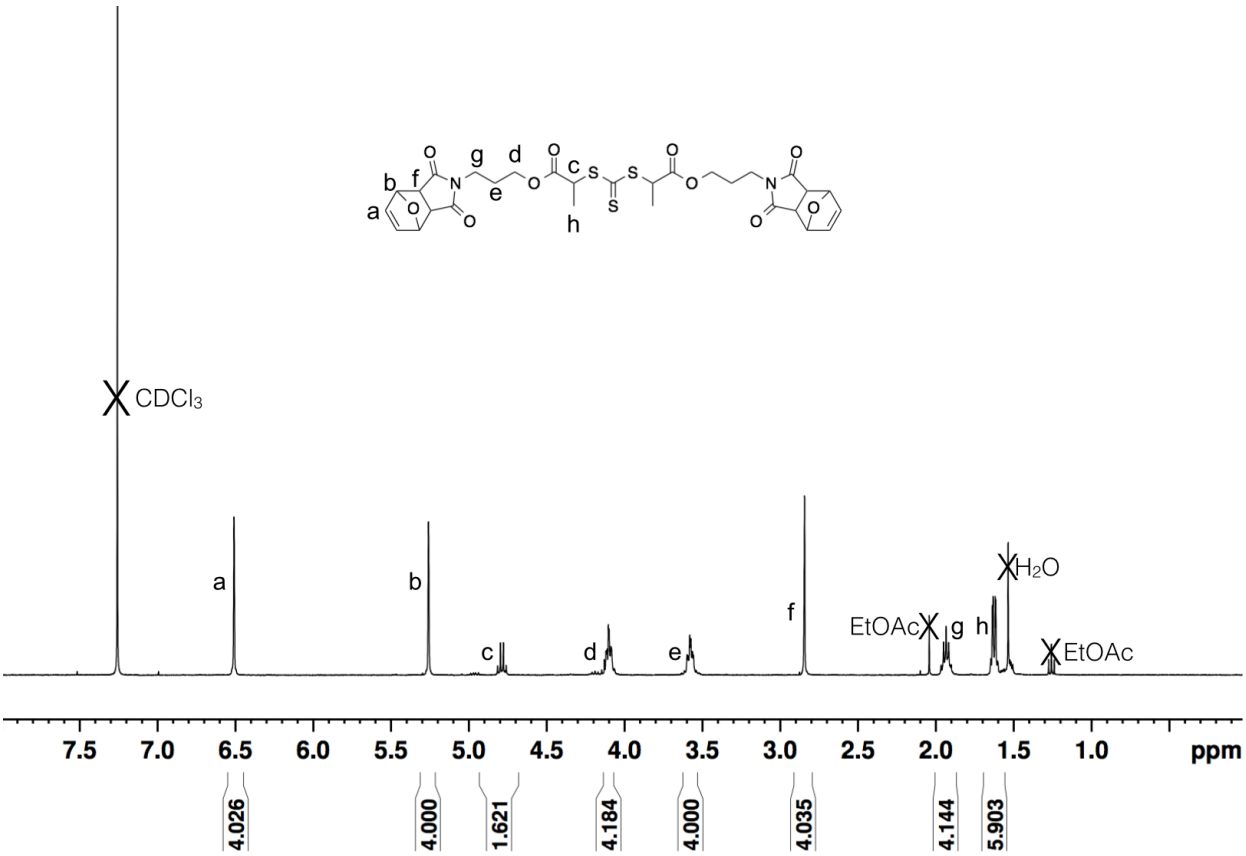

Figure 4-11. ^{1}H NMR (400 MHz, $CDCl_3$) of **CTA 2**

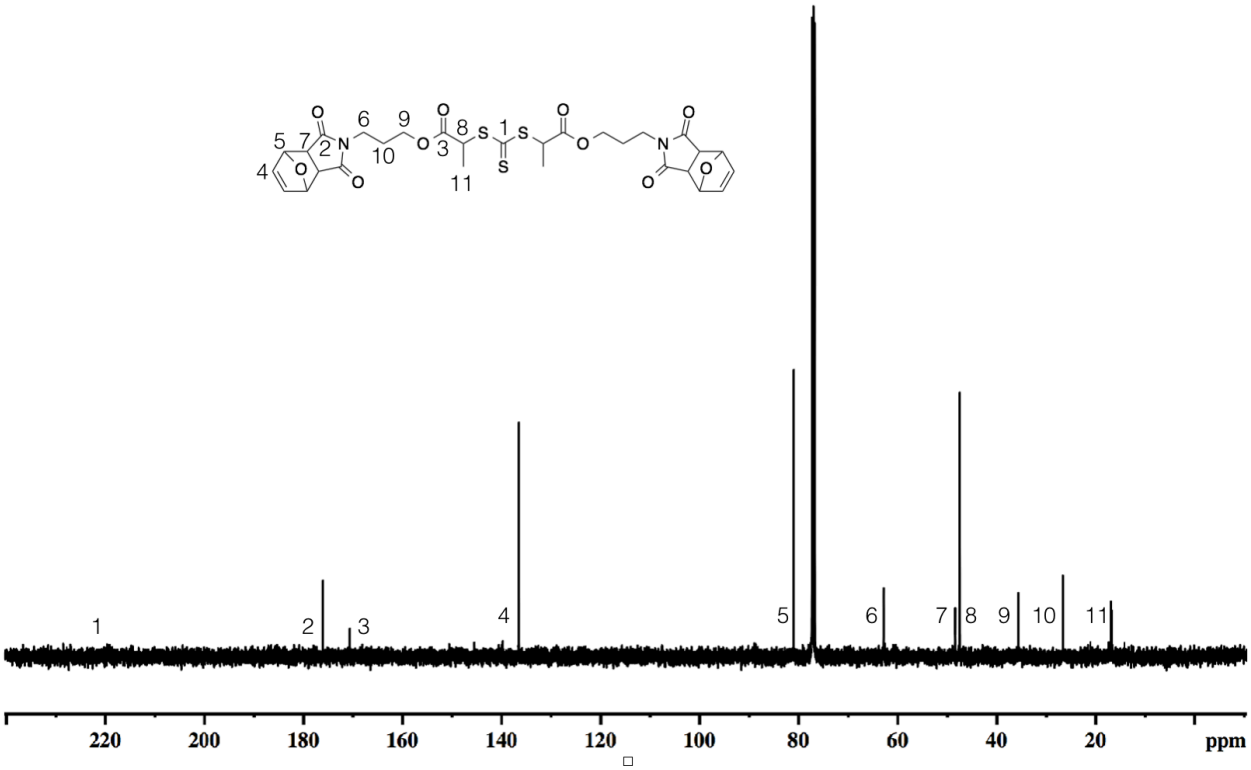

Figure 4-12. ^{13}C NMR (400 MHz, $CDCl_3$) of **CTA 2**

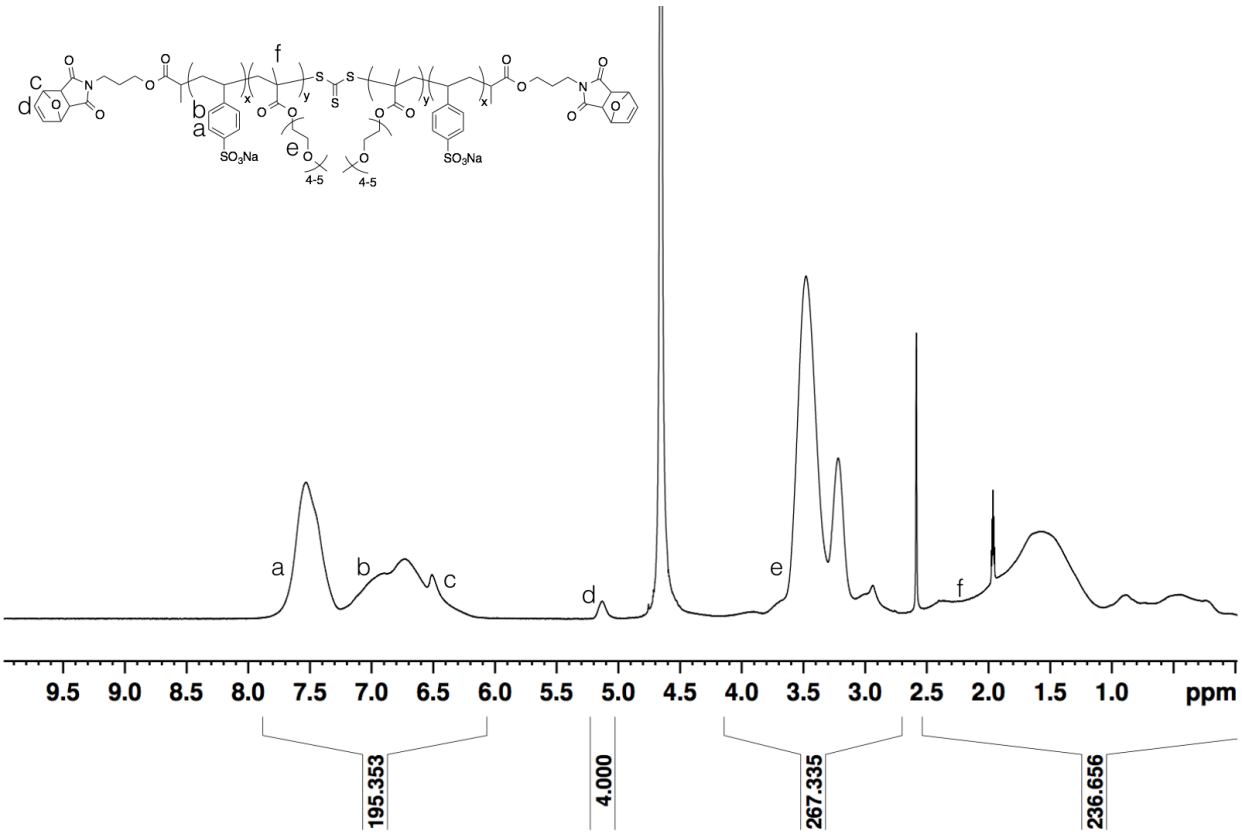

Figure 4-13. ^{1}H NMR (400 MHz, D_2O with CD_3CN) of FPM-p(SS-*co*-PEGMA)-FPM

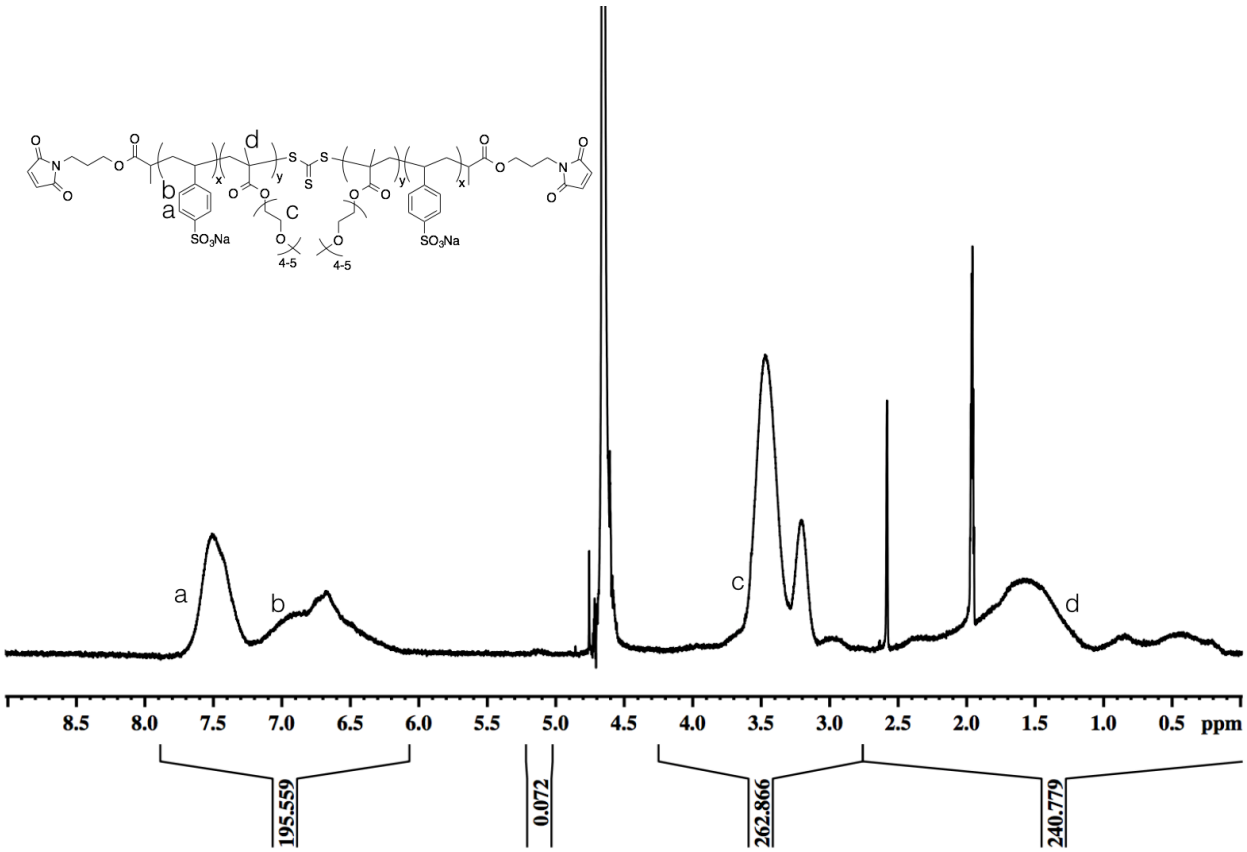

Figure 4.14. ^{1}H NMR (400 MHz, D_2O with CD_3CN) of MAL-p(SS-*co*-PEGMA)-MAL

4.6 References

† Portions of Chapter 4 are reproduced from Biomaterials, 81, Decker, C.G.; Wang, Y.; Paluck, S.J.; Shen, L.; Loo, J.A.; Levine, A.J.; Miller, L.S.; Maynard, H.D. Fibroblast growth factor 2 dimer with superagonist in vitro activity improves granulation tissue formation during wound healing. 157-168., Copyright 2016, with permission from Elsevier.

(1) Demidova-Rice, T. N.; Hamblin, M. R.; Herman, I. M. *Adv. Skin Wound Care* **2012**, *25*, 304.

(2) Greenhalgh, D. G. *J. Trauma Inj. Infect. Crit. Care* **1996**, *41*, 159.

(3) Barrientos, S.; Brem, H.; Stojadinovic, O.; Tomic-Canic, M. *Wound Repair Regen.* **2014**, *22*, 569.

(4) Steed, D. L.; Webster, M. W.; Ricotta, J. J.; Luterman, A.; Brown, S.; Comerota, A. J.; Walsh, D. B.; Bergamini, T. M.; Baker, W. H.; Boltax, R. S.; Schwarcz, T. H.; Donohoe, D. J.; Fleishman, A.; Krupski, W. C.; Harrington, M. E.; Gibbons, G.; Logerfo, F. *J. Vasc. Surg.* **1995**, *21*, 71.

(5) Wieman, T. J.; Smiell, J. M.; Su, Y. C. *Diabetes Care* **1998**, *21*, 822.

(6) Administration, F. a. D. 2008; Vol. 2017.

(7) Ornitz, D. M.; Itoh, N. *Genome Biol.* **2001**, *2*.

(8) Werner, S.; Grose, R. *Physiol. Rev.* **2003**, *83*, 835.

(9) Bikfalvi, A.; Klein, S.; Pintucci, G.; Rifkin, D. B. *Endocrine Rev.* **1997**, *18*, 26.

(10) Edelman, E. R.; Mathiowitz, E.; Langer, R.; Klagsbrun, M. *Biomaterials* **1991**, *12*, 619.

(11) Richard, J. L.; Bringer, J.; Parerrichard, C.; Rodier, M.; Daures, J. P.; Jacob, C.; Clouet, S.; Comtebardonnet, M.; Vannereau, D. *Diabetes Care* **1995**, *18*, 64.

(12) Whalen, G. F.; Shing, Y.; Folkman, J. *Growth Factors* **1989**, *1*, 157.

(13) Nguyen, T. H.; Kim, S.-H.; Decker, C. G.; Wong, D. Y.; Loo, J. A.; Maynard, H. D. *Nat. Chemistry* **2013**, *5*, 221.

(14) Paluck, S. J.; Nguyen, T. H.; Lee, J. P.; Maynard, H. D. *Biomacromolecules* **2016**.

(15) Ballinger, M. D.; Shyamala, V.; Forrest, L. D.; Deuter-Reinhard, M.; Doyle, L. V.; Wang, J. X.; Panganiban-Lustan, L.; Stratton, J. R.; Apell, G.; Winter, J. A.; Doyle, M. V.; Rosenberg, S.; Kavanaugh, W. M. *Nat. Biotechnol.* **1999**, *17*, 1199.

(16) Tassi, E.; Al-Attar, A.; Aigner, A.; Swift, M. R.; McDonnell, K.; Karavanov, A.; Wellstein, A. *J. Biol. Chem.* **2001**, *276*, 40247.

(17) Benjamin H. Chai L., F., M.A., Goodwin W., Hundal A., Israel D.I. (Praecis Pharmaceuticals Inc., USA). Peptide compounds useful for modulating FGF receptor activity. WO Patent PCT/US97/21070, Publication date May 22, 1998.

(18) Rudenko, O.; Tkach, V.; Berezin, V.; Bock, E. *Neurosci. Res.* **2010**, *68*, 35.

(19) Li, S. Z.; Christensen, C.; Kohler, L. B.; Kiselyov, V. V.; Berezin, V.; Bock, E. *Develop. Neurobiol.* **2009**, *69*, 837.

(20) Yayon, A.; Rom, E.; Chumakov, I.; Blumenstein, S. (Prochon Biotech Ltd., USA). FGF-2 variants having N-terminal deletions and increased receptor selectivity and uses thereof. US Patent Number 12/443,638. Publication date February 24, 2015.

(21) Springer, B.; Pantoliano, M.; Sharp, C.M. (3-Dimensional Pharmaceuticals, inc., USA). Analogs of human basic fibroblast growth factor mutated at one or more of the positions glutamate 89, aspartate 101 or leucine 137. US Patent Numbr 09/220,077, Publication date August 14, 2001.

(22) Bogin, O.; Yayon, A. (ProChon Biotech Ltd., USA). FGF variants and methods for use thereof. WO Patent Number PCT/IL2003/000379, Publication date November 20, 2003.

(23) Davis, J. C.; Venkataraman, G.; Shriver, Z.; Raj, P. A.; Sasisekharan, R. *Biochem. J.* **1999**, *341*, 613.

(24) Venkataraman, G.; Shriver, Z.; Davis, J. C.; Sasisekharan, R. *Proc. Nat. Acad. Sci. USA* **1999**, *96*, 1892.

(25) Platonova, N.; Miquel, G.; Chiu, L. Y.; Taouji, S.; Moroni, E.; Colombo, G.; Chevet, E.; Sue, S. C.; Bikfalvi, A. *Plos One* **2014**, *9*.

(26) Plotnikov, A. N.; Schlessinger, J.; Hubbard, S. R.; Mohammadi, M. *Cell* **1999**, *98*, 641.

(27) Schlessinger, J.; Plotnikov, A. N.; Ibrahimi, O. A.; Eliseenkova, A. V.; Yeh, B. K.; Yayon, A.; Linhardt, R. J.; Mohammadi, M. *Mol. Cell* **2000**, *6*, 743.

(28) Waksman, G.; Herr, A. B. *Nat. Struct. Biol.* **1998**, *5*, 527.

(29) Brown, A.; Robinson, C. J.; Gallagher, J. T.; Blundell, T. L. *Biophys. J.***2013**, *104*, 1720.

(30) Herr, A. B.; Ornitz, D. M.; Sasisekharan, R.; Venkataraman, G.; Waksman, G. *J.Biol. Chem.* **1997**, *272*, 16382.

(31) Kwan, C.-P.; Venkataraman, G.; Shriver, Z.; Raman, R.; Liu, D.; Qi, Y.; Varticovski, L.; Sasisekharan, R. *J. Biol. Chem.***2001**, *276*, 23421.

(32) Decker, C. G.; Wang, Y.; Paluck, S. J.; Shen, L.; Loo, J. A.; Levine, A. J.; Miller, L. S.; Maynard, H. D. *Biomaterials* **2016**, *81*, 157.

(33) Ornitz, D. M.; Yayon, A.; Flanagan, J. G.; Svahn, C. M.; Levi, E.; Leder, P. *Mol. Cell. Biol.***1992**, *12*, 240.

(34) Ishihara, M.; Ono, K. *Trends Glycosci. Glycotechnol.* **1998**, *10*, 223.

(35) Pantoliano, M. W.; Horlick, R. A.; Springer, B. A.; Vandyk, D. E.; Tobery, T.; Wetmore, D. R.; Lear, J. D.; Nahapetian, A. T.; Bradley, J. D.; Sisk, W. P. *Biochem.* **1994**, *33*, 10229.

(36) Bishop, E. T.; Bell, G. T.; Bloor, S.; Broom, I. J.; Hendry, N. F.; Wheatley, D. N. *Angiogenesis* **1999**, *3*, 335.

(37) Hetheridge, C.; Mavria, G.; Mellor, H. *Biochem. Soc. Trans.* **2011**, *39*, 1597.

(38) DeLisser, H. M.; ChristofidouSolomidou, M.; Strieter, R. M.; Burdick, M. D.; Robinson, C. S.; Wexler, R. S.; Kerr, J. S.; Garlanda, C.; Merwin, J. R.; Madri, J. A.; Albelda, S. M. *Am. J. Pathol.* **1997**, *151*, 671.

(39) Lappi, D. A.; Matsunami, R.; Martineau, D.; Baird, A. *Anal. Biochem.* **1993**, *212*, 446.

(40) Kim, Y. G.; Ho, S. O.; Gassman, N. R.; Korlann, Y.; Landorf, E. V.; Collart, F. R.; Weiss, S. *Bioconjugate Chem.* **2008**, *19*, 786.

(41) Heredia, K. L.; Grover, G. N.; Tao, L.; Maynard, H. D. *Macromolecules* **2009**, *42*, 2360.

(42) Chen, R.; John, J.; Lavrentieva, A.; Mueller, S.; Tomala, M.; Zhao, Y.; Zweigerdt, R.; Beutel, S.; Hitzmann, B.; Kasper, C.; Martin, U.; Rinas, U.; Stahl, F.; Scheper, T. *Eng. Life Sci.* **2012**, *12*, 29.

(43) Ornitz, D. M.; Leder, P. *J. Biol. Chem.* **1992**, *267*, 16305.

Chapter 5

Degradable Oxime and Hydrazone Based PEG-Like Polymers

5.1 Introduction

Proteins are an important class of therapeutics and are used to treat a wide range of diseases, including haemophilia, Crohn's disease, Kawasaki's disease, and diabetes.[1,2] Of the top 200 pharmaceuticals by sales in 2014, 38% were protein therapeutics.[3] While proteins are very useful therapeutic agents, barriers to their further use include poor solubility, rapid excretion, short shelf life, proteolysis, and immunological instability.[4,5] Many of these factors decrease the efficacy of protein therapeutics on the market, and in some cases even prevent the treatments from gaining FDA approval. Incorporation of polymers into protein therapeutics is one way to overcome some of these barriers.

Polymers have been used for biomedical applications since the 1940s. One of the first examples of polymers in biomedicine was the use of poly(vinyl pyrrolidone) (PVP) in plasma expanders.[4] Other early uses include as materials for wound dressings or coatings to treat anemia.[6] Since the 1960s, polymers have been used for various biomedical applications, which include polymeric gels, micelles and nanoparticles, and protein-polymer conjugates (Figure 5-1).[7] Protein-polymer conjugation, or the covalent attachment of a polymer to a protein, has been shown to improve the efficacy of proteins for use as therapeutics. The most widely used polymer used in these conjugates is poly(ethylene glycol) (PEG), which is non-toxic, soluble in both aqueous and organic solvents, non-ionic, and is hydrophilic.

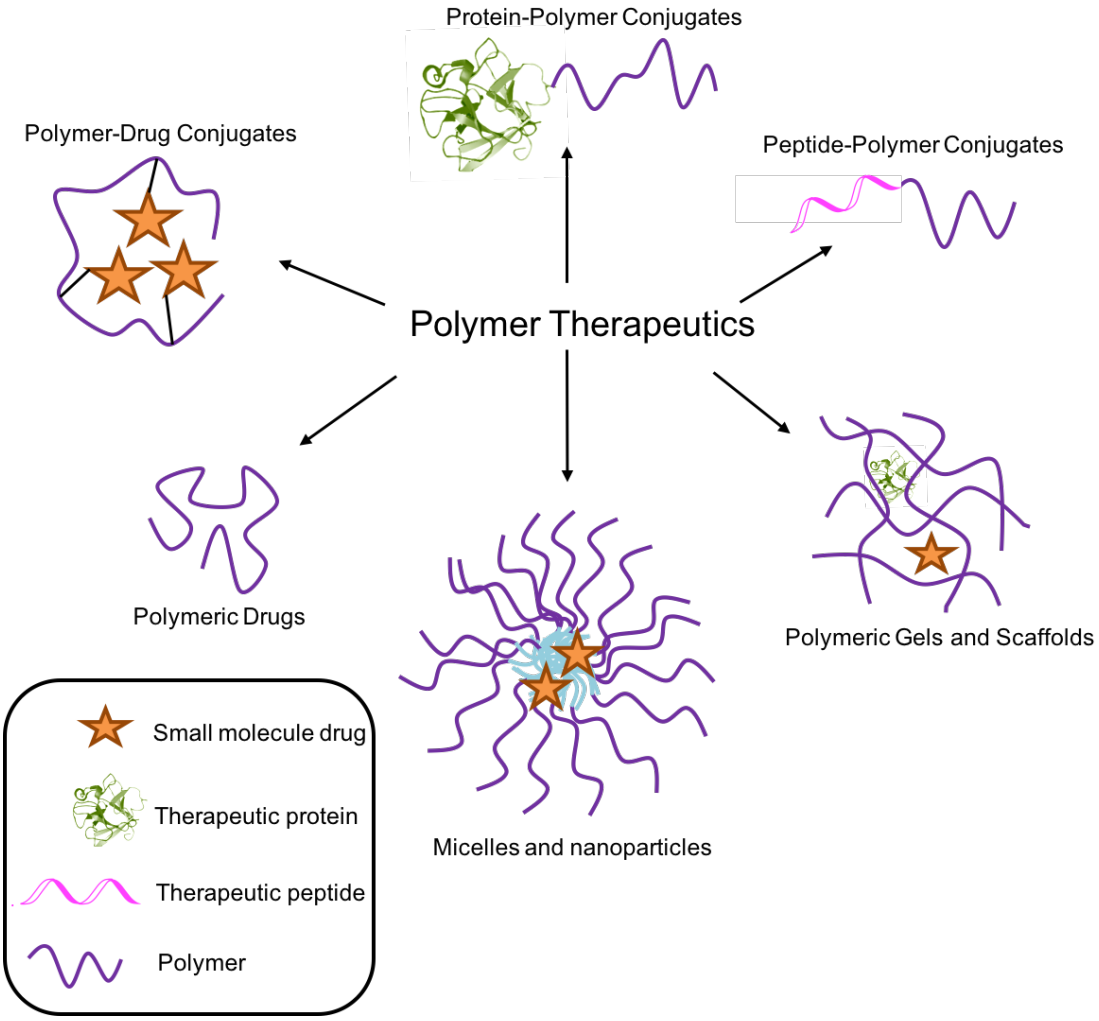

Figure 5-1. Incorporation of polymers in therapeutics

In the 1970s, Abuchowski and coworkers covalently attached PEG to bovine serum albumin (BSA), resulting in improved biological outcomes.[2] They found that covalently attaching PEG to the protein (termed PEGylation) greatly increased the hydrodynamic radius and solubility of the protein while decreasing the immunogenicity and blood clearance rate.[2,5,8-11] Importantly, PEGylated proteins decrease renal clearance and consequently reduce the frequency of drug administration and are thought to exhibit tumor-selective targeting due to the enhanced permeation and retention (EPR) effect.[12] Since this first report, many proteins have been

PEGylated and FDA-approved for clinical use, beginning with Adagen®, which was distributed on the market in 1990 to treat adenosine deaminase deficiency.[1,13] The number of FDA approved PEGylated proteins has since increased to 10.[14]

While PEGylation has greatly improved the outlook for protein therapeutics, the current strategy suffers from decreased activity of the conjugates as well as polymer buildup in the kidneys and liver due to the non-degradability of the polymer. The attachment of large polymers to the proteins can decrease the activity by blocking active or regulatory sites through steric crowding.[15] Reversible PEGylation is one solution to overcome the issue of decreased bioactivity. This method uses degradable linkages to conjugate the polymer to the protein. Under certain stimuli, such as pH, heat, or light changes, the polymer is released from the protein. When the polymer is released it leaves behind either native protein or protein with a small tag. If no tag is left behind the native protein is restored.[16,17] PEG-Intron, used to treat hepatitis C, was the first PEGylated protein on the market to use reversible PEGylation.[18,19]

Although reversible PEGylation mitigates attenuated bioactivity, it does not alleviate the issue of polymer accumulation in the kidneys. Larger PEGs tend to form protein-polymer conjugates with better pharmacokinetic properties, however, due to its non-degradable nature, PEG has been shown to persist *in vivo*, eventually causing the formation of vacuoles in the kidneys.[20,21] Additionally, patients treated with therapies incorporating PEG have shown development of antibodies, resulting in faster protein clearance and unwanted immunological response.[22,23] Polymers with degradable linkages throughout the backbone could provide a way to overcome this downfall. Covalently attaching degradable and/or reversible PEG-like polymers to proteins would provide the benefits of PEGylation while maintaining the native bioactivity and preventing unwanted polymer accumulation. Since PEG is not biodegradable, the

accumulated polymer may cause problems. Because of this, there is a molecular weight threshold allowed for PEGylated proteins, with current FDA approved therapeutics incorporating PEGs ranging from 5-40 kDa.[24] Thus, there is a strong driving force to developing degradable alternatives.

Degradable linkages that have been installed in the PEG polymer backbone include oximes,[25] polyesters,[26] disulfides,[27] acetals,[28] and vinyl ethers.[29] In this chapter we report the incorporation of hydrolyzable bonds such as oxime and hydrazone as degradable linkages within a PEG polymer. Both oxime and hydrazone bonds are degradable under acidic conditions as shown in Scheme 5.1. Herein we describe the functionalization of linear homo-bifunctional PEGs and their step-growth polymerization, as well as some preliminary degradation studies.

5.2 Results and Discussion

5.2.1 Synthesis of Monomers for Oxime and Hydrazone Polymers

This chapter focuses on the use of degradable oxime and hydrazone bonds as degradable linkages in PEG-like polymer backbones. Formation of oxime and hydrazone bonds was achieved by reacting an aldehyde/ketone carbonyl with aminooxy or hydrazide functionalities, respectively (Scheme 5-1).[13] Similar oxime and hydrazone chemistry was previously reported by Matthew Francis and coworkers for use in protein modification.[30] One advantage of hydrazones over oximes and other degradable systems is that they are known to be biocompatible and their degradation occurs at a biologically relevant time scale. Another advantage of hydrazones is that they are degradable under physiologically relevant conditions, whereas oximes require a more acidic environment to degrade on an appropriate time scale.[30] Two molecular weights of PEG

were bis-modified with either aldehyde or aminooxy groups, and the resulting homo-bifunctional monomers were mixed to form polymers containing oximes.

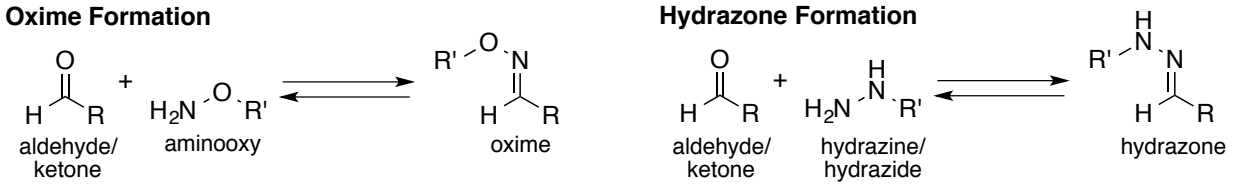

Scheme 5-1. Reversible formation of oxime and hydrazone bonds

Triethylene glycol-aminooxy (TEG-AO) was synthesized by a Mitsunobu reaction on the hydroxyl group of TEG with N-hydroxyphthalimide to yield TEG-phthalimide **1** (Scheme 5-2a), which was subsequently deprotected with hydrazine hydrate to obtain TEG-AO **2** (Scheme 5-2b). The deprotection of TEG-phthalimide to yield TEG-AO was verified by the disappearance of phthalimide proton and carbon peaks in ^{1}H NMR and ^{13}C NMR, respectively. The identity of the compound was further verified via ESI-MS and IR spectroscopy. Additionally, a larger molecular weight monomer was prepared by using 2 kDa PEG, resulting in PEG-AO **8**.

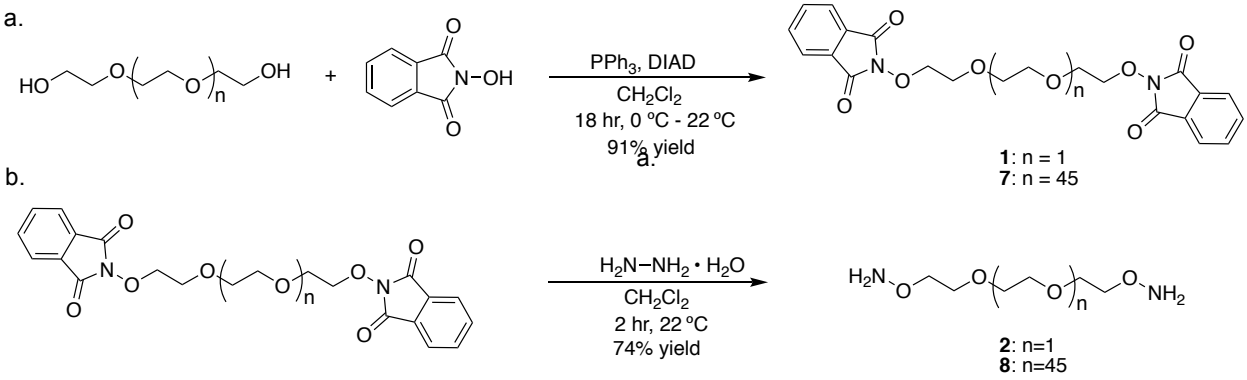

Scheme 5-2. Synthesis of monomers for degradable PEG. (a) Synthesis of TEG-phthalimide, **2**, and PEG-phthalimide, **7**, by Mitsunobu reaction. (b) Deprotection to yield and TEG-aminooxy, 2, and PEG-aminooxy **8.**

To synthesize the dialdehyde monomer **3**, various conditions were attempted. First, a PCC oxidation was attempted, but it resulted in over-oxidation to the undesired bis(carboxylic acid) (Scheme 5-3a). Next, a Pfitzner-Moffatt oxidation was performed, which resulted in formation of aldehyde **3** (Scheme 5-3b); however, purification of the product proved difficult. Silica and neutral alumina column chromatography, distillation, recrystallization, and precipitation were attempted, but the product was not successfully purified.

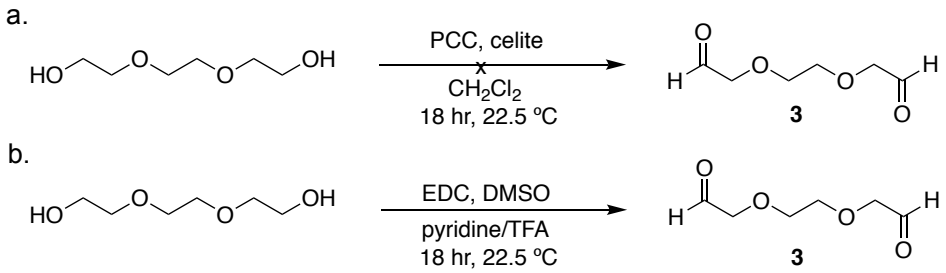

Scheme 5-3. Attempted syntheses of TEG-aldehyde via (a) PCC oxidation (b) and Pfitzner-Moffatt.

Finally, a protected aldehyde approach was utilized to obtain the dialdehyde monomer. TEG-acetal **4** was synthesized in 44% yield and was verified through ^{1}H NMR, ^{13}C NMR and ESI-mass spectrometry (Scheme 5-4a). The aldehyde was deprotected in acidic conditions to yield the aldehyde (Scheme 5-4b). The low yield of the acetal was due to the difficulty in chromatographic purification caused by the tendency of TEG to stick to silica or alumina. However, this route using a protected aldehyde allowed for larger quantities to be synthesized and stored before use, as the unprotected aldehyde is prone to degradation upon storage. Furthermore, deprotection could be performed *in situ* during the polymerization.

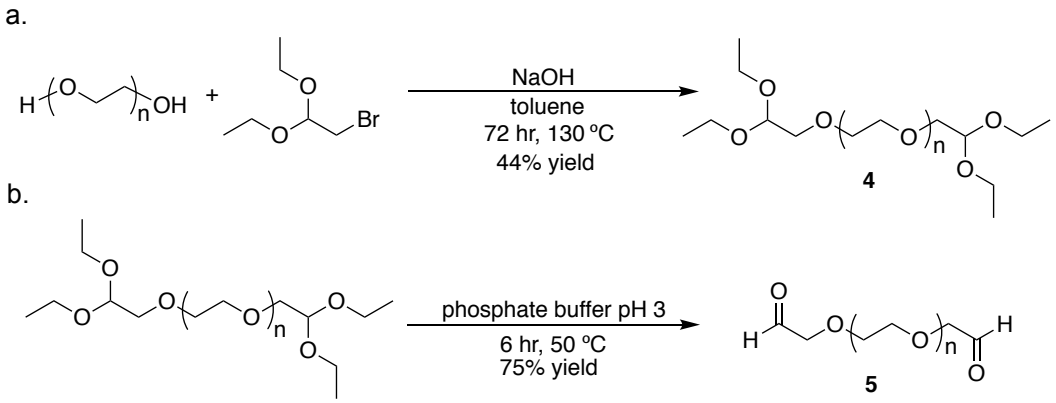

Scheme 5-4. Synthesis of (a) TEG-acetal, **4**, and (b) deprotection to yield TEG-aldehyde, **5**

5.2.2 Step-Growth Polymerization of Oxime and Hydrazone Polymers

Due to the low yield of TEG aldehyde (33% over two steps), commercially available diketone, diacetyl, was used in its place. Diacetyl was chosen due to its widespread use in butter flavorings for popcorn, and therefore is currently used for human consumption. Polymerization of TEG-AO **2** and diacetyl was performed using an acid catalyst under vacuum to remove water from the oxime condensation (Scheme 5-5). A solid yellow polymer **6** formed after one hour. Unlike PEG, the polymer was insoluble in H_2O and also in most organic solvents including DMF, DMSO, chloroform, and methanol; however, it was soluble in dichloromethane.

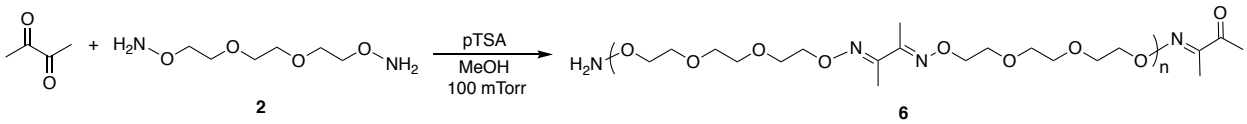

Scheme 5-5. Synthesis of oxime polymer **6** from TEG-aminooxy **2** and diacetyl

To analyze the polymer, the ^{1}H NMR and IR spectra of TEG-AO **2** (red), diacetyl (blue), and the oxime polymer **6** (black) were compared to confirm the complete consumption of the aminooxy units into oxime (Figure 5-2). In the ^{1}H NMR spectra there is a clear downfield shift in the ether protons **a** and **b** in the oxime polymer. In the IR spectra the disappearance of the N-H

stretch (aminooxy) at 3309 cm^{-1} and the appearance of C=N absorption (oxime) at 1693 cm^{-1} were observed for the polymer (Figure 5-2).

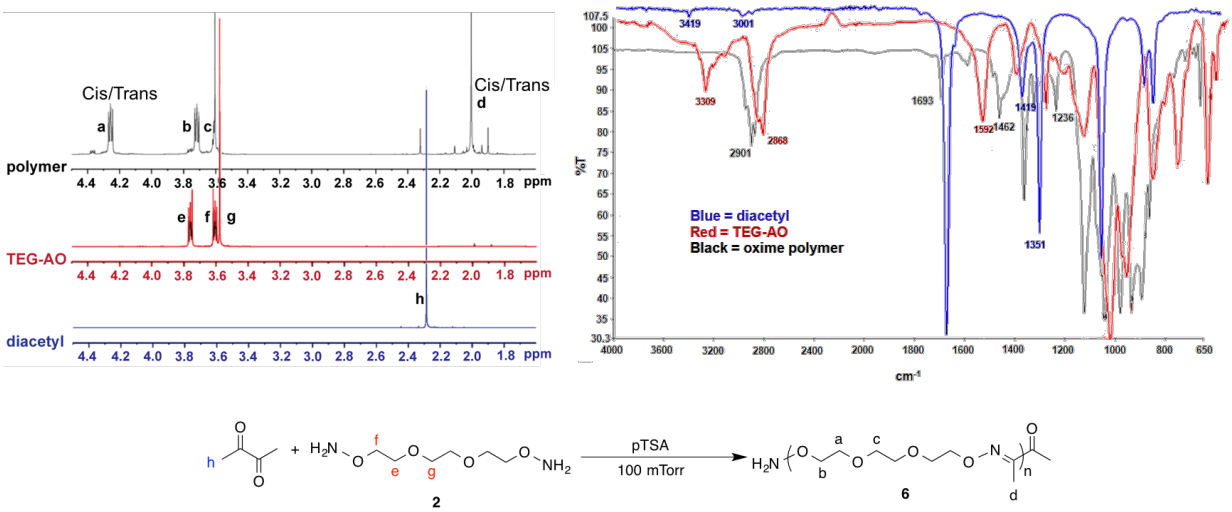

Figure 5-2. [1]HNMR and IR data for the synthesis of oxime polymer, **6**

Due to the insolubility of the polymer, molecular weight was not obtained by gel permeation chromatography (GPC). The data suggested that the limited number of ethylene oxide units between oxime bonds was insufficient for water solubility. To incorporate larger hydrophilic ethylene oxide segments, larger linear PEG with number-average molecular weight (M_n) of 2 kDa was functionalized for use as the monomer unit. The use of larger PEGs also allowed for easier purification through precipitations and dialysis rather than silica/alumina columns, resulting in higher yields.

Linear PEG (2 kDa) was modified with aminooxy and hydrazine functionalities for oxime- and hydrazone-linked polymers, respectively. For oxime polymers, PEG-AO **8** was synthesized from 2 kDa linear PEG using the Mitsunobu conditions previously used for TEG (Scheme 5-2) in 89% yield with 99% end group conversion. For hydrazone polymers, PEG-

hydrazide **9** was synthesized through functionalization of 2 kDa COOH-PEG-COOH with adipic acid dihydrazide (Scheme 5-6). The degree of PEG functionalization was determined to be 98% using ^{1}H NMR end group analysis and the functionalized polymer was obtained in 95% yield.

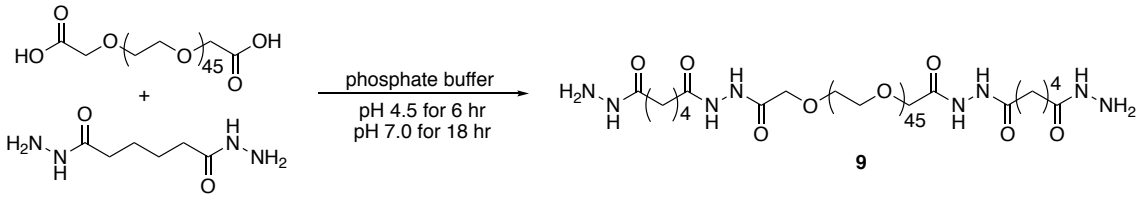

Scheme 5-6. Synthesis of PEG-dihydrazide **9**

Step-growth polymerizations of both oxime and hydrazone linked polymers were performed in aqueous acidic conditions. PEG-AO or PEG-hydrazide were polymerized with diacetyl to form oxime polymer **10** and hydrazone polymer **11**, respectively (Scheme 5-7a and 5-7b). GPC traces of the polymers were multimodal. Additionally, the polymers were poorly soluble in water. However, they were soluble in organic solvents such as DMF, DCM, and chloroform, allowing for GPC analysis. It is possible that the poor water solubility of the polymer resulted in low molecular weight since the polymerization was undertaken in water.

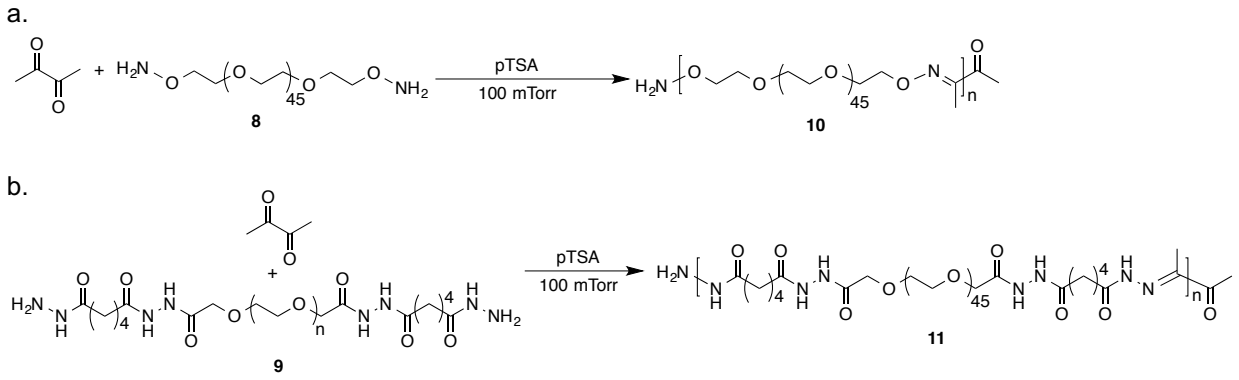

Scheme 5-7. Step-growth polymerization of (a) oxime polymer **10** and (b) hydrazone polymer **11**

To further improve the solubility of the polymers, the dialdehyde glyoxal was used in the place of diacetyl. It was hypothesized that the methyl groups on diacetyl were contributing to the poor solubility in water, and thus the absence of the methyl groups on glyoxal would improve water solubility of the polymers. Polymerizations were performed following previous literature procedures in water using aniline as a catalyst.[25] Oxime polymers were synthesized with glyoxal using TEG-AO to yield polymer **12** and PEG-AO to yield polymer **13** (Scheme 5-8a). Molecular weights of oxime polymers were determined by DMF GPC as 5.9 kDa ($Đ$ = 2.39) when polymerized with the TEG monomer and 2.8 kDa ($Đ$ = 1.05) when polymerized with the PEG monomer. The molecular weight of PEG-AO was also determined by DMF GPC to be 1.3 kDa. Additionally, glyoxal was polymerized with PEG-hydrazide (Scheme 5.8b) to yield hydrazone polymer **14** with a molecular weight of 4.5 kDa ($Đ$ = 1.45). Hydrazone polymer **14** was soluble in water whereas oxime polymers **13** was sparingly soluble in water and oxime polymer **12** was insoluble in water.

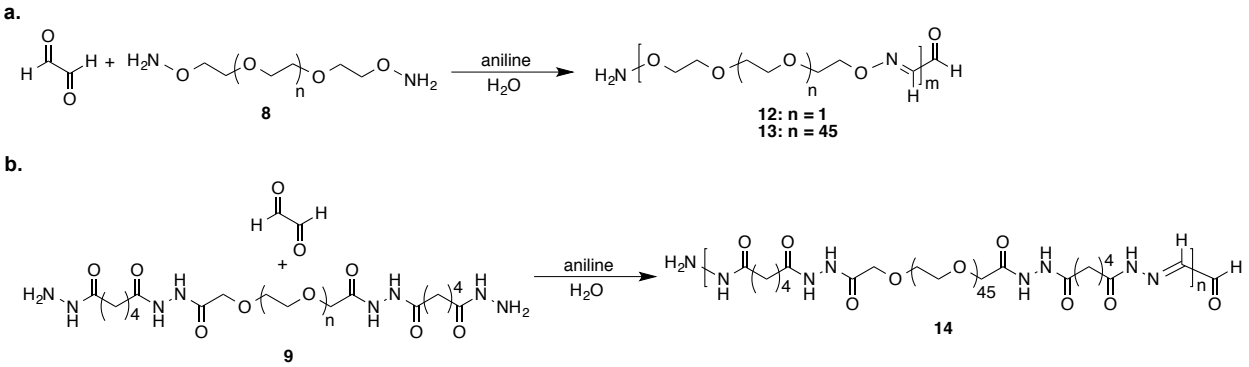

Scheme 5-8. Step-growth polymerization to synthesize oxime polymer (a) using TEG-AO or PEG-AO monomers to yield polymers **12** and **13**, respectively, and (b) synthesis of hydrazone polymer **14**

Due to the nature of step-growth polymerization, very high conversion is needed to obtain high molecular weights. Therefore, even small amounts of impurity can significantly

inhibit polymerization and reduce polymer molecular weight. In order to increase polymer molecular weight, monomers could be purified very carefully. PEG monomers could be resubjected for more complete functionalization, resulting in monomers with close to 100% functionality, resulting in less chain ending due to mono-functionalized monomers.

5.2.3 Degradation Study of Polymers

The glyoxal based polymers were used in degradation studies to determine whether the polymers could degrade in various types of media. Polymers tested included TEG-oxime (**12)**, PEG-oxime (**13**), and PEG-hydrazone (**14**). Polymer solutions were prepared in Eppendorf tubes at a concentration of 1 mg/mL in DPBS, phosphate buffer pH 6, or serum-free cell culture medium. The tubes were placed in an incubator set to 37 ºC with 5% CO_2 for twelve months. Typically, oximes do not degrade at neutral pH, but because the oxime was formed with the aldehyde glyoxal, they likelihood of degradation is greater over long time periods. After twelve months the polymers were removed and evaluated for solubility. The majority of samples had degraded or dissolved, with only the TEG-oxime polymer remaining insoluble.

Table 5-1. Degradation results comparing GPC of polymers in degradation study to polymers before degradation study

Polymer	PB pH 6	DPBS	Culture Media
PEG-oxime (**13**)	Mostly degrades	Mostly degrades	Does not degrade
TEG-oxime (**12**)	Does not degrade	Does not degrade	Does not degrade
PEG hydrazone (**14**)	Degrades	Degrades	Degrades

To evaluate whether any degradation occurred over this twelve-month period, the polymers were extracted into dichloromethane. The solvent was evaporated and the M_n of the resulting material was evaluated by DMF GPC. Polymers exposed to the degradation conditions were compared to both the monomer and the original polymer. Degradation results are shown in Table 5-1. The PEG-hydrazone polymer (14) exhibited the fastest degradation, reverting completely back to monomer in all buffers tested (Figure 5-3a). PEG-oxime polymer (13) showed degradation, though not completely back to the monomer (Figure 5-3b). TEG-oxime polymers were not sufficiently soluble to yield a GPC trace. It is suspected that the oxime-based polymers did not exhibit complete degradation due to the slower degradation rate and the need for more acidic buffer when compared to hydrazone polymers.

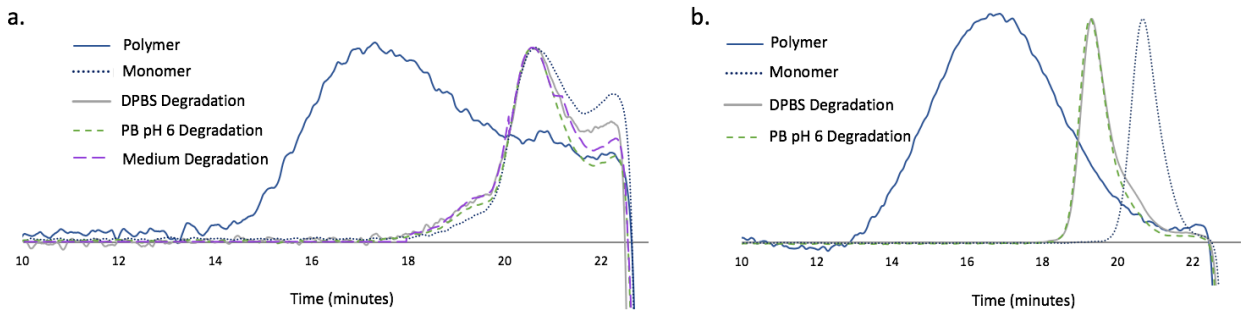

Figure 5-3. GPC traces showing the degradation of (a) PEG-hydrazone polymer 14 in DPBS, PB at pH 6, and serum free cell culture medium and (b) PEG-oxime polymer 13 in DPBS and PB at pH 6 after 12 months.

Since the polymers are expected to degrade in the body, it is important that the monomers and degradation by-products are not cytotoxic. For cytotoxicity studies, PEG-dialdehyde and PEG-dihydrazide (9) were incubated with 3T3-fibroblasts and human dermal fibroblasts (HDFs) for 24 hours. Neither monomer exhibited cytotoxic effects up to 1 mg/mL (Figure 5-4).

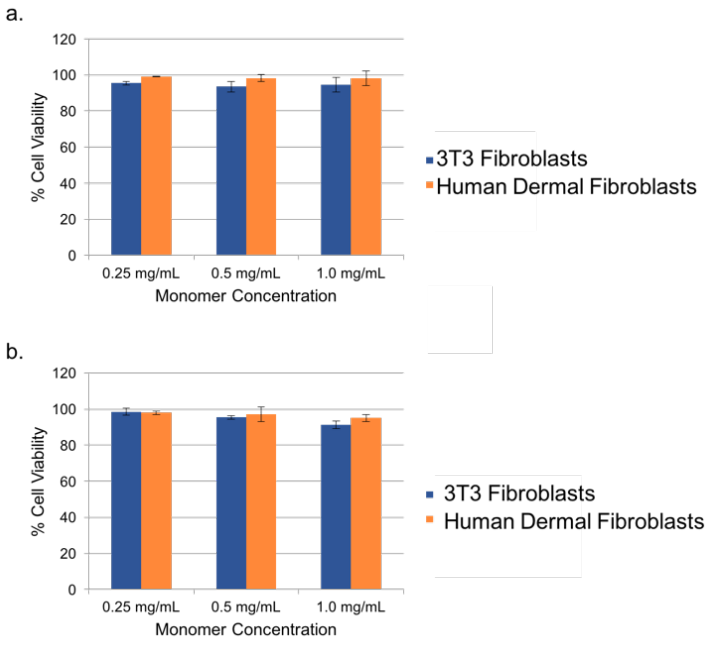

Figure 5-4. Cell viability assay performed on both 3T3 fibroblasts and human dermal fibroblasts for both (a) PEG-AO monomers and (b) PEG-hydrazine monomers. The experiment contained 6 replicates per sample. Error bars represent standard deviation.

5.3 Conclusion and Future Directions

TEG and PEG were functionalized with aminooxy and hydrazide functional groups for use in step-growth polymerizations to form PEG-like polymers with degradable linkages. While ethylene glycols with fewer ethylene oxide units, such as TEG, would degrade into smaller molecular weight fragments, these polymers exhibited poor solubility in most solvents. Therefore, low molecular-weight PEGs (M_n = 2 kDa) were used as polymer building blocks instead. Step-growth polymerization resulted in polymers with relatively low molecular weights (2-7 monomer repeats). Initial degradation studies showed complete degradation of polymers containing hydrazone bonds throughout the backbone. Oxime based polymers showed some

degradation at acidic pH, but did not completely degrade back to the monomer units. Polymers with TEG and oxime units did not degrade likely due to insolubility in water. Additionally, cytotoxicity studies were performed to prove that the monomers are not cytotoxic to fibroblasts up to 1 mg/mL. In the future, higher molecular weight polymers could be synthesized by attaining higher conversion during the polymerization, by in turn obtaining higher end group functionalization. These biodegradable polymers could be covalently conjugated to proteins to obtain protein-polymer conjugates with degradable PEGs, thus making them an attractive option for future protein drugs.

5.4 Experimental

5.4.1 Materials

Chemicals and reagents were purchased from Sigma-Aldrich and used as received unless otherwise indicated. Silica gel column chromatography was performed using Merck 60 (230-400 mesh) silica gel. Normal human dermal fibroblasts were purchased from ATCC. 3T3 Fibroblasts were purchased from PromoCell. Cell medium was purchased from ATCC or Invitrogen unless indicated otherwise. Cell Viability Assay kit was purchased from Promega. Near-monodisperse PEG standards for GPC calibration were purchased from Polymer Laboratories.

5.4.2 Analytical Techniques

^{1}H NMR and ^{13}C NMR spectroscopy was performed on an Avance DRX 400 instrument. Dimethylformamdide (DMF) GPC was conducted in DMF containing 0.10 M LiBr (40 °C, 0.6 mL/min) on a Shimadzu HPLC system equipped with a refractive index detector RID-10A, one Polymer Laboratories PLgel guard column, and two Polymer Laboratories PLgel 5 μm mixed D columns. Calibration was performed using near-monodisperse poly(ethylene glycol) standards from Polymer Laboratories. Chromatograms were processed using the EZStart 7.2

chromatography software. Cell images for cell viability/cytotoxicity were taken on an Axiovert 200 microscope equipped with an AxioCam MRm camera and FluoArc mercury lamp (Carl Zeiss, Thornwood). NIH ImageJ software was used to assist cell counting.

5.4.3 Methods

TEG-phthalimide **(1).** To a flame dried 2-neck round bottom flask, 2.09 g (7.96 mmol) of triphenylphosphine was added and dissolved in 15 mL of dry dichloromethane. After all of the triphenylphosphine was dissolved, 1.30 g (7.96 mmol) of N-hydroxyphthalimide was added followed by 0.50 mL (3.32 mmol) of triethylene glycol. The round bottom flask was placed in an ice bath and let stir for 30 minutes until the reaction mixture reached 0 ^{o}C. While stirring in the ice bath, 1.44 mL (7.30 mmol) of diisopropyl azodicarboxylate (DIAD) was added dropwise over 30 minutes. As the DIAD was added, the color of the reaction mixture went from clear-colorless to dark red. The reaction mixture was let warm to room temperature and stirred under argon for 18 hours, after which the color turned colorless to pale-yellow. To quench the reaction, 20 mL of EtOH was added and the dichloromethane was removed in vacuo. The residue was dissolved in 1:1 hexane:ethyl acetate and stirred for one hour. A white solid precipitated in a yellow liquid. The white solid was filtered and any excess solvent was removed in vacuo to give 2.67 g (91%) of product as a white solid. ^{1}H NMR (400 MHz, $CDCl_3$) δ: 7.85 (d, 4H), 7.70 (d, 4H), 4.30 (d, 4H), 3.80 (d, 4H), 3.60 (s, 4H). ^{13}C NMR (400 MHz, $CDCl_3$) δ: 163, 135, 129, 121, 72, 68. FT-IR(cm^{-1}): 2886, 1780, 1732, 1605, 1464, 1373, 1185, 1112, 1077, 1021, 976, 877.

PEG-phthalimide **(7)**. ^{1}H NMR (400 MHz, $CDCl_3$) δ: 7.70-7.74 (m, 4H), 7.79-7.83 (m, 4H), 4.31-4.38 (t, 4H), 2.29-2.34 (t, 4H), 3.45-3.68 (m, 178H). ^{13}C NMR (400 MHz, $CDCl_3$) δ:

163.23, 134.58, 128.98, 123.34, 70.25. FT-IR(cm^{-1}): 2883, 1790, 1732, 1467, 1360, 1342, 1280, 1241, 1188, 1147, 1101, 1061, 962, 878, 842, 702.

TEG-Aminooxy **(2)**. TEG-phthalimide (1.0 g, 2.27 mmol) was added to a clean, dry 1-neck round bottom flask and was dissolved in 10 mL of dichloromethane. Next, 3.15 mL (22.11 mmol) of hydrazine hydrate (35% in water) was added and the clear, colorless reaction was let stir at room temperature for 3 hours. After 3 hours, a white solid formed and was filtered off. The filtrate was evaporated to dryness *in vacuo* to give 0.3021 g of product as a colorless oil 74% yield. ^{1}H NMR (400 MHz, $CDCl_3$) δ: 4.8-6.1 (s, 4H), 3.8 (d, 4H), 4.30 (d, 4H), 3.60 (d, 8H). FT-IR (cm^{-1}): 3309, 2868, 1592, 1460, 1348, 1282, 1203, 1102, 1040, 940, 845, 730, 699. HRMS-ESI (expected, observed): (180.11, 181.24).

TEG-acetal **(4)**. Powdered NaOH (0.39 g, 9.67 mmol) was added to a flame dried 2-neck round bottom flask under argon followed by 0.27 mL (4.84 mmol) of ethylene glycol. Next, 1.48 mL (9.67 mmol) of bromoacetaldehyde diethyl acetal was added. The reaction mixture was light brown and some of the solid dissolved was not completely dissolved. The mixture was refluxed at 115°C under argon. After 72 hours, the reaction mixture was cooled to room temperature and diluted with 50 mL of water. The crude product was extracted 3 times with dichloromethane (50 mL). The combined organic layers were dried over $MgSO_4$, filtered, and concentrated. The yellow oil was run through a neutral alumina column with dichloromethane as the eluent. The product was collected and the solvent was evaporated in vacuo. An alumina column was run in $CHCl_3$ to give 1.5 g (44% yield) of a yellow oil as product. ^{1}HNMR (400 MHz, $CDCl_3$) δ: 4.6 (t, 2H), 3.65-3.74 (qd, 4H), 3.35 (s, 4H), 3.54-3.61 (qd, 4H), 3.52-3.54 (d, 4H), 1.18-1.24 (t, 12). ^{13}CNMR (400 MHz, $CDCl_3$) δ: 102, 74, 72, 63, 15. FT-IR (cm^{-1}): 2886, 1780, 1732, 1605, 1464, 1373, 1185, 1112, 1077, 1021, 976, 877. HRMS-ESI (expected, observed): (317.20, 318.19).

PEG-Aminooxy (**8**). PEG-phthalimide (1.0 g, 0.5 mmol) was added to a clean, dry 1-neck round bottom flask and was dissolved in 10 mL of dichloromethane. Next, 1.6 mL (11.05 mmol) of hydrazine hydrate (35% in water) was added and the clear, colorless reaction was let stir at room temperature for 3 hours. After 3 hours, a white solid formed and was filtered off. The filtrate was evaporated to dryness *in vacuo* to give a white powder with 100% conversion to the aminooxy. ^{1}H NMR (400 MHz, $CDCl_3$) δ: 3.30-3.80 (m, 182H), 1.70-2.00 (br s, 4H). ^{13}C NMR (400 MHz, $CDCl_3$) δ: 71.50. FT-IR (cm^{-1}): 496, 2884, 1467, 1360, 1341, 1280, 1241, 1147, 1099, 1061, 961, 842.

Representative Syntheses Oxime Polymers with diacetyl **(6, 10)**: TEG-aminooxy (100 mg, 0.55 mmol) and diacetyl (48.25 μL, 0.55 mmol) were added to a Schlenk tube along with 0.5 mL of 5% *p*-toluene sulfonic acid (PTSA) in MeOH. Vacuum was pulled and the reaction mixture was stirred under vacuum for 20 hours. After one hour a light yellow solid formed. The reaction product was a hard, yellow solid. ^{1}HNMR (400 MHz, CD_2Cl_2) δ: 4.24-4.27 (t, 30H), 3.71-3.73 (t, 30H), 3.60 (s, 30H), 2.32 (s, 3H) 1.90 (s, 3H). FTIR (cm^{-1}) 2901, 2875, 1693, 1588, 1462, 1362, 1323, 1236, 1123, 1041, 981, 936, 895, 864.

PEG-Aminooxy (**8**). PEG-phthalimide (1.0 g, 0.5 mmol) was added to a clean, dry 1-neck round bottom flask and was dissolved in 10 mL of dichloromethane. Next, 1.6 mL (11.05 mmol) of hydrazine hydrate (35% in water) was added and the clear, colorless reaction was let stir at room temperature for 3 hours. After 3 hours, a white solid formed and was filtered off. The filtrate was evaporated to dryness *in vacuo* to give a white powder with 99% conversion and 89% yield to the aminooxy. ^{1}H NMR (400 MHz, $CDCl_3$) δ: 3.30-3.80 (m, 182H), 1.70-2.00 (br s, 4H). ^{13}C NMR (400 MHz, $CDCl_3$) δ: 71.50. FT-IR (cm^{-1}): 496, 2884, 1467, 1360, 1341, 1280, 1241,

1147, 1099, 1061, 961, 842.

PEG-dihydrazide (**9**). To a round bottom flask, 100 mg (0.049 mmol) of COOH-PEG(2K)-COOH was added and dissolved in 3 mL of phosphate buffer at pH 6. Next, 679.8 mg (3.90 mmol) of adipic acid dihydrazide was dissolved in 2 mL of the phosphate buffer and added to the reaction mixture. Finally, 378.6 mg (2.44 mmol) of EDC was added to the reaction mixture in one portion. The pH value of the reaction was lowered to pH 4 by adding aqueous HCl dropwise. The reaction mixture was let stir for 18 hours at room temperature. The pH was controlled periodically throughout the reaction and adjusted to pH 4 as needed. After 18 hours the reaction was neutralized with aqueous NaOH. For purification, the product was dialyzed against 50:50 H_2O:MeOH for 72 hours. The dialysis solution was slowly increased to 100% H_2O over 48 hours. The product was lyophilized to give a white powder in 95% yield and 98% conversion. ^{1}HNMR (400 MHz, CD_2Cl_2) δ: 4.11-4.13 (s, 4H), 3.55-3.86 (s, 178H), 2.11-2.43 (10H). ^{13}CNMR (400 MHz, CD_2Cl_2) δ: 71.05. FTIR (cm^{-1}): 3237, 2885, 1667, 1469, 1361, 1343, 1281, 1242, 1148, 1104, 1061, 963, 841

Hydrazone Polymer **(11)**: Diacetyl and PEG-dihydrazide (5 mg, 0.0025 mmol) were added to a Schlenk tube and dissolved in 100 μL of MeOH. Oxygen was removed from the reaction flask through freeze- pump-thaw cycles. The reaction was stirred for 18 hours. After 18 hours, the reaction was lyophilized to dryness. The GPC in DMF was multimodal with three distinct peaks showing M_n of 14 kDa, 8.8 kDa and 4.3 kDa.

Oxime Polymer **(12)**: TEG-AO (50 mg, 0.278 mmol) was dissolved in 200 μL of water and then glyoxal (31.74 μL, 0.278 mmol) a 40% aniline solution (10.14 μL, 0.111 mmol) were added.

Upon aniline addition the solution became very cloudy. The polymerization was stirred for 1 hour at 60 °C. After 1 hour there was a white solid precipitated on the edges of the reaction vessel. The polymer was put on the high vac to remove any solvents. The GPC in DMF showed M_n of 2.8 kDa with $Đ$ of 1.05. ^{1}HNMR (400 MHz, CD_2Cl_2) δ: 8.28-8.30 (d, 1H), 7.76 (s, 2.5H), 7.70 (s, 0.4H), 4.27-4.31 (t, 10H) 3.73-3.76 (t, 10H), 3.65 (s, 10H).

Oxime Polymer (**13**): PEG-AO (107 mg, 0.0535 mmol) was dissolved in 175 μL of DMF and then glyoxal (6.11 μL, 0.0535 mmol) and aniline (1.95 μL, 0.0214 mmol) were added. The solution was placed on the thermoshaker at 60 °C at 1500 rpm. The polymerization was let stir for 16 hours. After 16 hours the solution was diluted with 5 mL of water and filtered through 3 kDa MWCO filter to remove DMF and any remaining aniline and glyoxal. The contents of the filter were washed 10 times with water at 12.6 rpm and then the remaining solution was lyophilized to dryness. The GPC in DMF showed M_n of 5.9 kDa with $Đ$ of 2.39. ^{1}HNMR (400 MHz, CD_2Cl_2) δ: 7.72 (s, 0.07H), 7.81 (s, 0.44H), 4.20-4.27 (m, 2H), 3.4-3.8 (m, 182H).

Hydrazone Polymer (**14**): PEG-hydrazide (100 mg, 0.0426 mmol) was dissolved in 200 μL of D_2O and then glyoxal (4.86 μL, 0.0426) and aniline (1.95 μL, 0.0214 mmol) were added. The polymerization was stirred for 16 hours at room temperature. The polymer was then purified by centriprep using a 3 kDa MWCO filter and was washed 10 times at 12.6 rpm with water. The resulting solution was lyophilized to dryness. The GPC in DMF showed M_n of 4.5 kDa with $Đ$ of 1.45. ^{1}HNMR (400 MHz, CD_2Cl_2) δ: 9.98-9.96 (d, 0.05H), 9.48-9.49 (d, 0.06H), 7.69-7.71 (s, 1H), 3.30-3.89 (s, 182H), 2.14-2.38 (s, 6H), 1.49-1.67 (s, 6H).

5.5 Appendix to Chapter 5 – Supplementary Figures

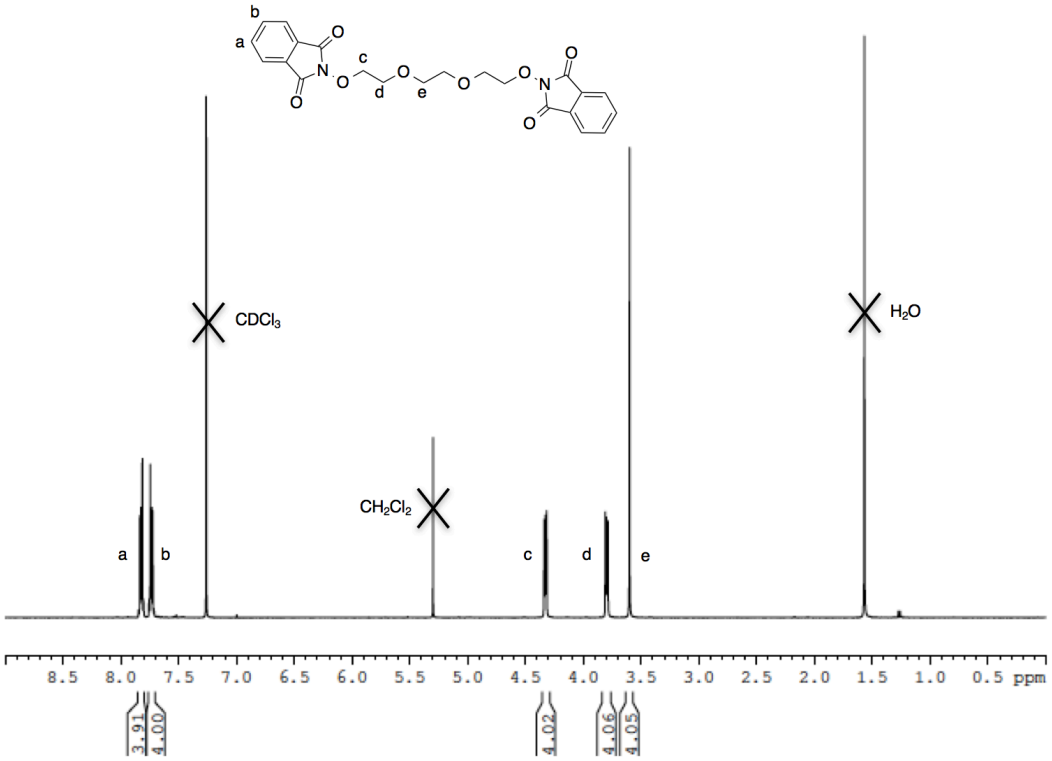

Figure 5-5. ^{1}H NMR (400 MHz, CD_2Cl_2) of TEG-phthalimide (**1**)

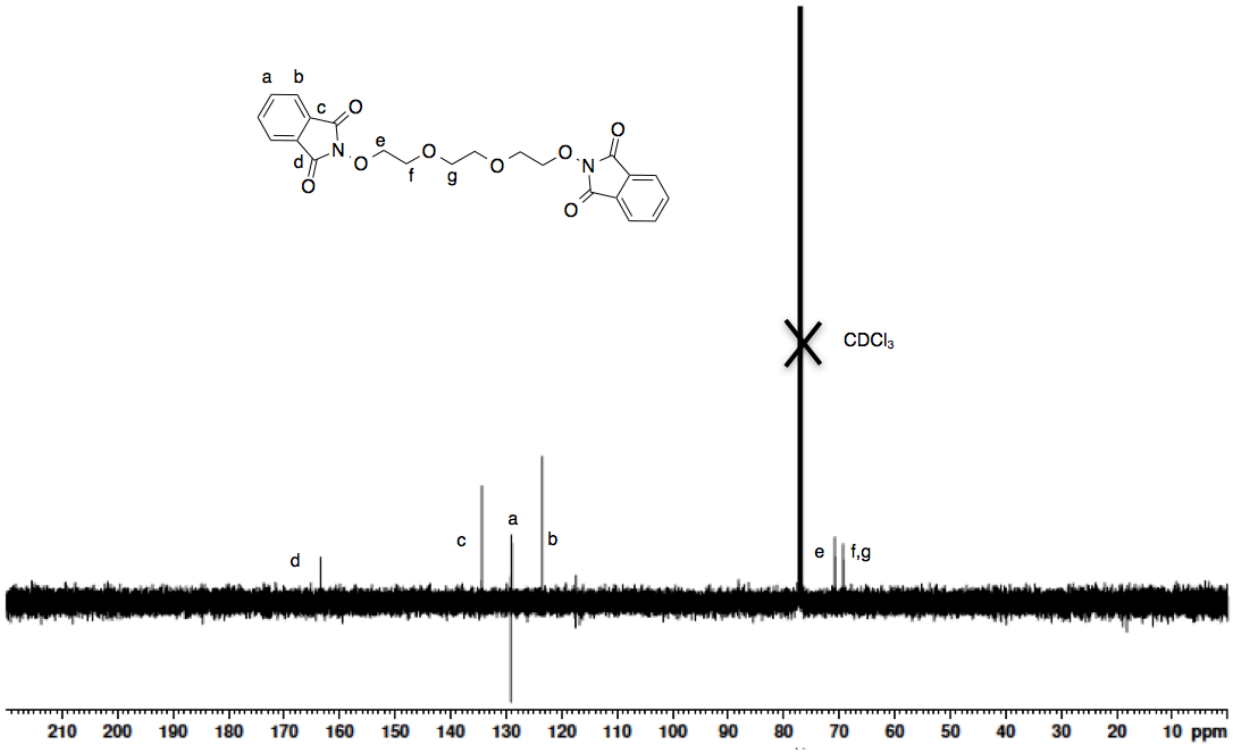

Figure 5-6. ^{13}C NMR (400 MHz, CD_2Cl_2) of TEG-phthalimide (**1**)

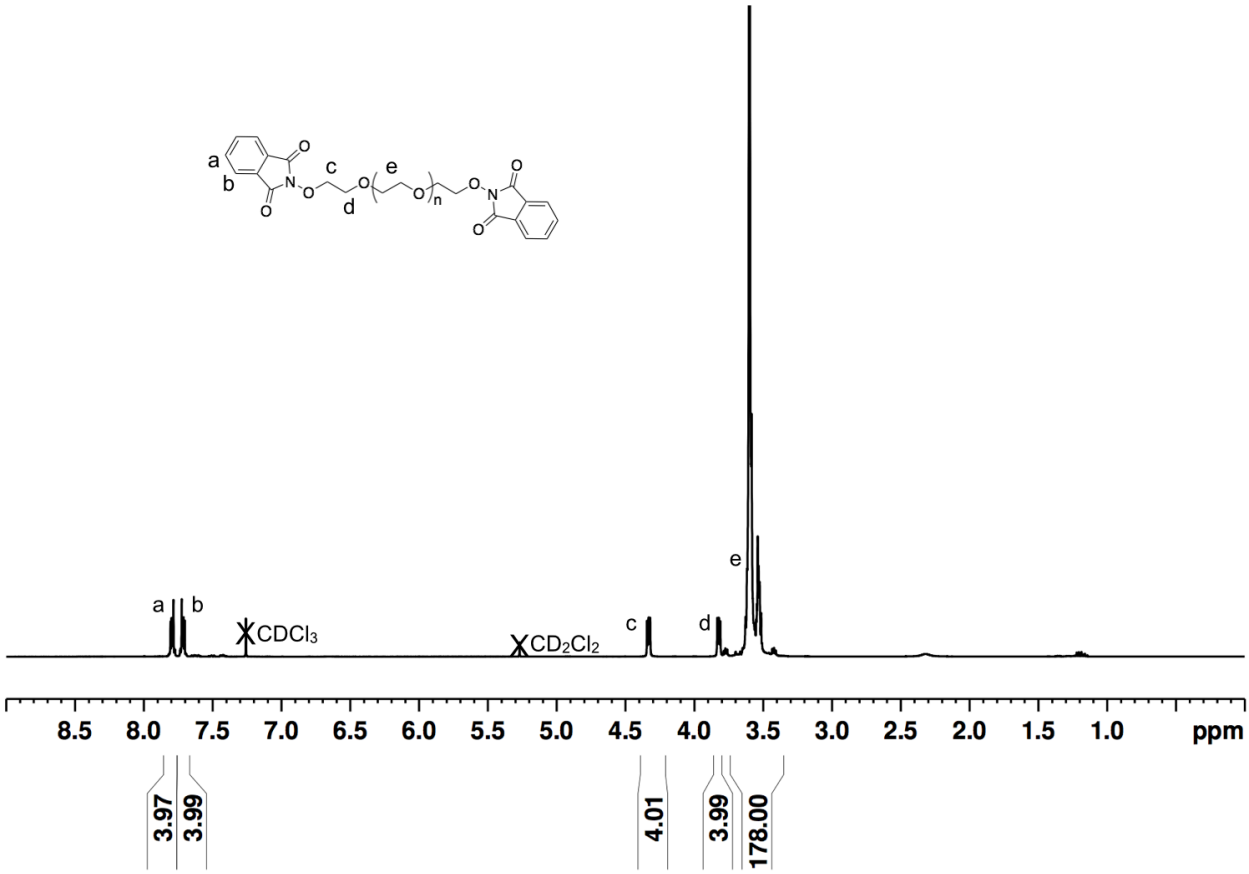

Figure 5-7. ^{1}H NMR (400 MHz, CD_2Cl_2) of PEG-phthalimide (**7**)

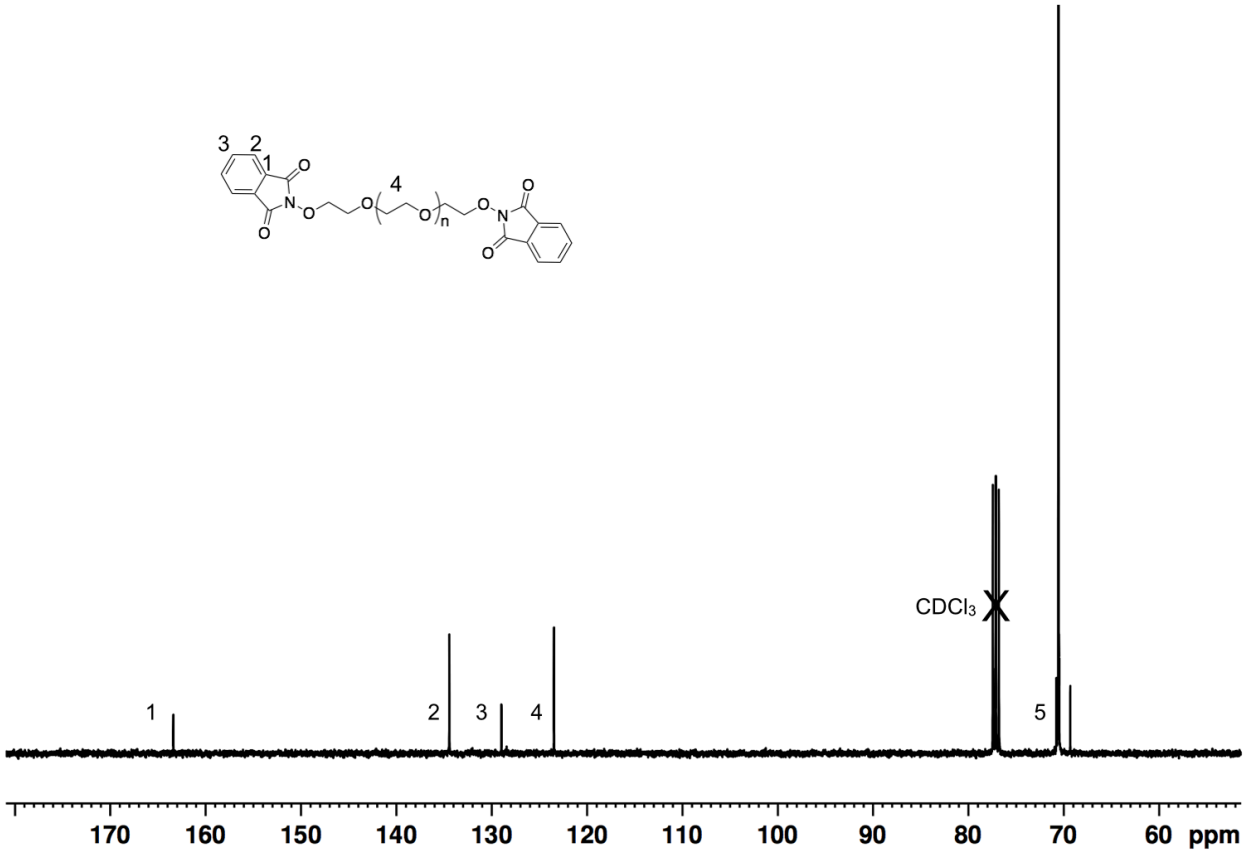

Figure 5-8. ^{13}C NMR (400 MHz, CD_2Cl_2) of PEG-phthalimide **(7)**

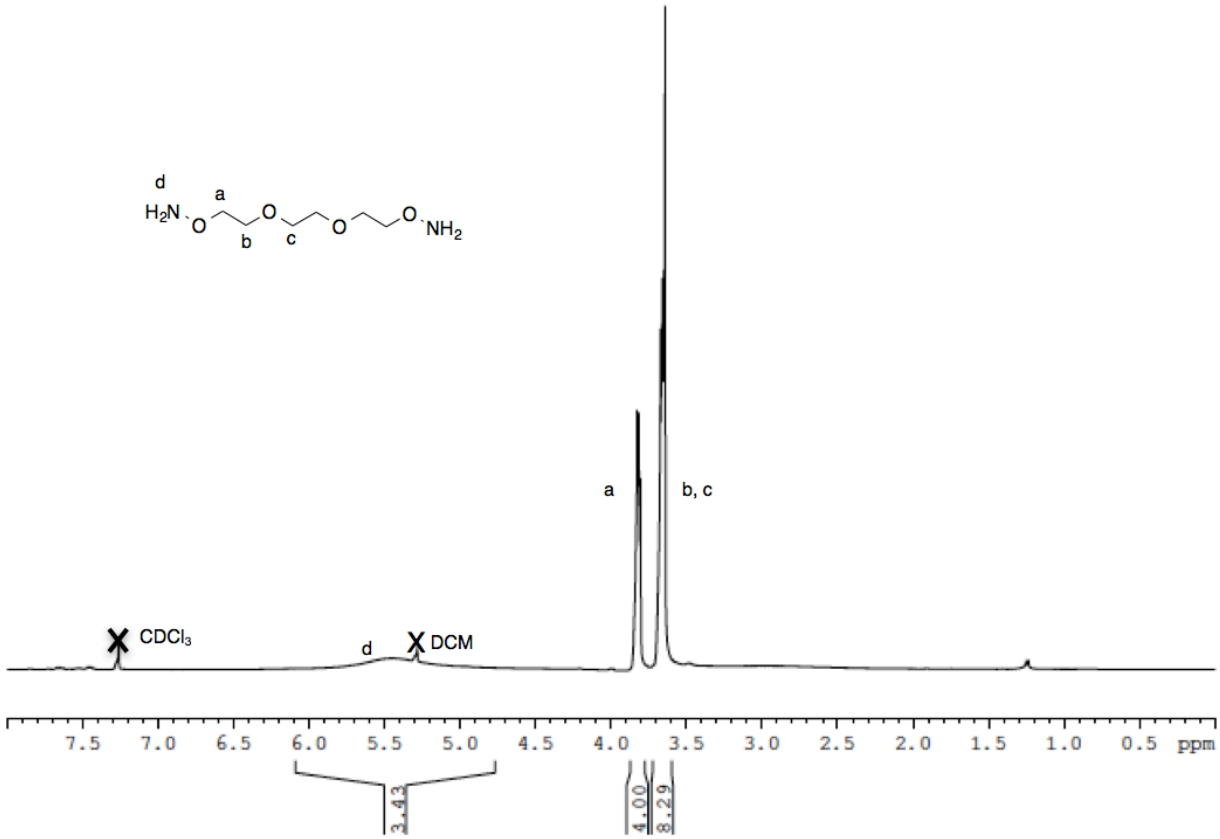

Figure 5-9. ^{1}H NMR (400 MHz, CD_2Cl_2) of TEG-AO (**2**)

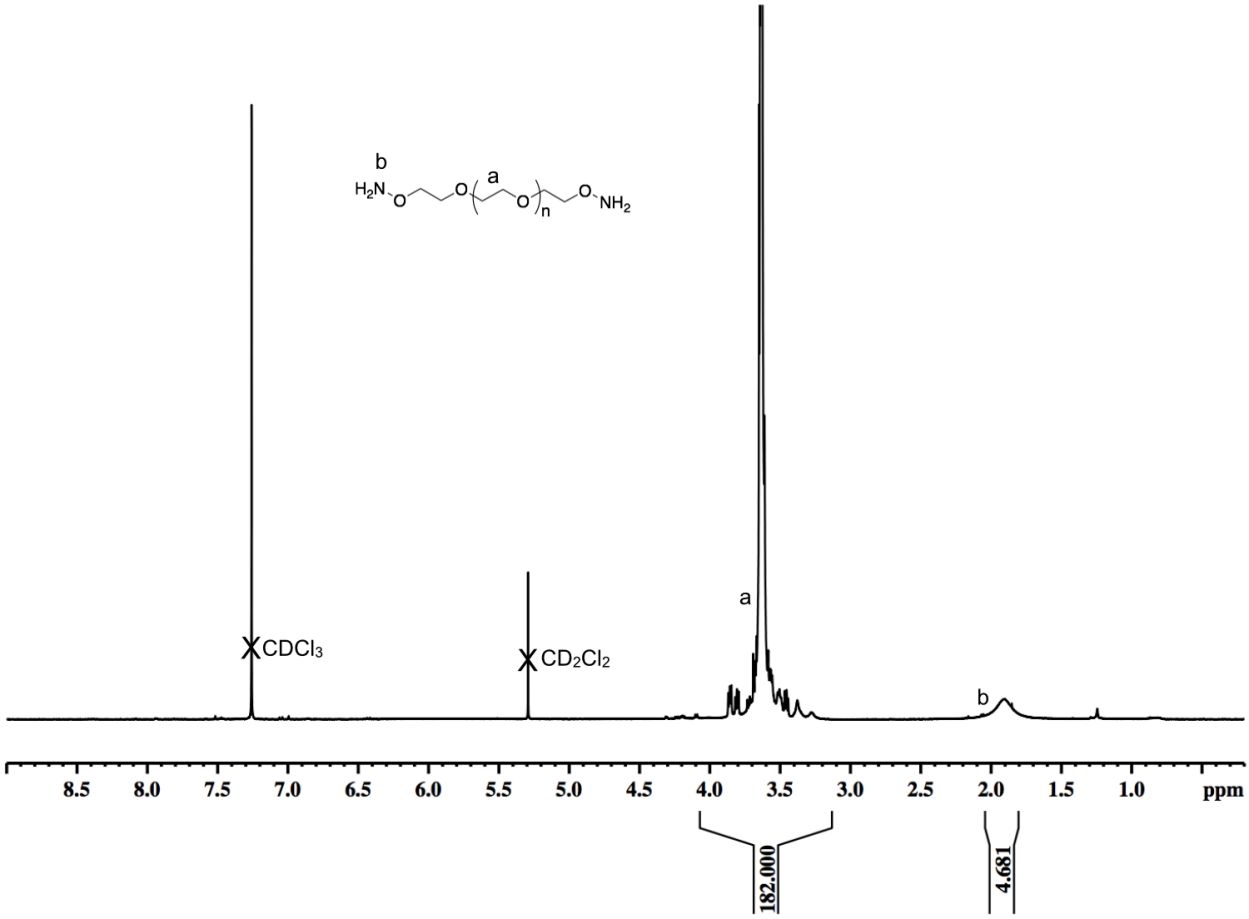

Figure 5-10. ^{1}H NMR (400 MHz, CD_2Cl_2) of PEG-AO (**8**)

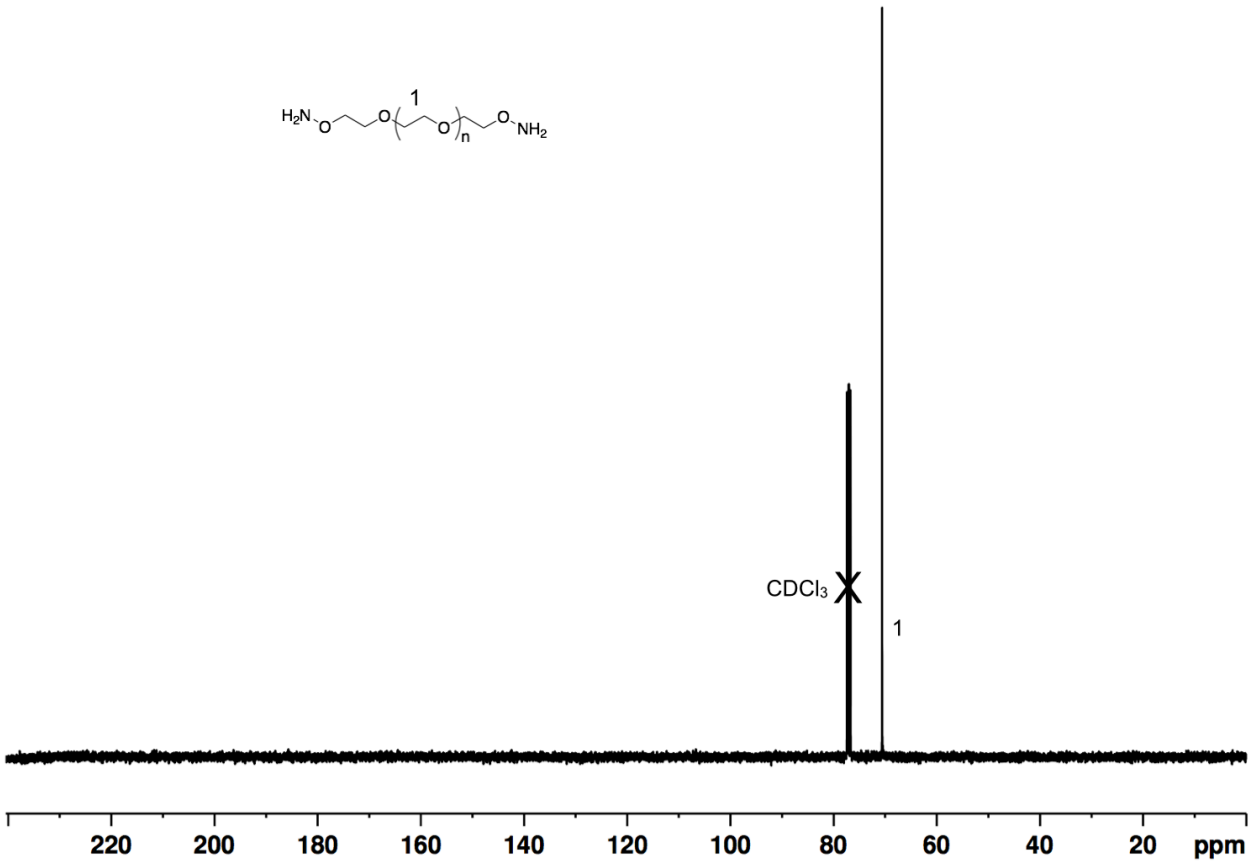

Figure 5-11. ^{13}C NMR (400 MHz, CD_2Cl_2) of PEG-AO (**8**)

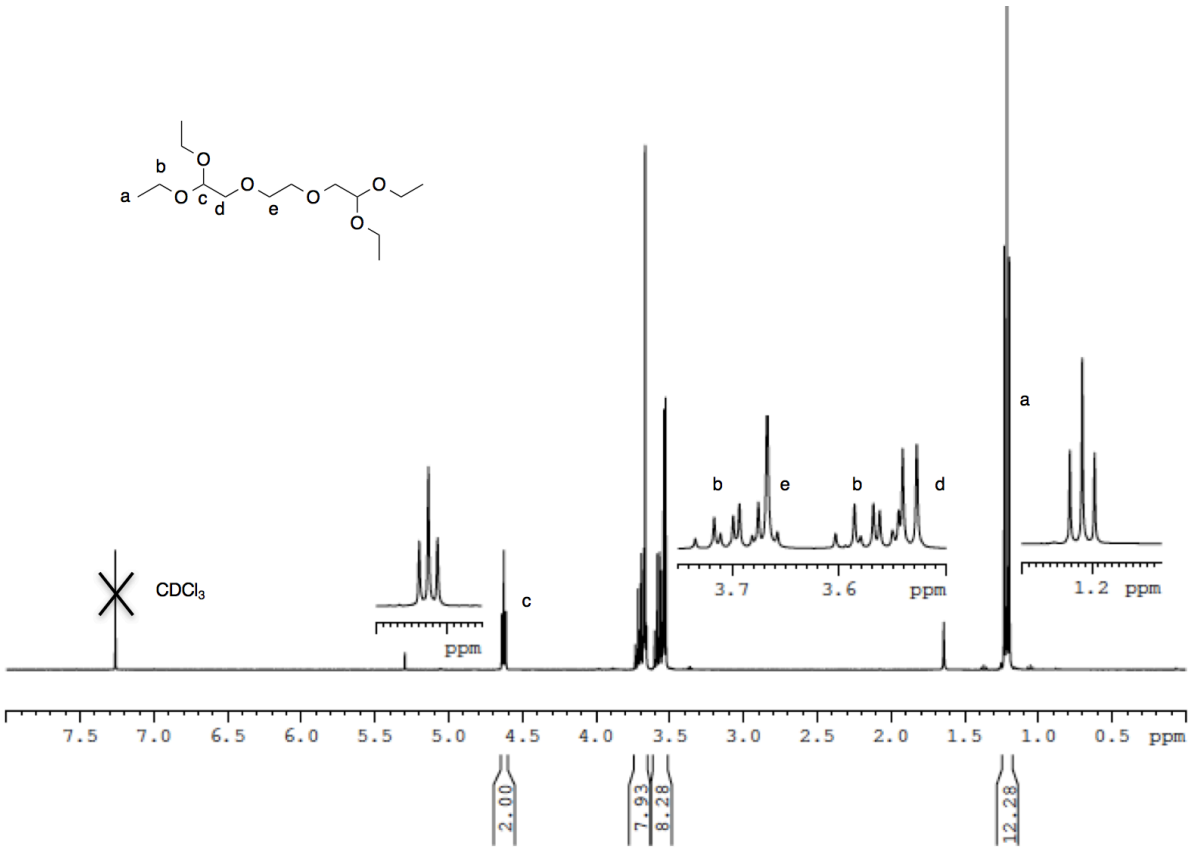

Figure 5-12. ^{1}H NMR (400 MHz, CD_2Cl_2) of TEG-acetal (**4**)

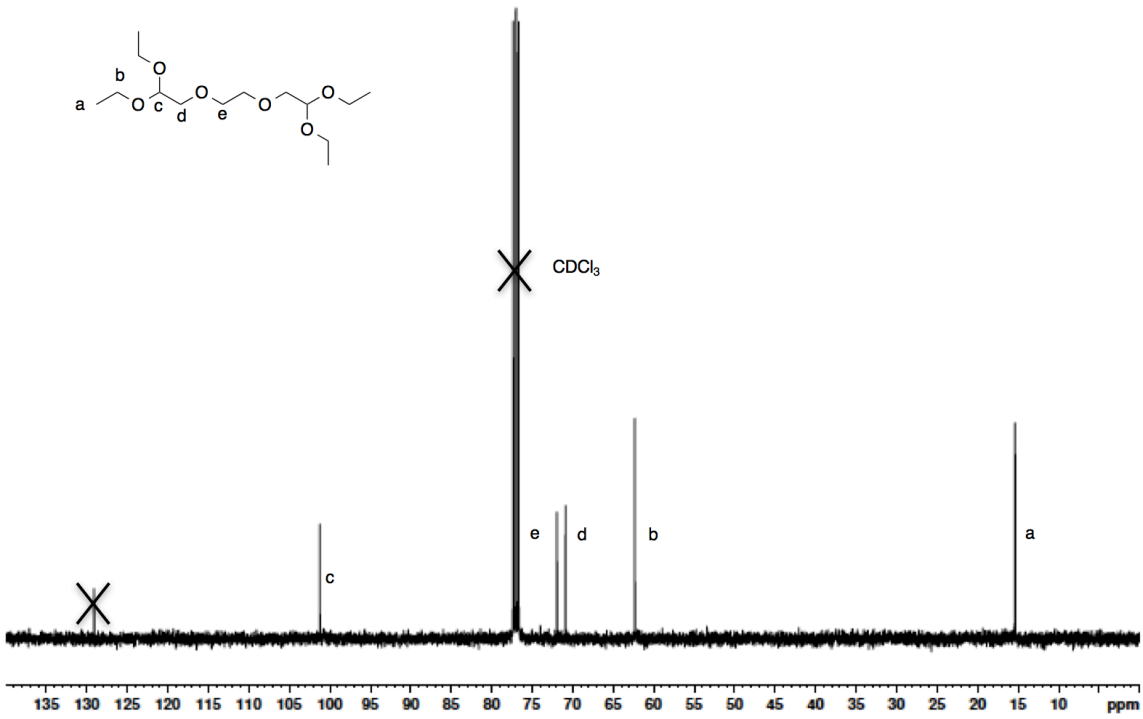

Figure 5-13. ^{13}C NMR (400 MHz, CD_2Cl_2) of TEG-acetal (**4**)

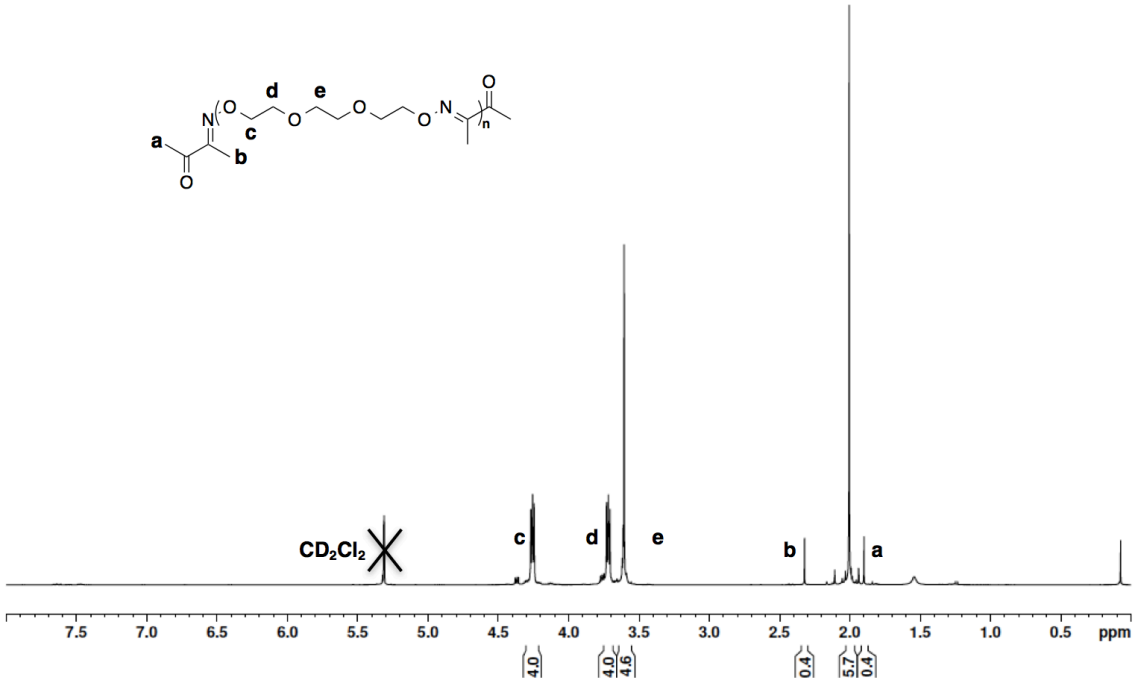

Figure 5-14. ^{1}H NMR (400 MHz, CD_2Cl_2) of oxime polymer (**6**)

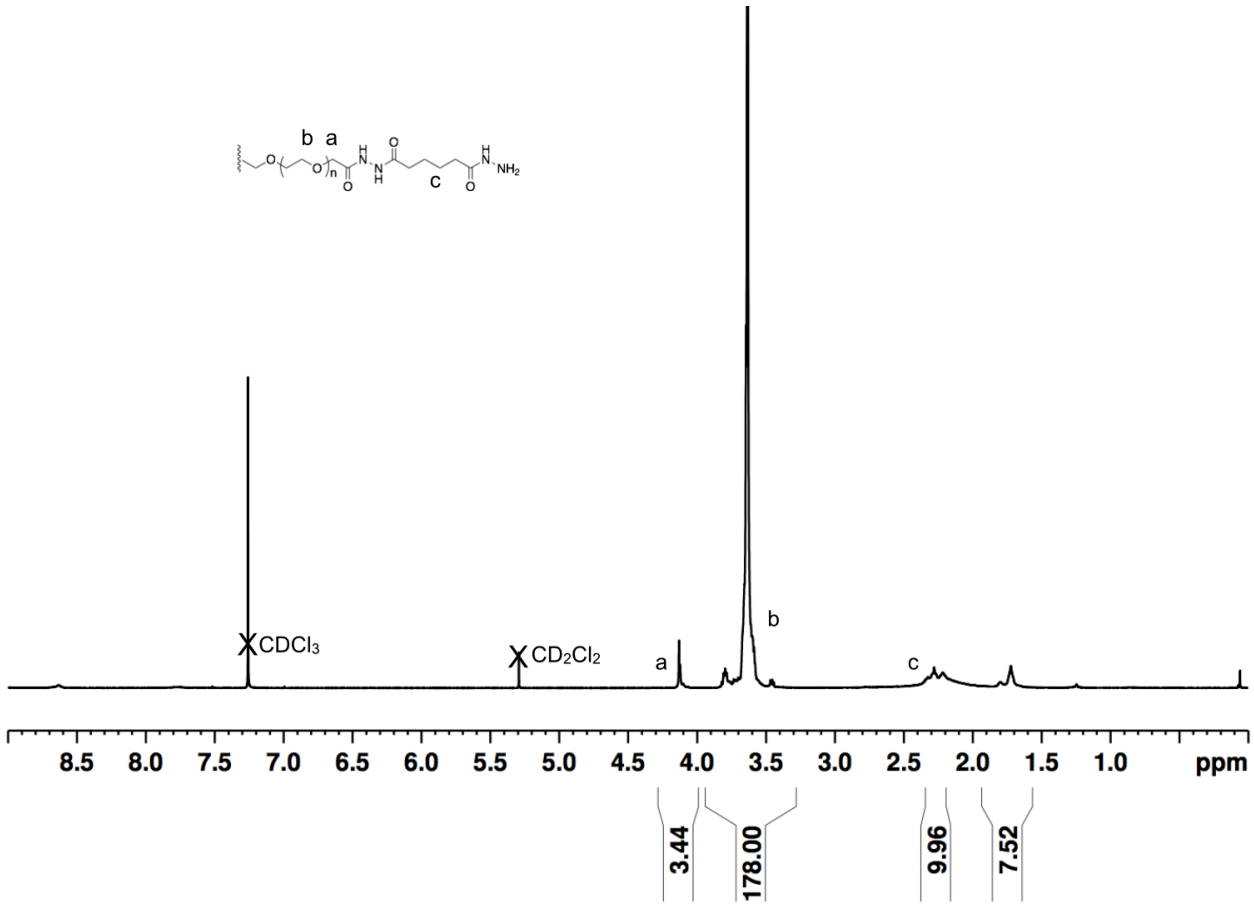

Figure 5-15. ^{1}H NMR (400 MHz, CD_2Cl_2) of PEG-hydrazide (**9**)

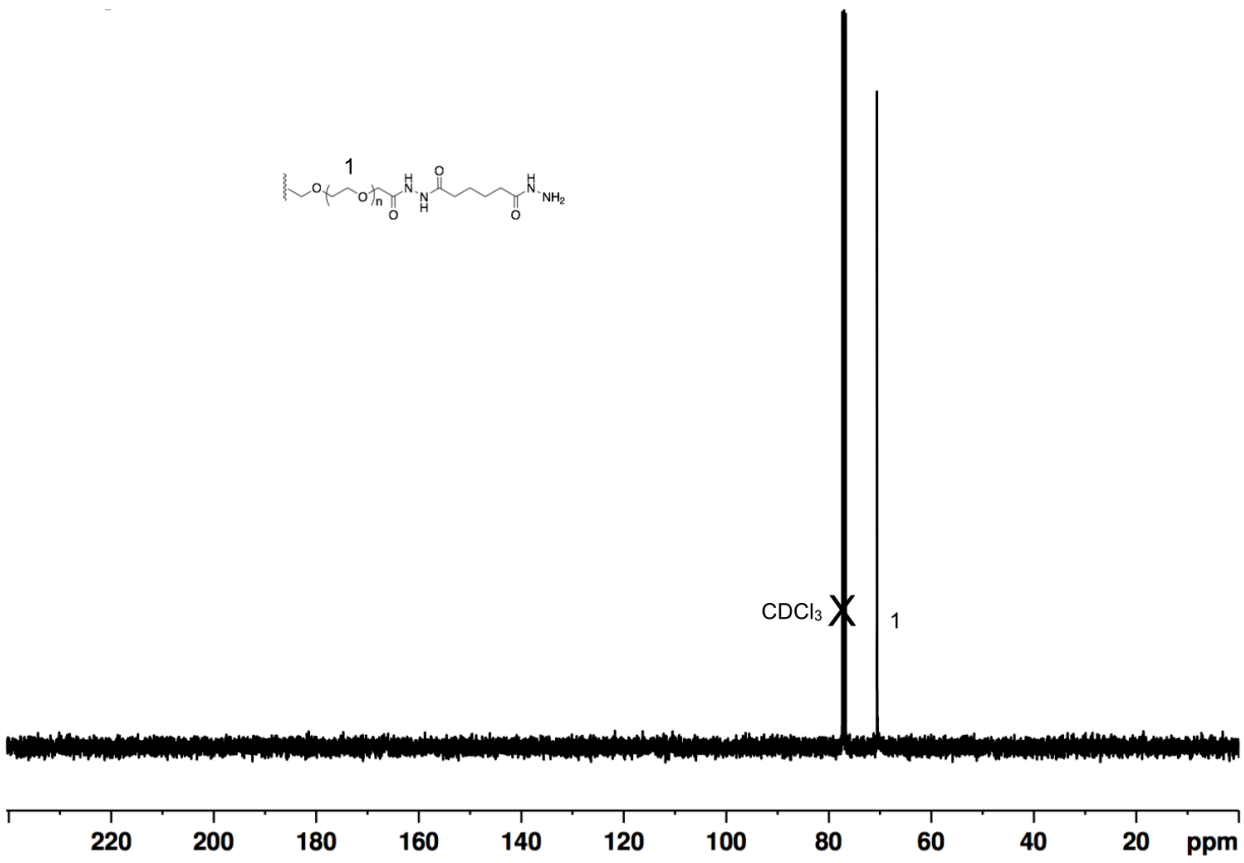

Figure 5-16. ^{13}C NMR (400 MHz, CD_2Cl_2) of PEG-hydrazide (**9**)

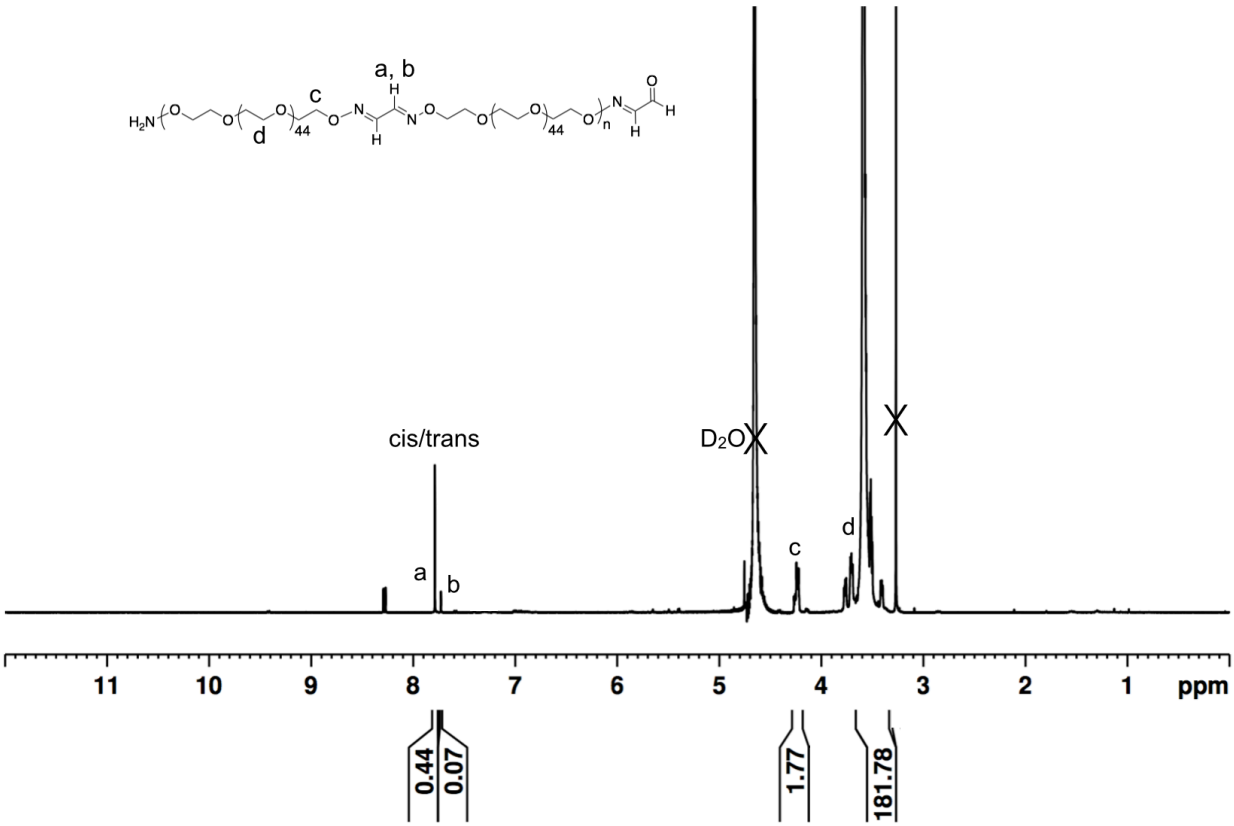

Figure 5.17. ^{1}H NMR (400 MHz, CD_2Cl_2) of oxime polymer (**13**)

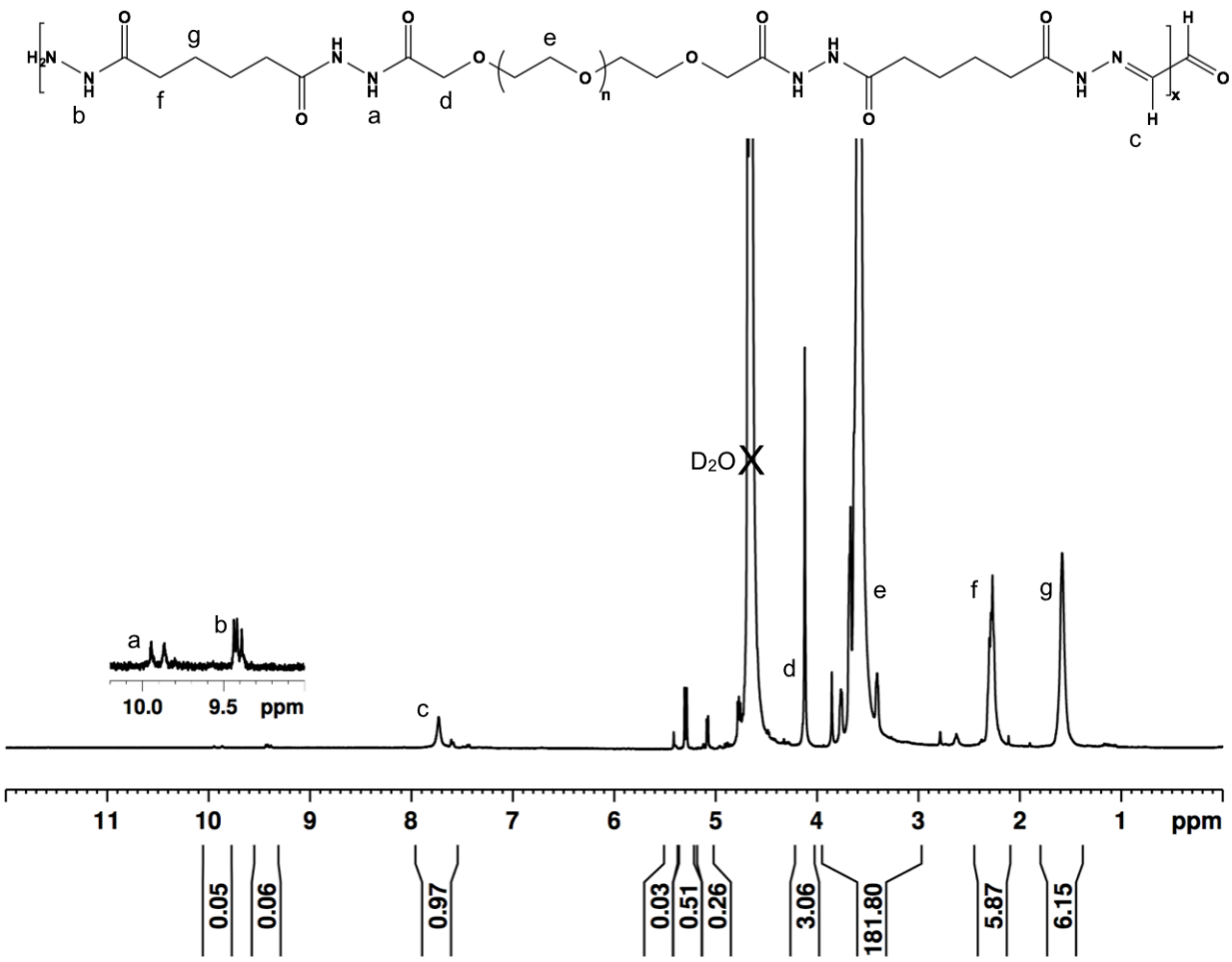

Figure 5-18. ^{13}H NMR (400 MHz, D_2O) hydrazone polymer (**14**)

5.6 References

(1) Alconcel, S. N. S.; Baas, A. S.; Maynard, H. D. *Polym. Chem.* **2011**, *2*, 1442.

(2) Abuchowski, A.; Vanes, T.; Palczuk, N. C.; Davis, F. F. *J. Biol. Chem.* **1977**, *252*, 3578.

(3) Nguyen, T. H.; Paluck, S. J.; McGahran, A. J.; Maynard, H. D. *Biomacromolecules* **2015**, *16*, 2684.

(4) Haag, R.; Kratz, F. *Angew, Chem. Int. Ed.* **2006**, *45*, 1198.

(5) Hinds, K. D.; Kim, S. W. *Adv. Drug Deliv. Rev.* **2002**, *54*, 505.

(6) Duncan, R.; Vicent, M. J. *Adv, Drug Deliv. Rev.* **2013**, *65*, 60.

(7) Ringsdorf, H. *J. Polym. Sci. C: Polym. Symp.* **1975**, 135.

(8) Abuchowski, A.; McCoy, J. R.; Palczuk, N. C.; Vanes, T.; Davis, F. F. *J. Biol. Chem.* **1977**, *252*, 3582.

(9) Abuchowski, A.; Vanes, T.; Palczuk, N. C.; Chen, R.; Davis, F. F. *Fed. Proc.* **1977**, *36*, 867.

(10) Bailey, F. E. K., T. *Nonionic Surf.* **1967**, 794.

(11) Harris, J. M. *Macromol. Chem. Phys.* **1985**, *C25*, 325.

(12) Mishra, P.; Nayak, B.; Dey, R. K. *Asian J. Pharm. Sci.* **2016**, *11*, 337.

(13) Levy, Y.; Hershfield, M. S.; Fernandezmejia, C.; Polmar, S. H.; Scudiery, D.; Berger, M.; Sorensen, R. U. *J. Ped.* **1988**, *113*, 312.

(14) Pelegri-O'Day, E. M.; Lin, E. W.; Maynard, H. D. *J. Am. Chem. Soc.* **2014**, *136*, 14323.

(15) Roberts, M. J.; Milton Harris, J. *J. Pharm. Sci.* **1998**, *87*, 1440.

(16) Sawhney, A. S.; Pathak, C. P.; Hubbell, J. A. *Macromolecules* **1993**, *26*, 581.

(17) Kretlow, J. D.; Klouda, L.; Mikos, A. G. *Adv. Drug Del. Rev.* **2007**, *59*, 263.

(18) *PEGylated Protein Drugs: Basic Science and Clinical Applications*, 2009.

(19) Wang, Y. S.; Youngster, S.; Grace, M.; Bausch, J.; Bordens, R.; Wyss, D. F. *Adv. Drug Del. Rev.* **2002**, *54*, 547.

(20) Rudmann, D. G.; Alston, J. T.; Hanson, J. C.; Heidel, S. *Tox. Path.* **2013**, *41*, 970.

(21) Markovsky, E.; Baabur-Cohen, H.; Eldar-Boock, A.; Omer, L.; Tiram, G.; Ferber, S.; Ofek, P.; Polyak, D.; Scomparin, A.; Satchi-Fainaro, R. *J. Contr. Rel.***2012**, *161*, 446.

(22) Hershfield, M. S.; Ganson, N. J.; Kelly, S. J.; Scarlett, E. L.; Jaggers, D. A.; Sundy, J. S. *Arthritis Res. Therapy* **2014**, *16*.

(23) Sizovs, A.; Xue, L.; Tolstyka, Z. P.; Ingle, N. P.; Wu, Y.; Cortez, M.; Reineke, T. M. *J. Am. Chem. Soc.***2013**, *135*, 15417.

(24) Pelegri-O'Day, E. M.; Lin, E.-W.; Maynard, H. D. *J. Am. Chem. Soc.* **2014**, *136*, 14323.

(25) Collins, J.; Xiao, Z. Y.; Espinosa-Gomez, A.; Fors, B. P.; Connal, L. A. *Polym. Chem.***2016**, *7*, 2581.

(26) Reddy, S. K.; Anseth, K. S.; Bowman, C. N. *Polym.* **2005**, *46*, 4212.

(27) Lee, Y.; Koo, H.; Jin, G.-w.; Mo, H.; Cho, M. Y.; Park, J.-Y.; Choi, J. S.; Park, J. S. *Biomacromolecules* **2005**, *6*, 24.

(28) Dingels, C.; Müller, S. S.; Steinbach, T.; Tonhauser, C.; Frey, H. *Biomacromolecules* **2013**, *14*, 448.

(29) Lundberg, P.; Lee, B. F.; van den Berg, S. A.; Pressly, E. D.; Lee, A.; Hawker, C. J.; Lynd, N. A. *ACS Macro Lett.* **2012**, *1*, 1240.

(30) In *Macro-Glycoligands: Methods and Protocols*; Sun, X. L., Sun, X. L., Eds. 2016; Vol. 1367.